CEA DSM DAPNIA-02-395 (2002)

ZGOUBI USERS' GUIDE

– VERSION 4.3 –

F. Méot

and

S. Valero

CEA Saclay, DSM/DAPNIA/SEA,

F-91191 Gif-sur-Yvette Cedex, France

January 6, 2003

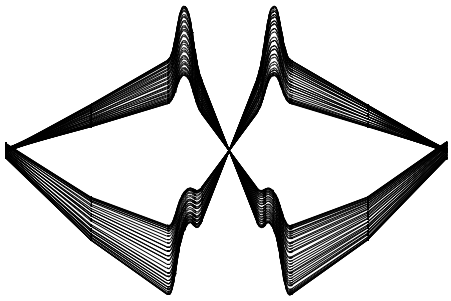

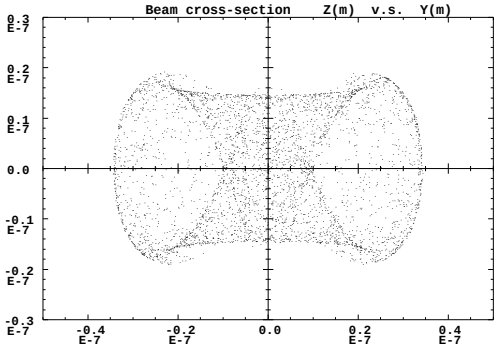

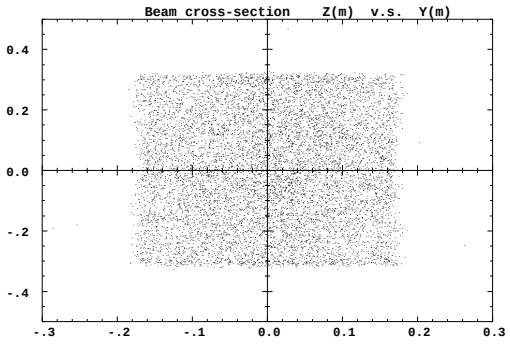

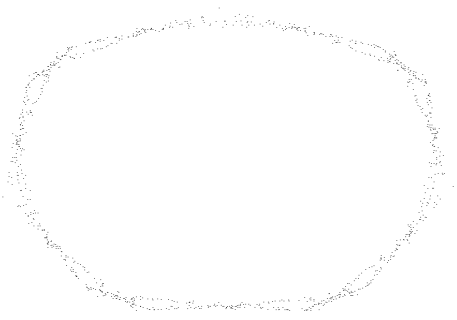

Cover figures :
upper left : colliding proton beams in LHC interaction regions,
upper right : sub-micronic non-monochromatic beam cross-section at the image plane of a second order achromatic micro-beam line,
lower left : uniform rectangular beam cross section at the downstream end of a non-linear beam expander,
lower right : a tracking of defect limited dynamic aperture in LHC.

Table of contents

PART A

Description of software contents

Glossary of keywords

Optical elements versus keywords

This glossary gives a list of keywords suitable for the simulation of common optical elements. These are classified in three categories: magnetic, electric and electromagnetic elements.

Field map procedures are also cataloged; they provide a mean for ray-tracing through measured fields, or as well through field maps obtained from numerical simulations of arbitrary geometries with such tools as POISSON, TOSCA, etc.

MAGNETIC ELEMENTS

Decapole	DECAPOLE, MULTIPOL
Dipole	AIMANT, BEND, DIPOLE, MULTIPOL, QUADISEX
Dodecapole	DODECAPO, MULTIPOL
Multipole	MULTIPOL, QUADISEX, SEXQUAD
Octupole	OCTUPOLE, MULTIPOL, QUADISEX, SEXQUAD
Quadrupole	QUADRUPO, MULTIPOL, SEXQUAD
Sextupole	SEXTUPOL, MULTIPOL, QUADISEX, SEXQUAD
Skewed multipoles	MULTIPOL
Solenoid	SOLENOID
Undulator	UNDULATOR

Field maps

1-D, cylindrical symmetry	BREVOL
2-D, mid-plane symmetry	CARTEMES, POISSON, TOSCA
2-D, no symmetry	MAP2D
2-D, polar mesh, mid-plane symmetry	POLARMES
3-D, no symmetry	TOSCA

ELECTRIC ELEMENTS

2-tube (bipotential) lens	EL2TUB
3-tube (unipotential) lens	UNIPOT
Decapole	ELMULT
Dipole	ELMULT
Dodecapole	ELMULT
Multipole	ELMULT
N-electrode mirror/lens, straight slits	ELMIR
N-electrode mirror/lens, circular slits	ELMIRC
Octupole	ELMULT
Quadrupole	ELMULT
R.F. (kick) cavity	CAVITE
Sextupole	ELMULT
Skewed multipoles	ELMULT

Field maps

1D, cylindrical symmetry	ELREVOL
2-D, no symmetry	MAP2D

ELECTROMAGNETIC ELEMENTS

Decapole	EBMULT
Dipole	EBMULT
Dodecapole	EBMULT
Multipole	EBMULT
Octupole	EBMULT
Quadrupole	EBMULT
Sextupole	EBMULT
Skewed multipoles	EBMULT
Wien filter	SEPARA, WIENFILT

INTRODUCTION

The computer code **zgoubi** calculates trajectories of charged particles in magnetic and electric fields. At the origin specially adapted to the definition and adjustment of beam lines and magnetic spectrometers, it has so evolved that it allows the study of systems including complex sequences of optical elements such as dipoles, quadrupoles, arbitrary multipoles and other magnetic or electric devices, and is able as well to handle periodic structures. Compared to other codes, it presents several peculiarities:

- a numerical method for integrating the Lorentz equation, based on Taylor series, which optimizes computing time and provides high accuracy and strong symplecticity,
- spin tracking, using the same numerical method as for the Lorentz equation,
- calculation of the synchrotron radiation electric field and spectra in arbitrary magnetic fields, from the ray-tracing outcomes,
- the possibility of using a mesh, which allows ray-tracing from simulated or measured (1-D, 2-D or 3-D) field maps,
- numerous Monte Carlo procedures: unlimited number of trajectories, in-flight decay, photon emission, etc.
- a built-in fitting procedure including arbitrary variables and a large variety of constraints,
- multiturn tracking in circular accelerators including features proper to machine parameter calculation and survey, simulation of time-varying power supplies.

The initial version of the Code, dedicated to ray-tracing in magnetic fields, was developed by D. Garreta and J.C. Faivre at CEN-Saclay in the early 1970's. It was perfected for the purpose of studying the four spectrometers SPES I, II, III, IV at the Laboratoire National Saturne (CEA-Saclay, France), and SPEG at Ganil (Caen, France). It is being used since long in several national and foreign laboratories.

The first manual was in French [1]. Since then many improvements have been implemented. In order to facilitate access to the program an English version of the manual was written at TRIUMF with the assistance of J. Doornbos. P. Stewart prepared the manuscript for publication [2]

An updating was necessary for accompanying the third version of the code which featured spin tracking and ray-tracing in combined electric and magnetic fields; this was done with the help of D. Bunel for the preparation of the document and lead to the third release [3].

Lately, provisions were introduced for the computation of synchrotron radiation electromagnetic impulse and spectra. In the mean time, several new optical elements were added, such as electro-magnetic and other electrostatic lenses. Used since several years for special studies in periodic machines (e.g., SATURNE at Saclay, COSY at Julich, LEP and LHC at Cern), **zgoubi** has also benefited from extensive development of storage ring related features.

These developments of **zgoubi** have strongly benefited of the environment of the Groupe Théorie, Laboratoire National SATURNE, CEA/DSM-Saclay.

The graphic interface to **zgoubi** (addressed in Part D) has also undergone concomitent extended developments, which make it a performant tool for post-processing **zgoubi** outputs.

This manual is intended only to describe the details of the most recent version of **zgoubi** , which is far from being a "finished product".

1 NUMERICAL CALCULATION OF MOTION AND FIELDS

1.1 zgoubi Frame

The reference frame of **zgoubi** is presented in Fig 1. Its origin is in the median plane on a reference curve which coincides with the optical axis of optical elements.

1.2 Integration of the Lorentz Equation

The Lorentz equation, which governs the motion of a particle of charge q, relativistic mass m and velocity $\vec{v}$ in electric and magnetic fields $\vec{e}$ and $\vec{b}$, is written

$$\frac{d(m\vec{v})}{dt} = q\,(\vec{e} + \vec{v} \times \vec{b}) \tag{1.2.1}$$

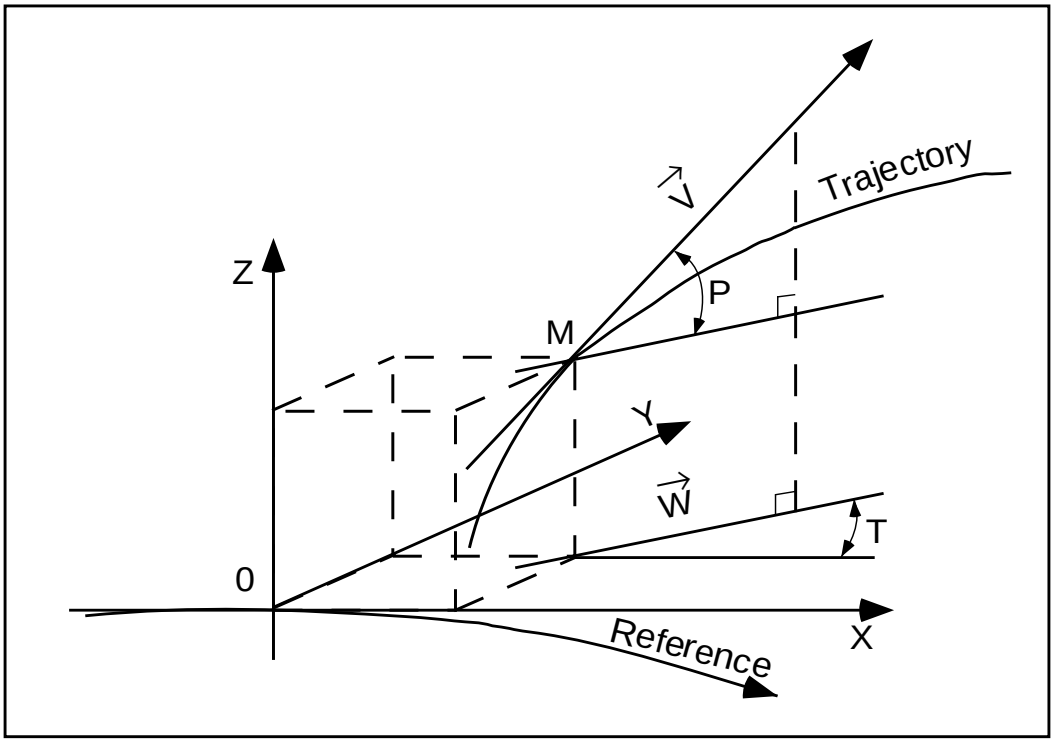

Figure 1: Reference frame and coordinates (Y, T, Z, P) in **zgoubi** .
OX: in the plane of the reference curve in the direction of motion,
OY: in the plane of the reference curve, normal to OX,
OZ: orthogonal to the (X, Y) plane,
$\vec{W}$: projection of the velocity, $\vec{v}$, in the (X, Y) plane,
T = angle between $\vec{W}$ and the X-axis,
P = angle between $\vec{W}$ and $\vec{v}$.

Taking

$$\vec{u} = \frac{\vec{v}}{v}, \quad ds = v\,dt, \quad \vec{u}' = \frac{d\vec{u}}{ds}, \quad m\vec{v} = mv\vec{u} = q\,B\rho\,\vec{u} \tag{1.2.2}$$

where $B\rho$ is the rigidity of the particle, this equation can be rewritten

$$(B\rho)'\,\vec{u} + B\rho\,\vec{u}\,' = \frac{\vec{e}}{v} + \vec{u} \times \vec{b} \tag{1.2.3}$$

From position $\vec{R}(M_0)$ and unit velocity $\vec{u}(M_0)$ at point M_0, position $\vec{R}(M_1)$ and unit velocity $\vec{u}(M_1)$ at point M_1 following a displacement Δs, are obtained from truncated Taylor expansions (Fig. 2)

$$\begin{aligned} \vec{R}(M_1) &\approx \vec{R}(M_0) + \vec{u}(M_0)\,\Delta s + \vec{u}\,'(M_0)\,\frac{\Delta s^2}{2!} + \ldots + \vec{u}\,'''''(M_0)\,\frac{\Delta s^6}{6!} \\ \vec{u}(M_1) &\approx \vec{u}(M_0) + \vec{u}\,'(M_0)\,\Delta s + \vec{u}\,''(M_0)\,\frac{\Delta s^2}{2!} + \ldots + \vec{u}\,'''''(M_0)\,\frac{\Delta s^5}{5!} \end{aligned} \tag{1.2.4}$$

The rigidity at M_1 is obtained in the same way from

$$(B\rho)(M_1) \approx (B\rho)(M_0) + (B\rho)'(M_0)\Delta s + \ldots + (B\rho)''''(M_0)\frac{\Delta s^4}{4!} \tag{1.2.5}$$

The equation of time of flight is written in a similar manner

$$T(M_1) \approx T(M_0) + \frac{dT}{ds}(M_0)\,\Delta s + \frac{d^2T}{ds^2}(M_0)\,\frac{\Delta s^2}{2} + \frac{d^3T}{ds^3}(M_0)\,\frac{\Delta s^3}{3!} + \frac{d^4T}{ds^4}(M_0)\,\frac{\Delta s^4}{4!} \tag{1.2.6}$$

The derivatives $\vec{u}^{(n)} = \dfrac{d^n\vec{u}}{ds^n}$ and $(B\rho)^{(n)} = \dfrac{d^n(B\rho)}{ds^n}$ involved in these expressions are calculated as described in the next sections. For the sake of computing speed, three distinct software procedures are involved, depending on whether $\vec{e}$ or $\vec{b}$ is zero, or $\vec{e}$ and $\vec{b}$ are both non-zero.

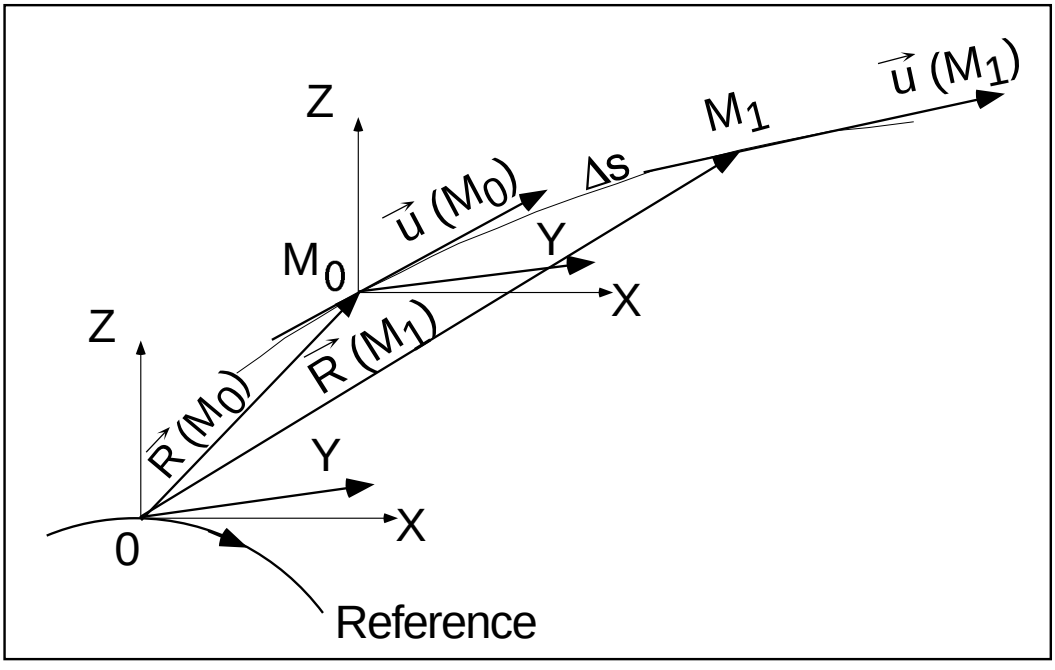

Figure 2: Position and velocity of a particle in the reference frame.

1.2.1 Integration in magnetic fields

Admitting that $\vec{e} = 0$, and noting $\vec{B} = \dfrac{\vec{b}}{B\rho}$, eq. (1.2.3) reduces to

$$\vec{u}\,' = \vec{u} \times \vec{B}$$

The successive derivatives $\vec{u}^{(n)} = \dfrac{d^n \vec{u}}{ds^n}$ of $\vec{u}$ needed in the Taylor expansions (eqs. 1.2.4) are calculated by differentiating $\vec{u}\,' = \vec{u} \times \vec{B}$

$$\begin{aligned}
\vec{u}\,'' &= \vec{u}\,' \times \vec{B} + \vec{u} \times \vec{B}\,' \\
\vec{u}\,''' &= \vec{u}\,'' \times \vec{B} + 2\vec{u}\,' \times \vec{B}\,' + \vec{u} \times \vec{B}\,'' \\
\vec{u}\,'''' &= \vec{u}\,''' \times \vec{B} + 3\vec{u}\,'' \times \vec{B}\,' + 3\vec{u}\,' \times \vec{B}\,'' + \vec{u} \times \vec{B}\,''' \\
\vec{u}\,''''' &= \vec{u}\,'''' \times \vec{B} + 4\vec{u}\,''' \times \vec{B}\,' + 6\vec{u}\,'' \times \vec{B}\,'' + 4\vec{u}\,' \times \vec{B}\,''' + \vec{u} \times \vec{B}\,''''
\end{aligned} \tag{1.2.7}$$

where $\vec{B}^{(n)} = \dfrac{d^n \vec{B}}{ds^n}$.

From $d\vec{B} = \dfrac{\partial \vec{B}}{\partial X}\,dX + \dfrac{\partial \vec{B}}{\partial Y}\,dY + \dfrac{\partial \vec{B}}{\partial Z}\,dZ = \sum_{i=1,3} \dfrac{\partial \vec{B}}{\partial X_i}\,dX_i$, and by successive differentiation, we get

$$\begin{aligned}
\vec{B}\,' &= \sum_i \frac{\partial \vec{B}}{\partial X_i}\,u_i \\
\vec{B}\,'' &= \sum_{ij} \frac{\partial^2 \vec{B}}{\partial X_i \partial X_j}\,u_i u_j + \sum_i \frac{\partial \vec{B}}{\partial X_i}\,u_i' \\
\vec{B}\,''' &= \sum_{ijk} \frac{\partial^3 \vec{B}}{\partial X_i \partial X_j \partial X_k}\,u_i u_j u_k + 3\sum_{ij} \frac{\partial^2 \vec{B}}{\partial X_i \partial X_j}\,u_i' u_j + \sum_i \frac{\partial \vec{B}}{\partial X_i}\,u_i'' \\
\vec{B}\,'''' &= \sum_{ijkl} \frac{\partial^4 \vec{B}}{\partial X_i \partial X_j \partial X_k \partial X_l}\,u_i u_j u_k u_l + 6\sum_{ijk} \frac{\partial^3 \vec{B}}{\partial X_i \partial X_j \partial X_k}\,u_i' u_j u_k \\
&\quad + 4\sum_{ij} \frac{\partial^2 \vec{B}}{\partial X_i \partial X_j}\,u_i'' u_j + 3\sum_{ij} \frac{\partial^2 \vec{B}}{\partial X_i \partial X_j}\,u_i' u_j' + \sum_i \frac{\partial \vec{B}}{\partial X_i}\,u_i'''
\end{aligned} \tag{1.2.8}$$

From the knowledge of $\vec{u}(M_0)$ and $\vec{B}(M_0)$ at point M_0 of the trajectory, we calculate alternately the derivatives of $\vec{u}(M_0)$ and $\vec{B}(M_0)$, by means of eqs. (1.2.7) and (1.2.8), and inject it in eq. (1.2.4) to get $\vec{R}(M_1)$ and $\vec{u}(M_1)$.

1.2.2 Integration in electric fields [4]

Admitting that $\vec{b} = 0$, eq. (1.2.3) reduces to

$$(B\rho)'\,\vec{u} + B\rho\vec{u}\,' = \frac{\vec{e}}{v} \tag{1.2.9}$$

which, by successive differentiations, gives the recursive relations

$$
\begin{aligned}
&(B\rho)'\,\vec{u} + B\rho\,\vec{u}\,' = \frac{\vec{e}}{v} \\
&(B\rho)''\,\vec{u} + 2(B\rho)'\,\vec{u}\,' + B\rho\,\vec{u}\,'' = \left(\frac{1}{v}\right)'\vec{e} + \frac{\vec{e}\,'}{v} \\
&(B\rho)'''\,\vec{u} + 3(B\rho)''\,\vec{u}\,' + 3(B\rho)'\,\vec{u}\,'' + B\rho\,\vec{u}\,''' = \left(\frac{1}{v}\right)''\vec{e} + 2\left(\frac{1}{v}\right)'\vec{e}\,' + \left(\frac{1}{v}\right)\vec{e}\,'' \\
&(B\rho)''''\,\vec{u} + 4(B\rho)'''\,\vec{u}\,' + 6(B\rho)''\,\vec{u}\,'' + 4(B\rho)'\,\vec{u}\,''' + B\rho\,\vec{u}\,'''' = \\
&\qquad \left(\frac{1}{v}\right)'''\vec{e} + 3\left(\frac{1}{v}\right)''\vec{e}\,' + 3\left(\frac{1}{v}\right)'\vec{e}\,'' + \frac{1}{v}\,\vec{e}\,'''
\end{aligned}
\tag{1.2.10}
$$

that provide the derivatives $\dfrac{d^n\vec{u}}{ds^n}$ needed in the Taylor expansions (eq. 1.2.4)

$$
\begin{aligned}
\vec{u}\,' &= \left(\frac{1}{v}\right)\vec{E} - \frac{(B\rho)'}{B\rho}\,\vec{u} \\
\vec{u}\,'' &= \left(\frac{1}{v}\right)'\vec{E} + \left(\frac{1}{v}\right)\vec{E}\,'\,|_{B\rho} - 2\frac{(B\rho)'}{B\rho}\vec{u}\,' - \frac{(B\rho)''}{B\rho}\vec{u} \\
\vec{u}\,''' &= \left(\frac{1}{v}\right)''\vec{E} + 2\left(\frac{1}{v}\right)'\vec{E}\,'\,|_{B\rho} + \frac{1}{v}\vec{E}\,''\,|_{B\rho} - 3\frac{(B\rho)'}{B\rho}\vec{u}\,'' - 3\frac{(B\rho)''}{B\rho}\vec{u}\,' - \frac{(B\rho)'''}{B\rho}\vec{u} \\
\vec{u}\,'''' &= \left(\frac{1}{v}\right)'''\vec{E} + 3\left(\frac{1}{v}\right)''\vec{E}\,'\,|_{B\rho} + 3\left(\frac{1}{v}\right)'\vec{E}\,''\,|_{B\rho} + \left(\frac{1}{v}\right)\vec{E}\,'''\,|_{B\rho} \\
&\quad - 4\frac{(B\rho)'}{B\rho}\vec{u}\,''' - 6\frac{(B\rho)''}{B\rho}\vec{u}\,'' - 4\frac{(B\rho)'''}{B\rho}\vec{u}\,' - \frac{(B\rho)''''}{B\rho}\vec{u} \\
\vec{u}\,''''' &= \left(\frac{1}{v}\right)''''\vec{E} + 4\left(\frac{1}{v}\right)'''\vec{E}\,'\,|_{B\rho} + 6\left(\frac{1}{v}\right)''\vec{E}\,''\,|_{B\rho} + 4\left(\frac{1}{v}\right)'\vec{E}\,'''\,|_{B\rho} + \left(\frac{1}{v}\right)\vec{E}\,''''\,|_{B\rho} \\
&\quad - 5\frac{(B\rho)'}{B\rho}\vec{u}\,'''' - 10\frac{(B\rho)''}{B\rho}\vec{u}\,''' - 10\frac{(B\rho)'''}{B\rho}\vec{u}\,'' - 5\frac{(B\rho)''''}{B\rho}\vec{u}\,' - \frac{(B\rho)'''''}{B\rho}\vec{u}
\end{aligned}
\tag{1.2.11}
$$

where $\vec{E} = \dfrac{\vec{e}}{B\rho}$, and $(\ )^{(n)}\,|_{B\rho}$ denotes differentiation at constant $B\rho$: $\vec{E}^{(n)}\,|_{B\rho} = \dfrac{1}{B\rho}\dfrac{d^n\vec{e}}{ds^n}$. These derivatives of the electric field are obtained from the total derivative

$$
d\vec{E} = \frac{\partial\vec{E}}{\partial X}\,dX + \frac{\partial\vec{E}}{\partial Y}\,dY + \frac{\partial\vec{E}}{\partial Z}\,dZ \tag{1.2.12}
$$

by successive differentiations

$$
\begin{aligned}
\vec{E}\,' &= \sum_i \frac{\partial\vec{E}}{\partial X_i}\,u_i \\
\vec{E}\,'' &= \sum_{ij} \frac{\partial^2\vec{E}}{\partial X_i\partial X_j}\,u_iu_j + \sum_i \frac{\partial\vec{E}}{\partial X_i}\,u_i' \\
\vec{E}\,''' &= \sum_{ijk} \frac{\partial^3\vec{E}}{\partial X_i\partial X_j\partial X_k}\,u_iu_ju_k + 3\sum_{ij} \frac{\partial^2\vec{E}}{\partial X_i\partial X_j}\,u_i'u_j + \sum_i \frac{\partial\vec{E}}{\partial X_i}\,u_i''
\end{aligned}
\tag{1.2.13}
$$

etc. as in eq. 1.2.8. These eqs. (1.2.11), as well as the calculation of the rigidity, following eq. (1.2.5), involve derivatives $(B\rho)^{(n)} = \dfrac{d^n(B\rho)}{ds^n}$, which are obtained in the following way. Considering that

$$
\frac{dp^2}{dt} = \frac{d\vec{p}^{\,2}}{dt} \quad i.e., \quad \frac{dp}{dt}\,p = \frac{d\vec{p}}{dt}\vec{p} \tag{1.2.14}
$$

with $\dfrac{d\vec{p}}{dt} = q\,(\vec{e} + \vec{v}\times\vec{b})$ (eq. 1.2.1), we obtain

$$\frac{dp}{dt}\,p = q\,(\vec{e} + v \times \vec{b}) \cdot \vec{p} = q\vec{e} \cdot \vec{p} \tag{1.2.15}$$

since $(\vec{v} \times \vec{b}) \cdot \vec{p} = 0$. Normalizing as previously with $\vec{p} = p\vec{u} = qB\rho\vec{u}$ and $ds = vdt$, and by successive differentiations, eq. (1.2.15) leads to the $(B\rho)^{(n)}$

$$\begin{aligned}
(B\rho)' &= \frac{1}{v}\,(\vec{e}\cdot\vec{u}) \\
(B\rho)'' &= \left(\frac{1}{v}\right)'(\vec{e}\cdot\vec{u}) + \frac{1}{v}\,(\vec{e}\cdot\vec{u})' \\
(B\rho)''' &= \left(\frac{1}{v}\right)''(\vec{e}\cdot\vec{u}) + 2\left(\frac{1}{v}\right)'(\vec{e}\cdot\vec{u})' + \frac{1}{v}\,(\vec{e}\cdot\vec{u})'' \\
(B\rho)'''' &= \left(\frac{1}{v}\right)'''(\vec{e}\cdot\vec{u}) + 3\left(\frac{1}{v}\right)''(\vec{e}\cdot\vec{u})' + 3\left(\frac{1}{v}\right)'(\vec{e}\cdot\vec{u})'' + \frac{1}{v}\,(\vec{e}\cdot\vec{u})'''
\end{aligned} \tag{1.2.16}$$

Note that the derivatives $(\vec{e}\cdot\vec{u})^{(n)} = \dfrac{d^n(\vec{e}\cdot\vec{u})}{ds^n}$ can be related to the derivatives of the kinetic energy W by $dW = \dfrac{d\vec{p}}{dt}\cdot\vec{v}\,dt = q\vec{e}\cdot\vec{v}\,dt$ which leads to

$$\frac{d^{n+1}W}{ds^{n+1}} = q\frac{d^n(\vec{e}\cdot\vec{u})}{ds^n} \tag{1.2.17}$$

Finally, the derivatives $\left(\dfrac{1}{v}\right)^{(n)} = \dfrac{d^n\left(\dfrac{1}{v}\right)}{ds^n}$ involved in eqs. (1.2.11,1.2.16) are obtained from $p = \dfrac{v}{c}\dfrac{W + m_0c^2}{c}$, ($m_0$ is the rest mass) by successive differentiations, that give the recursive relations

$$\begin{aligned}
\left(\frac{1}{v}\right) &= \frac{1}{c^2}\,\frac{W + m_0c^2}{qB\rho} \\
\left(\frac{1}{v}\right)' &= \frac{1}{c^2}\,\frac{(\vec{e}\cdot\vec{u})}{B\rho} - \frac{1}{v}\,\frac{(B\rho)'}{B\rho} \\
\left(\frac{1}{v}\right)'' &= \frac{1}{c^2}\,\frac{(\vec{e}\cdot\vec{u})'}{B\rho} - 2\left(\frac{1}{v}\right)'\frac{(B\rho)'}{B\rho} - \frac{1}{v}\,\frac{(B\rho)''}{B\rho} \\
\left(\frac{1}{v}\right)''' &= \frac{1}{c^2}\,\frac{(\vec{e}\cdot\vec{u})''}{B\rho} - 3\left(\frac{1}{v}\right)''\frac{(B\rho)'}{B\rho} - 3\left(\frac{1}{v}\right)'\frac{(B\rho)''}{B\rho} - \frac{1}{v}\,\frac{(B\rho)'''}{B\rho}
\end{aligned} \tag{1.2.18}$$

1.2.3 Integration in combined electric and magnetic fields

When both $\vec{e}$ and $\vec{b}$ are non-zero, the complete eq. (1.2.3) must be considered. Recursive differentiations give the following relations

$$\begin{aligned}
&(B\rho)'\vec{u} + B\rho\vec{u}\,' = \frac{\vec{e}}{v} + \vec{u}\times\vec{b} \\
&(B\rho)''\vec{u} + 2(B\rho)'\vec{u}\,' + B\rho\vec{u}\,'' = \left(\frac{1}{v}\right)'\vec{e} + \left(\frac{1}{v}\right)\vec{e}\,' + (\vec{u}\times\vec{b})' \\
&(B\rho)'''\vec{u} + 3(B\rho)''\vec{u}\,' + 3(B\rho)'\vec{u}\,'' + B\rho\vec{u}\,''' = \left(\frac{1}{v}\right)''\vec{e} + 2\left(\frac{1}{v}\right)'\vec{e}\,' + \left(\frac{1}{v}\right)\vec{e}\,'' + (\vec{u}\times\vec{b})'' \\
&(B\rho)''''\vec{u} + 4(B\rho)'''\vec{u}\,' + 6(B\rho)''\vec{u}\,'' + 4(B\rho)'\vec{u}\,''' + B\rho\vec{u}\,'''' = \\
&\qquad \left(\frac{1}{v}\right)'''\vec{e} + 3\left(\frac{1}{v}\right)''\vec{e}\,' + 3\left(\frac{1}{v}\right)'\vec{e}\,'' + \frac{1}{v}\vec{e}\,''' + (\vec{u}\times\vec{b})'''
\end{aligned} \tag{1.2.19}$$

that provide the derivatives $\dfrac{d^n\vec{u}}{ds^n}$ needed in the Taylor expansions (1.2.4)

$$
\begin{aligned}
\vec{u}\,' &= \left(\frac{1}{v}\right)\vec{E} + (\vec{u}\times\vec{B}) - \frac{(B\rho)'}{B\rho}\vec{u} \\
\vec{u}\,'' &= \left(\frac{1}{v}\right)'\vec{E} + \left(\frac{1}{v}\right)\vec{E}\,' \mid_{B\rho} + (\vec{u}\times\vec{B}\,')' \mid_{B\rho} - 2\frac{(B\rho)'}{B\rho}\vec{u}\,' - \frac{(B\rho)''}{B\rho}\vec{u} \\
\vec{u}\,''' &= \left(\frac{1}{v}\right)''\vec{E} + 2\left(\frac{1}{v}\right)'\vec{E}\,' \mid_{B\rho} + \frac{1}{v}\vec{E}\,'' \mid_{B\rho} + (\vec{u}\times\vec{B})'' \mid_{B\rho} - 3\frac{(B\rho)'}{B\rho}\vec{u}\,'' - 3\frac{(B\rho)''}{B\rho}\vec{u}\,' - \frac{(B\rho)'''}{B\rho}\vec{u} \\
\vec{u}\,'''' &= \left(\frac{1}{v}\right)'''\vec{E} + 3\left(\frac{1}{v}\right)''\vec{E}\,' \mid_{B\rho} + 3(\frac{1}{v})'\vec{E}\,'' \mid_{B\rho} + \left(\frac{1}{v}\right)\vec{E}\,''' \mid_{B\rho} \\
&\quad + (\vec{u}\times\vec{B})''' \mid_{B\rho} - 4\frac{(B\rho)'}{B\rho}\vec{u}\,''' - 6\frac{(B\rho)''}{B\rho}\vec{u}\,'' - 4\frac{(B\rho)'''}{B\rho}\vec{u}\,' - \frac{(B\rho)''''}{B\rho}\vec{u}
\end{aligned}
\tag{1.2.20}
$$

where $\vec{E} = \dfrac{\vec{e}}{B\rho}$, $\vec{B} = \dfrac{\vec{b}}{B\rho}$, and $^{(n)} \mid_{B\rho}$ denotes differentiation at constant $B\rho$

$$
\vec{E}^{(n)} \mid_{B\rho} = \frac{1}{B\rho}\frac{d^n\vec{e}}{ds^n} \quad \text{and} \quad (\vec{u}\times\vec{B})^{(n)} \mid_{B\rho} = \frac{1}{B\rho}(\vec{u}\times\vec{b})^{(n)}. \tag{1.2.21}
$$

These derivatives $\vec{E}^{(n)}$ and $\vec{B}^{(n)}$ of the electric and magnetic fields are calculated from the vector fields $\vec{E}(X,Y,Z)$, $\vec{B}(X,Y,Z)$ and their derivatives $\dfrac{\partial^{i+j+k}\vec{E}}{\partial X^i \partial Y^j \partial Z^k}$ and $\dfrac{\partial^{i+j+k}\vec{B}}{\partial X^i \partial Y^j \partial Z^k}$, following eqs. (1.2.8) and (1.2.13).

1.2.4 Calculation of the time of flight

The time of flight eq. (1.2.6) involves the derivatives $dT/ds = 1/v$, $d^2T/ds^2 = d(1/v)/ds$, etc. that are obtained from eq. (1.2.18). In the absence of electric field eq. (1.2.7) however redues to the simple form

$$
T(M_1) = T(M_0) + \Delta s/v \tag{1.2.22}
$$

1.3 Calculation of $\vec{B}$ and its Derivatives

$\vec{B}(X,Y,Z)$ and derivatives are calculated in various ways, depending whether field maps or analytic representations of optical elements are used. The five basic means are the following.

1.3.1 Extrapolation from 1-D axial field map [5]

A cylindrically symmetric field (e.g., using *BREVOL*) can be described by an axial 1-D field map of its longitudinal component $B_X(X, r=0)$ ($r = (Y^2+Z^2)^{1/2}$), while the radial component on axis $B_r(X, r=0)$ is assumed to be zero. $B_X(X, r=0)$ is obtained at any point along the X-axis by a polynomial interpolation from the map mesh (see section 1.4.1). Then the field components $B_X(X,r)$, $B_r(X,r)$ at the position of the particle, (X,r) are obtained from Taylor expansions truncated at the fifth order in r (hence, up to the fifth order derivative $\dfrac{\partial^5 B_X}{\partial X^5}(X,0)$), assuming cylindrical symmetry

$$\begin{aligned} B_X(X,r) &= B_X(X,0) - \frac{r^2}{4}\frac{\partial^2 B_X}{\partial X^2}(X,0) + \frac{r^4}{64}\frac{\partial^4 B_X}{\partial X^4}(X,0) \\ B_r(X,r) &= -\frac{r}{2}\frac{\partial B_X}{\partial X}(X,0) + \frac{r^3}{16}\frac{\partial^3 B_X}{\partial X^3}(X,0) - \frac{r^5}{384}\frac{\partial^5 B_X}{\partial X^5}(X,0) \end{aligned} \tag{1.3.1}$$

By differentiation with respect to X and r, up to the second order, these expressions provide the derivatives of $\vec{B}(X,r)$. Finally a conversion from the (X,r) coordinates to the (X,Y,Z) Cartesian coordinates of **zgoubi** is performed, thus providing the expressions $\frac{\partial^{i+j+k}\vec{B}}{\partial X^i \partial Y^j \partial Z^k}$ needed in the eq. (1.2.8).

1.3.2 Extrapolation from Median Plane Fields

In the median plane, $B_Z(X,Y,0)$, and its derivatives with respect to X or Y, may be calculated from analytical models (e.g. in Venus magnet - *VENUS*, and sharp edge multipoles *SEXQUAD* and *QUADISEX*) or numerically by polynomial interpolation from 2-D field maps (e.g. *CARTEMES, TOSCA*).

Median plane antisymmetry is assumed, which results in

$$\begin{aligned} B_X(X,Y,0) &= 0 \\ B_Y(X,Y,0) &= 0 \\ B_X(X,Y,Z) &= -B_X(X,Y,-Z) \\ B_Y(X,Y,Z) &= -B_Y(X,Y,-Z) \\ B_Z(X,Y,Z) &= B_Z(X,Y,-Z) \end{aligned} \tag{1.3.2}$$

Accomodated with Maxwell's equations, this results in Taylor expansions below, for the three components of $\vec{B}$ (here, B stands for $B_Z(X,Y,0)$)

$$\begin{aligned} B_X(X,Y,Z) &= Z\frac{\partial B}{\partial X} - \frac{Z^3}{6}\left(\frac{\partial^3 B}{\partial X^3} + \frac{\partial^3 B}{\partial X \partial Y^2}\right) \\ B_Y(X,Y,Z) &= Z\frac{\partial B}{\partial Y} - \frac{Z^3}{6}\left(\frac{\partial^3 B}{\partial X^2 \partial Y} + \frac{\partial^3 B}{\partial Y^3}\right) \\ B_Z(X,Y,Z) &= B - \frac{Z^2}{2}\left(\frac{\partial^2 B}{\partial X^2} + \frac{\partial^2 B}{\partial Y^2}\right) + \frac{Z^4}{24}\left(\frac{\partial^4 B}{\partial X^4} + 2\frac{\partial^4 B}{\partial X^2 \partial Y^2} + \frac{\partial^4 B}{\partial Y^4}\right) \end{aligned} \tag{1.3.3}$$

which are then differentiated one by one with respect to X, Y, or Z, up to second or fourth order (depending on optical element or *IORDRE* option, see section 1.4.2) so as to get the expressions involved in eq. (1.2.8).

1.3.3 Extrapolation from arbitrary 2-D Field Maps

2-D field maps that give the three components $B_X(X,Y,Z_0)$, $B_Y(X,Y,Z_0)$ and $B_Z(X,Y,Z_0)$ at each node (X,Y) of a Z_0 Z-elevation map may be used. $\vec{B}$ and its derivatives at any point (X,Y,Z) are calculated by polynomial interpolation followed by Taylor expansions in Z, without any hypothesis of symmetries (see section 1.4.3 and keywords *MAP2D*, *MAP2D-E*).

1.3.4 Interpolation in 3-D Field Maps [6]

In 3-D field maps $\vec{B}$ and its derivatives up to the second order with respect to X, Y, or Z are calculated by means of a second order polynomial interpolation, from 3-D $3 \times 3 \times$ 3-point grid (see section 1.4.4).

1.3.5 3-D Analytical Models of Fields

In analytical optical elements (such as *QUADRUPO, MULTIPOL, SEXTUPOL, EBMULT*, etc.) the three components of $\vec{B}$ and their derivatives with respect to X, Y or Z are obtained at any step along trajectories from analytical expression drawn from the scalar potential $V(X,Y,Z)$ following

$$B_X = \frac{\partial V}{\partial X}, \quad B_Y = \frac{\partial V}{\partial Y}, \quad B_Z = \frac{\partial V}{\partial Z}, \quad \frac{\partial B_X}{\partial X} = \frac{\partial^2 V}{\partial X^2}, \quad \frac{\partial B_X}{\partial Y} = \frac{\partial^2 V}{\partial X \partial Y}, \quad \text{etc.} \tag{1.3.4}$$

Multipoles

The scalar potential used for the calculation of $\frac{\partial^{i+j+k} \vec{B}_n(X,Y,Z)}{\partial X^i \partial Y^i \partial Z^k}$ ($i+j+k = 0$ to 4) in the case of magnetic and electro-magnetic multipoles with $2n$ poles (namely, *QUADRUPO* ($n = 2$) to *DODECAPO* ($n = 6$), *MULTIPOL* ($n = 1$ to 10), *EBMULT* ($n = 1$ to 10)) is [7]

$$V_n(X,Y,Z) = (n!)^2 \left(\sum_{q=0}^{\infty} (-1)^q \frac{G^{(2q)}(X)(Y^2+Z^2)^q}{4^q q!(n+q)!} \right) \left(\sum_{m=0}^{n} \frac{sin\left(m\frac{\pi}{2}\right) Y^{n-m} Z^m}{m!(n-m)!} \right) \tag{1.3.5}$$

where $G(X)$ is the longitudinal gradient, defined at the entrance or exit of the optical element by

$$G(s) = \frac{G_0}{1+\exp(P(s))}, \quad G_0 = \frac{B_0}{R_0^n} \tag{1.3.6}$$

and s is the distance to the EFB.

Skewed multipoles

A multipole component with arbitrary order n can be tilted independently of the others by an arbitrary angle A_n around the X-axis. If so, the calculation of the field and derivatives in the rotated axis (X, Y_R, Z_R) is done in two steps. First, they are calculated at the rotated position (X, Y_R, Z_R), in the (X, Y, Z) frame, as derived from expression (1.3.5) above. Second, $\vec{B}$ and its derivatives at (X, Y_R, Z_R) in the (X, Y, Z) frame are transformed to the rotated (X, Y_R, Z_R) frame by a rotation of the same angle A_n.

In particular a skewed $2n$-pole component is created by taking $A_n = \pi/2n$.

1.4 Calculation of $\vec{B}$ from Field Maps

1.4.1 1-D Axial Map, with Cylindrical Symmetry

Let B_i be the value of the longitudinal component $B_X(X, r = 0)$ of the field $\vec{B}$, at node i of a uniform mesh that defines a 1-D field map along the symmetry X-axis, while $B_r(X, r = 0)$ is assumed to be zero ($r = (Y^2+Z^2)^{1/2}$). The field component $B_X(X, r = 0)$ is calculated by a polynomial interpolation of the fifth degree in X, using a 5 points grid centered at the node of the 1-D map which is closest to the actual coordinate X of the particle. The interpolation polynomial is

$$B(X,0) = A_0 + A_1 X + A_2 X^2 + A_3 X^3 + A_4 X^4 + A_5 X^5 \tag{1.4.1}$$

and the coefficients A_i are calculated by expressions that minimize the quadratic sum

$$S = \sum_i \left(B(X,0) - B_i \right)^2 \tag{1.4.2}$$

Namely, the source code contains the explicit analytical expressions of the coefficients A_i solutions of the normal equations $\partial S/\partial A_i = 0$.

The derivatives $\frac{\partial^n B}{\partial X^n}(X,0)$ at the actual position X, as involved in eqs. (1.3.1), are then obtained by differentiation of the polynomial (1.4.1), giving

$$\begin{aligned}
\frac{\partial B}{\partial X}(X,0) &= A_1 + 2A_2X + 3A_3X^2 + 4A_4X^3 + 5A_5X^4 \\
\frac{\partial^2 B}{\partial X^2}(X,0) &= 2A_2 + 6A_3X + 12A_4X^2 + 20A_5X^3 \\
&\cdots \\
\frac{\partial^5 B}{\partial X^5}(X,0) &= 120A_5
\end{aligned} \tag{1.4.3}$$

1.4.2 2-D Median Plane Map, with Median Plane Antisymmetry

Let B_{ij} be the value of $B_Z(X,Y,0)$ at the nodes of a mesh which defines a 2-D field map in the (X,Y) plane while $B_X(X,Y,0)$ and $B_Y(X,Y,0)$ are assumed to be zero. Such a map may have been built or measured in either Cartesian or polar coordinates. Whenever polar coordinates are used, a change to Cartesian coordinates (described below) provides the expression of $\vec{B}$ and its derivatives as involved in eq. (1.2.8).

zgoubi provides three types of polynomial interpolation from the mesh (option *IORDRE*); namely, a second order interpolation, with either a 9- or a 25-point grid, or a fourth order interpolation with a 25-point grid (Fig. 3).

If the 2-D field map is built up from simulation, the grid simply aims at interpolating the field at a given point from its 9 or 25 neighbors. If the map results from measurements, the grid also smoothes field measurement fluctuations.

The mesh may be defined in Cartesian coordinates, (Figs. 3A and 3B) or in polar coordinates (Fig. 3C).

The interpolation grid is centered on the node which is closest to the projection in the (X,Y) plane of the actual point of the trajectory.

The interpolation polynomial is

$$B(X,Y,0) = A_{00} + A_{10}X + A_{01}Y + A_{20}X^2 + A_{11}XY + A_{02}Y^2 \tag{1.4.4}$$

in second order, or

$$\begin{aligned}
B(X,Y,0) =& A_{00} + A_{10}X + A_{01}Y + A_{20}X^2 + A_{11}XY + A_{02}Y^2 \\
&+ A_{30}X^3 + A_{21}X^2Y + A_{12}XY^2 + A_{03}Y^3 \\
&+ A_{40}X^4 + A_{31}X^3Y + A_{22}X^2Y^2 + A_{13}XY^3 + A_{04}Y^4
\end{aligned} \tag{1.4.5}$$

in fourth order. The coefficients A_{ij} are calculated by expressions that minimize, with respect to A_{ij}, the quadratic sum

$$S = \sum_{ij} (B(X,Y,0) - B_{ij})^2 \tag{1.4.6}$$

The source code contains the explicit analytical expressions of the coefficients A_{ij} solutions of the normal equations $\partial S/\partial A_{ij} = 0$.

The A_{ij} may then be identified with the derivatives of $B(X,Y,0)$ at the central node of the grid

$$A_{ij} = \frac{1}{i!j!} \frac{\partial^{i+j} B}{\partial X^i \partial Y^j}(0,0,0) \tag{1.4.7}$$

The derivatives of $B(X,Y,0)$ with respect to X and Y, at the actual point $(X,Y,0)$ are obtained by differentiation of the interpolation polynomial, which gives (e.g. from (1.4.4) in the case of second order interpolation)

$$\begin{aligned}\frac{\partial B}{\partial X}(X,Y,0) &= A_{10} + 2A_{20}X + A_{11}Y \\ \frac{\partial B}{\partial Y}(X,Y,0) &= A_{01} + A_{11}X + 2A_{02}Y \\ &\text{etc.}\end{aligned} \tag{1.4.8}$$

This allows stepping to the calculation of $\vec{B}(X,Y,Z)$ and its derivatives as described in subsection 1.3.2 (eq. 1.3.3).

The special case of polar maps

It is necessary to change from polar map frame (R,α,Z) to the Cartesian moving frame (X,Y,Z). This is done as follows.
In second order calculations the correspondence is (we note $B \equiv B_Z(Z=0)$)

$$\begin{aligned}
\frac{\partial B}{\partial X} &= \frac{1}{R}\frac{\partial B}{\partial \alpha} \\
\frac{\partial B}{\partial Y} &= \frac{\partial B}{\partial R} \\
\frac{\partial^2 B}{\partial X^2} &= \frac{1}{R^2}\frac{\partial^2 B}{\partial \alpha^2} + \frac{1}{R}\frac{\partial B}{\partial R} \\
\frac{\partial^2 B}{\partial X \partial Y} &= \frac{1}{R}\frac{\partial^2 B}{\partial \alpha \partial R} - \frac{1}{R^2}\frac{\partial B}{\partial \alpha} \\
\frac{\partial^2 B}{\partial Y^2} &= \frac{\partial^2 B}{\partial R^2} \\
\frac{\partial^3 B}{\partial X^3} &= \frac{3}{R^2}\frac{\partial^2 B}{\partial \alpha \partial R} - \frac{2}{R^3}\frac{\partial B}{\partial \alpha} \\
\frac{\partial^3 B}{\partial X^2 \partial Y} &= \frac{-2}{R^3}\frac{\partial^2 B}{\partial \alpha^2} - \frac{1}{R^2}\frac{\partial B}{\partial R} + \frac{1}{R}\frac{\partial^2 B}{\partial R^2} \\
\frac{\partial^3 B}{\partial X \partial Y^2} &= \frac{2}{R^3}\frac{\partial B}{\partial \alpha} - \frac{2}{R^2}\frac{\partial^2 B}{\partial \alpha \partial R} \\
\frac{\partial^3 B}{\partial Y^3} &= 0
\end{aligned} \tag{1.4.9}$$

In fourth order calculations the relations are the same up to second order, and then

$$\begin{aligned}
\frac{\partial^3 B}{\partial X^3} &= \frac{1}{R^3}\frac{\partial^3 B}{\partial \alpha^3} + \frac{3}{R^2}\frac{\partial^2 B}{\partial \alpha \partial R} - \frac{2}{R^3}\frac{\partial B}{\partial \alpha} \\
\frac{\partial^3 B}{\partial X^2 \partial Y} &= \frac{1}{R^2}\frac{\partial^3 B}{\partial \alpha^2 \partial R} - \frac{2}{R^3}\frac{\partial^2 B}{\partial \alpha^2} - \frac{1}{R^2}\frac{\partial B}{\partial R} + \frac{1}{R}\frac{\partial^2 B}{\partial R^2} \\
\frac{\partial^3 B}{\partial X \partial Y^2} &= \frac{1}{R}\frac{\partial^3 B}{\partial \alpha \partial R^2} + \frac{2}{R^3}\frac{\partial B}{\partial \alpha} - \frac{2}{R^2}\frac{\partial^2 B}{\partial \alpha \partial R} \\
\frac{\partial^3 B}{\partial Y^3} &= \frac{\partial^3 B}{\partial R^3} \\
\frac{\partial^4 B}{\partial X^4} &= \frac{1}{R^4}\frac{\partial^4 B}{\partial \alpha^4} - \frac{8}{R^4}\frac{\partial^2 B}{\partial \alpha^2} + \frac{6}{R^3}\frac{\partial^3 B}{\partial \alpha^2 \partial R} + \frac{3}{R^2}\frac{\partial^2 B}{\partial R^2} - \frac{3}{R^3}\frac{\partial B}{\partial R} \\
\frac{\partial^4 B}{\partial X^3 \partial Y} &= \frac{1}{R^3}\frac{\partial^4 B}{\partial \alpha^3 \partial R} - \frac{3}{R^4}\frac{\partial^3 B}{\partial \alpha^3} + \frac{3}{R^2}\frac{\partial^3 B}{\partial \alpha \partial R^2} - \frac{8}{R^3}\frac{\partial^2 B}{\partial \alpha \partial R} + \frac{6}{R^4}\frac{\partial B}{\partial \alpha} \\
\frac{\partial^4 B}{\partial X^2 2Y^2} &= \frac{1}{R^4}\frac{\partial^2 B}{\partial \alpha^2} - \frac{4}{R^3}\frac{\partial^3 B}{\partial \alpha^2 \partial R} - \frac{2}{R^2}\frac{\partial^2 B}{\partial R^2} + \frac{2}{R^3}\frac{\partial B}{\partial R} + \frac{1}{R^2}\frac{\partial^4 B}{\partial \alpha^2 \partial R^2} + \frac{1}{R}\frac{\partial^3 B}{\partial R^3} \\
\frac{\partial^4 B}{\partial X \partial Y^3} &= \frac{1}{R}\frac{\partial^4 B}{\partial \alpha \partial R^3} - \frac{3}{R^2}\frac{\partial^3 B}{\partial \alpha \partial R^2} + \frac{6}{R^3}\frac{\partial^2 B}{\partial \alpha \partial R} - \frac{6}{R^4}\frac{\partial^4 B}{\partial \alpha^4} \\
\frac{\partial^4 B}{\partial Y^4} &= \frac{\partial^4 B}{\partial R^4}
\end{aligned} \tag{1.4.10}$$

NOTE: If a particle goes beyond the limits of the field map, the field and its derivatives will be extrapolated by means of the same calculations, from the border grid which is the closest to the actual position of the particle. Its flag *IEX* is given the value -1 (see section 4.6.8).

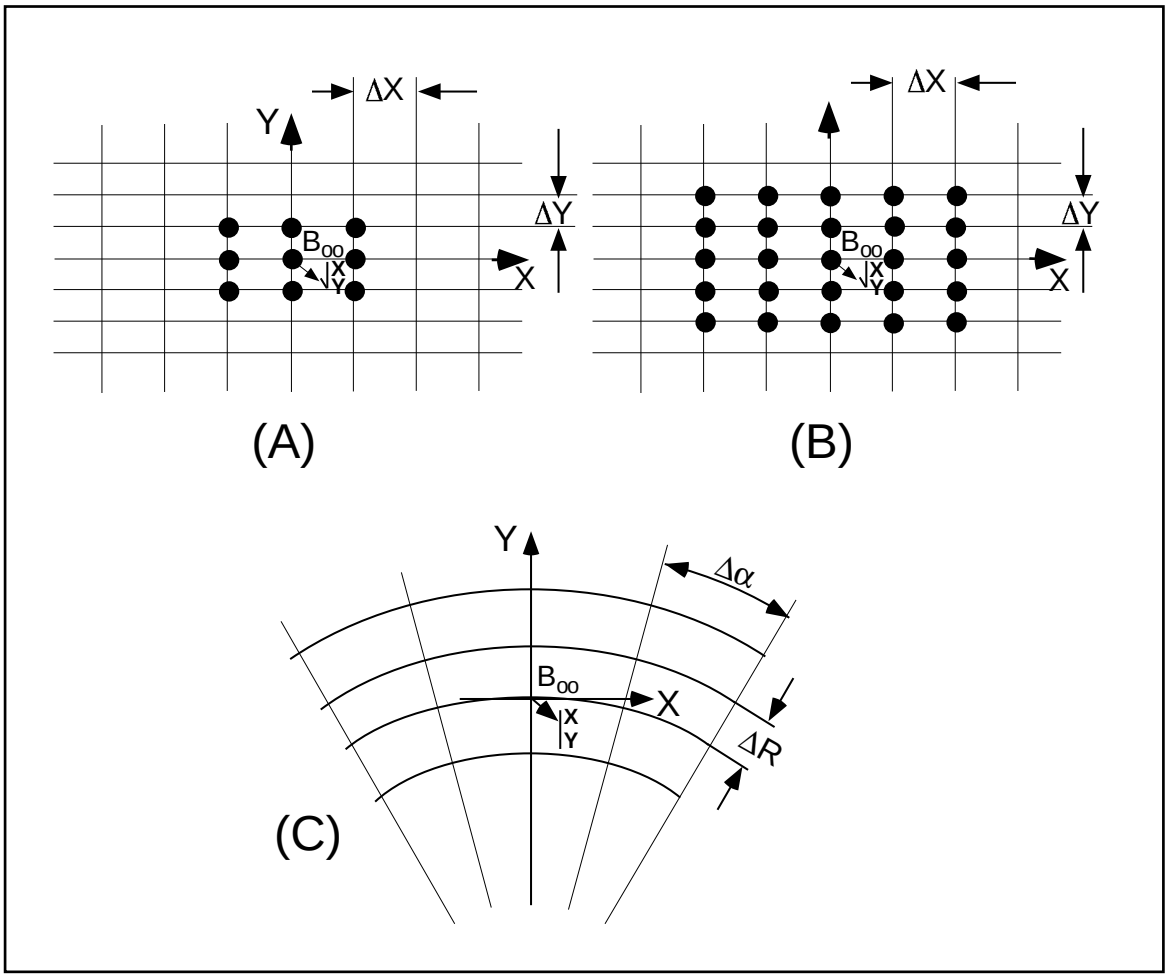

Figure 3: Mesh in the (X, Y) plane in Cartesian coordinates. The grid is centered
on the node which is closest to the actual position of the particle.
A: 9-point interpolation grid.
B: 25-point interpolation grid.
C: Mesh in the (X, Y) plane in polar coordinates.

1.4.3 Arbitrary 2-D Map, no Symmetry

The map is supposed to describe the field $\vec{B}(B_X, B_Y, B_Z)$ in the (X, Y) plane at elevation Z_0. It provides the components $B_{X,ij}$, $B_{Y,ij}$, $B_{Z,ij}$ at each node (i, j) of a 2-D mesh.
The value of $\vec{B}$ and its derivatives at the projection (X, Y, Z_0) of the actual position (X, Y, Z) of a particle is obtained by means of a polynomial interpolation from a 3×3 points grid centered at the node (i, j) which is closest to the position (X, Y)

$$B_\ell(X, Y, Z_0) = A_{00} + A_{10}X + A_{01}Y + A_{20}X^2 + A_{11}XY + A_{02}Y^2 \tag{1.4.11}$$

where B_ℓ stands for any of the three components B_X, B_Y or B_Z. Differentiating then gives the derivatives

$$\begin{aligned} \frac{\partial B_\ell}{\partial X}(X,Y,Z_0) &= A_{10} + 2A_{20}X + A_{11}Y \\ \frac{\partial^2 B_\ell}{\partial X \partial Y}(X,Y,Z_0) &= A_{11} \\ &\text{etc.} \end{aligned} \tag{1.4.12}$$

Then follows the procedure of extrapolation from (X, Y, Z_0) to the actual position (X, Y, Z).

No special symmetry is assumed, which allows the treatment of arbitrary field distribution.

Fourth order polynomial interpolation is available upon request (parameter *IORDRE* in keyword data list - see *MAP2D, MAP2D-E*), using the method above based on eq. (1.4.11 developped up to fourth order in X and Y.

1.4.4 Calculation of $\vec{B}$ from 3-D Field Map

The vector field $\vec{B}(X, Y, Z)$ and its derivatives necessary for the calculation of position and velocity of the particle are now defined by means of a 3-D field map, through second order polynomial interpolation

$$B_\ell(X,Y,Z) = A_{000} + A_{100}X + A_{010}Y + A_{001}Z + A_{200}X^2 + A_{020}Y^2 + A_{002}Z^2 + A_{110}XY + A_{101}XZ + A_{011}YZ \tag{1.4.13}$$

B_ℓ stands for any of the three components, B_X, B_Y or B_Z. By differentiation of B_ℓ one gets

$$\begin{aligned} \frac{\partial B_\ell}{\partial X} &= A_{100} + 2A_{200}X + A_{110}Y + A_{101}Z \\ \frac{\partial^2 B_\ell}{\partial X^2} &= 2A_{200} \end{aligned} \tag{1.4.14}$$

and so on for first and second order derivatives with respect to X, Y or Z.

The interpolation involves a $3 \times 3 \times 3$-point parallelipipedic grid (Fig. 4), the origin of which is positioned at the node of the 3-D field map which is closest to the actual position of the particle.

Let B^ℓ_{ijk} be the value of the — measured or computed — magnetic field at each one of the 27 nodes of the 3-D grid (B^ℓ stands for B_X, B_Y or B_Z), and $B_\ell(X, Y, Z)$ be the value at a position (X, Y, Z) with respect to the central node of the 3-D grid. Thus, any coefficient A_i of the polynomial expansion of B_ℓ is obtained by means of expressions that minimize, with respect to A_i, the sum

$$S = \sum_{ijk} \left(B_\ell(X,Y,Z) - B^\ell_{ijk} \right)^2 \tag{1.4.15}$$

where the indices i, j and k take the values -1, 0 or +1 so as to sweep the 3-D grid. The source code contains the explicit analytical expressions of the coefficients A_{ijk} solutions of the normal equations $\partial S / \partial A_{ijk} = 0$.

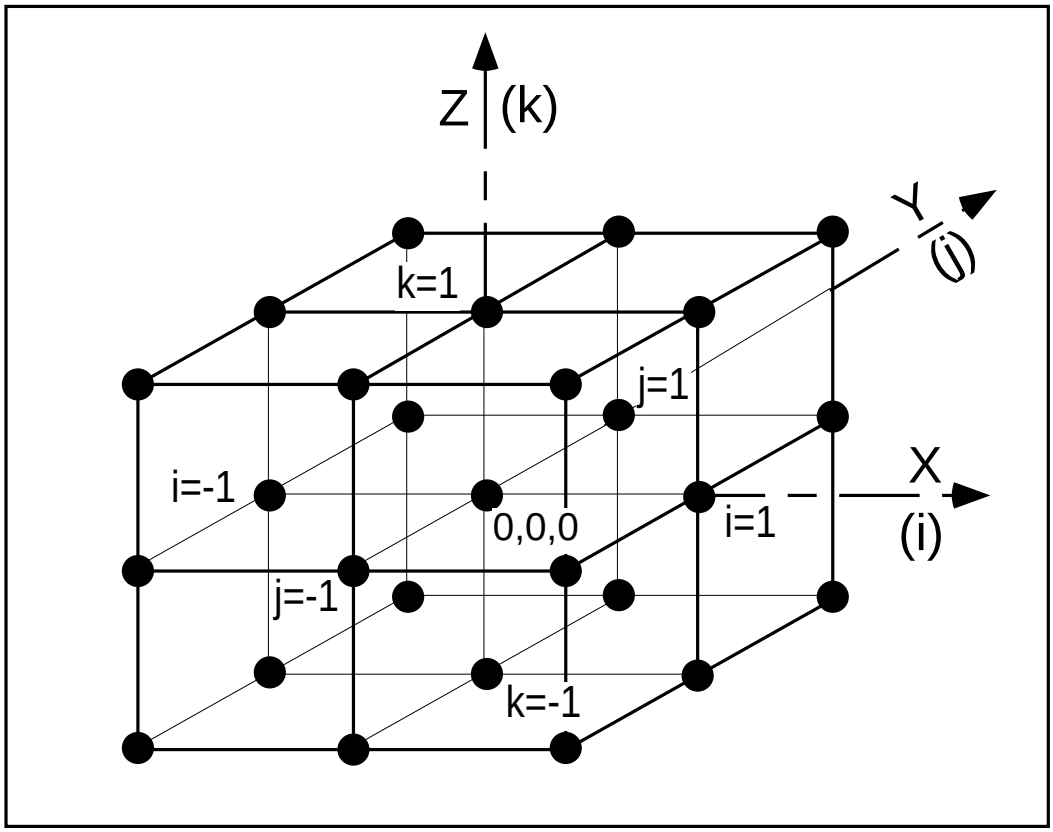

Figure 4: A 3-D 27-point grid is used for interpolation of $\vec{B}$ and its derivatives up to second order. The central node of the grid ($i = j = k = 0$) is at the closest vicinity of the actual position of the particle.

1.5 Calculation of $\vec{E}$ and its derivatives

zgoubi calculates $\vec{E}(X, Y, Z)$ and its derivatives in various ways, depending whether field maps or analytical representations of optical elements are used. The three basic means are the following [4].

1.5.1 Extrapolation from 1-D axial field map

A cylindrically symmetric field can be described by an axial 1-D field map of its longitudinal component $E_X(X, r = 0)$ ($r = (Y^2 + Z^2)^{1/2}$), while the radial component $E_r(X, r = 0)$ is assumed to be zero (e.g. in *ELREVOL*). $E_X(X, r = 0)$ is obtained at any point along the X-axis by a polynomial interpolation from the map mesh (see section 1.4.1). Then the field components $E_X(X, r)$, $E_r(X, r)$ at the position of the particle, (X, r) are obtained from Taylor expansions to the fifth order in r (hence, up to the fifth order derivative $\frac{\partial^5 E_X}{\partial X^5}(X, 0)$), assuming cylindrical symmetry

$$\begin{aligned} E_X(X,r) &= E_X(X,0) - \frac{r^2}{4}\frac{\partial^2 E_X}{\partial X^2}(X,0) + \frac{r^4}{64}\frac{\partial^4 E_X}{\partial X^4}(X,0) \\ E_r(X,r) &= -\frac{r}{2}\frac{\partial E_X}{\partial X}(X,0) + \frac{r^3}{16}\frac{\partial^3 E_X}{\partial X^3}(X,0) - \frac{r^5}{384}\frac{\partial^5 E_X}{\partial X^5}(X,0) \end{aligned} \tag{1.5.1}$$

By differentiation with respect to X and r, up to the second order, these expressions provide the derivatives of $\vec{E}(X,r)$. Finally a conversion from the (X,r) coordinates to the (X,Y,Z) Cartesian coordinates of **zgoubi** is performed, thus providing the expressions $\dfrac{\partial^{i+j+k}\vec{E}}{\partial X^i \partial Y^j \partial Z^k}$ needed in the eqs. (1.2.13).

1.5.2 Extrapolation from analytically defined axial fields

This procedure assumes cylindrical symmetry with respect to the X-axis. The longitudinal field component $E_X(X,r=0)$ ($r=(Y^2+Z^2)^{1/2}$), along this axis are derived from differentiation of an adequate model of the electrostatic potential $V(X)$ (e.g. in *EL2TUB, UNIPOT*). The longitudinal and radial field components $E_X(X,r)$, $E_r(X,r)$ and their derivatives off-axis $\dfrac{\partial^{i+j}E_X}{\partial X^i \partial r^j}$ and $\dfrac{\partial^{i+j}E_r}{\partial X^i \partial r^j}$ are obtained by Taylor expansions to the fifth order in r assuming cylindrical symmetry (see eq. (1.5.1)), and then transformed to the (X,Y,Z) Cartesian frame of **zgoubi** in order to provide the derivatives $\dfrac{\partial^{i+j+k}\vec{E}}{\partial X^i \partial Y^j \partial Z^k}$ needed in eq. (1.2.13).

1.5.3 3-D Analytical models of fields

In analytical elements (e.g. *WIENFILT, ELMULT, EBMULT*), the three components of $\vec{E}$, namely E_X, E_Y, E_Z, and their derivatives with respect to X, Y or Z are obtained at any step along trajectories, from analytical expressions drawn from models of the potential $V(X,Y,Z)$.

Multipoles and skewed multipoles

A right electric multipole is considered to have the same effect as the equivalent skewed magnetic multipole. Therefore, calculation of the right electric or electro-magnetic multipoles (*ELMULT, EBMULT*) uses the same eq. (1.3.5) together with the rotation process as described in section 1.3.5. The same method is used, for arbitrary rotation of arbitrary multipole component around the X-axis.

1.6 Calculation of $\vec{E}$ from field maps

1-D axial map, with cylindrical symmetry

The only type of field map treated in the actual version is the 1-D axial map, with cylindrical symmetry. The same procedure as for the case of magnetic fields is involved (see section 1.4.1).

2 SPIN TRACKING [8]

The depolarization of a particle beam travelling in a magnetic field $\vec{b}$ takes its origin in the spin precession undergone by each particle. This motion of the spin $\vec{S}$ is governed by the Thomas-BMT first order differential equation [9]

$$\frac{d\vec{S}}{dt} = \frac{q}{m}\,\vec{S} \times \vec{\Omega} \tag{2.1}$$

where

$$\vec{\Omega} = (1+\gamma G)\vec{b} + G(1-\gamma)\vec{b}_{/\!/} \tag{2.2}$$

q, m, γ and G are respectively the charge, mass, Lorentz relativistic factor, and anomalous magnetic moment of the particle. $\vec{b}_{/\!/}$ is the component of $\vec{b}$ which is parallel to the velocity $\vec{v}$ of the particle.
These equations are normalized by introducing the same notation as previously. Let $b = \| \vec{b} \|$ and $v = \| \vec{v} \|$; $ds = vdt$ is the differential path, $\frac{\gamma m v}{q} = B\rho$ is the rigidity of the particle; $\vec{S}\,' = \frac{d\vec{S}}{ds} = \frac{1}{v}\frac{d\vec{S}}{dt}$ is the derivative of the spin with respect to the path.
Introducing also $\vec{B} = \frac{\vec{b}}{B\rho}$, $\vec{B}_{/\!/} = \frac{\vec{b}_{/\!/}}{B\rho}$ and

$$\vec{\omega} = \frac{\vec{\Omega}}{B\rho} = (1+\gamma G)\vec{B} + G(1-\gamma)\vec{B}_{/\!/} \tag{2.3}$$

eq. (2.1) can be re-written in a normalized way

$$\vec{S}\,' = \vec{S} \times \vec{\omega} \tag{2.4}$$

This equation is then solved in the same way as the reduced Lorentz equation (1.2.3). From the values of the magnetic factor $\vec{\omega}(M_0)$ and the spin $\vec{S}(M_0)$ of the particle at position M_0 of its trajectory, the spin $\vec{S}(M_1)$ at position M_1, following a displacement Δs (fig. 2), is obtained from truncated Taylor expansion

$$\vec{S}(M_1) \approx \vec{S}(M_0) + \frac{d\vec{S}}{ds}(M_0)\,\Delta s + \frac{d^2\vec{S}}{ds^2}(M_0)\frac{\Delta s^2}{2} + \frac{d^3\vec{S}}{ds^3}(M_0)\frac{\Delta s^3}{3!} + \frac{d^4\vec{S}}{ds^4}(M_0)\frac{\Delta s^4}{4!} \tag{2.5}$$

The derivatives $\vec{S}^{(n)} = \frac{d^n\vec{S}}{ds^n}$ of $\vec{S}$ at M_0 are obtained by differentiating eq. (2.4)

$$\begin{aligned}
\vec{S}\,' &= \vec{S} \times \vec{\omega} \\
\vec{S}\,'' &= \vec{S}\,' \times \vec{\omega} + \vec{S} \times \vec{\omega}\,' \\
\vec{S}\,''' &= \vec{S}\,'' \times \vec{\omega} + 2\vec{S}\,' \times \vec{\omega}\,' + \vec{S} \times \vec{\omega}\,'' \\
\vec{S}\,'''' &= \vec{S}\,''' \times \vec{\omega} + 3\vec{S}\,'' \times \vec{\omega}\,' + 3\vec{S}\,' \times \vec{\omega}\,'' + \vec{S} \times \vec{\omega}\,'''
\end{aligned} \tag{2.6}$$

where the derivatives $\vec{\omega}^{(n)}$ are obtained from eq. (2.3).
The last point consists in getting $\vec{B}_{/\!/}$ and its derivatives. This can be done in the following way. Let $\vec{u} = \frac{\vec{v}}{v}$ be the normalized velocity of the particle, then,

$$\begin{aligned}
\vec{B}_{/\!/} &= (\vec{B}\cdot\vec{u})\,\vec{u} \\
\vec{B}'_{/\!/} &= (\vec{B}\,'\cdot\vec{u} + \vec{B}\cdot\vec{u}\,')\,\vec{u} + (\vec{B}\cdot\vec{u})\,\vec{u}\,' \\
\vec{B}''_{/\!/} &= (\vec{B}\,''\cdot\vec{u} + 2\vec{B}\,'\cdot\vec{u}\,' + \vec{B}\cdot\vec{u}\,'')\,\vec{u} + 2(\vec{B}\,'\cdot\vec{u} + \vec{B}\cdot\vec{u}\,')\,\vec{u}\,' + (\vec{B}\cdot\vec{u})\,\vec{u}\,'' \\
&\text{etc.}
\end{aligned} \tag{2.7}$$

The quantities $\vec{u}$, $\vec{B}$ and their n-th derivatives as involved in these equations are picked up from eqs. (1.2.7, 1.2.8).

3 SYNCHROTRON RADIATION

zgoubi allows the simulation of two types of synchrotron radiation (SR) related effects namely, on the one hand energy loss by stochastic emission of photon and the ensuing perturbation on particle dynamics and, on the other hand calculation of the radiated spectral-angular energy densities as observed in the lab.

3.1 Energy loss and related dynamical effects [10]

Given a particle wandering in the magnetic field of an arbitrary optical element or field map, **zgoubi** computes the energy loss undergone, and its effect on the particle motion. The energy loss is calculated in a classical manner, by calling upon two random processes that accompany the emission of a photon namely,

- the probability of emission,
- the energy of the photon.

The effects on the dynamic of the emitting particle is either limited to the alteration of the energy, or extended to angular kick effect, following user requested working options ; particle position is supposed not to change upon emission of a photon. These calculations and ensuing dynamics corrections are performed after each integration step. In a practical manner, this means every centimer or tens of centimers in smoothly varying magnetic fields.

Main aspects of the method are developped in the following.

Probability of emission of a photon

Given that the number of photons emitted within a step Δs can be very low (units or fractions of unit)[1] a Poisson probability law

$$p(k) = \frac{\lambda^{-k}}{k!} exp(-k) \tag{3.1.1}$$

is considered. k is the number of photons emitted over a $\Delta\theta$ (circular) arc of trajectory such that, the mean number of photons per radian expresses as[2]

$$\lambda = \frac{20 e r_0}{8\bar{h}\sqrt{3}} \beta^2 B\rho \Delta s \tag{3.1.2}$$

where $r_0 = e^2/4\pi\epsilon_0 m_0 c^2$ is the classical radius of the particle of rest-mass m_0, e is the elementary charge, $\bar{h} = h/2\pi$, h is the Planck constant, $\beta = v/c$, $B\rho$ is the particle stiffness. λ is evaluated at each integration step from the current values β, $B\rho$ and Δs, then a value of k is drawn by a rejection method [34, routine POIDEV].

Energy of the photons

These k photons are assigned energies $\epsilon = h\nu$ at random, in the following way. The cumulative distribution of the energy probability law $p(\epsilon/\epsilon_c)d\epsilon/\epsilon_c$ writes

$$\mathcal{P}(\epsilon/\epsilon_c) = \frac{3}{5\pi} \int_0^{\epsilon/\epsilon_c} \int_{\epsilon/\epsilon_c}^{\infty} K_{5/3}(x) dx \tag{3.1.3}$$

where $K_5/3$ is a modified Bessel function and, $\epsilon_c = \bar{h}\omega_c$ with $\omega_c = 2\pi 3\gamma^3 c/2\rho$ being the critical frequency of the radiation in constant field with bending radius ρ ; ω_c is evaluated at each integration step from the current values γ and ρ, in other words, this energy loss calculation assumes constant magnetic field [3] over the trajectory arc Δs. In the low frequency region ($\epsilon/\epsilon_c \ll 1$) it can be approximated by

$$\mathcal{P}(\epsilon/\epsilon_c) = \frac{12\sqrt{3}}{5\, 2^{1/3}\Gamma(\frac{1}{3})} (\frac{\epsilon}{\epsilon_c})^{1/3} \tag{3.1.4}$$

[1] For instance, a 1 GeV electron will emit about 20.6 photons per radian; an integration step size $\Delta s = 0.1$ m upon $\rho = 10$ m bending radius results in 0.2 photons per step.

[2] This leads for instance, in the case of electrons, to the classical formula $\lambda/\Delta\theta \approx 129.5\text{E(GeV)}/2\pi \approx \gamma/94.9$.

[3] From a practical viewpoint, note that the value of the magnetic field first computed for a one-step push of the particle (eqs. 1.2.4,1.2.7) is next used to obtain ρ and perform SR loss corrections afterwards.

About 40 values of $\mathcal{P}(\epsilon/\epsilon_c)$ computed from eq. 3.1.3 [35], honnestly spread over a range $\epsilon/\epsilon_c \leq 10$ are tabulated in **zgoubi** source file (see figure). In order to get ϵ/ϵ_c, first a random value $0 < \mathcal{P} < 1$ is generated uniformly, then ϵ/ϵ_c is drawn either by simple inverse linear interpolation of the tabulated values if $\mathcal{P} > 0.26$ (corresponding to $\epsilon/\epsilon_c > 10^{-2}$), or, if $\mathcal{P} < 0.26$ from eq. 3.1.4 that directly gives $\epsilon/\epsilon_c = \left(\frac{5\,2^{1/3}\Gamma(\frac{1}{3})}{12\sqrt{3}\mathcal{P}}\right)^3$ with precision no less than 1% at $\mathcal{P} \to 0.26$.

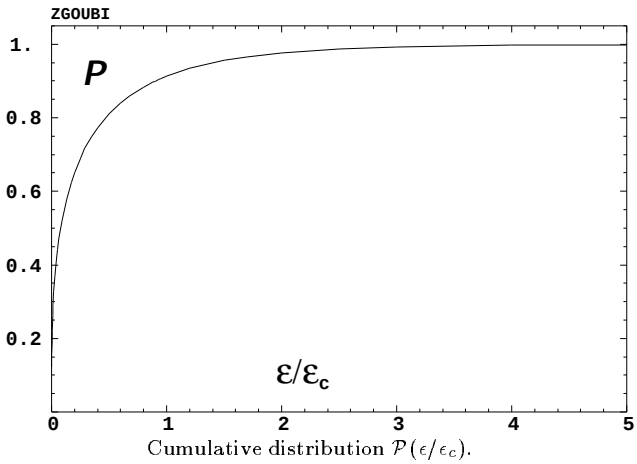

Cumulative distribution $\mathcal{P}(\epsilon/\epsilon_c)$.

Upon request of SR loss tracking, several optical elements that contain dipole magnetic field component (e.g., *MULTIPOL*) provide a printouot of various quantities related to SR emission, as drawn from classical theoretical expressions, such as for instance,
- energy loss per particle $\Delta E(eV) = \frac{2}{3} r_0 c \gamma^3 B(T) \Delta\theta$, ($B$ is the dipole field, exclusive of any other multipole component or non-linearity in the magnet; $\Delta\theta$ is the total deviation as calculated from B, the magnet length, and the reference rigidity *BORO*(as defined with, e.g., *OBJET*)
- energy $\epsilon_c(eV) = \frac{3\gamma^3 c}{2\rho}\frac{\hbar}{e}$, with $\rho = BORO/B$
- energy of radiated photons $< \epsilon >= \frac{8}{15\sqrt{3}}\epsilon_c$,
- r.m.s. energy of radiated photons $\epsilon_{rms} = 0.5591\epsilon_c$,
- number of radiated photons per particle $N = \Delta E / < \epsilon >$.

This is done in order to facilitate verifications, since on the other hand statistics regarding those values are drawn from the tracking and printed upon use of the dedicated keyword *SYNPRNL*.

Finally, upon user's request as well, SR loss can be limited to particular classes of optical elements, for instance dipole fields alone, or dipole + quadrupole magnets, etc. These tricks are made available in order to permit deeper insight, or easier comparison with other codes, for instance.

3.2 Spectral-angular radiated densities [11]

The ray-tracing procedures provide the ingredients necessary for the determination of the electric field radiated by the particle subject to acceleration, as shown in Fig. 5 (section 3.2.1). This allows calculation[4] of spectral-angular densities radiated by particles in magnetic fields (section 3.2.2).

3.2.1 Calculation of the radiated electric field

The expression for the radiated electric field $\vec{\mathcal{E}}(\vec{n}, \tau)$ as seen by the observer in the long distance approximation is [12]

$$\vec{\mathcal{E}}(\vec{n}, \tau) = \frac{q}{4\pi\varepsilon_0 c} \frac{\vec{n}(t) \times \left[\left(\vec{n}(t) - \vec{\beta}(t)\right) \times d\vec{\beta}/dt\right]}{r(t)\left(1 - \vec{n}(t)\cdot\vec{\beta}(t)\right)^3} \tag{3.2.1}$$

where t is the time in which the particle motion is described and τ is the observer time. Namely, when at position $\vec{r}(t)$ with respect to the observer [or as well at position $\vec{R}(t) = \vec{X} - \vec{r}(t)$ in the (O, x, y, z) frame] the particle emits a signal which reaches the observer at time τ, such that $\tau = t + r(t)/c$ where $r(t)/c$ is the delay necessary for the signal to travel from the emission point to the observer, which also leads by differentiation to the well-known relation

[4] These procedures are for the moment implemented in the post-processor **zpop**

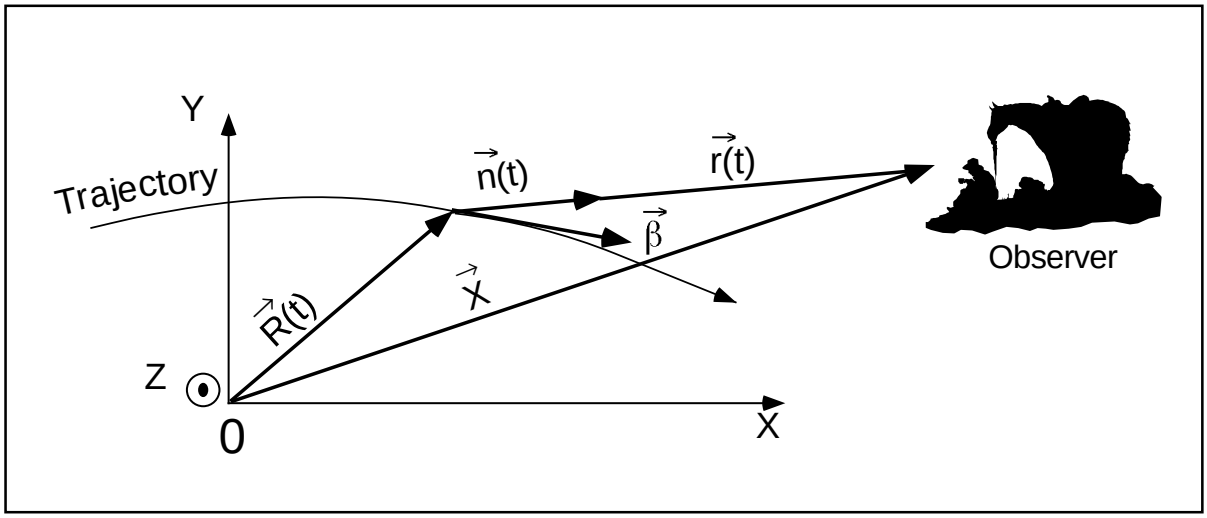

Figure 5: A scheme of the reference frame in **zgoubi** together with the vectors entering in the definition of the electric field radiated by the accelerated particle:
(x, y): horizontal plane; z: vertical axis.
$\vec{R}(t)$ = particle position in the fixed frame (O, x, y, z);
$\vec{X}$ (time-independent) = position of the observer in the (O, x, y, z) frame;
$\vec{r}(t) = \vec{X} - \vec{R}(t)$ = position of the particle with respect to the observer;
$\vec{n}(t)$ = (normalized) direction of observation = $\vec{r}(t)/|\vec{r}(t)|$;
$\vec{\beta}$ = normalized velocity vector of the particle $\vec{v}/c = (1/c)d\vec{R}/dt$.

$$d\tau/dt = 1 - \vec{n}(t) \cdot \vec{\beta}(t) \tag{3.2.2}$$

The vectors $\vec{R}(t)$ and $\vec{\beta}(t) = \frac{v}{c}\vec{u}$ (eq. 1.2.2) that describe the motion are obtained from the ray-tracing (eqs. 1.2.4). The acceleration is calculated from (eq. 1.2.1)

$$d\vec{\beta}/dt = (q/m)\ \vec{\beta}(t) \times \vec{b}(t) \tag{3.2.3}$$

Then, given the observer position $\vec{X}$ in the fixed frame, it is possible to calculate

$$\vec{r}(t) = \vec{X} - R(t) \text{ and } \vec{n}(t) = \vec{r}(t)/|\vec{r}(t)| \tag{3.2.4}$$

The calculation of $\vec{n} - \vec{\beta}$ and $1 - \vec{n} \cdot \vec{\beta}$

Owing to computer precision the crude computation of $\vec{n} - \vec{\beta}$ and $1 - \vec{n} \cdot \vec{\beta}$ may lead to

$$\vec{n} - \vec{\beta} = 0 \text{ and } 1 - \vec{n} \cdot \vec{\beta} = 0$$

since the preferred direction of observation is generally almost parallel to $\vec{\beta}$ (exactly parallel in the sense of computer precision), while $\beta \approx 1$ as soon as particle energies of a few hundred times the rest mass are concerned. It is therefore necessary to express $\vec{n} - \vec{\beta}$ and $1 - \vec{n} \cdot \vec{\beta}$ in an adequate form for achieving accurate software computation.
The expression for $\vec{n}$ is

$$\begin{aligned}\vec{n} = (n_x, n_y, n_z) &= (\cos\psi\ \cos\phi, \cos\psi\ \sin\phi, \sin\psi) \\ &= \left[1 - 2(\sin^2\phi/2 + \sin^2\psi/2) + 4\sin^2\phi/2 \sin^2\psi/2, \sin\phi(1 - 2\sin^2\psi/2), \sin\psi\right]\end{aligned} \tag{3.2.5}$$

where ϕ and ψ are the observation angles, given by

$$\phi = \mathrm{Atg}\left(\frac{r_y}{r_x}\right) \text{ and } \psi = \mathrm{Atg}\left(\frac{r_z}{\sqrt{r_x^2 + r_y^2}}\right) \tag{3.2.6}$$

with $\vec{r} = (r_x, r_y, r_z)$, while $\vec{\beta}$ can be written under the form

$$\begin{aligned}\vec{\beta} = (\beta_x, \beta_y, \beta_z) &= \left[\sqrt{(\beta^2 - \beta_y^2 - \beta_z^2)}, \beta_y, \beta_z\right] \\ &= \left[\sqrt{(1 - 1/\gamma^2 - \beta_y^2 - \beta_z^2)}, \beta_y, \beta_z\right] = (1 - a/2 + a^2/8 - a^3/16 + ..., \beta_y, \beta_z)\end{aligned} \tag{3.2.7}$$

where $a = 1/\gamma^2 + \beta_y^2 + \beta_z^2$. This leads to

$$n_x = 1 - \varepsilon_x \text{ and } \beta_x = 1 - \xi_x$$

with

$$\varepsilon_x = 2(\sin^2 \phi/2 + \sin^2 \psi/2) - 4 \sin^2 \phi/2 \sin^2 \psi/2$$

and

$$\xi_x = a/2 - a^2/8 + a^3/16 + ...$$

All this provides, on the one hand,

$$\vec{n} - \vec{\beta} = (-\varepsilon_x + \xi_x, n_y - \beta_y, n_z - \beta_z) \ , \tag{3.2.8}$$

whose components are combinations of terms of the same order of magnitude (ε_x and $\xi_x \sim 1/\gamma^2$ while n_y, β_y, n_z and $\beta_z \sim 1/\gamma$) and, on the other hand,

$$1 - \vec{n} \cdot \vec{\beta} = \varepsilon_x + \xi_x - n_y\beta_y - n_z\beta_z - \varepsilon_x\xi_x \ , \tag{3.2.9}$$

that combines terms of the same order of magnitude ($\varepsilon_x, \xi_x, n_y\beta_y$ and $n_z\beta_z \sim 1/\gamma^2$), plus $\varepsilon_x\beta_x \sim 1/\gamma^4$.
The precision of these expressions is directly related to the order at which the series

$$\xi_x = a/2 - a^2/8 + a^3/16 + ... \qquad (a = 1/\gamma^2 + \beta_y^2 + \beta_z^2)$$

is pushed, however the convergence is fast since $a \sim 1/\gamma^2 \ll 1$.

3.2.2 Calculation of the Fourier transform of the electric field

The Fourier transforms

$$FT_\omega[\vec{\mathcal{E}}(\tau)] = \int \vec{\mathcal{E}}(\tau) e^{-i\omega\tau} d\tau$$

of the σ and π electric field components provide the spectral angular energy density

$$\partial^3 W/\partial\phi\, \partial\psi\, \partial\omega = 2r^2 \left| FT_\omega \left(\vec{\mathcal{E}}(\tau)\right)\right|^2 / \mu_0 c \tag{3.2.10}$$

They are calculated in a regular way, without use of FFT technics, namely from

$$FT_\omega \left[\vec{\mathcal{E}}(\tau)\right] \approx \sum \vec{\mathcal{E}}(\tau_k)\, e^{-i\omega\tau_k}\, \Delta\tau_k \tag{3.2.11}$$

for two reasons. On the one hand, the number of integration steps Δs that define the trajectory (eqs. 1.2.4), is arbitrary and therefore in general not of order 2^n. On the other hand, the integration step defines a constant time differential element $\Delta t_k = \Delta s/\beta c$ which results in the observer differential time element $\Delta\tau_k$, which is also the differential element of the Fourier transform, being non-constant, since both are related by eq. 3.2.2 in which $\vec{\beta}$ and $\vec{n}$ vary as a function of the integration step number k.

Another major point is that $\Delta\tau_k$ may reach drastically small values in the region of the central peak of the electric impulse emitted in a dipole $(1-\vec{n}(t)\cdot\vec{\beta}(t)\rightarrow 1/2\gamma^2)$, whereas the total integrated time $\sum_{k=1}^{N}\Delta\tau_k$ may be several orders of magnitude larger. In terms of the physical phenomenon, the total duration of the electric field impulse as seen by the observer corresponds to the time delay $\sum_{k=1}^{N}\Delta\tau_k$ that separates photons emitted at the entrance of the magnet from photons emitted at the exit, but the significant part of it (in terms of energy density) which can be represented by the width $2\,\tau_c = \dfrac{2(1+\gamma^2\psi^2)^{3/2}\;2\rho}{3\gamma^3\;c}$ of the radiation peak [13], is a very small fraction of $\sum_{k=1}^{N}\Delta\tau_k$.
The consequence is that, once again in relation with computer precision, the differential element $\Delta\tau_k$ involved in the computation of eq. 3.2.11 cannot be derived from such relation as $\Delta\tau_k = \sum_{k=1}^{n}\Delta\tau_k - \sum_{k=1}^{n-1}\Delta\tau_k$ but instead must be stored as such beforehand in the couorse of the ray-tracing process.

4 DESCRIPTION OF THE AVAILABLE PROCEDURES

4.1 Introduction

This chapter gives a detailed description of how the **zgoubi** procedures work, and their associated keywords. It has been split into several sections. Sections 4.2 to 4.5 explain the underlying content and functioning of all available keywords. Section 4.6 is dedicated to the description of some general procedures that may be accessed by means of special data or flags (such as negative integration steps), or through the available keywords (such as multiturn tracking with *REBELOTE*).

4.2 Definition of an Object

The description of the object, *i.e.*, initial coordinates of the beam, must be the first element of the input data to **zgoubi** .

Several types of automatically generated objects are available, as described in the following pages.

MCOBJET: Monte-Carlo generation of a 6-D object

MCOBJET generates a set of up to 10^4 random 6-D initial conditions. It can be used in conjunction with the keyword *REBELOTE*, which moreover allows generating an arbitrarily high number of initial conditions.

The first datum is the reference rigidity (negative value allowed)

$$BORO = \frac{p_0}{q} \text{ (kG.cm)}$$

Depending on the value of the next datum, *KOBJ*, the *IMAX* ($\leq 10^4$) particles have their initial random conditions Y, T, Z, P, X and D (relative momentum) generated on 3 different types of supports, as described below.
Next come the data

$$KY, KT, KZ, KP, KX$$

that specify the type of probability density for the 6 coordinates.
KY, KT, KZ, KP, KX can take the following values:

1. uniform density, $p(x) = 1$ if $-\delta x \leq x \leq \delta x$, $p(x) = 0$ elsewhere,
2. Gaussian density, $p(x) = \frac{1}{\delta x\sqrt{2\pi}} e^{-\frac{x^2}{2\delta x^2}}$,
3. parabolic density, $p(x) = \frac{3}{4\delta x}(1 - \frac{x^2}{\delta x^2})$ if $-\delta x \leq x \leq \delta x$, $p(x) = 0$ elsewhere.

KD can take the following values:

1. uniform density, $p(D) = 1$ if $-\delta D \leq D \leq \delta D$, $p(D) = 0$ elsewhere,
2. exponential density, $p(D) = N_0 \exp(C_0 + C_1 l + C_2 l^2 + C_3 l^3)$ with $0 \leq l \leq 1$ and $-\delta D \leq D \leq \delta D$,
3. $p(D)$ is determined by a kinematic relation, namely, with T = horizontal angle, $D = \delta D * T$.

Next come the central value for the random sorting,

$$Y_0, \quad T_0, \quad Z_0, \quad P_0, \quad X_0, \quad D_0$$

namely, the probability density laws $p(x)$ ($x = Y, T, Z, P$ or X) and $p(D)$ described above apply to the variables $x - x_0$ ($\equiv Y - Y_0$, $T - T_0$, ...) and $D - D_0$ respectively. Negative value for D_0 is allowed (see section 4.6.9).

KOBJ = 1: Random generation of *IMAX* particles in a hyper-window with widths (namely the half-extent for uniform or parabolic distributions ($KY, KT, ... = 1$ or 3), and the r.m.s. width for Gaussian distributions ($KY, KT, ... = 2$))

$$\delta Y, \quad \delta T, \quad \delta Z, \quad \delta P, \quad \delta X, \quad \delta D$$

Then follow the cut-off values, in units of the r.m.s. widths δY, δT, ... (used only for Gaussian distributions, $KY, KT, ... = 2$)

$$N_{\delta Y}, \quad N_{\delta T}, \quad N_{\delta Z}, \quad N_{\delta P}, \quad N_{\delta X}, \quad N_{\delta D}$$

The last data are the parameters

$$N_0, \quad C_0, \quad C_1, \quad C_2, \quad C_3$$

needed for generation of the D coordinate upon option $KD = 2$ (unused if $KD = 1,\ 3$) and a set of three integer seeds for initialization of random sequences,

$$IR1, \quad IR2, \quad IR3 \quad (\text{all} \simeq 10^6)$$

All particles generated by *MCOBJET* are tagged with a (non-S) character, for further statistic purposes (e.g., with *HISTO* and *MCDESINT*).

KOBJ = 2: Random generation of $IY * IT * IZ * IP * IX * ID$ particles (maximum 10^4) in a hyper-grid. The input data are the number of bars in each coordinate

$$IY, \quad IT, \quad IZ, \quad IP, \quad IX, \quad ID$$

the spacing of the bars

$$PY, \quad PT, \quad PZ, \quad PP, \quad PX, \quad PD$$

the width of each bar

$$\delta Y, \quad \delta T, \quad \delta Z, \quad \delta P, \quad \delta X, \quad \delta D$$

the cut-offs, used with Gaussian densities (in units of the r.m.s. widths)

$$N_{\delta Y}, \quad N_{\delta T}, \quad N_{\delta Z}, \quad N_{\delta P}, \quad N_{\delta X}, \quad N_{\delta D}$$

This is illustrated in Fig. 6.

The last two sets of data in this option are the parameters

$$N_0, \quad C_0, \quad C_1, \quad C_2, \quad C_3$$

needed for generation of the D coordinate upon option KD= 2 (unused if KD= 1, 3) and a set of three integer seeds for initialization of random sequences, $IR1$, $IR2$, and $IR3$ (all $\simeq 10^6$).
All particles generated by *MCOBJET* are tagged with a (non-S) character, for further statistic purposes (see *HISTO and MCDESINT*).

KOBJ = 3: Distribution of *IMAX* particles inside a 6-D ellipsoid defined by the three sets of data (one set per 2-D phase-space)

$$\begin{array}{llllll} \alpha_Y, & \beta_Y, & \dfrac{\varepsilon_Y}{\pi}, & N_{\varepsilon_Y} & [, & N'_{\varepsilon_Y}, \text{ if } N_{\varepsilon_Y} < 0] \\ \alpha_Z, & \beta_Z, & \dfrac{\varepsilon_Z}{\pi}, & N_{\varepsilon_Z} & [, & N'_{\varepsilon_Z}, \text{ if } N_{\varepsilon_Z} < 0] \\ \alpha_X, & \beta_X, & \dfrac{\varepsilon_X}{\pi}, & N_{\varepsilon_X} & [, & N'_{\varepsilon_X}, \text{ if } N_{\varepsilon_X} < 0] \end{array}$$

where α, β are the ellipse parameters and ε/π the emittance, corresponding to an elliptical frontier $\dfrac{1+\alpha_Y^2}{\beta_Y} Y^2 + 2\alpha_Y YT + \beta_Y T^2 = \varepsilon_Y/\pi$ (idem for the (Z, P) or (X, D) planes). N_{ε_Y}, N_{ε_Z} and N_{ε_X} are the sorting cut-offs (used only for Gaussian distributions, $KY, KT, \ldots = 2$).
The sorting is uniform in surface (for $KY = 1$, or $KZ = 1$ or $KX = 1$) or Gaussian ($KY = 2$ or $KZ = 2$), and so on, as described above. A uniform sorting has the ellipse above for support. A Gaussian sorting has the ellipse above for r.m.s. frontier, leading to $\sigma_Y = \sqrt{\beta_Y \varepsilon_Y/\pi}$, $\sigma_T = \sqrt{\dfrac{(1+\alpha_Y^2)}{\beta_Y}} \varepsilon_Y/\pi$, and similar relations for σ_Z, σ_X.
If N_ε is negative, thus the sorting fills the elliptical ring that extends from $|N_\varepsilon|$ to N'_ε (rather than the inner region determined by the N_ε cut-off, as addressed above).

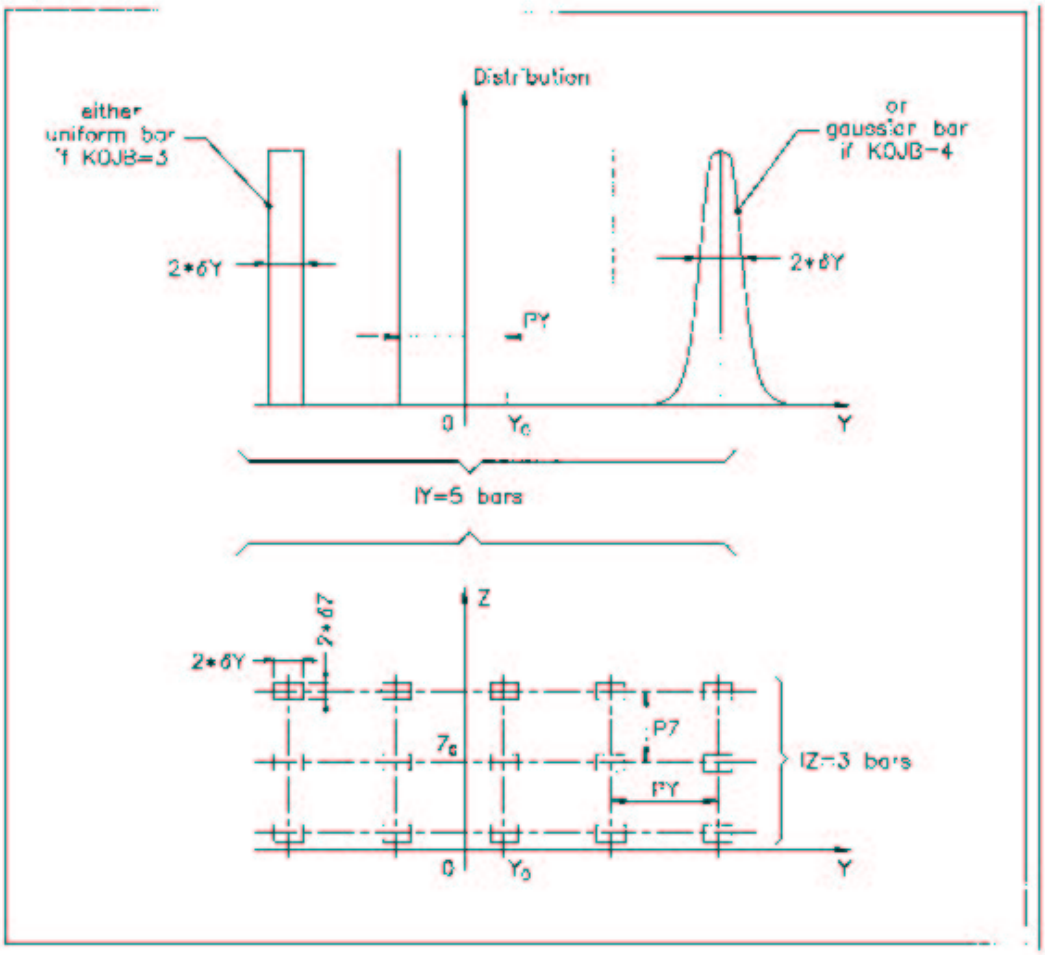

Figure 6: Scheme of the input parameters to *MCOBJET* when $KOBJ = 3, 4$
A: A distribution of the Y coordinate
B: A 2-D grid in (Y, Z) space.

OBJET: Generation of an object

OBJET is dedicated to the determination of the initial coordinates, in several ways.

The first datum is the reference rigidity (a negative value is allowed)

$$BORO = \frac{p_0}{q}$$

At the object, the beam is defined by a set of particles (maximum 10^4) with the initial conditions (Y, T, Z, P, X, D) where D is the relative momentum.
Depending on the value of the next datum *KOBJ*, these initial conditions may be generated in six different ways:

KOBJ = 1: Defines a grid in the Y, T, Z, P, X, D space. One gives the number of points desired,

$$IY, \quad IT, \quad IZ, \quad IP, \quad IX, \quad ID$$

(maximum 41 in each coordinate: $IY \leq 41 \ \ldots ID \leq 41$ and such that $IY * IT * \ldots * ID \leq 10^4$) and the sampling size

$$PY, \quad PT, \quad PZ, \quad PP, \quad PX, \quad PD$$

zgoubi then generates $IY * IT * IZ * IP * IX * ID$ ($\leq 10^4$) initial conditions with the following coordinates

$$\begin{array}{llll}
0, & \pm PY, & \pm 2 * PY, & \ldots, \quad \pm IY/2 * PY, \\
0, & \pm PT, & \pm 2 * PT, & \ldots, \quad \pm IT/2 * PT, \\
0, & \pm PZ, & \pm 2 * PZ, & \ldots, \quad \pm IZ/2 * PZ, \\
0, & \pm PP, & \pm 2 * PP, & \ldots, \quad \pm IP/2 * PP, \\
0, & \pm PX, & \pm 2 * PX, & \ldots, \quad \pm IX/2 * PX, \\
0, & \pm PD, & \pm 2 * PD, & \ldots, \quad \pm ID/2 * PD,
\end{array}$$

In this option relative momenta will be classified automatically for the purpose of the use of *IMAGES* for momentum analysis.
The particles are tagged with an index *IREP* possibly indicating a symmetry with respect to the (X,Y) plane, as explained in option $KOBJ = 3$. If two trajectories have mid-plane symmetry, only one will be ray-traced, while the other will be deduced using the mid-plane symmetries. This is done for the purpose of saving computing time. It may be incompatible with the use of some procedures (e.g. *MCDESINT*, which involves random processes).
The last datum is the reference of the problem (YR, TR, ZR, PR, XR, DR). For instance the reference rigidity is $DR*$ *BORO*, resulting in the rigidity of a particle of initial condition $I * PD$ to be $(DR + I * PD) *$ *BORO*.

KOBJ = 1.1: Same as $KOBJ = 1$ except for the Z symmetry. The initial Z and P conditions are the following

$$\begin{array}{llll}
0, & \pm PZ, & \pm 2 * PZ, & \ldots, \quad \pm (IZ - 1) * PZ, \\
0, & \pm PP, & \pm 2 * PP, & \ldots, \quad \pm (IP - 1) * PP,
\end{array}$$

This object results in shorter outputs/CPU-time when studying problems with Z symmetry.

KOBJ = 2: Next data: *IMAX* , *IDMAX* . Initial coordinates are entered explicitly for each trajectory. *IMAX* is the total number of particles ($IMAX \leq 10^4$). These may be classified in groups of equal number for each value of momentum, in order to fulfill the requirements of image calculations by *IMAGES*. *IDMAX* is the number of groups of momenta. The following initial conditions defining a particle are specified for each one of the *IMAX* particles

$$Y, \quad T, \quad Z, \quad P, \quad X, \quad D, \quad 'A'$$

where $D *$ *BORO* is the rigidity (negative value allowed) and $'A'$ is a (arbitrary) tagging character.
The last record *IEX* (I=1, *IMAX*) contains *IMAX* times either the string "1" (which indicates that the particle will be tracked) or the string "-2" (indicates that the particle will not be tracked).
This option $KOBJ = 2$ may be be useful for the definition of objects including kinematic effects.

KOBJ = 3**:** This option allows the reading of initial conditions from an external input file *FNAME*.
The next three data lines are:

IT1, IT2, ITStep
IP1, IP2, IPStep
YR,TR,ZR,PR,SR,DPR
InitC

followed by the storage file name *FNAME*.

IT1, IT2, ITStep specify reading coordinates of particles number IT1 through IT2 by step ITStep.

IP1, IP2, IPStep specify reading coordinates belonging in the sole pass IP1 through IP2 by step IPStep. Indeed, IP2 > IP1 assumes prior filling of *FNAME* in the course of a run (e.g., multiturn tracking) involving the keyword *REBELOTE*.

YR,TR,ZR,PR,SR,DPR are references added to the values of respectively Y, T, Z, P, S, DP as read from *FNAME*.

If InitC= 1 ray-tracing starts from the current coordinates $F(J, I)$,
if InitC= 0 ray-tracing starts from the initial coordinates $FO(J, I)$ as read from *FNAME*.

The file *FNAME* must be formatted so as to fit the following *FORTRAN* sequence

```
        OPEN (UNIT = NL, FILE = FNAME, STATUS = 'OLD')
 DO 1 I = 1, IMAX
    READ (NL,100) LET (I), IEX(I), (FO(J,I),J=1,6), (F(J,I),J=1,6), I, IREP(I),
     >      LET(I),IEX(I),-1.DO+FO(1,I),(FO(J,I),J=2,MXJ),
     >      -1.DO+F(1,I),F(2,I),F(3,I),
     >      (F(J,I),J=4,MXJ),ENEKI,
     >      ID,I,IREP(I), SORT(I),D,D,D,RET(I),DPR(I),
     >      D, D, D, BORO, IPASS, KLEY,LBL1,LBL2,NOEL
 100        FORMAT(1X,
C1   LET(IT),KEX,   1.DO-FO(1,IT),(FO(J,IT),J=2,MXJ),
     1           A1,1X,I2,1P,7E16.8,
C2   1.DO-F(1,IT),(FO(J,IT),J=2,MXJ),
     2         /,3E24.16,
C3   Z,P*1.D3,SAR,     TAR,     DS,
     3         /,4E24.16,E16.8,
C4   KART,  IT,IREP(IT),SORT(IT),X, BX,BY,BZ, RET(IT), DPR(IT),
     4         /,I1,2I6,7E16.8,
C5        EX,EY,EZ, BORO,  IPASS,  KLEY,  (LABEL(NOEL,I),I=1,2),NOEL
     5  /,4E16.8,          I6,1X,  A8,1X,  2A10,               I5)
    1    CONTINUE
```

where the meaning of the parameters (apart from D=dummy real, ID=dummy integer) is the following

LET(I) : one-character string (for tagging)
IEX(I) : flag, see $KOBJ = 2$
FO(1-6,I) : coordinates D, Y, T, Z, P and path length of the particle number I, at the origin. $D * BORO$ = rigidity
F(1-6,I) : idem, at the current position.

IREP is an index which indicates a symmetry with respect to median plane. For instance, if $Z(I+1) = -Z(I)$, then normally $IREP(I+1) = IREP(I)$. Consequently the coordinates of particle $I+1$ will not be obtained from ray-tracing but instead deduced without ray-tracing from those of particle I by simple symmetry. This results in gain of computing time.

$KOBJ = 3$ can be used directly for reading files filled by *FAISCNL*, *FAISTORE*.
If more than 10^4 particles are to be read from a file, use $IMAX \leq 10^4$ in conjunction with *REBELOTE*.

KOBJ = 3.1: Same as **KOBJ = 3**, except for the formatting of trajectory coordinate data in *FNAME* which is much simpler, namely, according to the following *FORTRAN* sequence

```
      OPEN (UNIT = NL, FILE = FNAME, STATUS = 'OLD')
 1    CONTINUE
 READ (NL,*,END=10,ERR=99) Y, T, Z, P, S, D
 GOTO 1
10    CALL ENDFIL
99    CALL ERREAD
```

KOBJ = 5: Mostly dedicated to the calculation of first order transfer matrix and various other optical parameters in conjunction with *MATRIX* or with *TWISS*. The input data are the stepsizes

$$PY, \quad PT, \quad PZ, \quad PP, \quad PX, \quad PD$$

The code generates 11 particles

$$0, \quad \pm PY, \quad \pm PT, \quad \pm PZ, \quad \pm PP, \quad \pm PX, \quad \pm PD$$

These values should be small enough, so that the paraxial ray approximation be valid.
The last data are the initial coordinates of the reference trajectory [normally $(YR, TR, ZR, PR, XR, DR) = (0, 0, 0, 0, 0, 1)$]. The reference rigidity is $DR * BORO$ (negative value allowed).

KOBJ = 5.1: Same as **KOBJ = 5**, except for an additional data line giving initial beam ellipse parameters $\alpha_Y, \beta_Y, \alpha_Z, \beta_Z, \alpha_X, \beta_X$, for further transport of these using *MATRIX*, or for possible use by the *FIT* procedure.

KOBJ = 6: Mostly dedicated to the calculation of first, second and other higher order transfer coefficients and various other optical parameters, in conjunction with *MATRIX* or with *TWISS*. The input data are the step sizes

$$PY, \quad PT, \quad PZ, \quad PP, \quad PX, \quad PD$$

to allow the building up of an object containing 61 particles. The last data are the initial coordinates of the reference trajectory [normally $(YR, TR, ZR, PR, XR, DR) = (0, 0, 0, 0, 0, 1)$]. The reference rigidity of the beam is $DR * BORO$.

KOBJ = 7: Object with kinematics
The data and functioning are the same as for $KOBJ = 1$, except for the following

- ID is not used,
- PD is the kinematic coefficient, such that for particle number I, the initial relative momentum D_I is calculated from the initial angle T_I following

  $$D_I = DR + PD * T_I$$

  while T_I is in the range

  $$0, \quad \pm PT, \quad \pm 2 * PT, \quad \ldots, \quad \pm IT/2 * PT$$

  as stated under $KOBJ = 1$

KOBJ = 8: Generation of phase-space coordinates on ellipses.
The ellipses are defined by the three sets of data (one set per ellipse)

$$\begin{array}{lll} \alpha_Y, & \beta_Y, & \varepsilon_Y/\pi \\ \alpha_Z, & \beta_Z, & \varepsilon_Z/\pi \\ \alpha_X, & \beta_X, & \varepsilon_X/\pi \end{array}$$

where α, β are the ellipse parameters and ε/π is the emittance encompassed, corresponding to an ellipse with equation $\dfrac{1+\alpha_Y^2}{\beta_Y} Y^2 + 2\alpha_Y YT + \beta_Y T^2 = \varepsilon_Y/\pi$ (idem for the (Z, P) or (X, D) planes).
The ellipses are centered respectively on (Y_0, T_0), (Z_0, P_0), (X_0, D_0).
The number of samples per plane is respectively IX, IY, IZ. If that value is zero, the central value above is assigned.

OBJETA: Object from Monte-Carlo simulation of decay reaction [14]

This generator simulates the reactions

$$M_1 + M_2 \longrightarrow M_3 + M_4$$

and then

$$M_4 \longrightarrow M_5 + M_6$$

where M_1 is the mass of the incoming body; M_2 is the mass of the target; M_3 is an outgoing body; M_4 is the rest mass of the decaying body; M_5 and M_6 are decay products. Example:

$$p + d \longrightarrow {}^3\mathrm{He} + \eta$$
$$\eta \longrightarrow \mu^+ + \mu^-$$

The first input data are the reference rigidity

$$BORO = \frac{p_0}{q}$$

an index *IBODY* which specifies the particle to be ray-traced, namely M3 ($IBODY = 1$), M5 ($IBODY = 2$) or M6 ($IBODY = 3$). In this last case, initial conditions for M6 must be generated by a first run of *OBJETA* with $IBODY = 2$; they are then stored in a buffer array, and restored as initial conditions at the next occurrence of *OBJETA* with $IBODY = 3$. Note that **zgoubi** by default assumes positively charged particles.

Another index, *KOBJ* specifies the type of distribution for the initial transverse coordinates Y, Z; namely either uniform ($KOBJ = 1$) or Gaussian ($KOBJ = 2$). The other three coordinates T, P and D are deduced from the kinematic of the reactions.

The next data are the number of particles to be generated, *IMAX* , and the masses involved in the two previous reactions.

$$M_1, \quad M_2, \quad M_3, \quad M_4, \quad M_5, \quad M_6$$

and the kinetic energy T_1 of the incoming body (M_1).
Then one gives the central value of the distribution for each coordinate

$$Y_0, \quad T_0, \quad Z_0, \quad P_0, \quad D_0$$

and the width of the distribution around the central value

$$\delta Y, \quad \delta T, \quad \delta Z, \quad \delta P, \quad \delta D$$

so that only those particles in the range

$$Y_0 - \delta Y \leq Y \leq Y_0 + \delta Y \qquad \ldots \qquad D_0 - \delta D \leq D \leq D_0 + \delta D$$

will be retained. The longitudinal initial coordinate is uniformly sorted in the range

$$-XL \leq X_0 \leq XL$$

The random sequences involved may be initialized with different values of the two integer seeds IR_1 and IR_2 ($\simeq 10^6$).

4.3 Declaration of options

These options allow the control of procedures that affect certain functions of the code. Some options are normally declared right after the object definition (e.g. *SPNTRK* - spin tracking, *MCDESINT* - in-flight decay), others are normally declared at the end of the data pile (e.g. *END* – end of a problem, *REBELOTE* – for tracking more than $10^4\tilde{\text{p}}$articles or for multi-turn tracking, *FIT* – fitting procedure).

BINARY: *BINARY/FORMATTED* data converter

This procedure translates field map data files from "BINARY" to "FORMATTED" – in the *FORTRAN* sense, or the other way.

The keyword is followed, next line, by NF (≤ 20), the number of files to be translated.
Then follow, line per line, the NF names of the files to be translated.

Iff a file name begins with the prefix "B_" or "b_", it is presumed "binary", and hence converted to "formatted", and given the same name after suppression of the prefix "B_" or "b_". Conversely, *iff* the file name does not begin with "B_" or "b_", the file is presumed "formatted" and hence translated to "binary", and is given the same name after addition of the prefix "B_".

In its present state, the procedure *BINARY* only supports files with standard *TOSCA* magnet code output format (see keyword *TOSCA*).

END or FIN: End of input data list ; see FIN

The end of a problem, or of a set of several problems stacked in the data file, should be stated by means of the keywords *FIN* or *END*.

Any information following these keywords will be ignored.

FIT: Fitting procedure

The keyword *FIT* allows the automatic adjustment of up to 20 variables, for fitting up to 20 constraints. It has been realized after existing routines used in the matrix transport code BETA [15]. Any physical parameter of any element (*i.e.* keyword) may be varied. Available constraints are, amongst others: any of the 6×6 coefficients of the first order transfer matrix $[R_{ij}]$ as defined in the keyword *MATRIX*, and its horizontal $(R_{11}R_{22} - R_{12}R_{21})$ and vertical $(R_{33}R_{44} - R_{34}R_{43})$ determinants; horizontal and vertical tunes (if periodical structure); any of the $6 \times 6 \times 6$ coefficients of the second order array $[T_{ijk}]$ as defined in *MATRIX* ; any of the 2×4 coefficients of the σ-matrix as defined by

$$[\sigma_{ij}] = \begin{pmatrix} \sigma_{11} & \sigma_{12} & & \\ \sigma_{21} & \sigma_{22} & & \\ & & \sigma_{33} & \sigma_{34} \\ & & \sigma_{43} & \sigma_{44} \end{pmatrix}$$

and any trajectory coordinates $F(J, I)$ as defined in *OBJET* (I = particle number, J = coordinate number = 1 to 6 for respectively D, Y, T, Z,P or S =path length).

Tunes $\nu_{Y,Z}$ and Twiss periodic functions $\beta_{Y,Z}, \alpha_{Y,Z}, \gamma_{Y,Z}$ are adjustable as well; they are defined by identification of the full optical structure transfer matrix $[R_{ij}]$ with the Twiss matrix, following $[R_{ij}] = Icos(2\pi\nu_{Y,Z}) + Jsin(2\pi\nu_{Y,Z})$ wherein $J = \begin{pmatrix} \alpha & \beta \\ -\gamma & -\alpha \end{pmatrix}$.

VARIABLES

The first input data in *FIT* are the number of variables *NV* , and for each one of them, the following parameters

$IR =$ number of the varied element in the structure
$IP =$ number of the physical parameter to be varied in this element
$XC =$ coupling parameter. Normally $XC = 0$. If $XC \neq 0$, coupling will occur (see below).
$DV =$ allowed relative range of variation of the physical parameter IP.

Numbering of the elements (*IR*):

The elements (*DIPOLE, QUADRUPO,* etc.) are numbered following their sequence in the **zgoubi** input data file, for the purpose of the *FIT* procedure. The number of any element just identifies to its position in the data sequence. However, a simple way to get IR is to make a preliminary run: **zgoubi** will then print the whole structure into the file zgoubi.res with all elements numbered.

Numbering of the physical parameters (*IP*):

In the elements *DIPOLE*, *AIMANT* and *EBMULT*, *ELMULT*, *MULTIPOL*, the numbering of the physical parameters just follows their sequence, as it is shown here after for *DIPOLE*: the left column below represents the input data, the right one the corresponding numbering to be used for the *FIT* procedure.

Input data	**Numbering for FIT**
DIPOLE	
NFACE, IC, IL	1, 2, 3
IAMAX, IRMAX	4, 5
B_0, N, B, G	6, 7, 8, 9
AT, ACENT, RM, RMIN, RMAX	10, 11, 12, 13, 14
λ , ξ	15,16
NC , C_0, C_1, C_2, C_3, C_4, C_5 shift	17, 18, 19, 20, 21, 22, 23, 24
ω, θ, R_1, U_1, U_2, R_2	25, 26, 27, 28, 29, 30
etc.	etc.

Parameters in *SCALING* also have a specific numbering, as follows.

Input data	**Numbering for FIT**
SCALING	
IOPT, NFAM	
NAMEF	
NT_1	
$SCL(I),\ I = 1,\ NT_1$	$10\ [, ...,\ 10 + NT_1]$
$TIM(I),\ I = 1,\ NT_1$	$10\ [, ...,\ 10 + 2 * NT_1]$
NAMEF	
NT_2	
$SCL(I),\ I = 1,\ NT_2$	$20\ [, ...,\ 20 + NT_2]$
$TIM(I),\ I = 1,\ NT_2$	$20\ [, ...,\ 20 + 2 * NT_2]$
...	
etc. up to *NFAM*	etc.

For all other keywords, the parameters are numbered in the following way

Input data	**Numbering for FIT**
KEYWORD	
first line	1, 2, 3,...
second line	10, 11, 12, 13,...
this is a comment	a line of comments is skipped
next line	20, 21, 22,...
and so on...	30, 31, 32, 33,...

The examples of *QUADRUPO* (quadrupole) and *TOSCA* (Cartesian mesh field map) are given below.

Input data	**Numbering for FIT**
QUADRUPO	
IL	1
$XL,\ R_0,\ B$	10, 11, 12
$X_E,\ \lambda_E$	20, 21
NCE , $C_0,\ C_1,\ C_2,\ C_3,\ C_4,\ C_5$	30, 31, 32, 33, 34, 35, 36
$X_S,\ \lambda_S$	40, 41
NCS , $C_0,\ C_1,\ C_2,\ C_3,\ C_4,\ C_5$	50, 51, 52, 53, 54, 55, 56
XPAS	60
KPOS, XCE, YCE, ALE	70, 71, 72, 73
TOSCA	
IC, IL	1, 2
BNORM, X-[Y-,Z-]NORM	10, 11 [,12, 13]
TIT	This is text
$IX,\ IY,\ IZ$	20, 21
FNAME	This is text
$ID,\ A,\ B,\ C\ [A',\ B',\ C'$, etc. if $ID \geq 2]$	30, 31, 32, 33 [34, 35, 36, etc if $ID \geq 2$]
IORDRE	40
XPAS	50
KPOS, XCE, YCE, ALE	60,61,62,63

Coupled variables (XC)

Coupling a variable parameter to any other parameter in the structure is possible. This is done by giving XC a value of the form $r \cdot pp$ where the integer part r is the number of the coupled element in the structure (equivalent to IR, see above), and the decimal part pp is the number of its parameter of concern (equivalent to IP, see above) (if the parameter number is in the range 1,...,9, then pp must take the form $0p$). For example, $XC = 20 \cdot 01$ is a request for coupling with the parameter number 1 of element number 20 of the structure, while $XC = 20 \cdot 10$ is a request for coupling with the parameter number 10 of element 20.

An element of the structure which is coupled (by means of $XC \neq 0$) to a variable declared in the data list of the *FIT* keyword, needs not appear as one of the *NV* variables in that data list (this would be redundant information).

XC can be either positive or negative. If $XC > 0$, then the coupled parameter will be given the same value as the variable parameter (for example, symmetric quadrupoles in a lens triplet will be given the same field). If $XC < 0$, then the coupled parameter will be given a variation opposite to that of the variable, so that the sum of the two parameters stays constant (for example, an optical element can be shifted while preserving the length of the structure, by coupling together its upstream and downstream drift spaces).

Variation range (DV)

For a parameter IP of initial value p, the *FIT* procedure is allowed to explore the range $p(1 \pm DV)$.

IC	=	type of constraint (see table below).
I, J	=	constraint (*i.e.* R_{ij}, determinant, tune; T_{ijk}; σ_{ij}; trajectory $\#I$ and coordinate $\#J$)
IR	=	number of the element in the **zgoubi** input data file, right after which the constraint applies
V	=	desired value of the constraint
W	=	weight of the constraint (smaller W for higher weight)

CONSTRAINTS

The next input data in *FIT* are the number of constraints, *NC* , and for each one of them the following parameters.

IC=0 : The coefficients σ_{11} (σ_{33}) = horizontal (vertical) beta values and σ_{22} (σ_{44}) = horizontal (vertical) derivatives ($\alpha = -\beta'/2$) are obtained by transport of their initial values at line start as introduced using for instance *OBJET, KOBJ=5.1*.

IC=0.1 : Twiss functions: $\sigma_{11} = \beta_Y, \sigma_{12} = \sigma_{21} = -\alpha_Y, \sigma_{22} = \gamma_Y$, $\sigma_{33} = \beta_Z, \sigma_{34} = \sigma_{43} = -\alpha_Z, \sigma_{44} = \gamma_Z$; periodic dispersion: $\sigma_{16} = D_Y$, $\sigma_{26} = D'_Y$, $\sigma_{36} = D_Z, \sigma_{46} = D'_Z$, all quantities derived by assuming periodic structure and identifying the first order transfer matrix to its Twiss form.

IC=1, 2 : The coefficients R_{ij} and T_{ijk} are calculated following the procedures described in *MATRIX*, option *IFOC* = 0. The fitting of the $[R_{ij}]$ matrix coefficients or determinants supposes the tracking of particles having initial coordinates sampled as described in *MATRIX* (these particles are normally defined with *OBJET*, *KOBJ* = 5 or 6). The same is true for the T_{ijk} second order coefficients (Initial coordinates normally defined with *OBJET*, *KOBJ* = 6).

IC=3 : If $1 < I <$ *IMAX* then the value of coordinate type J ($J = 1, 6$ for respectively D, Y, T, Z, P, S) of particle number I ($1 < I <$ *IMAX*) is constrained. If $I = -1$ the constraint is the mean value of coordinate of type J.

IC=4 : The coefficients σ_{11} (σ_{33}) = horizontal (vertical) beta values and σ_{22} (σ_{44}) = horizontal (vertical) derivatives ($\alpha = -\beta'/2$) are derived from an ellipse match of the current particle population (as generated for instance using *MCOBJET, KOBJ=3*).
The fitting of the $[\sigma_{ij}]$ coefficients supposes the tracking of a relevant population of particles within an adequate emittance.

IC=5 : If $I = -1$ then the constraint value is the ratio of particles still on the run. If $I \geq 1$ then the constraint value is the ratio of particles encompassed within a given I-type ($I = 1-3$ for respectively Y, Z, D) phase-space surface.

Type of constraint	**Parameters defining the constraints**				**Object definition (recommended)**
	IC	**I**	**J**	**Constraint**	
σ-matrix	0	1 - 6	1 - 6	σ_{IJ} $(\sigma_{11} = \beta_Y,\ \sigma_{12} = \sigma_{21} = \alpha_Y,$ etc.)	*OBJET, KOBJ=5 or 6*
Periodic (Twiss) coefficients	0.1	1 - 6	1 - 6	σ_{IJ} $(\sigma_{11} = \cos\mu_Y + \alpha_Y \sin\mu_Y,$ etc.)	*OBJET, KOBJ=5 or 6*
		7	any	Y-tune $= \mu_Y/2\pi$	
		8	any	Z-tune $= \mu_Z/2\pi$	
First order parameters	1	1 - 6	1 - 6	Transport coeff. R_{IJ}	*OBJET, KOBJ=5*
		7	any	Y-determinant	
		8	any	Z-determinant	
Second order parameters	2	1 - 6	11 - 66	Transport coeff. $T_{I,j,k}$ $(j = [J/10], k = J - 10[J/10])$	*OBJET, KOBJ=6*
Trajectory coordinates	3	1 - IMAX	1 - 6	$F(J, I)$	*OBJET, MCOBJET*
		-1	1 - 6	$< F(J, i) >_{i=1,IMAX}$	
Matched ellipse parameters	4	1 - 6	1 - 6	σ_{IJ} $(\sigma_{11} = \beta_Y,\ \sigma_{12} = \sigma_{21} = \alpha_Y,$ etc.)	*OBJET, KOBJ=8; MCOBJET, KOBJ=3*
Number of particles	5	-1	any	Ratio $N_{survived}/IMAX$	*OBJET, MCOBJET*
		1 - 3	any	$N_{survived}/IMAX$ through ϵ_I	

Table 1: This table shows the constraints available, depending on the values of IC, I and J. [ ] denotes the integer part. When $IC = 3$, I designates the particle number and J the coordinate number (i.e., D, Y, T, Z, P or X).

OBJECT DEFINITION

Depending on the type of constraint (see Table), constraint calculations are performed either from transport coefficient calculation and in such case need *OBJET* with either $KOBJ = 5$ or $KOBJ = 6$, or from particle distributions and in this case need object definition using for instance *OBJET* with $KOBJ = 8$, *MCOBJET* with either $KOBJ = 3$.

THE FITTING METHOD [15]

The numerical procedure is a direct sequential minimization of the quadratic sum of all errors (*i.e.*, differences between desired and actual values of the NC constraints), each normalized by its specified weight W (the smaller W, the stronger the constraint).
The step sizes for the variation of the physical parameters depend on their initial values, and cannot be accessed by the user. At each iteration, the optimum value of the step size, as well as the optimum direction of variation, is determined for each one of the NV variables. Then follows an iterative global variation of all NV variables, until the minimization fails which results in a next iteration on the optimization of the step sizes.

GASCAT: Gas scattering

Modification of particle momentum and velocity vector, performed at each integration step, under the effect of scattering by residual gas.

To be documented

MCDESINT: Monte-Carlo simulation of in-flight decay[16]

As soon as *MCDESINT* appears in a structure (normally, after *OBJET* or after *CIBLE*), in-flight decay simulation starts. It must be preceded by *PARTICUL* for the definition of mass M_1 and *COM* lifetime τ_1.
The two-body decay simulated is

$$1 \longrightarrow 2 + 3$$

The decay is isotropic in the center of mass. 1 is the incoming particle, with mass M_1, momentum $p_1 = \gamma_1 M_1 \beta_1 c$ (relative momentum $D_1 = \frac{p_1}{q}\frac{1}{BORO}$ with *BORO*= reference rigidity, see *OBJET*), and position Y_1, Z_1 in the **zgoubi** frame. 2 and 3 are decay products with respective masses and momenta M_2, M_3 and $p_2 = \gamma_2 M_2 \beta_2 c$, $p_3 = \gamma_3 M_3 \beta_3 c$.
The decay length s_1 of particle 1 is related to its center of mass lifetime τ_1 by

$$s_1 = c\tau_1\sqrt{\gamma_1^2 - 1}$$

The path length s up to the decay point is then calculated from a random number $0 < R_1 \leq 1$ by using the exponential decay formula

$$s = -s_1 \ell n R_1$$

After decay, particle 2 will be ray-traced with assumed positive charge, while particle 3 is discarded. Its scattering angles in the center of mass θ^* and ϕ are generated from two other random numbers $0 < R_2 \leq 1$ and $0 < R_3 \leq 1$ by

$$\begin{aligned} \theta^* &= 2\pi(R_2 - 0.5) \qquad (-\pi < \theta^* \leq \pi) \\ \phi &= 2\pi R_3 \qquad\qquad\quad (0 < \phi \leq 2\pi) \end{aligned}$$

ϕ is a relativistic invariant, and θ in the laboratory frame (Fig. 7) is given by

$$\tan\theta = \frac{1}{\gamma_1}\frac{\sin\theta^*}{\frac{\beta_1}{\beta_2^*} + \cos\theta^*}$$

β_2^* and momentum p_2 are given by

$$\begin{aligned} \gamma_2^* &= \frac{M_1^2 + M_2^2 - M_3^2}{2M_1M_2} \\ \beta_2^* &= \left(1 - \frac{1}{\gamma^2}\right)^{1/2} \\ \gamma_2 &= \gamma_1\gamma_2^*\,(1 + \beta_1\beta_2^*\cos\theta^*) \\ p_2 &= M_2\sqrt{\gamma_2^2 - 1} \end{aligned}$$

Finally, θ and ϕ are transformed into the angles T_2 and P_2 in the **zgoubi** frame, and the relative momentum takes the value $D_2 = \frac{p_2}{q}\frac{1}{BORO}$ (where *BORO*is the reference rigidity, see *OBJET*), while the starting position of M_2 is $Y_2 = Y_1$ and $Z_2 = Z_1$.

The decay simulation by **zgoubi** obeys the following procedures. In optical elements and field maps, after each integration step *XPAS*, the actual path length of the particle, $F(6, I)$, is compared to its limit path length s. If s is passed, then the particle is considered as having decayed at $F(6, I) - \frac{XPAS}{2}$, at a position obtained by a linear translation from the position at $F(6, I)$. [Presumably, the smaller *XPAS*, the smaller the error on position and angles at the decay point].

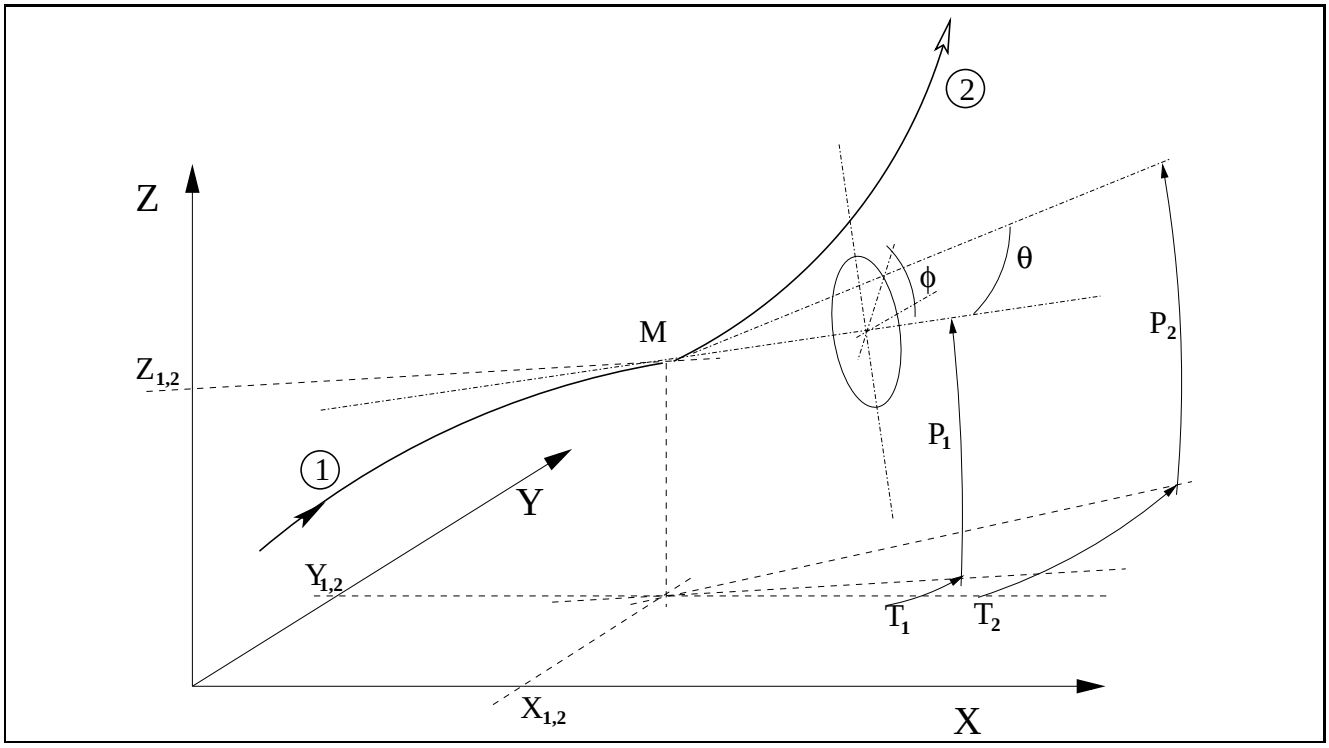

Figure 7: At position $M(X_1, Y_1, Z_1)$, particle 1 decays into 2 and 3; **zgoubi** then calculates the trajectory of 2, while 3 is discarded.
θ and ϕ are the scattering angles of particle 2 relative to the direction of the incoming particle 1; they transform to T_2 and P_2 in **zgoubi** frame.

In *ESL* and *CHANGREF*, $F(6, I)$ is compared to s at the end of the element. If the decay occurs inside the element, the particle is considered as having decayed at its actual limit path length s, and its coordinates at s are recalculated by translation.

The limit path length of all particles ($I = 1$, *IMAX*) is stored in the array *FDES*$(6, I)$, for further statistical purposes. For the same purpose (e.g., use of *HISTO*), any particle of type 2 (resulting from decay of 1) will be tagged with an S standing for "secondary". When a particle decays, its coordinates D, Y, T, Z, P at the decay point are stored in *FDES*(J, I), $J = 1, 5$.

NOTE on negative drifts:
The use of negative drifts with *MCDESINT* is allowed and correct. For instance, negative drifts may occur in a structure for some of the particles when using *CHANGREF* (due to the Z-axis rotation or negative *XCE)*, or when using *DRIFT* with $XL < 0$. Provision has been made to take it into account during the *MCDESINT* procedure, as follows.
If, due to a negative drift, a secondary particle reaches back the decay spot of the primary particle from which it originated, then that primary particle is regenerated with its original coordinates at that spot. Then the secondary particle is discarded while ray-tracing resumes in a regular way for the primary particle which is again susceptible of decay at the same time-of-flight. This procedure is made possible by prior storage of the coordinates of the primary particles (in array *FDES*(J, I)) each time a decay occurs.
Negative steps (*XPAS*< 0) in optical elements are not compatible with *MCDESINT*.

ORDRE: Taylor expansions order

The position $\vec{R}$ and velocity $\vec{u}$ of a particle are obtained from Taylor expansions as described in eq. (1.2.4). By default, these expansions are up to the fourth order derivative of $\vec{u}$,

$$\vec{R}_1 \approx \vec{R}_0 + \vec{u}_0 \Delta s + \ldots + \vec{u}_0^{(4)} \frac{\Delta s^5}{5!}$$
$$\vec{u}_1 \approx \vec{u}_0 + \vec{u}_0' \Delta s + \ldots + \vec{u}_0^{(4)} \frac{\Delta s^4}{4!}$$

which corresponds to third order derivatives of $\vec{B}$, since (eq. (1.2.7))

$$\vec{u}^{(4)} = \vec{u}''' \times \vec{B} + 3\vec{u}'' \times \vec{B}' + 3\vec{u}' \times \vec{B}'' + \vec{u} \times \vec{B}'''$$

and to the third order derivatives of $\vec{E}$ (eq. (1.2.11)) as well.

However $\vec{B}'''$, or $\vec{E}'''$, and higher order derivatives may be zero in second order type optical elements, for instance in a sharp edge quadrupole. Also, in several elements, no more than first and second order field derivatives are implemented in the code. One may also wish to fasten calculations by limiting the time-consuming calculation of lengthy (while possibly ineffective in terms of accuracy) Taylor expansions.

In that spirit, the purpose of *ORDRE*, option $IO = 2 - 5$, is to allow for expansions to the $\vec{u}_0^{(IO)}$ term in eq. 1.2.4. Default functionning is $IO = 4$.

Note the following:

As concerns the optical elements

QUADRUPO, SEXTUPOL, OCTUPOLE, DECAPOLE, DODECAPO, MULTIPOL, ELMULT, EBMULT

magnetic field derivatives (see eq. 1.2.8) have been installed in the code according to $\vec{u}_0^{(5)}$ developement order; it may not be as complete for some other optical elements, as well as for the possible electric field component whose field derivatives may not be provided to more than second order.

In electric optical elements field derivatives (eq. 1.2.13) are usually provided to no more than second order, which justifies saving computing time by not pushing Taylor expansions as high as $\vec{u}_0^{(5)}$.

NOTE: see also the option *IORDRE* in field map declarations (*DIPOLE, TOSCA*, etc.).

PARTICUL: Particle characteristics

PARTICUL allows the definition of several characteristics of the particles (mass, charge, gyromagnetic factor and life-time in the center of mass), that are needed in several procedures, as follows

MCDESINT	: mass, COM life-time
SPNTRK	: mass, gyromagnetic factor
SRLOSS	: mass, charge
SYNRAD	: mass, charge
Electric and Electro-Magnetic elements	: mass, charge

The declaration of *PARTICUL* must **precede** these keywords.
Note that, in the case of electric or electro-magnetic optical elements, the mass and charge are needed in order to compute the particle velocity v, as involved in eq. 1.2.3.

REBELOTE: Jump to the beginning of zgoubi input data file

As soon as *REBELOTE* is encountered in the input data file, the code execution jumps back to the beginning of the data file to start a new run, and so on up to *NPASS* times. When the following random procedures are used: *MCOBJET, OBJETA, MCDESINT, SPNTRK* ($KSO = 5$), their random seeds are not reset, and therefore independent statistics will add up. *REBELOTE* is dedicated either to Monte Carlo calculations when more than 10^4 particles are to be tracked (due to *IMAX* $\leq 10^4$, see *MCOBJET*), or to the tracking in circular machines (e.g. Synchrotron accelerators). The option index K is then used to either generate new initial coordinates ($K = 0$ see section 4.6.7), when using *MCOBJET* or any other generator of random initial coordinates, or in order that the final coordinates at the last run be taken as the initial coordinates of the next ($K = 99$ — see section 4.6.4).

Monte Carlo simulations: normally $K = 0$. *NPASS* runs through the same structure will follow, resulting in the calculation of $(1 + NPASS) * IMAX$ trajectories.

Circular machines: normally $K = 99$. *NPASS* turns in the same structure will follow, resulting in the tracking of *IMAX* particles over $1 + NPASS$ turns (Note: for the simulation of accelerators and synchrotron motion, see *SCALING*).

Output prints over *NPASS* runs might result in a prohibitively big file. They may be inhibited by means of the option *KWRIT*= 0.

REBELOTE provides statistical calculations and related informations on particle decay *(MCDESINT)*, spin tracking *(SPNTRK)*, stopped particles (*CHAMBR, COLLIMA*).

RESET: Reset counters and flags

Piling up problems in **zgoubi** input data file is allowed, with normally no particular precaution, except that each new problem must begin with a new object definition (with *MCOBJET, OBJET*, etc.). Nevertheless, when calling upon certain keywords, flags, counters or integrating procedures are involved. It may therefore be necessary to reset them. This is the purpose of *RESET* which normally appears right after the object definition and causes each problem to be treated as a new and independent one.

The keywords or procedures of concern and the effect of *RESET* are the following

CHAMBR	:	*NOUT* = number of stopped particles = 0; *CHAMBR* option switched off
COLLIMA	:	*NOUT* = number of stopped particles = 0
HISTO	:	Histograms are emptied
INTEG	:	*NRJ* = number of particles out of range = 0 (*INTEG* is the numerical integration subroutine; *NRJ* is incremented when a particle goes out of a field map)
MCDESINT	:	Decay in flight option switched off
SCALING	:	Scaling options disabled
SPNTRK	:	Spin tracking option switched off

SCALING: Time scaling of power supplies and R.F.

SCALING acts as a function generator dedicated to varying fields in optical elements, or potentials in electrostatic devices, or frequency in *CAVITE*. It is normally intended to be declared right after the object definition, and used in conjunction with *REBELOTE*, for the simulation of multiturn tracking - possibly including acceleration cycles.

SCALING acts on families of elements, a family being designated by its name that coincides with the keyword of the corresponding element. For instance, declaring *MULTIPOL* as to be varied will result in the same timing law being applied to all *MULTIPOL*'s in the **zgoubi** optical structure data file. Subsets can be selected by labeling keywords in the data file (section 4.6.3, page 124) and adding the corresponding *LABEL*('s) in the *SCALING* declarations (two *LABEL*'s maximum). The family name of concern, as well as the field versus timing scaling law of that family (or frequency versus timing in the case of *CAVITE*) are given as input data to the keyword *SCALING*. Up to 9 families can be declared as subject to a scaling law; a scaling law can be made of up to 10 successive timings; between two successive timings, the variation law is linear.

An example of data formatting is given in the following.

SCALING		- Scaling
1 4		Active. 4 families of elements are concerned, as listed below
QUADRUPO QFA QFB		- Quadrupoles labeled 'QFA' and Quadrupoles labeled 'QFB'
2		2 timings
18131.E-3	24176.E-3	The field increases (linearly) from 18131E-3$*B_0$ to 24176E-3$*B_0$
1	6379	from turn 1 to turn 6379
MULTIPOL QDA QDB		- Multipoles labeled 'QDA' and Multipoles labeled 'QDB'
2		
18131.E-3	24176.E-3	Fields increase from 18131E-3$*B_i$ to 24176E-3$*B_i$ ($\forall i$ = 1, 10 poles)
1	6379	from turn 1 to turn 6379
BEND		- All *BEND*'s (regardless of any LABEL)
2		
18131.E-3	24176.E-3	Same scaling
1	6379	
CAVITE		- Accelerating cavity
2		
1 1.22	1.33352	The synchronous rigidity $(B\rho)_s$ increases,
1 1200	6379	from $(B\rho)_{s_o}$ to 1.22 $*(B\rho)_{s_o}$ from turn 1 to 1200, and
		from 1.22 $*(B\rho)_{s_o}$ to 1.33352 $(B\rho)_{s_o}$ from turn 1200 to 6379

The timing is in unit of turns. In this example, TIMING = 1 to 6379 (turns). Therefore, at turn number N, B and B_i are updated in the following way. Let $SCALE(TIMING = N)$ be the updating scale factor

$$\text{SCALE}(N) = 18.131\frac{24.176 - 18.131}{1 + 6379 - 1}(N - 1)$$

and then

$$B(N) = SCALE(N)B_0$$
$$B_i(N) = SCALE(N)B_{i\,0}$$

The cavity R.F. is calculated from

$$f_{RF} = \frac{hc}{\mathcal{L}}\frac{q(B\rho)_s}{(q^2(B\rho)_s^2 + (Mc^2)^2)^{1/2}}$$

where the rigidity is updated in the following way. Let $(B\rho)_{s_o}$ be the initial rigidity (namely, $(B\rho)_{s_o} = BORO$as defined in the keyword *OBJET* for instance). Then, at turn number N,

$$\text{if } 1 \leq N \leq 1200 \text{ then, } SCALE(N) = 1 + \frac{1.22 - 1}{1 + 1200 - 1}(N - 1)$$
$$\text{if } 1200 \leq N \leq 6379 \text{ then, } SCALE(N) = 1.22 + \frac{1.33352 - 1.22}{1 + 6379 - 1200}(N - 1200)$$

and then,

$$(B\rho)_s(N) = SCALE(N) \cdot (B\rho)_{s_o}$$

from which value the calculations of $f_{RF}(N)$ follow.

Note : It may happen that some optical elements won't scale, for source code developement reasons. This should be paid attention to.

SPNTRK: Spin tracking

The keyword *SPNTRK* permits switching on the spin tracking option. It also permits the attribution of an initial spin component to each one of the *IMAX* particles of the beam, following a distribution that depends on the option index *KSO*. It must be preceded by *PARTICUL* for the definition of mass and gyromagnetic factor.

KSO = 1 (respectively 2, 3): the *IMAX* particles of the beam are given a longitudinal (1,0,0) spin component (respectively transverse horizontal (0,1,0), vertical (0,0,1)).

KSO = 4: initial spin components are entered explicitly for each one of the *IMAX* particles of the beam.

KSO = 5: random generation of *IMAX* initial spin conditions as described in Fig. 8. Given a mean polarization axis (S) defined by its angles T_0 and P_0, and a cone of angle A with respect to this axis, the *IMAX* spins are sorted randomly in a Gaussian distribution

$$p(a) = \exp\left[-\frac{(A-a)^2}{2\delta A^2}\right] / \delta A\sqrt{2\pi}$$

and within a cylindrical uniform distribution around the (S) axis. Examples of simple distributions available by this mean are given in Fig. 9.

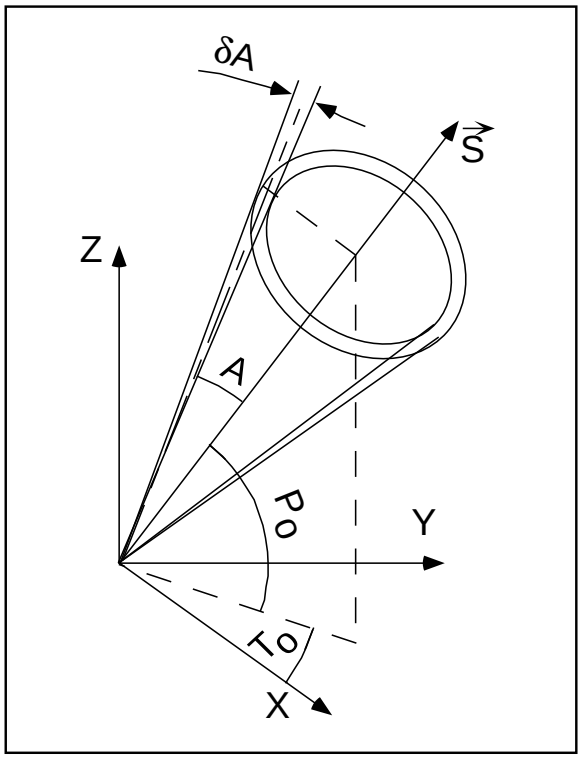

Figure 8: Spin distribution as obtained with option $KSO = 5$.
The spins are distributed within an annular strip δA (standard deviation) at an angle A with respect to the axis of mean polarization (S) defined by T_0 and P_0.

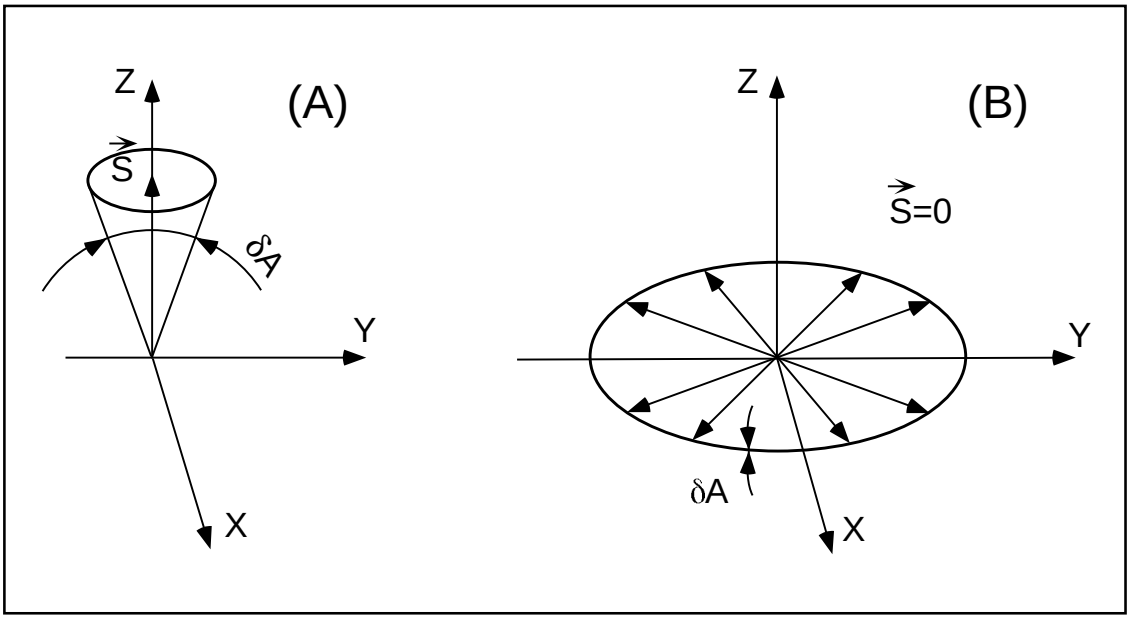

Figure 9: Examples of the use of KSO =5.
A: Gaussian distribution around a mean vertical polarization axis, obtained with T_0 = arbitrary, $P_0 = \pi/2$, $A = 0$ and $\delta A \neq 0$.
B: Isotropic distribution in the median plane, obtained with $P_0 = \pm\pi/2$, $A = \pi/2$, and $\delta A = 0$.

SRLOSS: Synchrotron radiation loss

[10]
The keyword *SRLOSS* allows activating or stopping (option $KSR = 1, 0$ respectively) stepwise tracking of energy loss by emission of photons in magnetic fields and the ensuing particle energy perturbation. It must be preceded by *PARTICUL* for defining mass and charge values as they enter in the definition of SR parameters.

Statistics on SR parameters are perform while tracking, results of which can be obtained by means of keyword SRPRNL.

SYNRAD: Synchrotron radiation spectral-angular densities

The keyword *SYNRAD* enables (or disables) the calculation of synchrotron radiation (SR) electric field and spectral angular energy density. It must be preceded by *PARTICUL* for defining mass and charge values, as they enter in the definition of SR parameters.

SYNRAD is supposed to appear a first time at the location where SR calculations should start, with the first data *KSR* set to 1. It results in on-line storage of the electric field vector and other relevant quantities in zgoubi.sre, as step by step integration proceeds. The observer position (XO, YO, ZO) is specified next to *KSR*.

Data stored in zgoubi.sre:

(ELx, ELy, ELz): electric field vector $\vec{\mathcal{E}}$ (eq. 3.2.1)
$(btx, bty, btz) = \vec{\beta} = \frac{1}{c} \times$ particle velocity
$(gx, gy, gz) = \frac{d\vec{\beta}}{dt}$ = particle acceleration (eq. 3.2.3)
$\Delta\tau$ = observer time increment (eq. 3.2.2)
$t' = \tau - r(t')/c$ = retarded (particle) time
$(rtx, rty, rtz) : \vec{R}(t)$, particle to observer vector (eq. 3.2.4)
(x, y, z) = particle coordinates
Δs = step size in the magnet (fig. 2)
NS = step number
I = particle number
$LET(I)$ = tagging letter
$IEX(I)$ = stop flag (see section 4.6.8)

SYNRAD is supposed to appear a second time at the location where SR calculations should stop, with *KSR* set to 2. It results in the output of the angular energy density $\int_{\nu_1}^{\nu_2} \partial^3 W/\partial\phi\,\partial\psi\,\partial\nu$ (eq. 3.2.11) as calculated from the Fourier transform of the electric field (eq. 3.2.11). The spectral range of interest and frequency sampling (ν_1, ν_2, N) are specified next to *KSR*.

Note that *KSR* = 0 followed by a dummy line of data allows temporary inhibition of SR procedures.

4.4 Optical Elements and related numerical procedures

AIMANT: Generation of a dipole magnet 2-D map

The keyword *AIMANT* provides an automatic generation of a dipole median plane field map in polar coordinates. A more recent and improved version will be found in *DIPOLE*. The extent of the map is defined by the following parameters, as shown in Figs. 10A and 10B.

AT	:	total angular aperture
RM	:	mean radius used for the positioning of field boundaries
RMIN, RMAX	:	minimum and maximum radial boundaries of the map

The 2 or 3 effective field boundaries (EFB) inside the map are defined from geometric boundaries, the shape and position of which are determined by the following parameters.

ACENT	:	arbitrary angle, used for the positioning of the EFB's.
ω	:	azimuth of an EFB with respect to *ACENT*
θ	:	angle of a boundary with respect to its azimuth (wedge angle)
R_1, R_2	:	radius of curvature of an EFB
U_1, U_2	:	extent of the linear part of the EFB.

At any node of the map mesh, the value of the Z component of the field is calculated as

$$B_Z = \mathcal{F} * B_0 * \left(1 + N * \left(\frac{R-RM}{RM}\right) + B * \left(\frac{R-RM}{RM}\right)^2 + G * \left(\frac{R-RM}{RM}\right)^3\right) \tag{4.4.1}$$

where N, B and G are respectively the first, second and third order field indices and $\mathcal{F}$ is the fringe field coefficient, while the X and Y components of the field are assumed to be zero on the map mesh.

Calculation of the Fringe Field Coefficient

With each EFB a realistic extent of the fringe field, λ, is associated (Figs. 10A and 10B), and a fringe field coefficient F is calculated. In the following λ stands for either λ_E (Entrance), λ_S (Exit) or λ_L (Lateral EFB). If a node of the map mesh is at a distance of the EFB larger than λ, then $F = 0$ outside the field map and $\mathcal{F} = 1$ inside. If a node is inside the fringe field zone, then F is calculated as follows.
Two options are available, for the calculation of F, depending on the value of ξ.
If $\xi \geq 0$, F is a second order type fringe field (Fig. 11) given by

$$F = \frac{1}{2}\frac{(\lambda - s)^2}{\lambda^2 - \xi^2} \quad \text{if } \xi \leq s \leq \lambda \tag{4.4.2}$$

$$F = 1 - \frac{1}{2}\frac{(\lambda - s)^2}{\lambda^2 - \xi^2} \quad \text{if } -\lambda \leq s \leq -\xi \tag{4.4.3}$$

where s is the distance to the EFB, and

$$F = \frac{1}{2} + \frac{s}{\lambda + \xi} \quad \text{if } 0 \leq s \leq \xi \tag{4.4.4}$$

$$F = \frac{1}{2} - \frac{s}{\lambda + \xi} \quad \text{if } -\xi \leq s \leq 0 \tag{4.4.5}$$

This simple model allows a rapid calculation of the fringe field, but may lead to erratic behavior of the field when extrapolating out of the median plane, due to the discontinuity of d^2B/ds^2 at $s = \pm\xi$ and $s = \pm\lambda$. For more accuracy it is better to use the next option.

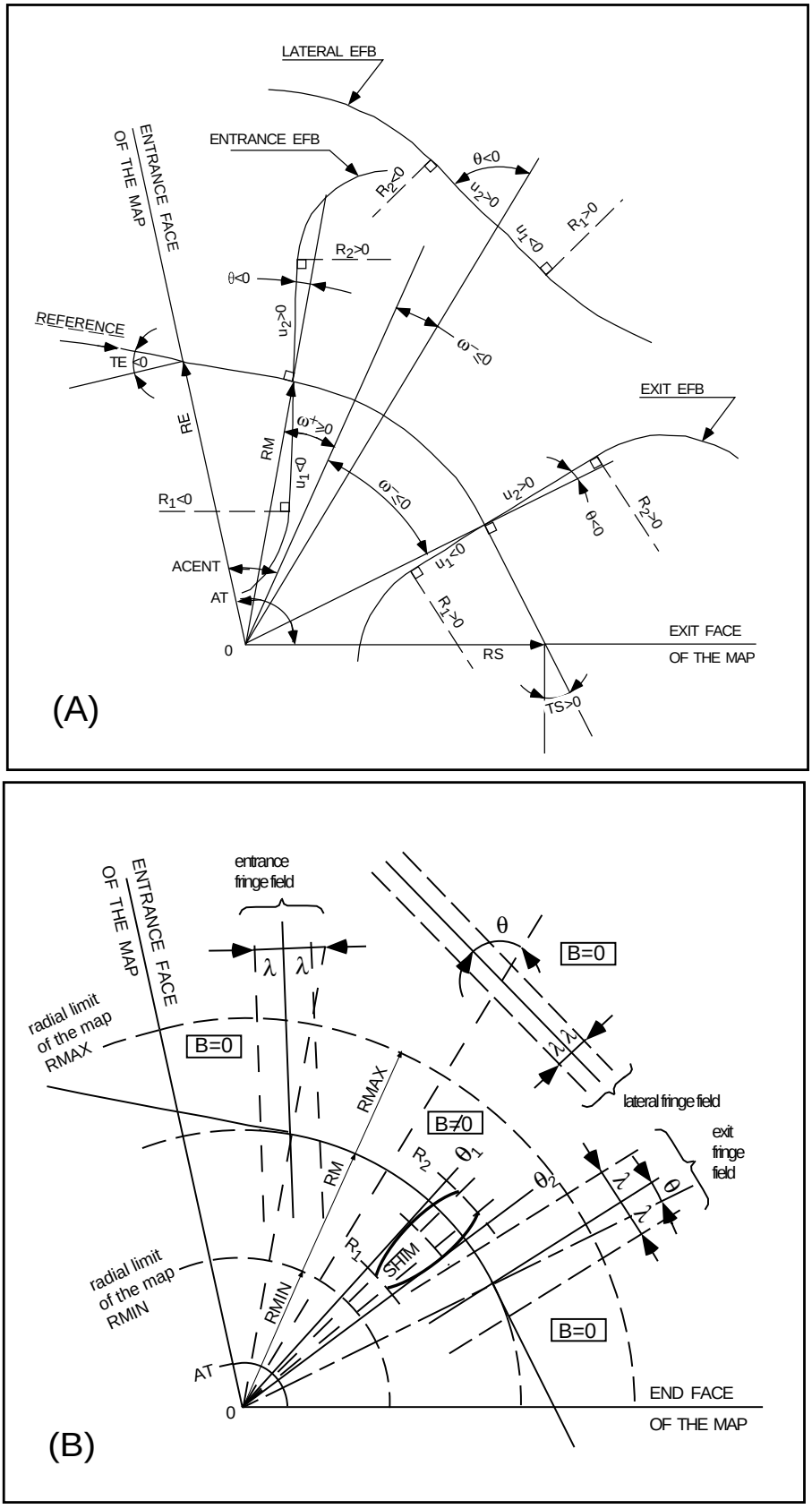

Figure 10: A: Parameters used to define the field map and geometric boundaries.
B: Parameters used to define the field map and fringe fields.

If $\xi = -1$, F is an exponential type fringe field (Fig. 11) given by [17]

$$F = \frac{1}{1 + \exp P(s)} \tag{4.4.6}$$

where s is the distance to the EFB, and

$$P(s) = C_0 + C_1 \left(\frac{s}{\lambda}\right) + C_2 \left(\frac{s}{\lambda}\right)^2 + C_3 \left(\frac{s}{\lambda}\right)^3 + C_4 \left(\frac{s}{\lambda}\right)^4 + C_5 \left(\frac{s}{\lambda}\right)^5 \tag{4.4.7}$$

The values of the coefficients C_0 to C_5 should be such that the derivatives of B_Z with respect to s be negligible at $s = \pm\lambda$, so as not to perturb the extrapolation of $\vec{B}$ out of the median plane (this restriction no longer holds in the improved version *DIPOLE*).
It is also possible to simulate a shift of the EFB, by giving a non zero value to the parameter *SHIFT*. s is then changed to $s-$ *SHIFT* in the previous equation. This allows small variations of the total magnetic length.
Let F_E (respectively F_S, F_L) be the fringe field coefficient attached to the entrance (respectively exit, lateral) EFB following eqs. above. At any node of the map mesh, the resulting value of the fringe field coefficient (eq. 4.4.1) is (Fig. 12)

$$\mathcal{F} = F_E * F_S * F_L$$

($F_L = 1$ if no lateral EFB is requested).

The Mesh of the Field Map

The magnetic field is calculated at the nodes of a mesh with polar coordinates, in the median plane. The radial step is given by

$$\delta R = \frac{RMAX \text{ - } RMIN}{IRMAX - 1}$$

and the angular step by

$$\delta\theta = \frac{AT}{IAMAX - 1}$$

where, *RMIN* and *RMAX* are the lower and upper radial limits of the field map, and AT is its total angular aperture (Fig. 10B). *IRMAX* and *IAMAX* are the total number of nodes in the radial and angular directions.

Simulating Field Defects and Shims

Once the initial map is calculated, it is possible to modify it by means of the parameter *NBS*, so as to simulate field defects or shims.

If NBS $= -2$, the map is globally modified by a perturbation proportional to $R - R_0$, where R_0 is an arbitrary radius, with an amplitude $\Delta B_Z / B_0$, so that B_Z at the nodes of the mesh is replaced by

$$B_Z * \left(1 + \frac{\Delta B_Z}{B_0} \frac{R - R_0}{RMAX - RMIN}\right)$$

If NBS $= -1$, the perturbation is proportional to $\theta - \theta_0$, and B_Z is replaced by

$$B_Z * \left(1 + \frac{\Delta B_Z}{B_0} \frac{\theta - \theta_0}{AT}\right)$$

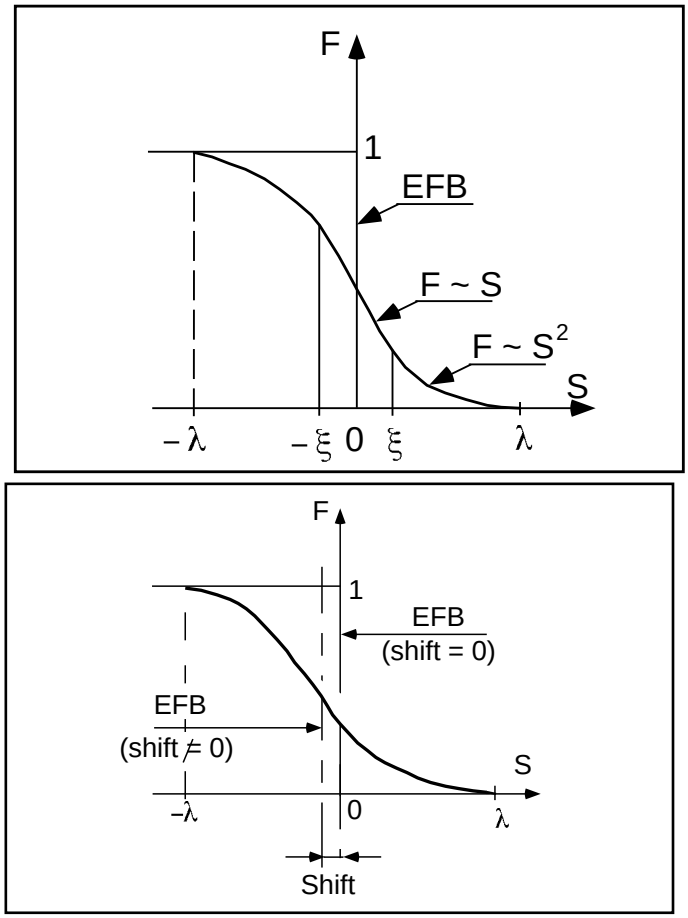

Figure 11: Second order type fringe field (upper plot) and exponential type fringe field (lower plot).

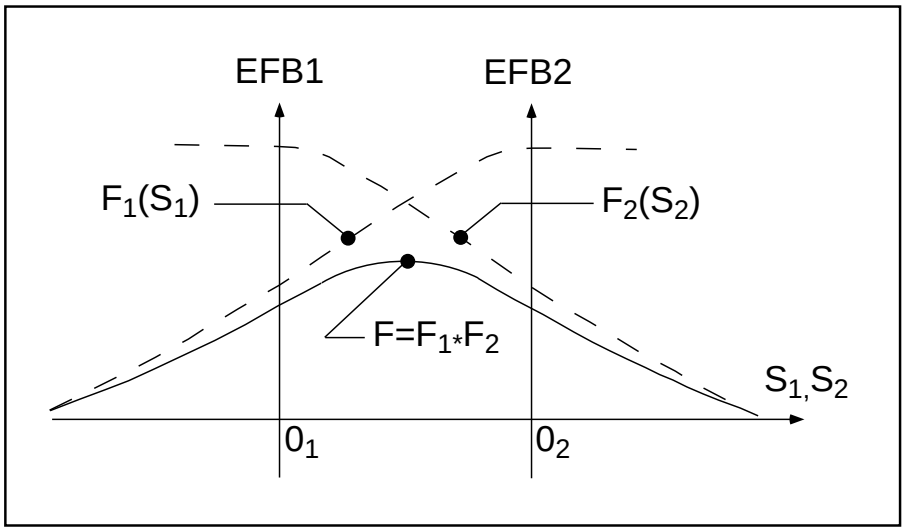

Figure 12: Effective value of $\mathcal{F}$ for overlapping fringe fields F_1 and F_2 centered at O_1 and O_2.

If NBS $\geq$ 1, then *NBS* shims are introduced at positions $\frac{R_1+R_2}{2}$, $\frac{\theta_1+\theta_2}{2}$ (Fig. 13) [18]
The initial field map is modified by shims with second order profiles given by

$$\theta = \left(\gamma + \frac{\alpha}{\mu}\right) \beta \frac{X^2}{\rho^2}$$

where X is shown in Fig. 13, $\rho = \frac{R_1+R_2}{2}$ is the central radius, α and γ are the angular limits of the shim, β and μ are parameters.
At each shim, the value of B_Z at any node of the initial map is replaced by

$$B_Z * \left(1 + F\theta * FR * \frac{\Delta B_Z}{B_0}\right)$$

where $F\theta = 0$ or $FR = 0$ outside the shim, and $F\theta = 1$ and $FR = 1$ inside.

Extrapolation Off Median Plane

The vector field $\vec{B}$ and its derivatives in the median plane are calculated by means of a second or fourth order polynomial interpolation, depending on the value of the parameter *IORDRE* (*IORDRE*=2, 25 or 4, see section 1.4.2). The transformation from polar to Cartesian coordinates is performed following eqs. (1.4.9 or 1.4.10). Extrapolation off median phase is then performed by means of Taylor expansions following the procedure described in section 1.3.2.

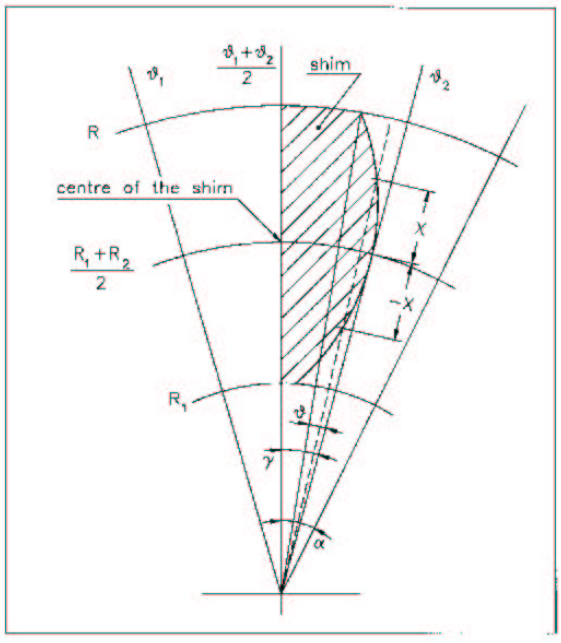

Figure 13: A second order profile shim. The shim is centered at $\frac{(R_1+R_2)}{2}$ and $\frac{(\theta_1+\theta_2)}{2}$.

AUTOREF: Automatic transformation to a new reference frame

AUTOREF positions the new reference frame following 3 options:

If I = 1, *AUTOREF* is equivalent to

$$CHANGREF[XCE = 0, YCE = Y(1), ALE = T(1)]$$

so that the new reference frame is at the exit of the last element, with particle 1 at the origin with its horizontal angle set to $T = 0$.

If I = 2, it is equivalent to

$$CHANGREF[XW, YW, T(1)]$$

so that the new reference frame is at the position (XW, YW) of the waist (calculated automatically in the same way as for *IMAGE*) of the three rays number 1, 4 and 5 (compatible for instance with *OBJET*, *KOBJ* = 5, 6 together with the use of *MATRIX*) while $T(1)$ is set to zero.

If I = 3, it is equivalent to

$$CHANGREF[XW, YW, T(I1)]$$

so that the new reference frame is at the position (XW, YW) of the waist (calculated automatically in the same way as for *IMAGE*) of the three rays number I1, I2 and I3 specified as data, while $T(1)$ is set to zero.

BEND: Bending magnet

BEND is one of the several keywords available for the simulation of dipole magnets. It presents the interest of easy handling, and is well adapted for the simulation of synchrotron dipoles and such other regular dipoles as sector magnets with wedge angles.
The dipole simulation is performed from the magnet geometrical length XL, from the skew angle (rotation *wrt.* the X axis, useful for obtaining vertical deviation magnet), and from the field $B1$ such that in absence of fringe field the deviation θ satisfies $XL = 2\frac{BORO}{B1}\sin(\frac{\theta}{2})$.
Then follows the description of the entrance and exit EFB's and fringe fields. The model is the same as for *DIPOLE*. The wedge angles W_E (entrance) and W_S (exit) are defined with respect to the sector magnet, with the signs described in Fig. 14. Within a distance $\pm X_E(\pm X_S)$ on both sides of the entrance (exit) EFB, the fringe field model is used; elsewhere, the field is supposed to be uniform.
If λ_E (resp. λ_S) is zero sharp edge field model is assumed at entrance (resp. exit) of the magnet and X_E (resp. X_S) is set to zero. In this case, the wedge angle vertical first order focusing effect (if $\vec{B}1$ is non zero) is simulated at magnet entrance and exit by a kick $P_2 = P_1 - Z_1\tan(\epsilon/\rho)$ applied to each particle (P_1, P_2 are the vertical angles upstream and downstream the EFB, Z_1 the vertical particle position at the EFB, ρ the local horizontal bending radius and ϵ the wedge angle experienced by the particle ; ϵ depends on the horizontal angle T).
Magnet (mis-)alignement is assured by *KPOS*, with special features allowing some degrees of automatism useful for periodic structures (section 4.6.5).

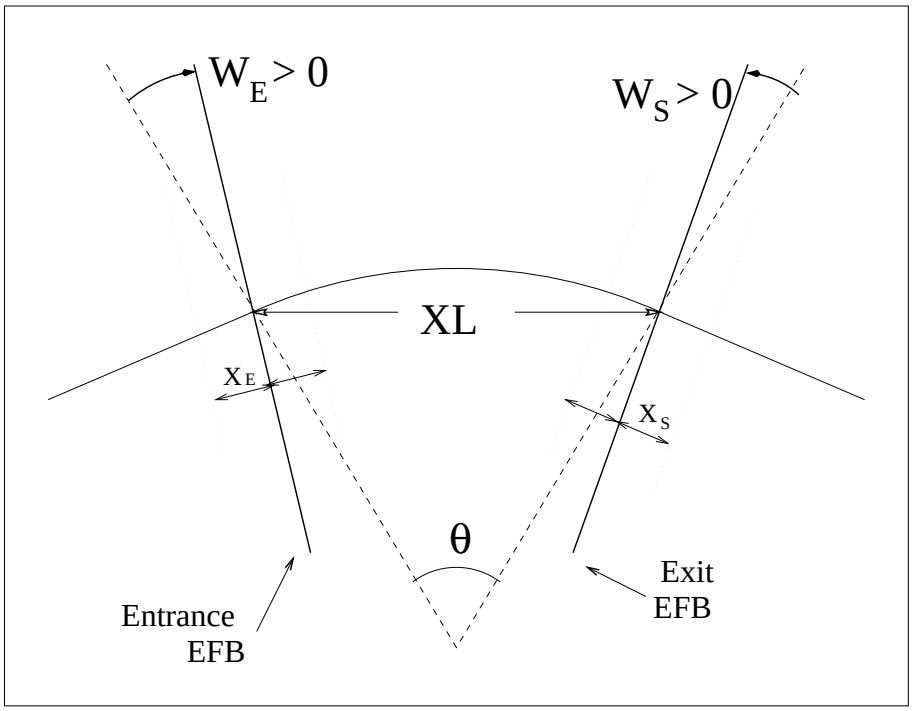

Figure 14: Geometry and parameters in *BEND*: XL = length, θ = deviation, W_E, W_S are the entrance and exit wedge angles.

BREVOL: 1-D uniform mesh magnetic field map

BREVOL reads a 1-D axial field map from a storage data file, whose content must fit the following *FORTRAN* reading sequence

```
      OPEN (UNIT = NL, FILE = FNAME, STATUS = 'OLD' [,FORM='UNFORMATTED'])
      DO 1 I = 1, IX
        IF (BINARY) THEN
              READ(NL) X(I), BX(I)
        ELSE
              READ(NL,*) X(I), BX(I)
        ENDIF
1     CONTINUE
```

where IX is the number of nodes along the (symmetry) X-axis, $X(I)$ their coordinates, and $BX(I)$ the values of the X component of the field. BX is normalized with *BNORM* factor prior to ray-tracing, as well X is normalized with a *XNORM* coefficient (usefull to convert to centimeters, the working units in **zgoubi**). For binary files, *FNAME* must begin with 'B_ ' or 'b_ ', a flag 'BINARY' will thus be set to '.TRUE.'.

X-cylindrical symmetry is assumed, resulting in BY and BZ taken to be zero on axis. $\vec{B}(X,Y,Z)$ and its derivatives along a particle trajectory are calculated by means of a 5-point polynomial fit followed by second order off-axis Taylor series extrapolation (see sections 1.3.1, 1.4.1).

Entrance and/or exit integration boundaries may be defined in the same way as in *CARTEMES* by means of the flag ID and coefficients A, B, C, etc.

CARTEMES: 2-D Cartesian uniform mesh magnetic field map

CARTEMES was originally dedicated to the reading and processing of the measured median plane field maps of the QDD spectrometer SPES2 at Saclay. However, it can be used for the reading of any other 2-D median plane maps, provided that the format of the field data storage file fits the following *FORTRAN* sequence

```
OPEN (UNIT = NL, FILE = FNAME, STATUS = 'OLD' [,FORM='UNFORMATTED'])
       IF (BINARY) THEN
         READ(NL) (Y(J), J=1, JY)
       ELSE
         READ(NL,FMT='(10F8.2)') (Y(J), J=1, JY)
       ENDIF
       DO 1 I=1, IX
  IF (BINARY) THEN
    READ(NL) X(I), (BMES(I,J), J=1, JY)
  ELSE
    READ(NL,FMT='(10F8.1)') X(I), (BMES(I,J), J=1, JY)
         ENDIF
  1    CONTINUE
```

where, IX and JY are the number of longitudinal and transverse horizontal nodes of the uniform mesh, and $X(I)$, $Y(J)$ their coordinates. *FNAME* is the file containing the field data. For binary files, *FNAME* must begin with 'B_ ' or 'b_', a flag 'BINARY' will thus be set to '.TRUE.'.

The measured field *BMES* is normalized with *BNORM*,

$$B(I,J) = BMES(I,J) \times BNORM$$

As well the longitudinal coordinate X is normalized with a *XNORM* coefficient (usefull to convert to centimeters, the working units in **zgoubi** .
The vector field, $\vec{B}$, and its derivatives out of the median plane are calculated by means of a second or fourth order polynomial interpolation, depending on the value of the parameter *IORDRE* (*IORDRE* = 2, 25 or 4, see section 1.4.2).

In case a particle exits the mesh, its *IEX* flag is set to -1 (see section 4.6.8 on page 126), however it is still tracked with the field being *extrapolated* from the closest mesh nodes of the map. Note that such extrapolation process may induce eratic behavior if the distance from the mesh gets too large.

Entrance and/or exit integration boundaries can be defined with the flag ID, as follows (Fig. 15).

If ID = 1: the integration in the field is terminated on a boundary with equation $A'X + B'Y + C' = 0$, and then the trajectories are extrapolated linearly onto the exit end of the map.

If ID = −1: an entrance boundary is defined, with equation $A'X + B'Y + C' = 0$, up to which trajectories are first extrapolated linearly from the map entrance end, prior to being integrated in the field.

If ID ≥ 2: one entrance boundary, and $ID - 1$ exit boundaries are defined, as above. The integration in the field terminates on the last $(ID - 1)$ exit boundary. No extrapolation onto the map exit end is performed in this case.

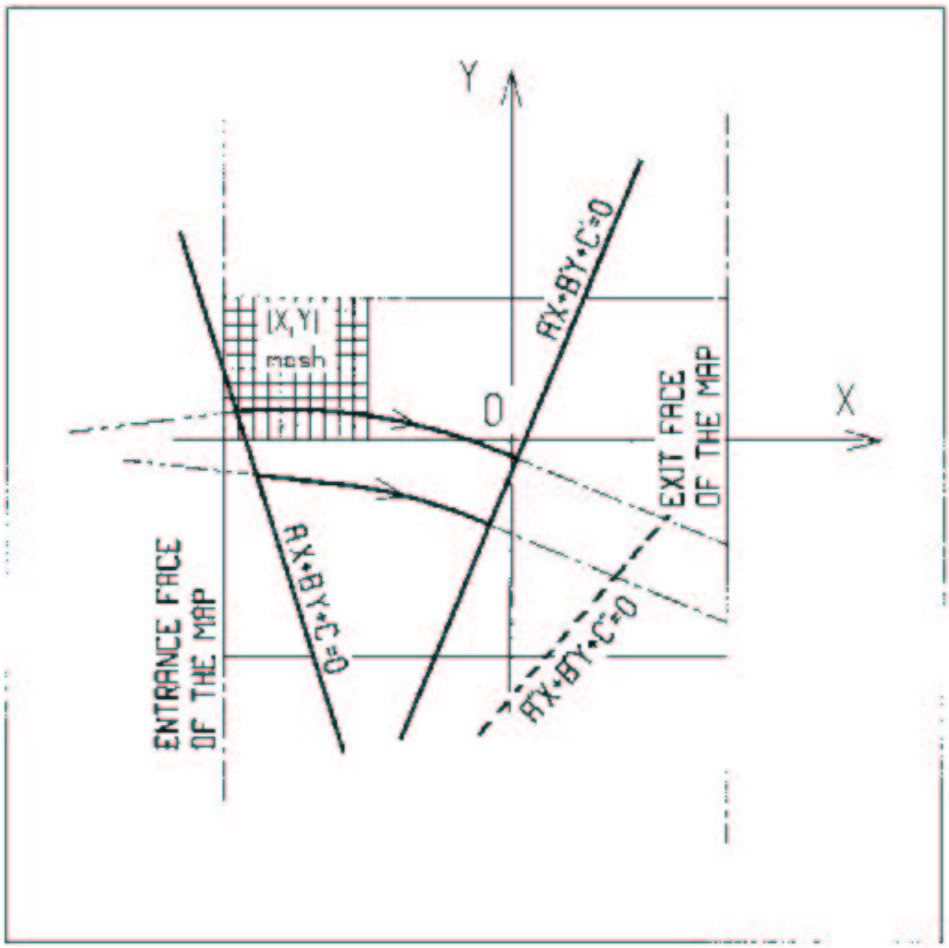

Figure 15: OXY is the coordinate system of the mesh. Integration boundaries may be defined, using $ID \neq 0$: particle coordinates are extrapolated linearly from the entrance face of the map, onto the boundary $A'X+B'Y+C'=0$; after ray-tracing inside the map and terminating on the boundary $AX+BY+C=0$, coordinates are extrapolated linearly onto the exit face of the map if $ID=2$, or terminated on the last $(ID-1)$ boundary if $ID>2$.

CAVITE: Accelerating cavity

CAVITE provides an analytical simulation of a (zero length) accelerating cavity; it can be used in conjunction with keywords *REBELOTE* and *SCALING* for the simulation of multiturn tracking with synchrotron acceleration (see section 4.6.7). It must be preceded by *PARTICUL* for the definition of mass M and charge q.

If IOPT = 0: *CAVITE* is switched off.

If IOPT = 1: *CAVITE* simulates the R.F. cavity of a synchrotron accelerator. Normally the keyword *CAVITE* appears **at the end** of the optical structure (the periodic motion over $IT = 1$, $NPASS + 1$ turns is simulated by means of the keyword *REBELOTE*, option K = 99 while R.F. and optical elements timings are simulated by means of *SCALING* — see section 4.6.7). The synchrotron motion of any of the *IMAX* particles of a beam is obtained by solving the following mapping

$$\begin{cases} \phi_2 - \phi_1 = 2\pi\, f_{RF} \left(\dfrac{\ell}{\beta c} - \dfrac{\mathcal{L}}{\beta_s c} \right) \\ W_2 - W_1 = q\hat{V} \sin\phi_1 \end{cases}$$

where

ϕ	=	R.F. phase; $\phi_2 - \phi_1$ = variation of ϕ between two traversals
W	=	kinetic energy; $W_2 - W_1$ = energy gain at a traversal of *CAVITE*
$\mathcal{L}$	=	length of the synchronous closed orbit (to be calculated by prior ray-tracing, see the bottom NOTE)
ℓ	=	orbit length of the particle between two traversals
$\beta_s c$	=	velocity of the (virtual) synchronous particle
βc	=	velocity of the particle
$\hat{V}$	=	peak R.F. voltage
q	=	particle electric charge.

The R.F. frequency f_{RF} is a multiple of the synchronous revolution frequency, and is obtained from the input data, following

$$f_{RF} = \frac{hc}{\mathcal{L}} \frac{q(B\rho)_s}{(q^2(B\rho)_s^2 + (Mc)^2)^{1/2}}$$

where

h	=	harmonic number of the R.F
M	=	mass of the particle
c	=	velocity of light.

The current rigidity $(B\rho)_s$ of the synchronous particle is obtained from the timing law specified by means of *SCALING* following $(B\rho)_s$ = *BORO* · *SCALE(TIMING)* (see *SCALING* for the meaning and calculation of the scale factor *SCALE(TIMING)*). If *SCALING* is not used, $(B\rho)_s$ is assumed to keep the constant value *BORO*given in the object description (see *OBJET* for instance).
The velocity βc of a particle is calculated from its current rigidity

$$\beta = \frac{q(B\rho)}{\sqrt{q^2(B\rho)^2 + (Mc)^2}}$$

The velocity $\beta_s c$ of the synchronous particle is obtained in the same way from

$$\beta_s = \frac{q(B\rho)_s}{\sqrt{q^2(B\rho)_s^2 + (Mc)^2}}$$

The kinetic energies and rigidities involved in these formulae are related by

$$q(B\rho) = \sqrt{W(W + 2Mc^2)}$$

Finally, the initial conditions for the mapping, at the first turn, are the following

- For the (virtual) synchronous particle

$$\phi_1 = \phi_s = \text{synchronous phase}$$
$$(B\rho)_{1s} = BORO$$

- For any of the $I = 1$, $IMAX$ particles of the beam

$$\phi_{1I} = \phi_s = \text{synchronous phase}$$
$$(B\rho)_{1I} = BORO * D_I$$

where the quantities $BORO$and D_I are given in the object description.

Calculation of the coordinates

Let $p_I = \left[p_{XI}^2 + p_{YI}^2 + p_{ZI}^2\right]^{1/2}$ be the momentum of particle I at the exit of the cavity, while $p_{I_0} = \left[p_{XI_0}^2 + p_{YI_0}^2 + p_{ZI_0}^2\right]^{1/2}$ is its momentum at the entrance. The kick in momentum is assumed to be fully longitudinal, resulting in the following relations between the coordinates at the entrance (denoted by the index zero) and at the exit

$$\begin{aligned} p_{XI} &= \left[p_I^2 - (p_{I_0}^2 - p_{XI_0}^2)\right]^{1/2} \\ p_{YI} &= p_{YI_0}, \quad \text{and} \quad p_{ZI} = p_{ZI_0} \quad \text{(longitudinal kick)} \\ X_I &= X_{I_0}, \quad Y_I = Y_{I_0} \quad \text{and} \quad Z_I = Z_{I_0} \quad \text{(zero length cavity)} \end{aligned}$$

and for the angles (see Fig. 1)

$$\left.\begin{aligned} T_I &= \text{Atg}\left(\frac{p_{YI}}{p_{XI}}\right) \\ P_I &= \text{Atg}\left(\frac{P_{ZI}}{(p_{XI}^2 + p_{YI}^2)^{1/2}}\right) \end{aligned}\right\} \quad \text{(damping of the transverse motion)}$$

If IOPT = 2 : the same simulation of a synchrotron R.F. cavity, as for **IOPT = 1**, is performed, except that the keyword *SCALING* (family *CAVITE*) is not taken into account in this option : the increase in kinetic energy at each traversal, for the synchronous particle, is

$$\Delta W_s = q\hat{V} \sin\phi_s$$

where the synchronous phase ϕ_s is given in the input data. From this, the calculation of the law $(B\rho)_s$ and the R.F. frequency f_{RF} follows, according to the formulae given in $IOPT = 1$.

If IOPT = 3: acceleration without synchrotron motion. Any particle will be given a kick

$$\Delta W = q\hat{V} \sin\phi_s$$

where $\hat{V}$ and ϕ_s are input data.

NOTE: Calculation of the closed orbit.
Due to the fringe fields, the horizontal closed orbit may not coincide with the ideal axis of the optical elements. One way to calculate it at the beginning of the structure (*i.e.* where the initial particle coordinates have to be defined) is to ray-trace a single particle over a significantly high number of turns, starting with the initial condition ($Y_0 = T_0 = Z_0 = P_0 = 0$), and so as to obtain a statistically well-defined phase-space ellipse. The initial conditions of the closed orbit then correspond to the coordinates Y_c and T_c of the center of this ellipse. Next, ray-tracing over one turn a particle starting with the initial condition (Y_c, T_c, $Z_0 = P_0 = 0$) will provide the length $\mathcal{L}$ (namely, the $F(6,1)$ coordinate) of the closed orbit.

CHAMBR: Long transverse aperture limitation

CHAMBR causes the identification, counting and stopping of particles that reach the transverse limits of the vacuum chamber. The chamber can be either rectangular (*IFORM* = 1) or elliptic (*IFORM* = 2). The chamber is centered at YC, ZC and has transverse dimensions $\pm YL$ and $\pm ZL$ such that any particle will be stopped if its coordinates Y, Z satisfy

$$(Y - YC)^2 \geq YL^2 \text{ or } (Z - ZC)^2 \geq ZL^2 \quad \text{if} \quad IFORM = 1$$
$$\frac{(Y - YC)^2}{YL^2} + \frac{(Z - ZC)^2}{ZL^2} \geq 1 \quad \text{if} \quad IFORM = 2$$

The conditions introduced with *CHAMBR* are valid along the optical structure until the next occurrence of the keyword *CHAMBR*. Then, if $IL = 1$ the aperture is possibly modified by introducing new values of YC, ZC, YL and ZL, or, if $IL = 2$ the chamber ends and information is printed concerning those particles that have been stopped.

The testing is done in optical elements at each integration step, between the *EFB*'s. For instance, in *QUADRUPO* there will be no testing from $-X_E$ to 0 and from XL to $XL + X_S$, but only from 0 to XL; in *DIPOLE*, there is no testing as long as the *ENTRANCE EFB* is not reached, and testing is stopped as soon as the *EXIT* or *LATERAL EFB*'s are passed.

In polar coordinate optical elements Y stands for the radial coordinate (e.g. with *DIPOLE*, see Figs. 3C and 10). Therefore, centering *CHAMBR* at $YC = RM$ simulates a chamber curved with radius RM, and having a radial acceptance $RM \pm YL$. The testing is done in *ESL* (*DRIFT*) at the beginning and the end, and only for positive drifts. There is no testing in *CHANGREF*.

When a particle is stopped, its index *IEX* (see *OBJET* and section 4.6.8) is set to the value -4, and its actual path length is stored in the array *SORT* for possible further statistical purposes.

CHANGREF: Transformation to a new reference frame

CHANGREF transports the particles to a new reference frame. It can be used anywhere in a structure. The new coordinates of the particles Y_2, T_2, Z_2 and P_2 and the path length S_2 are deduced from the old ones Y_1, T_1, Z_1, P_1 and S_1 by

$$\begin{aligned} T_2 &= T_1 - ALE \\ Y_2 &= \frac{(Y_1 - YCE)\cos T_1 + XCE \sin T_1}{\cos T_2} \\ DL^2 &= (XCE - Y_2 \sin ALE)^2 + (YCE - Y_1 + Y_2 \cos ALE)^2 \\ Z_2 &= Z_1 + DL \mathrm{tg} P_1 \\ S_2 &= S_1 + \frac{DL}{\cos P_1} \\ P_2 &= P_1 \end{aligned}$$

where, XCE and YCE are shifts in the horizontal plane along,respectively, X- and Y-axis, and ALE is a rotation around the Z-axis. DL is given the sign of $XCE - Y_2 \sin(ALE)$. This keyword may for instance be used for positioning optical elements, or for setting a reference frame at the entrance or exit of field maps. Effects of *CHANGREF* on spin tracking, particle decay and gas-scattering are taken into account (but not on synchrotron radiation).

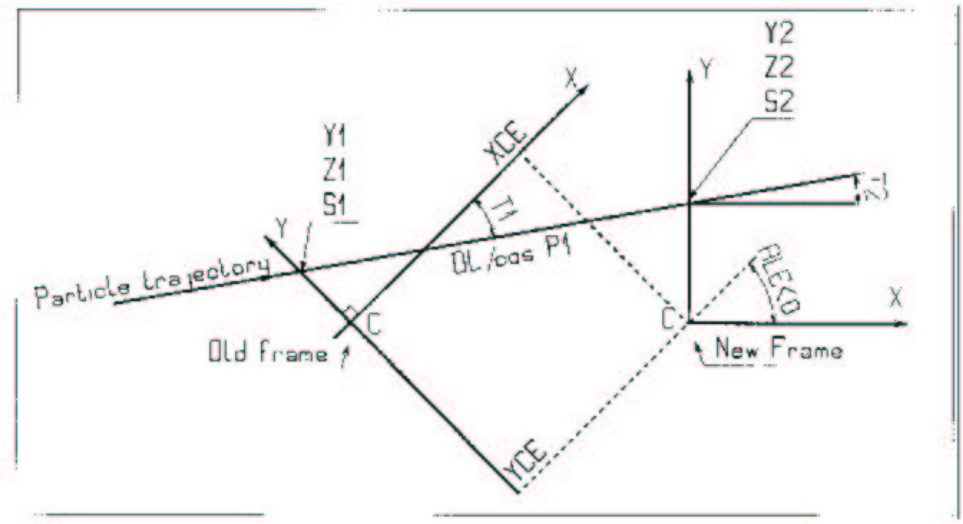

Figure 16: Scheme of the *CHANGREF* procedure.

CIBLE or TARGET: Generate a secondary beam from target interaction

The reaction is $1 + 2 \longrightarrow 3 + 4$ with the following parameters

Laboratory momentum	$p_1 \equiv 0$	p_2	p_3	p_4
Rest mass	M_1	M_2	M_3	M_4
Total energy in laboratory	$M_1 c^2$	W_2	W_3	W_4

The geometry of the interaction is shown in Fig. 17.

The angular sampling at the exit of the target consists of the NT coordinates $0, \pm TS, \pm 2{*}TS \ldots \pm(NT-1){*}TS/2$ in the median plane, and the NP coordinates $0, \pm PS, \pm 2 * PS \ldots \pm(NP-1) * PS/2$ in the vertical plane.

The position of B downstream is deduced from that of A upstream by a transformation equivalent to two transformations using *CHANGREF*, namely

$$CHANGREF(XCE = YCE = 0, \quad ALE = \beta)$$

followed by

$$CHANGREF(XCE = YCE = 0, \quad ALE = \theta - \beta).$$

Particle 4 is discarded, while particle 3 continues. The energy loss Q is related to the variable mass M_4 by

$$Q = M_1 + M_2 - (M_3 + M_4) \qquad \text{and} \qquad dQ = -dM_4$$

The momentum sampling of particle 3 is derived from conservation of energy and momentum, according to

$$M_1 c^2 + W_2 = W_3 + W_4$$
$$p_4^2 = p_2^2 + p_3^2 - 2 p_2 p_3 \cos(\theta - T)$$

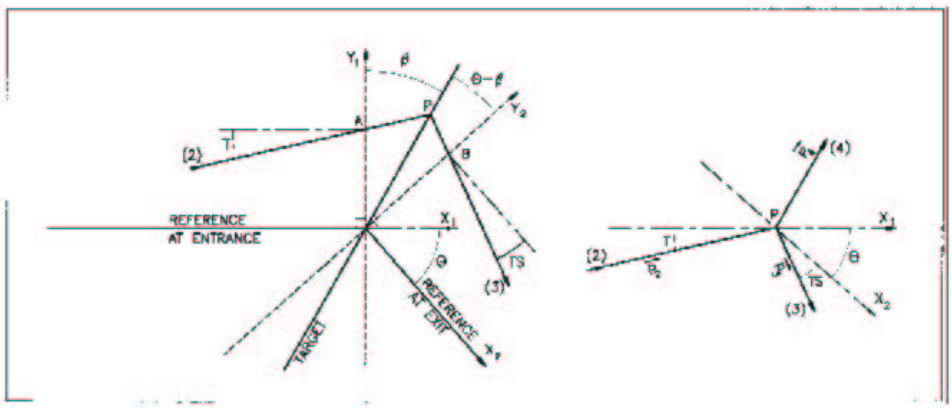

Figure 17: Scheme of the principles of *CIBLE (TARGET)*
A, T = position, angle of incoming particle 2 in the entrance reference frame
P = position of the interaction
B, T = position, angle of the secondary particle in the exit reference frame
θ = angle between entrance and exit frames
β = tilt angle of the target

COLLIMA: Collimator

COLLIMA acts as a mathematical aperture of zero length. It causes the identification, counting and stopping of particles that reach the aperture limits.

Phisical aperture

A physical aperture can be either rectangular (*IFORM* = 1) or elliptic (*IFORM* = 2). The collimator is centered at YC, ZC and has transverse dimensions $\pm YL$ and $\pm ZL$ such that any particle will be stopped if its coordinates Y, Z satisfy

$$(Y - YC)^2 \geq YL^2 \text{ or } (Z - ZC)^2 \geq ZL^2 \quad \text{if} \quad IFORM = 1$$
$$\frac{(Y - YC)^2}{YL^2} + \frac{(Z - ZC)^2}{ZL^2} \geq 1 \quad \text{if} \quad IFORM = 2$$

Longitudinal phase-space collimation

COLLIMA can act as a longitudinal phase-space aperture, coordinates acted on are selected with *IFORM.J*. Any particle will be stopped if its horizontal (h) and vertical (v) coordinates satisfy

$$(h \leq h_m inorh \geq hmax) or (v \leq v_m inorv \geq vmax)$$

wherein, h is path length S if *IFORM*=6 or time if *IFORM*=7, and v is 1+DP/P if J=1 or kinetic energy if J=2 (provided mass and charge have been defined using the keyword *PARTICUL*).
If *IFORM*=11 (respectively 12) then ϵ_Y/π (respectively ϵ_Z/π) is to be specified by the user as well as $\alpha_{Y,Z}$, $\beta_{Y,Z}$. If *IFORM*=14 (respectively 15) then α_Y and β_Y (respectively α_Z, β_Z) are computed by **zgoubi** by prior matching of the particle population, only $\epsilon_{Y,Z}/\pi$ need be specified by the user.

Phase-space collimation

COLLIMA can act as a phase-space aperture. Any particle will be stopped if its coordinates satisfy

$$\gamma_Y Y^2 + 2\alpha_Y YT + \beta_Y T^2 \geq \epsilon_Y/\pi \quad \text{if} \quad IFORM = 11 \text{ or } 14$$
$$\gamma_Z Z^2 + 2\alpha_Z ZP + \beta_Z P^2 \geq \epsilon_Z/\pi \quad \text{if} \quad IFORM = 12 \text{ or } 15$$

If *IFORM*=11 (respectively 12) then ϵ_Y/π (respectively ϵ_Z/π) is to be specified by the user as well as $\alpha_{Y,Z}$, $\beta_{Y,Z}$. If *IFORM*=14 (respectively 15) then α_Y and β_Y (respectively α_Z, β_Z) are computed by **zgoubi** by prior matching of the particle population, only $\epsilon_{Y,Z}/\pi$ need be specified by the user.

When a particle is stopped, its index *IEX* (see *OBJET* and section 4.6.8) is set to the value -4, and its actual path length is stored in the array *SORT* for possible further statistical purposes (e.g. with *HISTO*).

DECAPOLE: Decapole magnet (Fig. 18)

The meaning of parameters for *DECAPOLE* is the same as for *QUADRUPO*.
In fringe field regions the magnetic field $\vec{B}(X,Y,Z)$ and its derivatives up to fourth order are derived from the scalar potential approximated to the 5th order in Y and Z

$$V(X,Y,Z) = G\left(Y^4Z - 2Y^2Z^3 + \frac{Z^5}{5}\right)$$
$$\text{with } G_0 = \frac{B_0}{R_0^4}$$

Outside fringe field regions, or everywhere in sharp edge decapole ($\lambda_E = \lambda_S = 0$) , $\vec{B}(X,Y,Z)$ in the magnet is given by

$$B_X = 0$$
$$B_Y = 4G_0(Y^2 - Z^2)YZ$$
$$B_Z = G_0(Y^4 - 6Y^2Z^2 + Z^4)$$

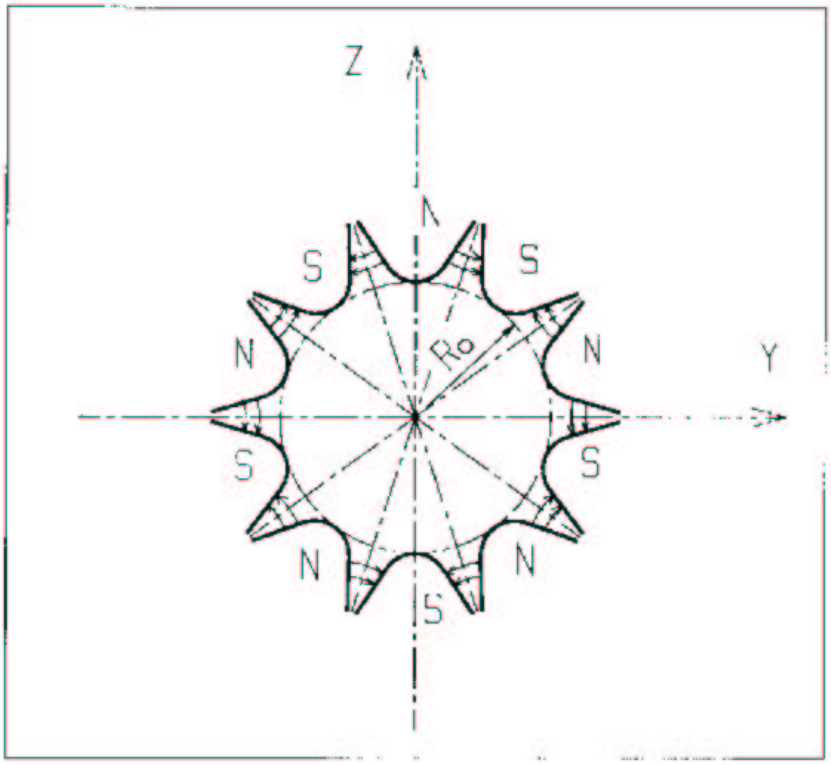

Figure 18: Decapole magnet

DIPOLE: Generation of a dipole magnet 2-D map

DIPOLE is a more recent, simpler and improved version of *AIMANT*.

The keyword *DIPOLE* provides an automatic generation of a dipole field map in polar coordinates. The extent of the map is defined by the following parameters, as shown in Figs. 10A and 10B.

AT	:	total angular aperture
RM	:	mean radius used for the positioning of field boundaries
RMIN, RMAX	:	minimum and maximum radii

The 2 or 3 effective field boundaries (EFB) inside the map are defined from geometric boundaries, the shape and position of which are determined by the following parameters.

ACENT	:	arbitrary inner angle, used for EFB's positioning
ω	:	azimuth of an EFB with respect to *ACENT*
θ	:	angle of an EFB with respect to its azimuth (wedge angle)
R_1, R_2	:	radius of curvature of an EFB
U_1, U_2	:	extent of the linear part of an EFB.

At any node of the map mesh, the value of the field is calculated as

$$B = \mathcal{F} * B_0 * \left(1 + N * \left(\frac{R - RM}{RM}\right) + B * \left(\frac{R - RM}{RM}\right)^2 + G * \left(\frac{R - RM}{RM}\right)^3\right) \tag{4.4.8}$$

where N, B and G are respectively the first, second and third order field indices and $\mathcal{F}$ is the fringe field coefficient, while the X and Y components of the field are assumed to be zero on the mesh plane.

Calculation of the Fringe Field Coefficient

With each EFB a realistic extent of the fringe field, λ (normally equal to the gap size), is associated and a fringe field coefficient F is calculated. In the following λ stands for either λ_E (Entrance), λ_S (Exit) or λ_L (Lateral EFB).

F is an exponential type fringe field (Fig. 11) given by [17]

$$F = \frac{1}{1 + \exp P(s)}$$

where s is the distance to the EFB, and

$$P(s) = C_0 + C_1\left(\frac{s}{\lambda}\right) + C_2\left(\frac{s}{\lambda}\right)^2 + C_3\left(\frac{s}{\lambda}\right)^3 + C_4\left(\frac{s}{\lambda}\right)^4 + C_5\left(\frac{s}{\lambda}\right)^5$$

It is also possible to simulate a shift of the *EFB*, by giving a non zero value to the parameter *SHIFT*. s is then changed to $s - SHIFT$ in the previous equation. This allows small variations of the total magnetic length.

Let F_E (respectively F_S, F_L) be the fringe field coefficient attached to the entrance (respectively exit, lateral) EFB. At any node of the map mesh, the resulting value of the fringe field coefficient (eq. 4.4.8) is

$$\mathcal{F} = F_E * F_S * F_L$$

($F_L = 1$ if no lateral EFB is requested).

The Mesh of the Field Map

The magnetic field is calculated at the nodes of a mesh with polar coordinates, in the median plane. The radial step is given by

$$\delta R = \frac{RMAX - RMIN}{IRMAX - 1}$$

and the angular step by

$$\delta\theta = \frac{AT}{IAMAX - 1}$$

where, *RMIN* and *RMAX* are the lower and upper radial limits of the field map, and AT is its total angular aperture (Fig. 10B). $IRMAX$ and $IAMAX$ are the total number of nodes in the radial and angular directions.

Simulating Field Defects and Shims

Once the initial map is calculated, it is possible to modify it by means of the parameter *NBS*, so as to simulate field defects or shims.

If NBS = −2, the map is globally modified by a perturbation proportional to $R - R_0$, where R_0 is an arbitrary radius, with an amplitude $\Delta B_Z/B_0$, so that B_Z at the nodes of the mesh is replaced by

$$B_Z * \left(1 + \frac{\Delta B_Z}{B_0}\,\frac{R - R_0}{RMAX\ -\ RMIN}\right)$$

If NBS = −1, the perturbation is proportional to $\theta - \theta_0$, and B_Z is replaced by

$$B_Z * \left(1 + \frac{\Delta B_Z}{B_0}\,\frac{\theta - \theta_0}{AT}\right)$$

If NBS ≥ 1, then *NBS* shims are introduced at positions $\frac{R_1 + R_2}{2}$, $\frac{\theta_1 + \theta_2}{2}$ (Fig. 13) [18]
The initial field map is modified by shims with second order profiles given by

$$\theta = \left(\gamma + \frac{\alpha}{\mu}\right)\beta\,\frac{X^2}{\rho^2}$$

where X is shown in Fig. 11, $\rho = \frac{R_1 + R_2}{2}$ is the central radius, α and γ are the angular limits of the shim, β and μ are parameters.
At each shim, the value of B_Z at any node of the initial map is replaced by

$$B_Z * \left(1 + F\theta * FR * \frac{\Delta B_Z}{B_0}\right)$$

where $F\theta = 0$ or $FR = 0$ outside the shim, and $F\theta = 1$ and $FR = 1$ inside.

Extrapolation Off Median Plane

The vector field $\vec{B}$ and its derivatives in the median plane are calculated by means of a second or fourth order polynomial interpolation, depending on the value of the parameter *IORDRE* (*IORDRE*=2, 25 or 4, see section 1.4.2). The transformation from polar to Cartesian coordinates is performed following eqs (1.4.9 or 1.4.10). Extrapolation off median plane is then performed by means of Taylor expansions, following the procedure described in section 1.3.2.

DODECAPO: Dodecapole magnet (Fig. 19)

The meaning of parameters for *DODECAPO* is the same as for *QUADRUPO*.
In fringe field regions the magnetic field $\vec{B}(X,Y,Z)$ and its derivatives up to fourth order are derived from the scalar potential approximated to the 6th order in Y and Z

$$V(X,Y,Z) = G\left(Y^4 - \frac{10}{3}Y^2Z^2 + Z^4\right)YZ$$
$$\text{with } G_0 = \frac{B_0}{R_0^5}$$

Outside fringe field regions, or everywhere in sharp edge dodecapole ($\lambda_E = \lambda_S = 0$) , $\vec{B}(X,Y,Z)$ in the magnet is given by

$$B_X = 0$$
$$B_Y = G_0(5Y^4 - 10Y^2Z^2 + Z^4)Z$$
$$B_Z = G_0(Y^4 - 10Y^2Z^2 + 5Z^4)Y$$

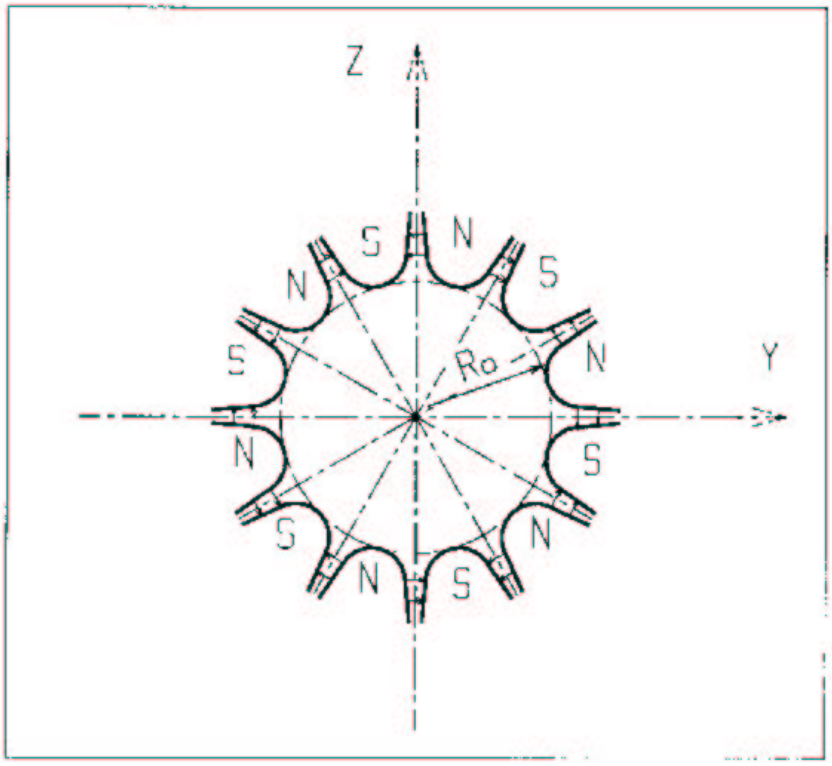

Figure 19: Dodecapole magnet

DRIFT or ESL: Field free drift space

DRIFT or *ESL* allow introduction of a drift space with length XL with positive or negative sign, anywhere in a structure. The associated equations of motion are (Fig. 20)

$$Y_2 = Y_1 + XL * \mathrm{tg}T$$
$$Z_2 = Z_1 + \frac{XL}{\cos T}\,\mathrm{tg}P$$
$$SAR_2 = SAR_1 + \frac{XL}{\cos T * \cos P}$$

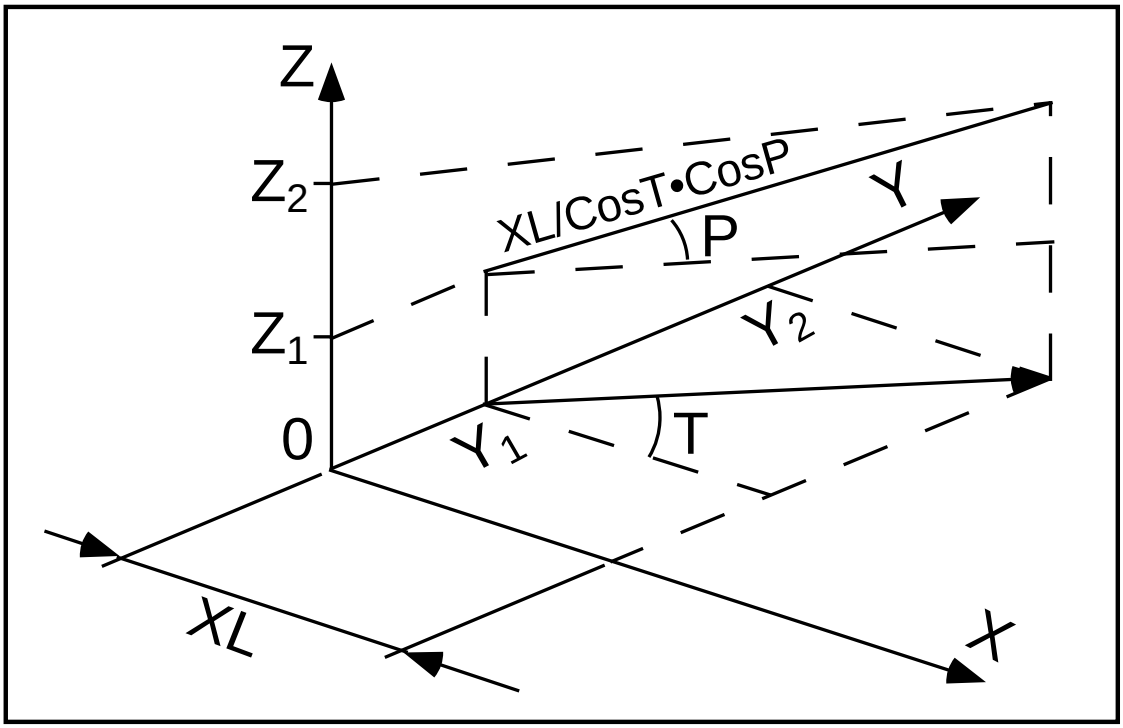

Figure 20: Transfer of particles in a drift space.

EBMULT: Electro-magnetic multipole

EBMULT simulates an electro-magnetic multipole, by addition of electric ($\vec{E}$) and magnetic ($\vec{B}$) multipole components (dipole to 20-pole). $\vec{E}$ and its derivatives $\frac{\partial^{i+j+k}\vec{E}}{\partial X^i \partial Y^j \partial Z^k}$ $(i+j+k \leq 4)$ are derived from the general expression of the multipole scalar potential (eq. 1.3.5), followed by a $\frac{\pi}{2n}$ rotation (n = pole order), as described in section 1.5.3 (see also *ELMULT*). $\vec{B}$ and its derivatives are derived from the same general potential, as described in section 1.3.5 (see also *MULTIPOL*).
The entrance and exit fringe fields of the $\vec{E}$ and $\vec{B}$ components are treated separately, in the same way as described under *ELMULT* and *MULTIPOL*, for each one of these two fields. Wedge angle correction is applied in sharp edge field model if $\vec{B}1$ is non zero, as in *MULTIPOL*. Any of the $\vec{E}$ or $\vec{B}$ multipole field component can be rotated independently of the others.
Use *PARTICUL* prior to *EBMULT*, for the definition of particle mass and charge.

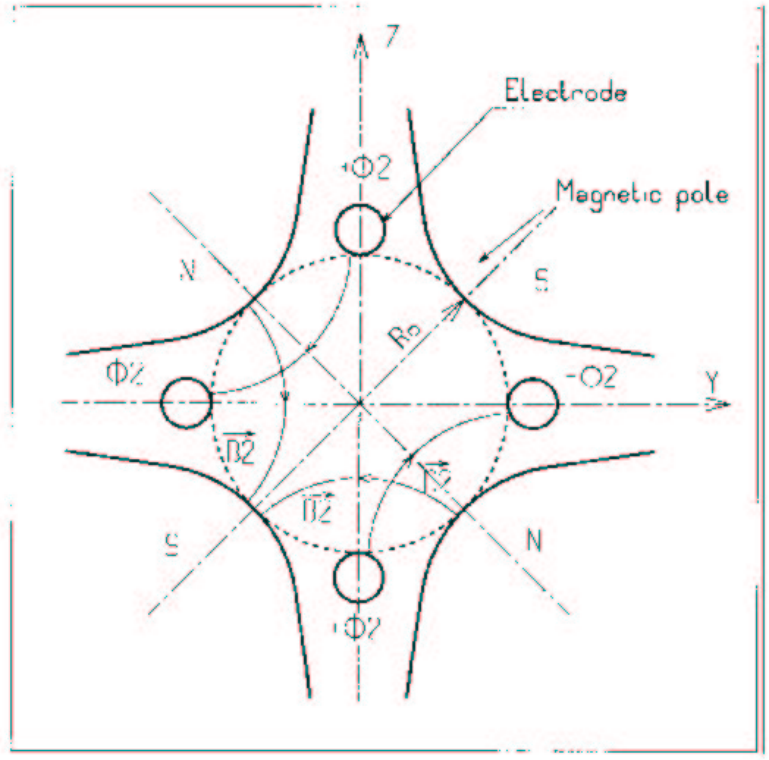

Figure 21: An example of $\vec{E}$, $\vec{B}$ multipole: the achromatic quadrupole (known for its allowing null second order chromatic aberrations [19]).

EL2TUB: Two-tube electrostatic lens

The lens is cylindrically symmetric about the X-axis.
The length and potential of the first (resp. second) electrode are $X1$ and $V1$ ($X2$ and $V2$). The distance between the two electrodes is D, and their inner radius is R_0 (Fig. 22). X-axis cylindrical symmetry is assumed. The model for the electrostatic potential along the axis is [21]

$$V(X) = \frac{V_2 - V_1}{2} \operatorname{th} \frac{\omega x}{R_0} \left[+ \frac{V_1 + V_2}{2} \right] \qquad \text{if } D = 0$$

$$V(X) = \frac{V_2 - V_1}{2} \frac{1}{2\omega D} \ell n \frac{\operatorname{ch} \omega \dfrac{x + D}{R_0}}{\operatorname{ch} \omega \dfrac{x - D}{R_0}} \left[+ \frac{V_1 + V_2}{2} \right] \qquad \text{if } D \neq 0$$

(x = distance from half-way between the electrodes; $\omega = 1.318$; th = hyperbolic tangent; ch = hyperbolic cosine) from which the field $\vec{E}(X, Y, Z)$ and its derivatives are derived following the procedure described in section 1.5.2 (note that they don't depend on the constant term $\left[\dfrac{V_1 + V_2}{2} \right]$ which disappears when differentiating).
Use *PARTICUL* prior to *EL2TUB*, for the definition of particle mass and charge.

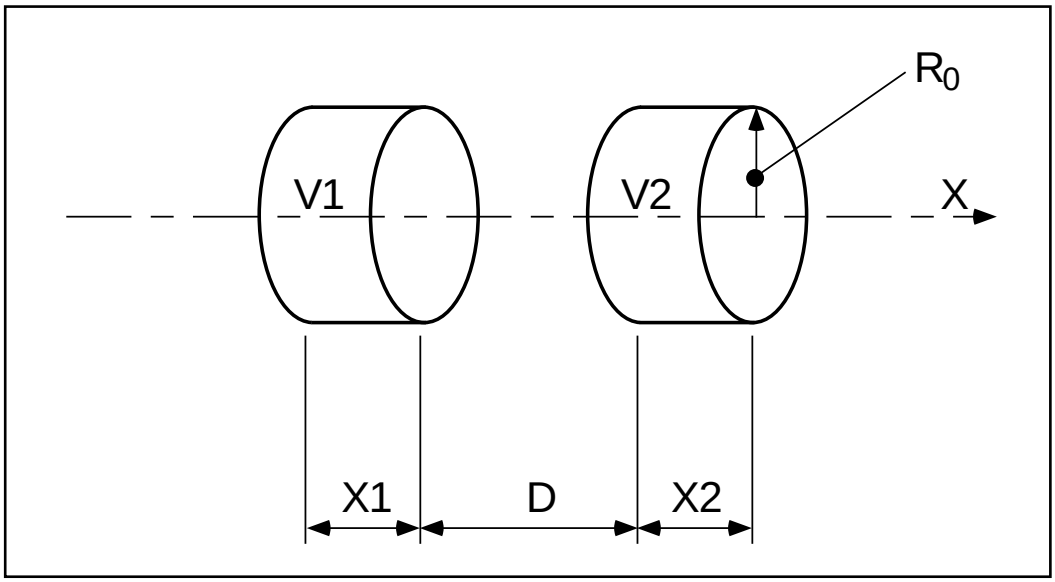

Figure 22: Two-electrode cylindrical electric lens.

ELMIR: Electrostatic N-electrode mirror/lens, straight slits

The device works as mirror or lens, horizontal or vertical. It is made of N 2-plate electrodes and has mid-plane symmetry.

Electrode lengths are $L1$, $L2$, ..., LN. D is the mirror/lens gap. The model for the Y-independent electrostatic potential is (after Ref. [22, p.412])

$$V(X,Z) = \sum_{i=2}^{N} \frac{Vi - Vi-1}{\pi} \arctan \frac{\sinh(\pi(X - Xi-1)/D)}{\cos(\pi Z/D)}$$

where Vi are the potential at the N electrodes (and normally $V1 = 0$ refers to the incident beam energy), Xi are the locations of the slits, X is the distance from the origin taken at the first slit (located at $X1 \equiv 0$ between the first and second electrodes). From $V(X,Z)$ the field $\vec{E}(X,Y,Z)$ and derivatives are deduced following the procedure described in section 1.5.3 (page 26).
The total X-extent of the mirror/lens is $L = \sum_{i=1}^{N} Li$.
In the mirror mode (*i.e.*, option flag $MT = 11$ for vertical mid-plane or 12 for horizontal mid-plane) stepwise integration starts at $X = -L1$ (entrance of the first electrode) and terminates either when back to $X = -L1$ or when reaching $X = L - L1$ (end of the $N - th$ electrode). In the latter case particles are stopped with their index *IEX* set to -8 (see section 4.6.8 on page 126). Normally $X1$ should exceed $3D$ (possibly sensibly, so that $V(X < X1)$ have negligible effect in terms of trajectory behavior).
In the lens mode (*i.e.*, option flag $MT = 21$ for vertical mid-plane or 22 for horizontal mid-plane) stepwise integration starts at $X = -L1$ (entrance of the first electrode) and terminates either when reaching $X = L - L1$ (end of the $N - th$ electrode) or when the particle deflection exceeds $\pi/2$. In the latter case the particle is stopped with their index *IEX* set to -3.

Use *PARTICUL* prior to *ELMIR*, for the definition of particle mass and charge.

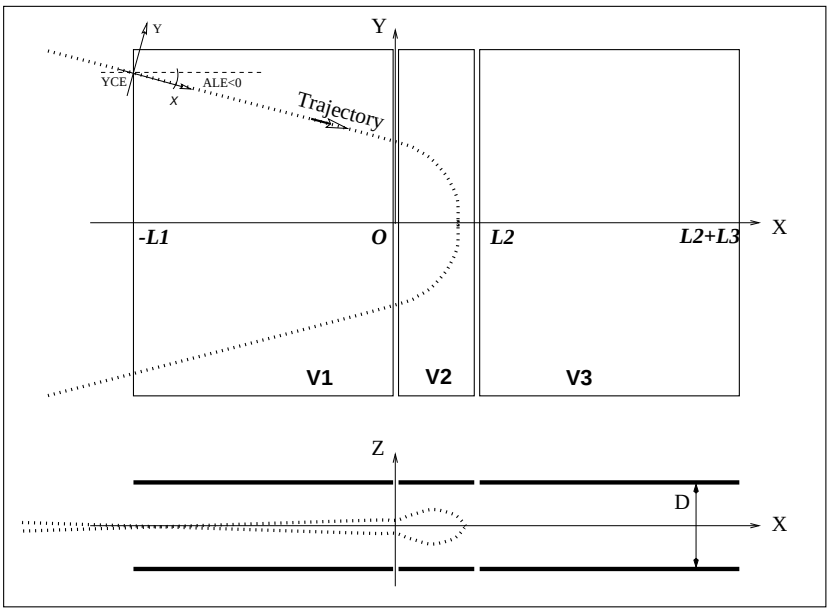

Figure 23: Electrostatic N-electrode mirror/lens, straight slits, in the case $N = 3$, in horizontal mirror mode ($MT = 11$).
Possible non-zero entrance quantities YCE, ALE should be specified using *CHANGREF*, or using *KPOS*=3 with *YCE*=pitch, *ALE*=half-deviation.

ELMIRC: Electrostatic N-electrode mirror/lens, circular slits [22]

The device works as mirror or lens, horizontal or vertical. It is made of N 2-plate electrodes and has mid-plane symmetry[5].

Electrode slits are circular, concentric with radii $R1$, $R2$, ..., $R_{N\text{-}1}$, D is the mirror/lens gap. The model for the mid-plane ($Z = 0$) radial electrostatic potential is (after Ref. [22, p.443])

$$V(r) = \sum_{i=2}^{N} \frac{Vi - Vi{-}1}{\pi} \arctan\left(\sinh \frac{\pi(r - Ri{-}1)}{D}\right)$$

where Vi are the potential at the N electrodes (and normally $V1 = 0$ refers to the incident beam energy). r is the current radius.

The mid-plane field $\vec{E}(r)$ and its r-derivatives are first derived by differentiation, then $\vec{E}(r, Z)$ and derivatives are obtained from Taylor expansions and Maxwell relations. Eventually a transformation to the rotating frame provides $\vec{E}(X, Y, Z)$ and derivatives as involved in eq. 1.2.13.
Stepwise integration starts at entrance (defined by RE, TE) of the first electrode and terminates when rotation of the reference rotating frame (RM, X, Y) has reached the value AT. Normally, $R1 - RE$ and $R1 - RS$ should both exceed $3D$ (possibly sensibly, so that $V(r < RE)$ and $V(r < RS)$ have negligible effect in terms of trajectory tails).

Positioning of the element is performed by means of *KPOS* (see section 4.6.5).

Use *PARTICUL* prior to *ELMIRC*, for the definition of particle mass and charge.

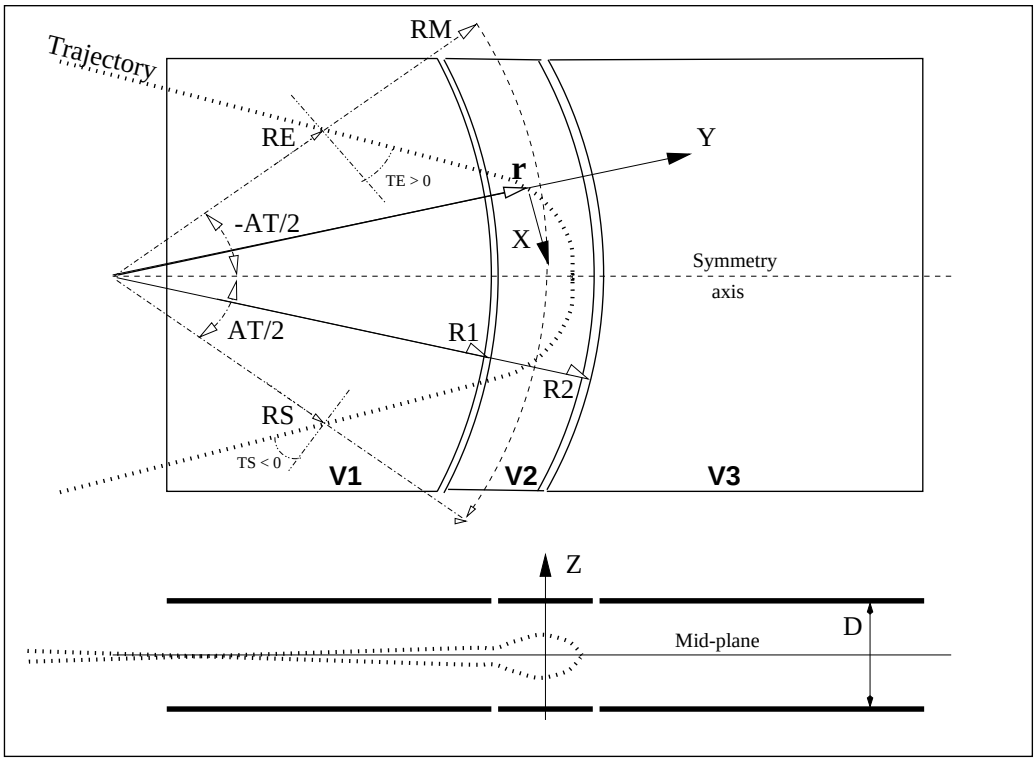

Figure 24: Electrostatic N-electrode mirror/lens, circular slits, in the case $N = 3$, in horizontal mirror mode.

[5]NOTE : in the present version of the code, the sole horizontal mirror mode is operational, and N is limited to 3.

ELMULT: Electric multipole

The simulation of multipolar electric field $\vec{M}_E$ proceeds by addition of the dipolar ($\vec{E}1$), quadrupolar ($\vec{E}2$), sextupolar ($\vec{E}3$), etc., up to 20-polar ($\vec{E}10$) components, and of their derivatives up to fourth order, following

$$\begin{aligned}
\vec{M}_E &= \vec{E}1 + \vec{E}2 + \vec{E}3 + \ \ldots\ + \vec{E}10 \\
\frac{\partial \vec{M}_E}{\partial X} &= \frac{\partial \vec{E}1}{\partial X} + \frac{\partial \vec{E}2}{\partial X} + \frac{\partial \vec{E}3}{\partial X} + \ \ldots\ + \frac{\partial \vec{E}10}{\partial X} \\
\frac{\partial^2 M_E}{\partial X \partial Z} &= \frac{\partial^2 \vec{E}1}{\partial X \partial Z} + \frac{\partial^2 \vec{E}2}{\partial X \partial Z} + \frac{\partial^2 \vec{E}3}{\partial X \partial Z} + \ \ldots\ + \frac{\partial^2 \vec{E}10}{\partial X \partial Z} \\
&\text{etc.}
\end{aligned}$$

The independent components $\vec{E}1$ to $\vec{E}10$ and their derivatives up to the second order are calculated by differentiating the general multipole potential given in eq. 1.3.5 (page 20), followed by a $\frac{\pi}{2n}$ rotation about the X-axis, so that the so defined right electric multipole of order n, and of strength [19, 20]

$$K_n = \frac{1}{2} \frac{\gamma}{\gamma^2 - 1} \frac{V_n}{R_0^n}$$

(V_n = potential at the electrode, R_0 = radius at pole tip, γ = relativistic Lorentz factor of the particle) has the same focusing effect than the right magnetic multipole of order n and strength $K_n = \dfrac{B_n}{R_0^{n-1} B\rho}$ (B_n = field at pole tip, $B\rho$ = particle rigidity, see *MULTIPOL*).
Such $\dfrac{\pi}{2n}$ rotation of the multipole components is obtained following the procedure described in section 1.5.3.

The entrance and exit fringe fields are treated separately. They are characterized by the integration zone X_E at entrance and X_S at exit, as for *QUADRUPO*, and by the extent λ_E at entrance, λ_S at exit. The fringe field extents for the dipole component are λ_E and λ_S. The fringe field for the quadrupolar (sextupolar, ..., 20-polar) component is given by a coefficient E_2 (E_3, ..., E_{10}) at entrance, and S_2 (S_3, ..., S_{10}) at exit, such that the fringe field extent is $\lambda_E * E_2$ ($\lambda_E * E_3$, ..., $\lambda_E * E_{10}$) at entrance and $\lambda_S * S_2$ ($\lambda_S * S_3$, ..., $\lambda_S * S_{10}$) at exit.

If $\lambda_E = 0$ ($\lambda_S = 0$) the multipole lens is considered to have a sharp edge field at entrance (exit), and then, X_E (X_S) is forced to zero (for the mere purpose of saving computing time).

If $E_i = 0$ ($S_i = 0$) ($i = 2,\ 10$), the entrance (exit) fringe field for multipole component i is considered as a sharp edge field.

Overlapping of fringe fields inside the element is treated separately for each component, in the way described in *QUADRUPO*.

Moreover, any multipole component $\vec{E}i$ can be rotated independently by an angle RXi around the longitudinal X-axis, for the simulation of positioning defects, as well as skewed lenses.

Use *PARTICUL* prior to *ELMULT*, for the definition of particle mass and charge.

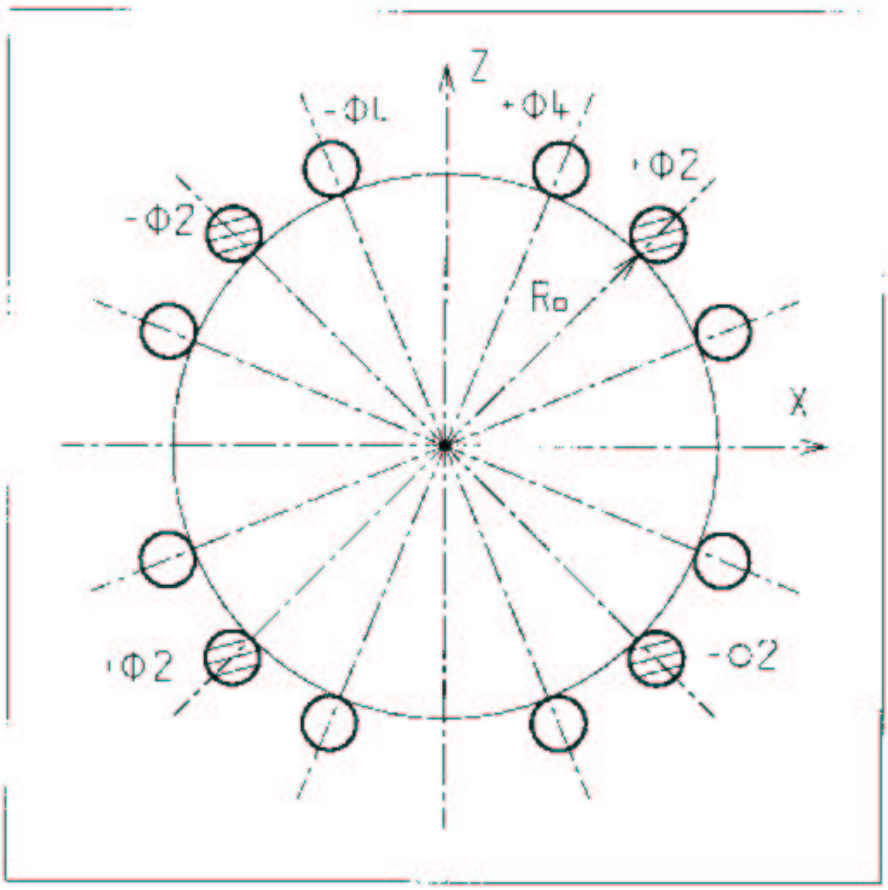

Figure 25: An electric multipole combining skew-quadrupole ($\vec{E}2 \neq \vec{0},\ \vec{R}2 = \pi/4$) and skew-octupole ($\vec{E}4 \neq \vec{0},\ \vec{R}4 = \pi/8$) components ($\vec{E}1 = \vec{E}3 = \vec{E}5 = \ \ldots\ = \vec{E}10 = \vec{0}$) [20].

ELREVOL: 1-D uniform mesh electric field map

ELREVOL reads a 1-D axial field map from a storage data file, whose content must fit the following *FORTRAN* reading sequence

```
OPEN (UNIT = NL, FILE = FNAME, STATUS = 'OLD' [,FORM='UNFORMATTED'])
DO 1 I=1, IX
   IF (BINARY) THEN
      READ(NL) X(I), EX(I)
   ELSE
      READ(NL,*) X(I), EX(I)
   ENDIF
  1     CONTINUE
```

where IX is the number of nodes along the (symmetry) X-axis, $X(I)$ their coordinates, and $EX(I)$ the values of the X component of the field. EX is normalized with *ENORM* prior to ray-tracing. As well the longitudinal coordinate X is normalized with a *XNORM* coefficient (usefull to convert to centimeters, the working units in **zgoubi** .

X-cylindrical symmetry is assumed, resulting in EY and EZ taken to be zero on axis. $\vec{E}(X,Y,Z)$ and its derivatives along a particle trajectory are calculated by means of a 5-points polynomial fit followed by second order off-axis Taylor series extrapolation (see sections 1.5.1 and 1.6).

Entrance and/or exit integration boundaries may be defined in the same way as in *CARTEMES* by means of the flag ID and coefficients A, B, C, A', B', C'.

Use *PARTICUL* prior to *ELREVOL*, for the definition of particle mass and charge.

MAP2D: 2-D Cartesian uniform mesh field map - arbitrary magnetic field [23]

MAP2D reads a 2-D field map that provides the three components B_X, B_Y, B_Z of the magnetic field at all nodes of a 2-D Cartesian uniform mesh in an (X, Y) plane. No particular symmetry is assumed, which allows the treatment of any type of field (e.g., dipole field with arbitrary Z elevation - the map needs not be a mid-plane map, solenoidal field, etc.). The data file should be filed with a format that fits the following *FORTRAN* reading sequence (presumably compatible with *TOSCA* code outputs)

```
      OPEN (UNIT = NL, FILE = FNAME, STATUS = 'OLD' [,FORM='UNFORMATTED'])
       DO 1 J=1,JY
          DO 1 I=1,IX
             IF (BINARY) THEN
                READ(NL) Y(J), Z(1), X(I), BY(I,J), BZ(I,J), BX(I,J)
             ELSE
                READ(NL,100) Y(J), Z(1), X(I), BY(I,J), BZ(I,J), BX(I,J)
100             FORMAT (1X, 6E11.4)
             ENDIF
      1       CONTINUE
```

where IX (JY) is the number of longitudinal (transverse horizontal) nodes of the 2-D uniform mesh, $Z(1)$ is the considered Z-elevation of the map. For binary files, FNAME must begin with 'B_' or 'b_', a flag 'BINARY' will thus be set to '.TRUE.'. The field $\vec{B} = (B_X, B_Y, B_Z)$ is next normalized with BNORM, prior to ray-tracing. As well the coordinates X, Y are normalized with *X-,Y-NORM* coefficients (usefull to convert to centimeters, the working units in **zgoubi** .

At each step of the trajectory of a particle, the field and its derivatives are calculated by a polynomial interpolation followed by a Z extrapolation (see sections 1.3.3, 1.4.3). Entrance and/or exit integration boundaries may be defined, in the same way as for *CARTEMES*.

MAP2D-E: 2-D Cartesian uniform mesh field map - arbitrary electric field

MAP2D-E reads a 2-D field map that provides the three components E_X, E_Y, E_Z of the electric field at all nodes of a 2-D Cartesian uniform mesh in an (X, Y) plane. No particular symmetry is assumed, which allows the treatment of any type of field (e.g., field of a parallel-plate mirror with arbitrary Z elevation - the map needs not be a mid-plane map). The data file should be filed with a format that fits the following *FORTRAN* reading sequence

```
      OPEN (UNIT = NL, FILE = FNAME, STATUS = 'OLD' [,FORM='UNFORMATTED'])
       DO 1 J=1,JY
          DO 1 I=1,IX
             IF (BINARY) THEN
                READ(NL) Y(J), Z(1), X(I), EY(I,J), EZ(I,J), EX(I,J)
             ELSE
                READ(NL,100) Y(J), Z(1), X(I), EY(I,J), EZ(I,J), EX(I,J)
100             FORMAT (1X, 6E11.4)
             ENDIF
      1       CONTINUE
```

where IX (JY) is the number of longitudinal (transverse horizontal) nodes of the 2-D uniform mesh, $Z(1)$ is the considered Z-elevation of the map. For binary files, FNAME must begin with 'E_' or 'b_', a flag 'BINARY' will thus be set to '.TRUE.'. The field $\vec{E} = (E_X, E_Y, E_Z)$ is next normalized with ENORM, prior to ray-tracing. As well the coordinates X, Y re normalized with *X-,Y-NORM* coefficients (usefull to convert to centimeters, the working units in **zgoubi** .

At each step of the trajectory of a particle, the field and its derivatives are calculated by a polynomial interpolation followed by a Z extrapolation (see sections 1.3.3, 1.4.3). Entrance and/or exit integration boundaries may be defined, in the same way as for *CARTEMES*.

MATPROD: Matrix transfer

MATPROD performs a matrix transfer of the particle coordinates in the following way

$$X_i = \sum_j R_{ij} X_j^0 + \sum_{j,k} T_{ijk} X_j^0 X_k^0$$

where, X_i stands for any of the current coordinates Y, T, Z, P, path length and dispersion, and X_i^0 stands for any of the initial coordinates. $[R_{ij}]$ ($[T_{ijk}]$) is the first order (second order) transfer matrix as usually involved in second order beam optics [15]. Second order transfer is optional. The length of the element represented by the matrix may be introduced for the purpose of path length updating. Note : *MATRIX* delivers $[R_{ij}]$ and $[T_{ijk}]$ matrices in a format suitable for straightforward use with *MATPROD*.

MULTIPOL: Magnetic multipole

The simulation of multipolar magnetic field $\vec{M}$ by *MULTIPOL* proceeds by addition of the dipolar ($\vec{B}1$), quadrupolar ($\vec{B}2$), sextupolar ($\vec{B}3$), etc., up to 20-polar ($\vec{B}10$) components, and of their derivatives up to fourth order, following

$$\vec{M} = \vec{B}1 + \vec{B}2 + \vec{B}3 + \ \ldots\ + \vec{B}10$$
$$\frac{\partial \vec{M}}{\partial X} = \frac{\partial \vec{B}1}{\partial X} + \frac{\partial \vec{B}2}{\partial X} + \frac{\partial \vec{B}3}{\partial X} + \ \ldots\ + \frac{\partial \vec{B}10}{\partial X}$$
$$\frac{\partial^2 \vec{M}}{\partial X \partial Z} = \frac{\partial^2 \vec{B}1}{\partial X \partial Z} + \frac{\partial^2 \vec{B}2}{\partial X \partial Z} + \frac{\partial^2 \vec{B}3}{\partial X \partial Z} + \ \ldots\ + \frac{\partial^2 \vec{B}10}{\partial X \partial Z}$$
etc.

The independent components $\vec{B}1$, $\vec{B}2$, $\vec{B}3$, ..., $\vec{B}10$ and their derivatives up to the fourth order are calculated as described in section 1.3.5.

The entrance and exit fringe fields are treated separately. They are characterized by the integration zone X_E at entrance and X_S at exit, as for *QUADRUPO*, and by the extent λ_E at entrance, λ_S at exit. The fringe field extents for the dipole component are λ_E and λ_S. The fringe field for the quadrupolar (sextupolar, ..., 20-polar) component is given by a coefficient E_2 (E_3, ..., E_{10}) at entrance, and S_2 (S_3, ..., S_{10}) at exit, such that the extent is $\lambda_E * E_2$ ($\lambda_E * E_3$, ..., $\lambda_E * E_{10}$) at entrance and $\lambda_S * S_2$ ($\lambda_S * S_3$, ..., $\lambda_S * S_{10}$) at exit.

If $\lambda_E = 0$ ($\lambda_S = 0$) the multipole lens is considered to have a sharp edge field at entrance (exit), and then, X_E (X_S) is forced to zero (for the mere purpose of saving computing time). If $E_i = 0$ ($S_i = 0$) ($i = 2, 10$), the entrance (exit) fringe field for the multipole component i is considered as a sharp edge field. In sharp edge field model, the wedge angle vertical first order focusing effect (if $\vec{B}1$ is non zero) is simulated at magnet entrance and exit by a kick $P_2 = P_1 - Z_1 \tan(\epsilon/\rho)$ applied to each particle (P_1, P_2 are the vertical angles upstream and downstream the EFB, Z_1 the vertical particle position at the EFB, ρ the local horizontal bending radius and ϵ the wedge angle experienced by the particle ; ϵ depends on the horizontal angle T).

Overlapping of fringe fields inside the optical element is treated separately for each component, in the way described in *QUADRUPO*.

Any multipole component $\vec{B}i$ can be rotated independently by an angle RXi around the longitudinal X-axis, for the simulation of positioning defects, as well as skewed lenses.

(Mis-)alignement of the optical element is assured by *KPOS*, with special features allowing some degrees of automatism useful for periodic structures (section 4.6.5).

OCTUPOLE: Octupole magnet (Fig. 26)

The meaning of parameters for *OCTUPOLE* is the same as for *QUADRUPO*. In fringe field regions the magnetic field $\vec{B}(X,Y,Z)$ and its derivatives up to fourth order are derived from the scalar potential approximated to the 8-th order in Y and Z

$$V(X,Y,Z) = \left(G - \frac{G''}{20}(Y^2+Z^2) + \frac{G''''}{960}(Y^2+Z^2)^2\right)(Y^3Z - YZ^3)$$

$$\text{with } G_0 = \frac{B_0}{R_0^3}$$

Outside fringe field regions, or everywhere in sharp edge dodecapole ($\lambda_E = \lambda_S = 0$) , $\vec{B}(X,Y,Z)$ in the magnet is given by

$$B_X = 0$$
$$B_Y = G_0(3Y^2Z - Z^3)$$
$$B_Z = G_0(Y^3 - 3YZ^2)$$

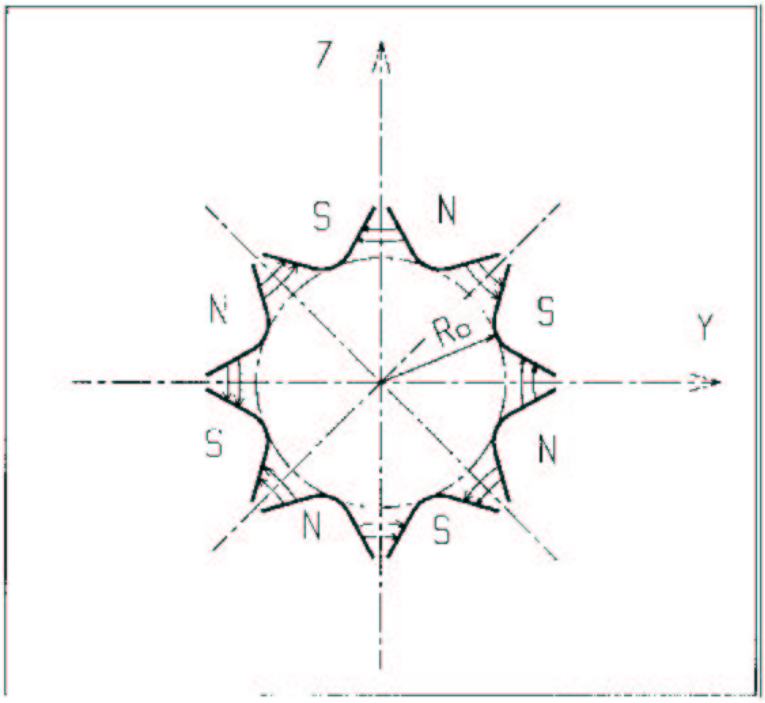

Figure 26: Octupole magnet

POISSON:Read magnetic field data from *POISSON* output

This keyword allows reading a field profile $B(X)$ from *POISSON* output. Let *FNAME* be the name of this output file (normally, *FNAME* = outpoi.lis); the data are read following the *FORTRAN* statements hereunder

```
I = 0
  11    CONTINUE
  I = I + 1
          READ(LUN,101,ERR=10,END=10) K, K, K, R, X(I), R, R, B(I)
  101     FORMAT(I1, I3, I4, E15.6, 2F11.5, 2F12.3)
        GOTO 11
  10    CONTINUE
        ...
```

where X(I) is the longitudinal coordinate, and B(I) is the Z component of the field at a node (I) of the mesh. K's and R's are dummy variables appearing in the *POISSON* output file outpoi.lis but not used here.

From this field profile, a 2-D median plane map is built up, with a rectangular and uniform mesh; mid-plane symmetry is assumed. The field at each node (X_i, Y_j) of the map is $B(X_i)$, independent of Y_j (*i.e.*, the distribution is uniform in the Y direction).

For the rest, *POISSON* works in a way similar to *CARTEMES*.

POLARMES: 2-D polar mesh magnetic field map

Similar to *CARTEMES*, apart from the polar mesh frame: IX is the number of angular nodes, JY the number of radial nodes; $X(I)$ and $Y(J)$ are respectively the angle and radius of a node (these parameters are similar to those entering in the definition of the map in *DIPOLE*).

PS170: Simulation of a round shape dipole magnet

PS170 is dedicated to a 'rough' simulation of CERN's *PS170* dipole.

The field B_0 is constant inside the magnet, and zero outside. The pole is a circle of radius R_0, centered on X axis. The output coordinates are generated at the distance XL from the entrance (Fig. 25).

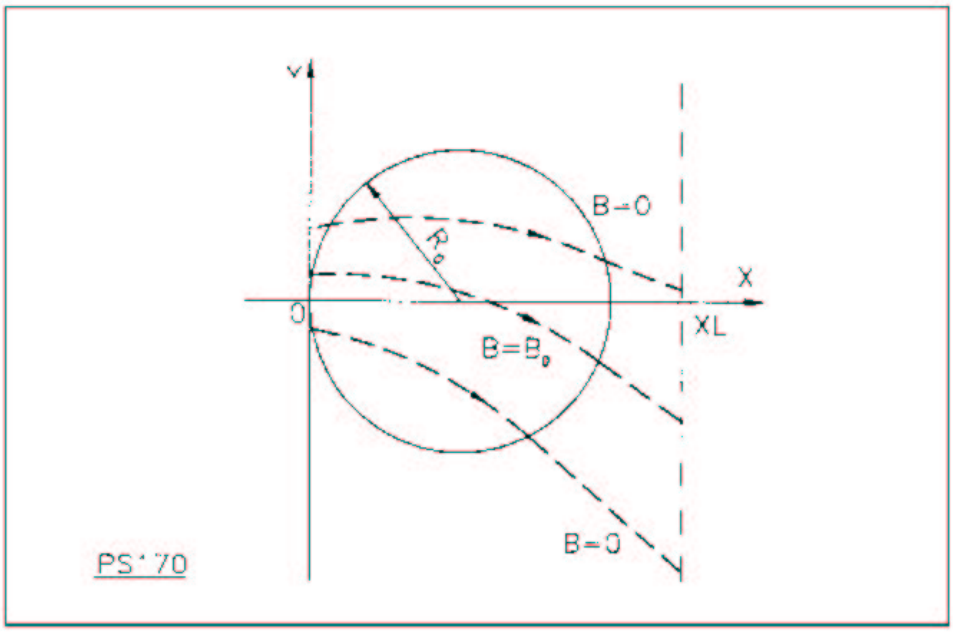

Figure 27: Scheme of the PS170 magnet simulation.

QUADISEX, SEXQUAD: Sharp edge magnetic multipoles

SEXQUAD defines in a simple way a sharp edge field with quadrupolar, sextupolar and octupolar components. *QUADISEX* adds a dipole component. The length of the element is XL. The vertical component $B \equiv B_Z(X, Y, Z = 0)$ of the field and its derivatives in median plane are calculated at each step from the following expressions

$$\begin{aligned} B &= B_0 \left(U + \frac{N}{R_0} Y + \frac{B}{R_0^2} Y^2 + \frac{G}{R_0^3} Y^3 \right) \\ \frac{\partial B}{\partial Y} &= B_0 \left(\frac{N}{R_0} + 2\frac{B}{R_0^2} Y + 3\frac{G}{R_0^3} Y^2 \right) \\ \frac{\partial^2 B}{\partial Y^2} &= B_0 \left(2\frac{B}{R_0^2} + 6\frac{G}{R_0^3} Y \right) \\ \frac{\partial^3 B}{\partial Y^3} &= 6 B_0 \frac{G}{R_0^3} \end{aligned}$$

and then extrapolated out of the median plane by Taylor expansion in Z (see section 1.3.2).

With option *SEXQUAD*, $U = 0$, while with *QUADISEX*, $U = 1$.

QUADRUPO: Quadrupole magnet (Fig. 28)

The length of the magnet XL is the distance between the effective field boundaries (EFB). The field at the pole tip R_0 is B_0.
The extent of the entrance (exit) fringe field is characterized by $\lambda_E(\lambda_S)$. The distance of ray-tracing on both sides of the EFB's, in the field fall off regions, will be $\pm\ X_E$ at the entrance, and $\pm\ X_S$ at the exit (Fig. 29), by prior and further automatic changes of frame.
In the fringe field regions $[-X_E, X_E]$ and $[-X_S, X_S]$ on both sides of the EFB's, $\vec{B}(X,Y,Z)$ and its derivatives up to fourth order are calculated at each step of the trajectory from the analytical expressions of the three components B_X, B_Y, B_Z obtained by differentiation of the scalar potential (see section 1.3.5) approximated to the 8th order in Y and Z.

$$V(X,Y,Z) = \left(G - \frac{G''}{12}(Y^2+Z^2) + \frac{G''''}{384}(Y^2+Z^2)^2 - \frac{G''''''}{23040}(Y^2+Z^2)^3\right) YZ$$
$$(G' = dG/dX, \quad G'' = d^2G/dX^2, \ldots)$$

where G is the gradient on axis [17]:

$$G(s) = \frac{G_0}{1+\exp P(s)} \qquad \text{with} \quad G_0 = \frac{B_0}{R_0}$$

and,

$$P(s) = C_0 + C_1\left(\frac{s}{\lambda}\right) + C_2\left(\frac{s}{\lambda}\right)^2 + C_3\left(\frac{s}{\lambda}\right)^3 + C_4\left(\frac{s}{\lambda}\right)^4 + C_5\left(\frac{s}{\lambda}\right)^5 \; P(s) = C_0 + C_1\left(\frac{s}{\lambda}\right) + C_2\left(\frac{s}{\lambda}\right)$$

where, s is the distance to the field boundary and λ stands for λ_E or λ_S (normally, $\lambda \simeq 2 * R_0$).
When fringe fields overlap inside the magnet ($XL \leq X_E + X_S$), the gradient G is expressed as

$$G = G_E + G_S - 1$$

where, G_E is the entrance gradient and G_S is the exit gradient.
If $\lambda_E = 0$ ($\lambda_S = 0$), the field at entrance (exit) is considered as sharp edged, and then $X_E(X_S)$ is forced to zero (for the mere purpose of saving computing time).
Outside of the fringe field regions (or everywhere when $\lambda_E = \lambda_S = 0$) $\vec{B}(X,Y,Z)$ in the magnet is given by

$$B_X = 0$$
$$B_Y = G_0 Z$$
$$B_Z = G_0 Y$$

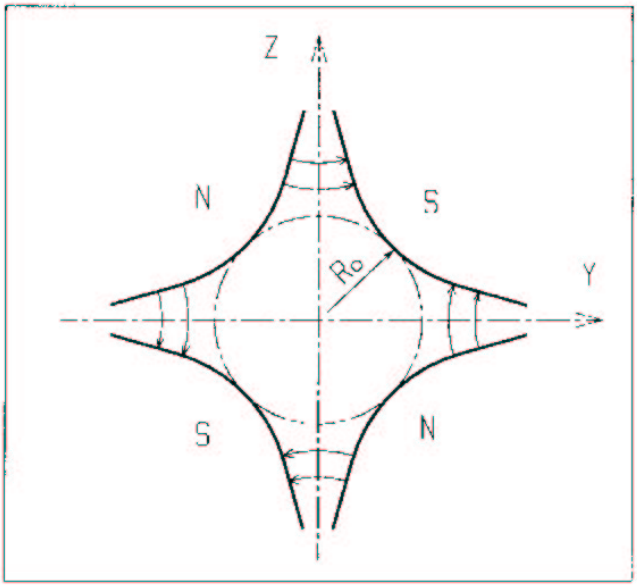

Figure 28: Quadrupole magnet

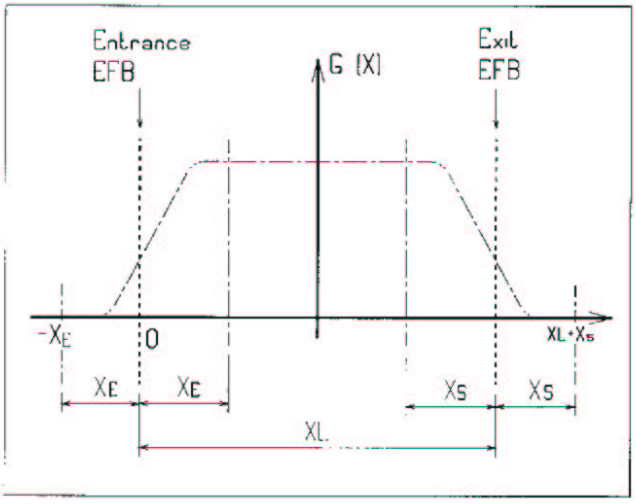

Figure 29: Scheme of the longitudinal field gradient $G(X)$.
(OX) is the longitudinal axis of the reference frame $(0, X, Y, Z)$ of **zgoubi** . The length of the element is XL, but trajectories are ray-traced from $-X_E$ to $XL + X_S$, by means of prior and further automatic changes of frame.

SEPARA: Wien Filter - analytical simulation

SEPARA provides an analytic simulation of an electrostatic separator. Input data are the length L of the element, the electric field E and the magnetic field B. The mass m and charge q of the particles are entered by means of the keyword *PARTICUL*.

The subroutines involved in this simulation solve the following system of three equations with three unknown variables S, Y, Z (while $X \equiv L$), that describe the cycloidal motion of a particle in $\vec{E}$, $\vec{B}$ static fields (Fig. 30).

$$X = -R\cos\left(\frac{\omega S}{\beta c} + \epsilon\right) - \frac{\alpha S}{\omega \beta c} + \frac{C_1}{\omega}$$
$$Y = R\sin\left(\frac{\omega S}{\beta c} + \epsilon\right) - \frac{\alpha}{\omega^2} - \frac{C_2}{\omega} + Y_0$$
$$Z = S\sin(P_0) + Z_0$$

where, S is the path length in the separator, $\alpha = -\dfrac{Ec^2}{\gamma}$, $\omega = -\dfrac{Bc^2}{m\gamma}$, $C_1 = \beta\sin(T_0)\cos(P_0)$ and $C_2 = \beta c\cos(T_0)\cos(P_0)$ are initial conditions. c = velocity of light, βc = velocity of the particle, $\gamma = (1-\beta^2)^{-\frac{1}{2}}$ and $\tan\epsilon = (C_2 + \frac{\alpha}{\omega})/C_1$. Y_0, T_0, Z_0, P_0 are the initial coordinates of the particle in the **zgoubi** reference frame. Here βc and γ are assumed constant, which is true as long as the change of momentum due to the electric field remains negligible all along the separator.

The index IA in the input data allows switching to inactive element (thus equivalent to *ESL*), horizontal or vertical separator. Normally, E, B and the value of β_W for wanted particles are related by

$$B(T) = -\frac{E\left(\dfrac{V}{m}\right)}{\beta_W \cdot c\left(\dfrac{m}{s}\right)}$$

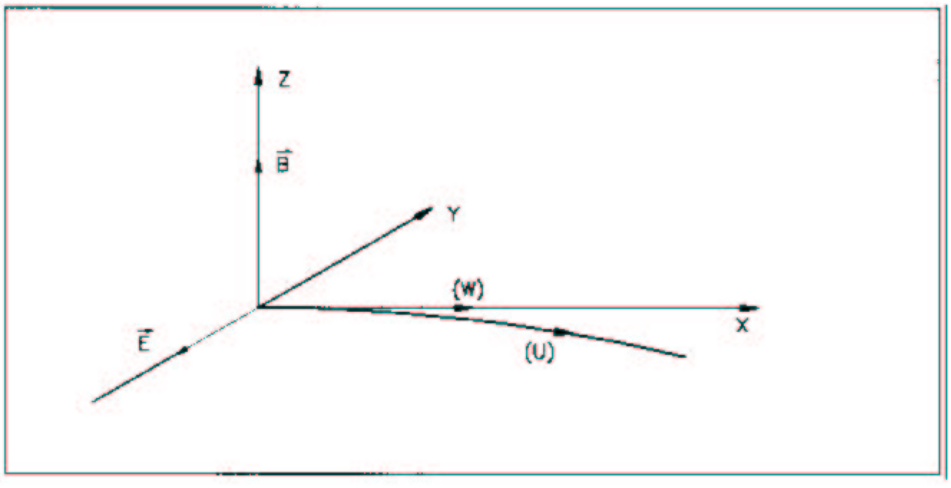

Figure 30: Horizontal separation between a wanted particle, (W), and an unwanted particle, (U). (W) undergoes a linear motion while (U) undergoes a cycloidal motion.

SEXTUPOL: Sextupole magnet (Fig. 31)

The meaning of parameters for *SEXTUPOL* is the same as for *QUADRUPO*.

In fringe field regions the magnetic field $\vec{B}(X,Y,Z)$ and its derivatives up to fourth order are derived from the scalar potential approximated to 7th order in Y and Z

$$V(X,Y,Z) = \left(G - \frac{G''}{16}(Y^2+Z^2) + \frac{G''''}{640}(Y^2+Z^2)^2\right)\left(Y^2Z - \frac{Z^3}{3}\right)$$
$$\text{with } G_0 = \frac{B_0}{R_0^2}$$

Outside fringe field regions, or everywhere in sharp edge sextupole ($\lambda_E = \lambda_S = 0$), $\vec{B}(X,Y,Z)$ in the magnet is given by

$$B_X = 0$$
$$B_Y = 2G_0YZ$$
$$B_Z = G_0(Y^2 - Z^2)$$

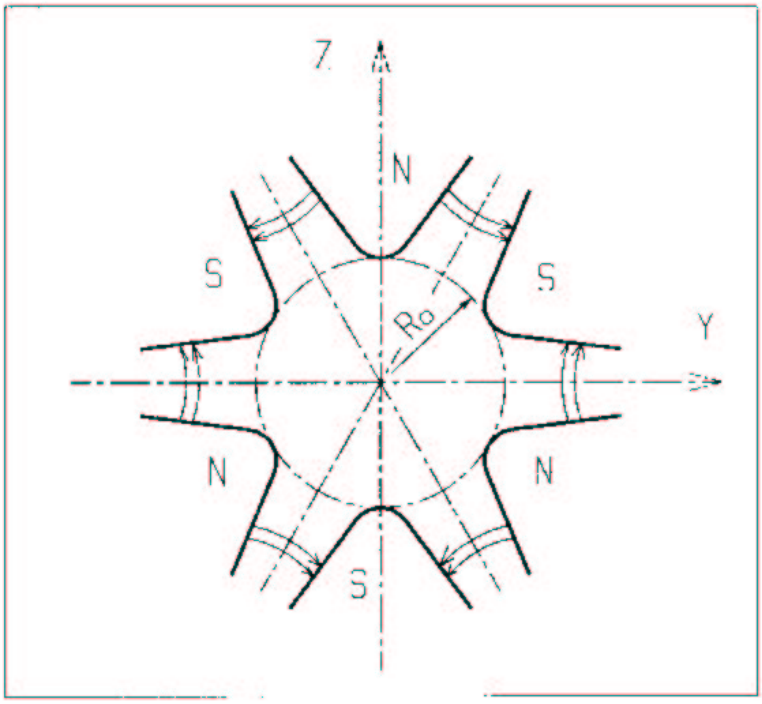

Figure 31: Sextupole magnet

SOLENOID: Solenoid (Fig. 32)

The solenoidal magnet has an effective length XL, a mean radius R_0 and an asymptotic field $B_0 = \mu_0 NI/XL$ (i.e., $\int_{-\infty}^{\infty} B_X(X,r)dX = \mu_0 NI$, $\forall r < R_0$), wherein B_X=longitudinal field component, NI = number of Ampere-Turns, $\mu_0 = 4\pi 10^{-7}$.

The distance of ray-tracing beyond the effective length XL, is X_E at the entrance, and X_S at the exit (Fig. 32).

The field $\vec{B}(X,r)$, $r = (Y^2 + Z^2)^{1/2}$, and its derivatives up to the second order with respect to X, Y or Z are obtained after the method proposed in ref. [24], that involves the three complete elliptic integrals K, E and Π. These are calculated with the algorithm proposed in the same reference. Their derivatives are calculated by means of recursive relations [25].

This analytical model for the solenoidal field allows simulating an extended range of coil geometries (legnth and radius) provided that the coil thickness is small enough compared to the mean radius R_0.

In particular the field on-axis writes (taking $x = r = 0$ as solenoid center)

$$B_X(x, r=0) = \frac{\mu_0 NI}{2XL}\left[\frac{XL/2 - x}{\sqrt{(XL/2-x)^2 + R_0^2}} + \frac{XL/2 + x}{\sqrt{(XL/2+x)^2 + R_0^2}}\right]$$

and yields the magnetic length

$$L_{mag} \equiv \frac{\int_{-\infty}^{\infty} B_X(x, r < R_0)dx}{B_X(x=r=0)} = XL\sqrt{1 + \frac{4R_0^2}{XL^2}} > XL$$

with in addition

$$B_X(\text{center}) \equiv B_X(x=r=0) = \frac{\mu_0 NI}{XL\sqrt{1 + \frac{4R_0^2}{XL^2}}}.$$

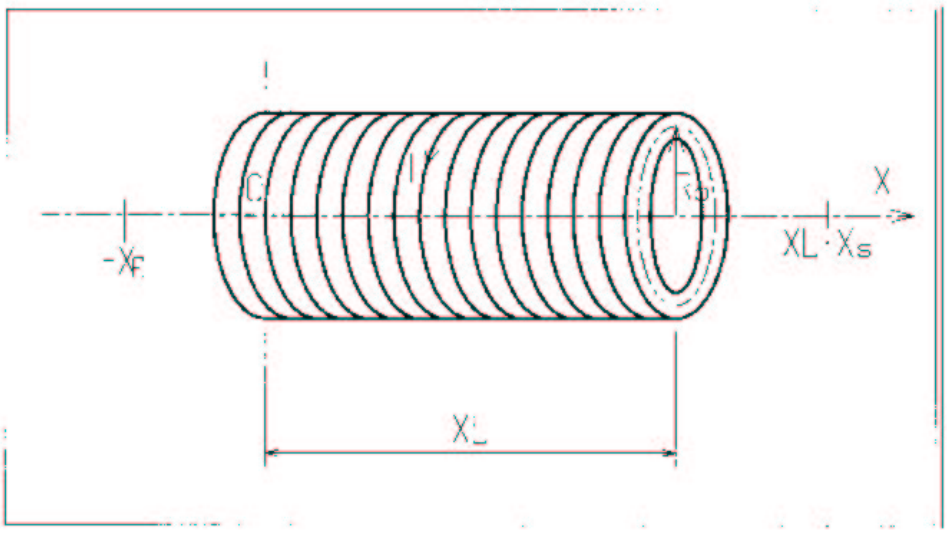

Figure 32: Solenoidal magnet.

TOSCA: 2-D and 3-D Cartesian uniform mesh magnetic field map

TOSCA is dedicated to the reading and treatment of 2-D or 3-D Cartesian mesh field maps as delivered by the *TOSCA* magnet computer code standard output.

The total number of field data files to be read is given by the parameter IZ that appears in the data list following the keyword. Each file contains the field components B_X, B_Y, B_Z on an (X, Y) mesh at a given Z coordinate. $IZ = 1$ for 2-D maps, and in this case B_X and B_Y are assumed zero all over the map[6]. For 3-D maps with mid-plane symmetry, IZ should be positive, and thus, the first data file whose name follows in the data list is supposed to contain the median plane field (assuming $Z = 0$ and $B_X = B_Y = 0$), while the next files contain the next maps in increasing Z order. For arbitrary 3-D maps (and in particular, contrary to what precedes without mid-plane symmetry assumption) IZ should be odd and negative, and thus, the total number of maps (whose names follow in the data list) is $|IZ|$, while map number $[IZ/2] + 1$ is the $Z = 0$ one.

The field map data files should be formatted following the *FORTRAN* reading sequence below.

```
DO  1  K = 1, KZ
  OPEN (UNIT = NL, FILE = FNAME, STATUS = 'OLD' [,FORM='UNFORMATTED'])
  DO  1  J = 1,  JY
    DO  1 I = 1, IX
              IF (BINARY) THEN
                READ(NL) Y(J), Z(K), X(I), BY(J,K,I), BZ(J,K,I), BX(J,K,I)
              ELSE
        READ(NL,100) Y(J), Z(K), X(I), BY(J,K,I), BZ(J,K,I), BX(J,K,I)
 100            FORMAT(1X,6E11.2)
              ENDIF
  1     CONTINUE
```

where, IX (JY, KZ) is the number of longitudinal (transverse horizontal, vertical) nodes of the 3-D uniform mesh. For binary files, FNAME must begin with 'B_' or 'b_', a flag 'BINARY' will thus be set to '.TRUE.'.

The field $\vec{B} = (B_X, B_Y, B_Z)$ is normalized by means of *BNORM* in a similar way as in *CARTEMES*. As well the coordinates X (and Y, Z with 3-D field maps) is normalized with a *X-[Y-,Z-]NORM* coefficient (usefull to convert to centimeters, the working units in **zgoubi** .

At each step of the trajectory of a particle inside the map, the field and its derivatives are calculated

- in the case of 2-D map, by means of a second or fourth order polynomial interpolation, depending on *IORDRE* (*IORDRE* = 2, 25 or 4), as for *CARTEMES*,

- in the case of 3-D map, by means of a second order polynomial interpolation with a $3 \times 3 \times 3$-point parallelipipedic grid, as described in section 1.4.4.

Entrance and/or exit integration boundaries between which the trajectories are integrated in the field may be defined, in the same way as in *CARTEMES*.

[6] Use *MAP2D* in case non-zero B_X, B_Y are to be taken into account in a 2-D map.

TRAROT: Translation-Rotation of the reference frame

This procedure transports particles into a new frame by translation and rotation. Effect on spin tracking, particle decay and gas-scattering are taken into account (but not on synchrotron radiation).

UNDULATOR: Undulator magnet

UNDULATOR

To be documented

Figure 33: Undulator magnet.

UNIPOT: Unipotential cylindrical electrostatic lens

The lens is cylindrically symmetric about the X-axis.

The length of the first (resp. second, third) electrode is $X1$ (resp. $X2$, $X3$). The distance between the electrodes is D. The potentials are $V1$ and $V2$. The inner radius is R_0 (Fig. 34). The model for the electrostatic potential along the axis is [26]

$$V(x) = \frac{V2 - V1}{2\omega D}\left[\ln \frac{\cosh \frac{\omega\left(x + \frac{X2}{2} + D\right)}{R_0}}{\cosh \frac{\omega\left(x + \frac{X2}{2}\right)}{R_0}} + \ln \frac{\cosh \frac{\omega\left(x - \frac{X2}{2} - D\right)}{R_0}}{\cosh \frac{\omega\left(x - \frac{X2}{2}\right)}{R_0}}\right]$$

(x = distance from the center of the central electrode; ω = 1,318; cosh = hyperbolic cosine), from which the field $\vec{E}(X, Y, Z)$ and its derivatives are deduced following the procedure described in section 1.5.2.
Use *PARTICUL* prior to *UNIPOT*, for the definition of particle mass and charge.

The total length of the lens is $X1 + X2 + X3 + 2\,D$; stepwise integration starts at entrance of the first electrode and terminates at exit of the third one.

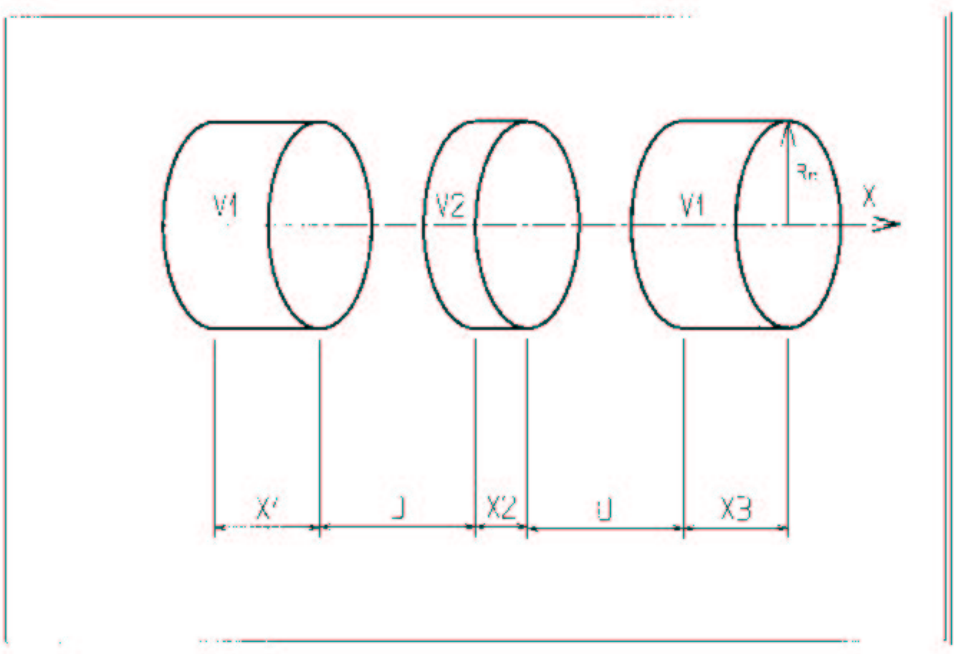

Figure 34: Three-electrode cylindrical unipotential lens.

VENUS: Simulation of a rectangular dipole magnet

VENUS is dedicated to a 'rough' simulation of Saturne Laboratory's *VENUS* dipole. The field B_0 is constant inside the magnet, with longitudinal extent XL and transverse extent $\pm YL$; outside these limits, $B_0 = 0$ (Fig. 35).

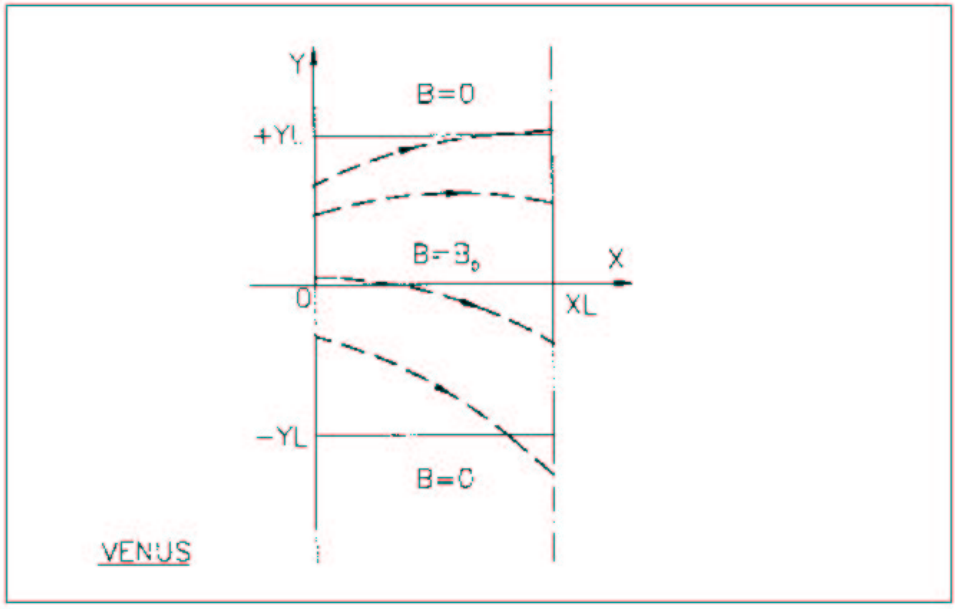

Figure 35: Scheme of *VENUS* rectangular dipole.

WIENFILT: Wien filter

WIENFILT simulates a Wien Filter, with transverse and orthogonal electric and magnetic fields $\vec{E}_Y$, $\vec{B}_Z$ or $\vec{E}_Z$, $\vec{B}_Y$ (Fig. 30). It must be preceded by *PARTICUL* for the definition of particle mass and charge.

The length XL of the element is the distance between its entrance and exit EFB's. The electric and magnetic field intensities E_0 and B_0 in the central, uniform field region, normally satisfy the relation

$$B_0 = -\frac{E_0}{\beta_W c}$$

for the selection of " wanted" particles of velocity $\beta_W c$. Ray-tracing in field fall-off regions extends over a distance X_E (X_S) beyond the entrance (exit) EFB by means of prior and further automatic changes of frame. Four sets of coefficients λ, $C_0 - C_5$ allow the description of the entrance and exit fringe fields outside the uniform field region, following the model [17]

$$F = \frac{1}{1 + \exp(P(s))}$$

where $P(s)$ is of the term

$$P(s) = C_0 + C_1 \left(\frac{s}{\lambda}\right) + C_2 \left(\frac{s}{\lambda}\right)^2 + C_3 \left(\frac{s}{\lambda}\right)^3 + C_4 \left(\frac{s}{\lambda}\right)^4 + C_5 \left(\frac{s}{\lambda}\right)^5$$

and s is the distance to the EFB. When fringe fields overlap inside the element (*i.e.* $XL \leq X_E + X_S$), the field fall-off is expressed as

$$F = F_E + F_S - 1$$

where $F_E(F_S)$ is the value of the coefficient respective to the entrance (exit) EFB.
If $\lambda_E = 0$ ($\lambda_S = 0$) for either the electric or magnetic component, then both are considered as sharp edge fields and $X_E(X_S)$ is forced to zero (for the purpose of saving computing time). In this case, the magnetic wedge angle vertical first order focusing effect is simulated at entrance and exit by a kick $P_2 = P_1 - Z_1 \tan(\epsilon/\rho)$ applied to each particle (P_1, P_2 are the vertical angles upstream and downstream the EFB, Z_1 the vertical particle position at the EFB, ρ the local horizontal bending radius and ϵ the wedge angle experienced by the particle ; ϵ depends on the horizontal angle T). This is not done for the electric field, however it is advised not to use a sharp edge electric dipole model since this entails non symplectic mapping, and in particular precludes focusing effects of the non zero longitudinal electric field component.

YMY: Reverse signs of Y and Z reference axes

YMY performs a 180° rotation of particle coordinates with respect to the X-axis, as shown in Fig. 36. This is done by means of a change of sign of Y and Z axes, and therefore coordinates, as follows

$$Y2 = -Y1, \quad T2 = -T1, \quad Z2 = -Z1 \quad \text{and} \quad P2 = -P1$$

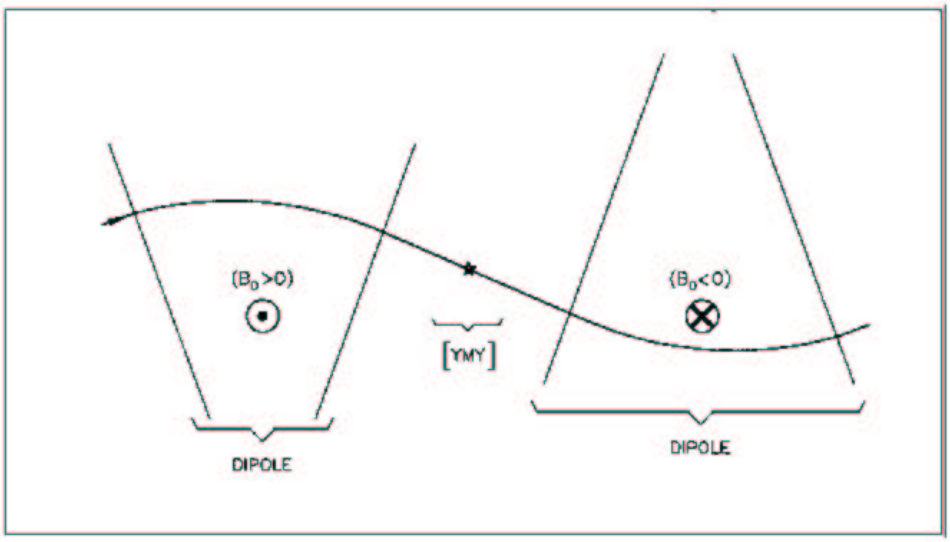

Figure 36: The use of YMY in a sequence of two identical dipoles of opposite signs.

4.5 Output Procedures

These procedures are dedicated to the printing of particle coordinates, histograms, spin coordinates, etc. They may be called for at any spot in the data pile.

CLORB: Beam centroid path; closed orbit

CLORB computes the beam centroid path, from average value of particle coordinates as observed at *LABEL*'ed keywords.

In conjunction with *REBELOTE*, this procedure computes by the same method the closed orbit in the periodic structure as delimited by means *REBELOTE*.

The *LABEL* list of concern follows the keyword *CLORB*.

FAISCEAU, FAISCNL, FAISTORE: Print/Store particle coordinates

FAISCEAU can be introduced anywhere in a structure. It produces a print of initial and actual coordinates of the particles at the location where it stands, together with their tagging indices and letters, following the same format as for *FAISCNL* (except for *SORT(I)* which is not printed) .

FAISCNL has a similar effect, except that the information is stored in a dedicated file *FNAME* (standard name is *FNAME* = 'zgoubi.fai' for post-processing with **zpop**). This file may further on be read by means of *OBJET*, option *KOBJ* = 3, or used for other purposes such as graphics (see Part D of the Guide). The data written to that file are formatted and ordered according to the *FORTRAN* sequence below

```
   OPEN (UNIT = NL, FILE = FNAME, STATUS = 'NEW')
   DO  1  I=1, IMAX
     WRITE(NL,110) LET(I),IEX(I),(FO(J,I),J=1,7),(F(J,I),J=1,7),KineticE,
  >  I(I),IREP(I),SORT(I),Mass,Charge,G-Factor,com-Life-time,unused,RET(I), DPR(I),
  >                                    BORO,IPASS,KLEY,LBL1,LBL2,NOEL
110     FORMAT(1X,A1,I2,1P,7E16.8,
    2         /,3E24.16,
    3         /,4E24.16,E16.8,
    4         /,2I6,8E16.8,
    5         /,E16.8,   I6,  A8,  2A10, I5)
```

The meaning of main data is the following (see the keyword *OBJET*)

$LET(I)$	:	one-character string, for tagging particle number I
IEX, I, $IREP(I)$	:	flag, particle number, index
$FO(1-6, I)$	:	coordinates D, Y, T, Z, P and path length at the origin of the structure
$F(1-6, I)$	:	idem, at the current position
$SORT(I)$	:	path length at which the particle has possibly been stopped (see *CHAMBR* or *COLLIMA*)
$RET(I)$, $DPR(I)$	:	synchrotron phase space coordinates; RET =phase (radian), DPR = momentum dispersion (MeV/c) (see *CAVITE*)
IPASS	:	turn number (see *REBELOTE*)
etc.	:	

FAISTORE has an effect similar to *FAISCNL*, with two more features. On the first data line, *FNAME* may be followed by a series of up to 10 *LABEL*'s proper to the elements of the data file at the exit of which the print should occur; if there is no label, the print occurs by default at the location of *FAISTORE*; if there are labels the print occurs right downstream of all optical elements wearing those labels (and no longer at the *FAISTORE* location). The next data line gives a parameter IP: printing will occur every IP other pass, if using *REBELOTE* with *NPASS* $\geq IP - 1$. For instance the data list

FAISTORE
zgoubi.fai *HPCKUP* *VPCKUP*
12

will result in output prints into zgoubi.fai, every 12 other pass, each time elements of the zgoubi.dat data list labeled either *HPCKUP* or *VPCKUP* are encountered.

Note
Binary storage can be obtained from *FAISCNL* and *FAISTORE*. This for the sake of compactness and access speed, for instance in case voluminous amounts of data would have to be manipulated.

This is achieved by giving the storage file a name of the form *b_FNAME* or *B_FNAME* (e.g., 'b_zgoubi.fai'). The FORTRAN *WRITE* list is the same as in the *FORMATTED* case above.

This is compatible with the *READ* statements in **zpop** that will recognize binary storage from that very radical 'b_' or 'B_'.

FOCALE, IMAGE[S]: Particle coordinates and beam size; localization and size of horizontal waist

FOCALE calculates the dimensions of the beam and its mean transverse position, at a longitudinal distance XL from the position corresponding to the keyword *FOCALE*.

IMAGE computes the location and size of the closest horizontal waist.

IMAGES has the same effect as *IMAGE*, but, in addition, for a non-monochromatic beam it calculates as many waists as there are distinct momenta in the beam, provided that the object has been defined with a classification of momenta (see *OBJET*, *KOBJ* = 1, 2 for instance).

Optionally, for each of these three procedures, **zgoubi** can list a trace of the coordinates in the X, Y and in the Y, Z planes.

The following quantities are calculated for the N particles of the beam (*IMAGE, FOCALE*) or of each group of momenta (*IMAGES*)

- Longitudinal position:

$$\begin{aligned} \textit{FOCALE}: \quad & X = XL \\ \textit{IMAGE[S]}: \quad & X = -\frac{\sum_{i=1}^{N} Y_i * tgT_i - \left(\sum_{i=1}^{N} Y_i * \sum_{i=1}^{N} tgT_i\right) /N}{\sum_{i=1}^{N} tg^2T_i - \left(\sum_{i=1}^{N} tgT_i\right)^2 /N} \\ & Y = Y_1 + X * \mathrm{tg}T_1 \end{aligned}$$

  where Y_1 and T_1 are the coordinates of the first particle of the beam (*IMAGE, FOCALE*) or the first particle of each group of momenta (*IMAGES*).

- Transverse position of the center of mass of the waist (*IMAGE[S]*) or of the beam (*FOCALE*), with respect to the reference trajectory

$$YM = \frac{1}{N}\sum_{i=1}^{N}(Y_i + X\mathrm{tg}T_i) - Y = \frac{1}{N}\sum_{i=1}^{N} Y\ M_i$$

- FWHM of the image (*IMAGE[S]*) or of the beam (*FOCALE*), and total width, respectively, W and WT

$$\begin{aligned} W &= 2.35\left(\frac{1}{N}\sum_{i=1}^{N} Y\ M_i^2 - Y\ M^2\right)^{\frac{1}{2}} \\ WT &= \max(Y\,M_i) - \min(Y\,M_i) \end{aligned}$$

FOCALEZ, IMAGE[S]Z: Particle coordinates and beam size; localization and size of vertical waist

Similar to *FOCALE* and *IMAGE[S]*, but the calculations are performed with respect to the vertical coordinates Z_i and P_i, in place of Y_i and T_i.

HISTO: 1-D histogram

Any of the coordinates used in **zgoubi** may be histogrammed, namely initial Y_0, T_0, Z_0, P_0, S_0, D_0 or actual Y, T, Z, P, S, D particle coordinates (S = path length ; D may change in decay process simulation with *MCDESINT*, or when ray-tracing in $\vec{E}$ fields), and also spin coordinates and modulus S_X, S_Y, S_Z and $\left\|\vec{S}\right\|$.

HISTO can be used in conjunction with *MCDESINT*, for statistics on the decay process, by means of *TYP*. *TYP* is a one-character variable. If it is set equal to 'S', only secondary particles will be histogrammed. If it is set equal to 'P', then only primary particles will be histogrammed. For no discrimination between S-econdary and P-rimary particles, *TYP* = 'Q' must be used.

The dimensions of the histogram (number of lines and columns) may be modified. It can be normalized with *NORM* = 1, to avoid saturation.

Histograms are indexed with the parameter NH. This allows making independent histograms of the same coordinate at several spots in a structure. This is also useful when piling up problems in an input data file (see also *RESET*). NH is in the range 1-5.

If *REBELOTE* is used, the statistics on the 1+*NPASS* runs in the structure will add up.

IMAGE[S][Z]: Localization and size of vertical waists

See FOCALE[Z].

MATRIX: Calculation of transfer coefficients, periodic parameters

MATRIX causes the calculation of the transfer coefficients of the structure, at the spot where it is introduced in the structure, or at the closest horizontal focus. In this last case the position of the focus is calculated automatically in the same way as the position of the waist in *IMAGE*. Depending on option *IFOC*, *MATRIX* also delivers the Twiss functions, tune numbers, chromaticities and other perturbation parameters in the hypothesis of a periodic structure.

Depending on the value of option *IORD*, different procedures follow

- If $IORD = 0$, *MATRIX* is inhibited (equivalent to *FAISCEAU*, whatever *IFOC*).
- If $IORD = 1$, the first order transfer matrix $[R_{ij}]$ is calculated, from a third order expansion of the coordinates, for instance

$$Y^+ = \left(\frac{Y}{T_0}\right) T_0 + \left(\frac{Y}{T_0^2}\right) T_0^2 + \left(\frac{Y}{T_0^3}\right) T_0^3$$
$$Y^- = -\left(\frac{Y}{T_0}\right) T_0 + \left(\frac{Y}{T_0^2}\right) T_0^2 - \left(\frac{Y}{T_0^3}\right) T_0^3$$

  which gives, neglecting third order terms

$$R_{11} = \left(\frac{Y}{T_0}\right) = \frac{Y^+ - Y^-}{2T_0}$$

- If $IORD = 2$, fifth order Taylor expansions are used for the calculation of the first order transfer matrix $[R_{ij}]$ and the second order matrix $[T_{ijk}]$. Other higher order coefficients are also calculated.

The object necessary for the calculation of $[R_{ij}]$ with $IORD = 1$ may be generated automatically by means of *OBJET* with option $KOBJ = 5$. When using $IORD = 2$, the object may be generated automatically with *OBJET* and $KOBJ = 6$.

The next option, *IFOC*, acts as follows

- If $IFOC = 0$, the transfer coefficients are calculated at the position of *MATRIX*, and with respect to particle 1 taken as a reference (for instance, Y^+ and T^+ above are defined for particle I as $Y^+ = Y^+(I) - Y(1)$, and $T^+ = T^+(I) - T(1)$).
- If $IFOC = 1$, the transfer coefficients are calculated at the horizontal focus closest to *MATRIX* (determined automatically), while the reference direction is that of particle 1 (for instance, Y^+ is defined for particle I as $Y^+ = Y^+(I) - Y_{\text{focus}}$, and T^+ is defined as $T^+ = T^+(I) - T(1)$).
- If $IFOC = 2$, no change of reference frame is performed: the coordinates refer to the current frame. Namely, $Y^+ = Y^+(I)$, $T^+ = T^+(I)$, etc.

Periodic structures

- If $IFOC = 10 + NPeriod$, *MATRIX* calculates periodic parameters characteristic of the structure such as Twiss functions and tune numbers, assuming that it is *NPeriod*-periodic; no change of reference is performed for these calculations. If $IFOC = 2$ additional periodic parameters are computed such as chromaticities, beta-function momentum dependence, etc.

  These quantities are derived from the first order perturbed and unperturbed transfer matrices as obtained in the way described above, and by identification with the Twiss form $[R_{ij}] = Icos(\mu) + Jsin(\mu)$.

PLOTDATA: Intermediate output for the PLOTDATA graphic software [27]

To be documented

SPNPRNL, SPNPRNLA, SPNPRT: Print/Store spin coordinates

SPNPRNL has the same effect as *SPNPRT* (see below), except that the information is stored in a dedicated file *FNAME* (standard is *FNAME* = 'zgoubi.spn' for post-processing with **zpop**). The data are formatted and ordered according to the *FORTRAN* sequence below

```
OPEN (UNIT = NL, FILE = FNAME, STATUS = 'NEW')
DO  1  I=1, IMAX
    WRITE (NL,100) LET(I), IEX(I), (SI(J,I)J=1,4), (SF(J,I),J=1,4), GAMMA, I
 100   FORMAT(1X, A1, I2, 1P, 8E15.7, /, E15.7, 2I3, I6)
  1     CONTINUE
```

The meaning of these parameters is the following

LET(I),IEX(I)	:	tagging character and flag (see *OBJET*)
SI(1-4,I)	:	spin components SX, SY, SZ and modulus, at the origin
SF(1-4,I)	:	idem, at the current position
GAMMA	:	Lorentz relativistic factor
I	:	particle number
IMAX	:	total number of particles ray-traced (see *OBJET*)
IPASS	:	turn number (see *REBELOTE*)

SPNPRNLA has an effect similar to *SPNPRNL*, with one more feature. The line next to *FNAME* gives a parameter IP printing will occur every IP other pass, when using *REBELOTE* with *NPASS* $\geq IP - 1$.

SPNPRT can be introduced anywhere in a structure. It produces a listing (into zgoubi.res) of the initial and actual coordinates and modulus of the spin of the *IMAX* particles, at the location where it stands, together with their Lorentz factor γ, following the format detailed above. The mean values of the spin components are also printed.

SRPRNT: Print SR loss statistics

SRPRNT may be introduced anywhere in a structure. It produces a listing (into zgoubi.res) of current state of statistics on several parameters related to SR loss presumably activated beforehand with keyword *SRLOSS*.

TWISS: Calculation of optical parameters ; periodic parameters

TWISS causes the calculation of transfer coefficients and various other parameters, in particular periodical quantities such as tunes, chromaticies, etc.
If $KTWISS = 1$, the object necessary for these calculations can be generated automatically by means of *OBJET* with option $KOBJ = 5$. When using $KTWISS = 2$, the object can be generated automatically with *OBJET* and $KOBJ = 6$.

4.6 Complementary Features

4.6.1 Backward Ray-tracing

For the purpose of parameterization for instance, it may be interesting to ray-trace backward from the image toward the object. This can be performed by first reversing the position of optical elements in the structure, and then reversing the integration step sign in all the optical elements.

An illustration of this feature is given in the following Figure 37.

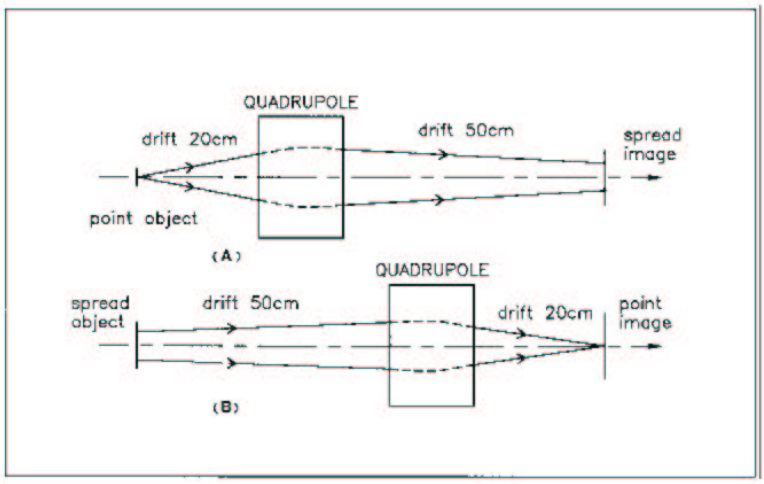

Figure 37: A. Regular forward ray-tracing, from object to image.
B. Same structure, with backward ray-tracing from image to object: negative integration step XPAS is used in the quadrupole.

4.6.2 Checking Fields and Trajectories inside Optical Elements

In all optical elements, an option index IL is available. It is normally set to 0 and in this case has no effect.
$IL = 1$ causes a print in zgoubi.res of particle coordinates and field along trajectories in the optical element. In the meantime, a calculation and summation of the values of $\vec{\nabla} \cdot \vec{B}$, $\vec{\nabla} \times \vec{B}$ and $\nabla^2 \vec{B}$ (same for $\vec{E}$) at all integration steps is performed, which allows a check of the behavior of $\vec{B}$ (or $\vec{E}$) in field maps (all these derivatives should normally be zero).
$IL = 2$ causes a print of particle coordinates and other informations in zgoubi.plt at each integration step ; this information can further be processed with **zpop**[7]. In order to limit the volume of that storage file (when dealing with small step size, large number of particles, etc.) it is possible to print out every other 10^n integration step by taking $IL = 2 \times 10^n$ (for instance, $IL = 200$ would cause output into zgoubi.plt every 100 other step).

When dealing with maps (e.g., *CARTEMES*, *ELREVOL*), another option index IC is available. It is normally set to 0 and in this case has no effect.
$IC = 1$ causes a print of the field map in zgoubi.res.
$IC = 2$ will cause a print of field maps in zgoubi.map which can further be processed with **zpop**.

[7] See Part D of the Guide.

4.6.3 Labeling keywords

Keywords in **zgoubi** data file zgoubi.dat can be *LABEL*'ed, for the purpose of the execution of such procedures as *CLORB*, *FAISCNL*, *FAISTORE* , *SCALING*.
Each keyword accepts two *LABEL*'s, of which the first one is used for the above mentioned purposes. The keyword and related *LABEL*['s] should fit within a 80-character long string on a single line.

4.6.4 Multiturn tracking in circular machines

Multiturn tracking in circular machines can be performed by means of the keyword *REBELOTE*, put at the end of the optical structure with its argument *NPASS*+1 being the number of turns to be performed. In order that the *IMAX* particles of the beam start a new turn with the coordinates they have reached at the end of the previous one, the option $K = 99$ has to be specified in *REBELOTE*.

Synchrotron acceleration can be simulated, following the procedure below

- *CAVITE* appears at the end of the structure (before *REBELOTE*), with option *IOPT*= 1
- the R.F. frequency of the cavity is given a timing law by means of *SCALING*, family *CAVITE*
- the magnets are given the same timing law $B\rho(T)$, (where $T = 1$ to *NPASS*+1 is the turn number) by means of *SCALING*.

Eventually some families of magnets may be given a law which does not follow $B\rho(T)$, for the simulation of special processes (e.g. fast crossing of spin resonances with independent families of quadrupoles).

4.6.5 Positioning of optical elements and field maps

The last record in most optical elements and field maps is the positioning flag *KPOS*, followed by the parameterss *XCE*, *YCE* for translation and *ALE* for rotation. The positioning works in two different ways, depending whether they are defined in Cartesian (X, Y, Z) coordinates (e.g., *QUADRUPO*, *TOSCA*), or polar (R, θ, Z) coordinates (*DIPOLE*).

Cartesian Coordinates:

If $KPOS = 1$, the X-axis of the element coincides with the X-axis of the incoming reference.
If $KPOS = 2$, the shifts *XCE* and *YCE*, and the tilt angle *ALE* are taken into account, for the positioning of the element with respect to the incoming reference, as shown in Fig. 38. $KPOS = 2$ can also be used to simulate a misalignment. The effect is equivalent to a *CHANGREF* transformation placed right upstream the optical element, followed by the reverse transformation right downstream.
$KPOS = 3$ option is available for some magnets (e.g., *BEND*, *MULTIPOL*); it positions automatically the device in the following way, convenient for periodic structures. It is effective only if a non zero dipole component $B1$ is present; entrance and exit frames are shifted by *YCE* (*XCE* is not used) and tilted w.r.t. the magnet

- either, if ALE≠0 by an angle *ALE*,
- or, if ALE=0 by half the deviation $\theta/2$ (such that $L = 2\frac{BORO}{B1}\sin(\theta/2)$ wherein L = geometrical length, *BORO*= reference rigidity as defined in *OBJET*). This is equivalent to the sequence *CHANGREF(0,0,-θ/2)*, *CHANGREF(0,YCE,0)* right upstream the magnet, followed by *CHANGREF(0,-YCE,-θ/2)*.

Polar Coordinates

If $KPOS = 1$, the element is positioned automatically in such a way that a particle entering with zero initial coordinates and $1 + DP = B\rho/BORO$ relative momentum will reach position $(RM, \frac{AT}{2})$ in the element with $T = 0$ angle with respect to the moving frame in the polar coordinates system of the element (Fig. 39; see *DIPOLE* and *POLARMES*).
If $KPOS = 2$, the map is positioned in such a way that the incoming particle will enter it at radius RE with angle TE. The reference frame of **zgoubi** is positioned in a similar way with respect to the map, at the exit face, by means of the two parameters RS (radius) and TS (angle) (see Fig. 10A.).

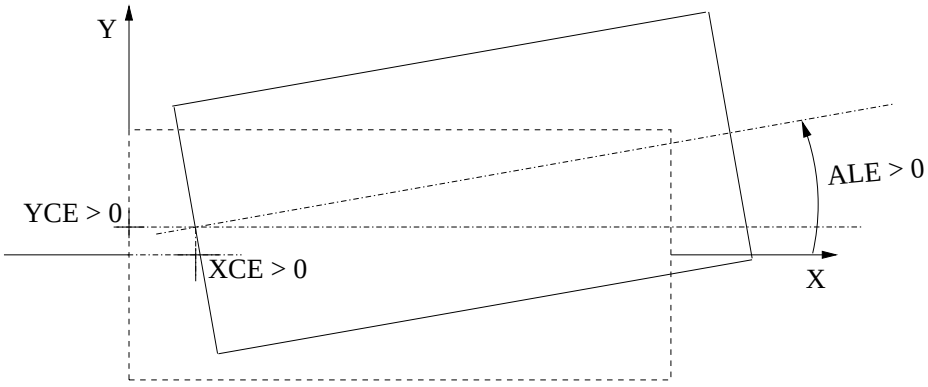

Figure 38: Positioning of a Cartesian coordinate optical element when *KPOS*= 2.

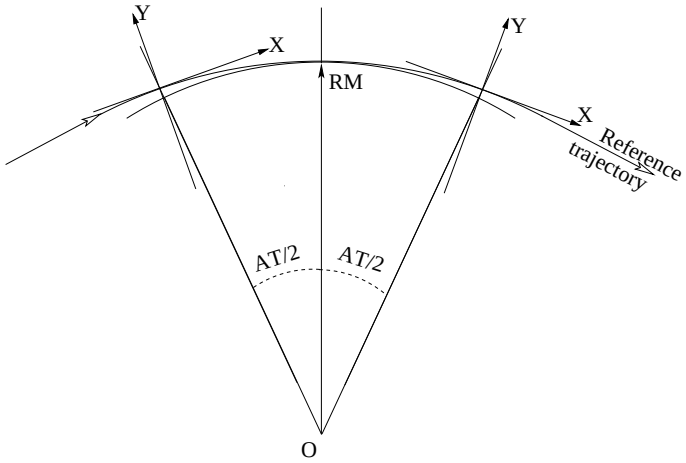

Figure 39: Positioning of a polar field map when *KPOS*= 1.

4.6.6 Coded integration step

In several optical elements (e.g., all multipoles, *BEND*) the integration step (in general noted *XPAS*) can be coded under the form *XPAS* = b.fffE10 in order to allow two different step sizes in the uniform part of the field (the optical element body) and in the field fall-off regions. b is an arbitrary integer and fff is a 3-digit integer; they give the number of steps respectively in the body and fringe field regions. For instance 120.012E10 requests 120 steps in the body and 12 in the fringe field regions. The maximum allowed value for fff is 999 steps.

4.6.7 Ray-tracing of an arbitrarily large number of particles

Monte Carlo multiparticle simulations involving an arbitrary number of particles can be performed by means of *REBELOTE*, put at the end of the optical structure, with its argument *NPASS* being the number of passes through *REBELOTE*, and (*NPASS*+1) * *IMAX* the number of particles to be ray-traced. In order that new initial conditions (D, Y, T, Z, P, X) be generated at each pass, $K = 0$ has to be specified in *REBELOTE*.

Statistics on coordinates, spins, and other histograms can be performed by means of such procedures as *HISTO*, *SPNTRK*, etc. that stack the information from pass to pass.

4.6.8 Stopped particles: the IEX flag

As described in *OBJET*, each particle $I = 1$, *IMAX* is attached a value $IEX(I)$ of the *IEX* flag. Normally, $IEX(I) = 1$. Under certain circumstances, *IEX* may take negative values, as follows

-1 : the trajectory happened to wander outside the limits of a field map

-2 : too many integration steps in an optical element

-3 : deviation happened to exceed $\frac{\pi}{2}$ in an optical element

-4 : stopped by walls (procedures *CHAMBR*, *COLLIMA*)

-5 : too many iterations in subroutine *DEPLA*

-6 : energy loss exceeds particle energy

-7 : field discontinuities larger than 50% wthin a field map

-8 : reached field limit in an optical element

Only in the case $IEX = -1$ will the integration not be stopped since in this case the field outside the map is extrapolated from the map data, and the particle may possibly get back into the map (see section 1.4.2 on page 21). In all other cases the particle of concern will be stopped.

4.6.9 Negative rigidity

zgoubi can handle negative rigidities $B\rho = p/q$. This is equivalent to considering either particles of negative charges ($q < 0$), or counter going particles ($p < 0$), or virtually reversed fields (w.r.t. the field sign that shows in the optical element data list).
Negative rigidities may be specified in terms of *BORO*< 0 or $D = B\rho/BORO < 0$ when defining the initial coordinates with *OBJET* and *MCOBJET*.

PART B

Keywords and input data formatting

Glossary of keywords

Optical elements versus keywords

This glossary gives a list of keywords suitable for the simulation of common optical elements. These are classified in three categories: magnetic, electric and electromagnetic elements.

Field map procedures are also cataloged; they provide a mean for ray-tracing through measured fields, or as well through field maps obtained from numerical simulations of arbitrary geometries with such tools as POISSON, TOSCA, etc.

MAGNETIC ELEMENTS

Decapole	DECAPOLE, MULTIPOL
Dipole	AIMANT, BEND, DIPOLE, MULTIPOL, QUADISEX
Dodecapole	DODECAPO, MULTIPOL
Multipole	MULTIPOL, QUADISEX, SEXQUAD
Octupole	OCTUPOLE, MULTIPOL, QUADISEX, SEXQUAD
Quadrupole	QUADRUPO, MULTIPOL, SEXQUAD
Sextupole	SEXTUPOL, MULTIPOL, QUADISEX, SEXQUAD
Skewed multipoles	MULTIPOL
Solenoid	SOLENOID
Undulator	UNDULATOR

Field maps

1-D, cylindrical symmetry	BREVOL
2-D, mid-plane symmetry	CARTEMES, POISSON, TOSCA
2-D, no symmetry	MAP2D
2-D, polar mesh, mid-plane symmetry	POLARMES
3-D, no symmetry	TOSCA

ELECTRIC ELEMENTS

2-tube (bipotential) lens	EL2TUB
3-tube (unipotential) lens	UNIPOT
Decapole	ELMULT
Dipole	ELMULT
Dodecapole	ELMULT
Multipole	ELMULT
N-electrode mirror/lens, straight slits	ELMIR
N-electrode mirror/lens, circular slits	ELMIRC
Octupole	ELMULT
Quadrupole	ELMULT
R.F. (kick) cavity	CAVITE
Sextupole	ELMULT
Skewed multipoles	ELMULT

Field maps

1D, cylindrical symmetry	ELREVOL
2-D, no symmetry	MAP2D

ELECTROMAGNETIC ELEMENTS

Decapole	EBMULT
Dipole	EBMULT
Dodecapole	EBMULT
Multipole	EBMULT
Octupole	EBMULT
Quadrupole	EBMULT
Sextupole	EBMULT
Skewed multipoles	EBMULT
Wien filter	SEPARA, WIENFILT

INTRODUCTION

Here after is given a detailed description of input data formatting and units. All available keywords appear in alphabetical order.

Keywords are read from the input data file by an unformatted *FORTRAN READ* statement. They may therefore need be enclosed between quotes (e.g., '*DIPOLE*').

Text string data such as comments or file names, are read by formatted READ statements. Therefore no quotes are needed. Numerical variables and indices are read by unformatted READ. It may therefore be necessary that integer variables be assigned an integer value.

In the following tables

- the first column states the input numerical variables, indices and text strings,
- the second column gives brief explanations,
- the third column gives the units or ranges of the input variables and indices,
- the fourth column indicates whether the inputs are integers (I), reals (E) or text strings (A). For example, 'I, 3*E' means that one integer followed by 3 reals must be entered. 'A80' means that a text string of maximum 80 characters must be entered.

AIMANT	**Generation of a dipole magnet 2-D map** $B_Z = \mathcal{F} B_0 \left(1 - N\left(\frac{R-RM}{RM}\right) + B\left(\frac{R-RM}{RM}\right)^2 + G\left(\frac{R-RM}{RM}\right)^3\right)$		
NFACE, IC, IL	Number of field boundaries $IC = 1, 2$: print field map $IL = 1, 2$: print field and coordinates on trajectories	2-3, 0-2, 0-2	3*I
IAMAX, IRMAX	Azimuthal and radial number of nodes of the mesh	≤ 400, $\leq 10^4$	2*I
B_0, N, B, G	Field and field indices	kG, 3* no dim.	4*E
AT, ACENT, RM, RMIN, RMAX	Mesh parameters: total angle of the map; azimuth for positioning of EFB's; mean radius; minimum and maximum radii	2*deg, 3*cm	5*E
	ENTRANCE FIELD BOUNDARY		
λ, ξ	Fringe field extent (normally $\simeq$ gap size); flag: - if $\xi \geq 0$: second order type fringe field with linear variation over distance ξ - if $\xi = -1$: exponential type fringe field: $F = (1 + \exp(P(s)))^{-1}$ $P(s) = C_0 + C_1(\frac{s}{\lambda}) + C_2(\frac{s}{\lambda})^2 + ... + C_5(\frac{s}{\lambda})^5$	cm, (cm)	2*E
NC, $C_0 - C_5$, shift	NC = 1 + order of $P(s)$; C_0 to C_5: see above; EFB shift (ineffective if $\xi \geq 0$)	0-6, 6* no dim., cm	I, 7*E
ω^+, θ, R_1, U_1, U_2, R_2	Azimuth of entrance EFB with respect to *ACENT*; wedge angle of EFB; radii and linear extents of EFB (use $\mid U_{1,2} \mid = \infty$ when $R_{1,2} = \infty$) (Note : $\lambda = 0$, ω^+ = ACENT and $\theta = 0$ for <u>sharp edge</u>)	2*deg, 4*cm	6*E
	EXIT FIELD BOUNDARY (See ENTRANCE FIELD BOUNDARY)		
λ, ξ	Fringe field parameters	cm, (cm)	2*E
NC, $C_0 - C_5$, shift		0-6, 6* no dim., cm	1, 7*E
ω^-, θ, R_1, U_1, U_2, R_2	Positioning and shape of the exit EFB (Note : $\lambda = 0$, ω^- =-AT+ACENT and $\theta = 0$ for <u>sharp edge</u>)	2*deg, 4*cm	6*E

if NFACE = 3	LATERAL FIELD BOUNDARY (See ENTRANCE FIELD BOUNDARY) Next 3 records *only* if *NFACE* = 3		
λ, ξ	Fringe field parameters	cm, (cm)	2*E
NC, $C_0 - C_5$, shift		0-6, 6* no dim., cm	I, 7*E
ω^-, θ, R_1, U_1, U_2, R_2, $RM3$	Positioning and shape of the lateral EFB; RM3 is the radial position on azimut *ACENT*	2*deg, 5cm	7*E
NBS	Option index for perturbations to the field map	normally 0	I
if NBS = 0	Normal value. No other record required		
if NBS = -2	The map is modified as follows:		
R_0, $\Delta B/B_0$	B transforms to $B * \left(1 + \frac{\Delta B}{B_0} \frac{R-R_0}{RMAX-RMIN}\right)$	cm, no dim.	2*E
if NBS = -1	the map is modified as follows:		
θ_0, $\Delta B/B_0$	B transforms to $B * \left(1 + \frac{\Delta B}{B_0} \frac{\theta-\theta_0}{AT}\right)$	deg, no dim.	2*E
if NBS $\geq$ 1	Introduction of NBS shims		
For I = 1, NBS ¿	The following 2 records must be repeated NBS times		
R_1, R_2, θ_1, θ_2, λ	Radial and angular limits of the shim; λ is unused	2*cm, 2*deg, cm	5*E
γ, α, μ, β	geometrical parameters of the shim	2*deg, 2*no dim.	4*E
IORDRE	Order of interpolation polynomial: 2 = second order, 9-point grid 25 = second order, 25-point grid 4 = fourth order, 25-point grid	2, 4 or 25	I
XPAS	Integration step	cm	E
KPOS	Positioning of the map, normally 2. Two options:	1-2	I
if KPOS = 2 RE, TE, RS, TS	Positioning as follows: Radius and angle of reference, respectively, at entrance and exit of the map.	cm, rad, cm, rad	4*E
if KPOS = 1 *DP*	Automatic positioning of the map, by means of reference relative momentum	no dim.	E

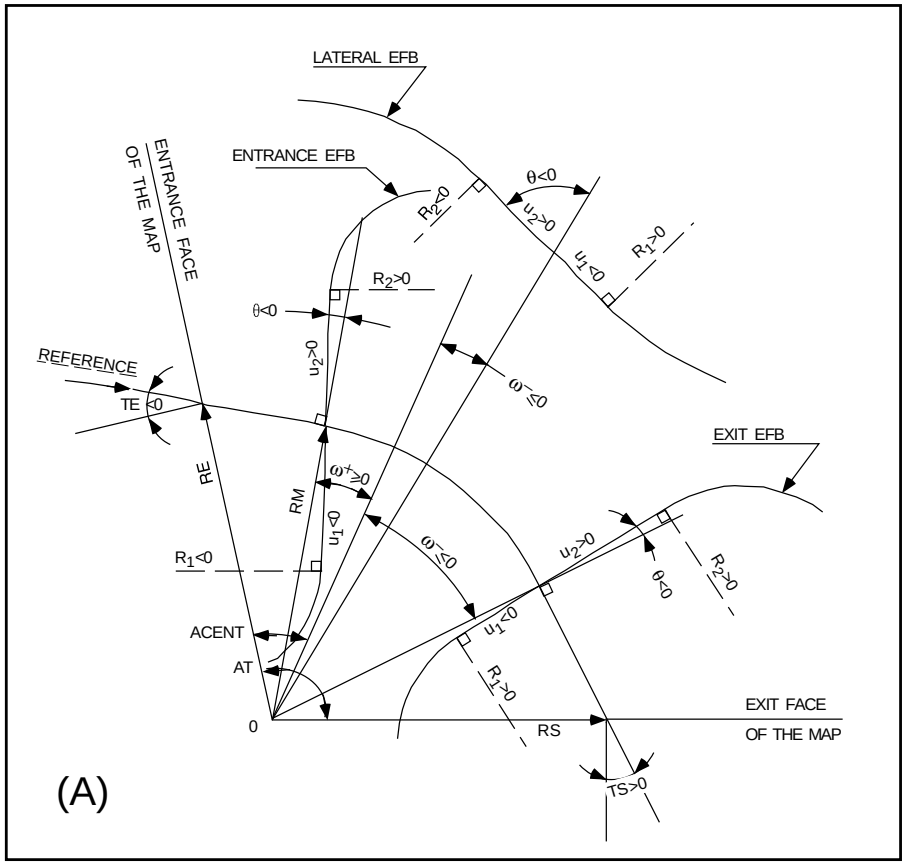

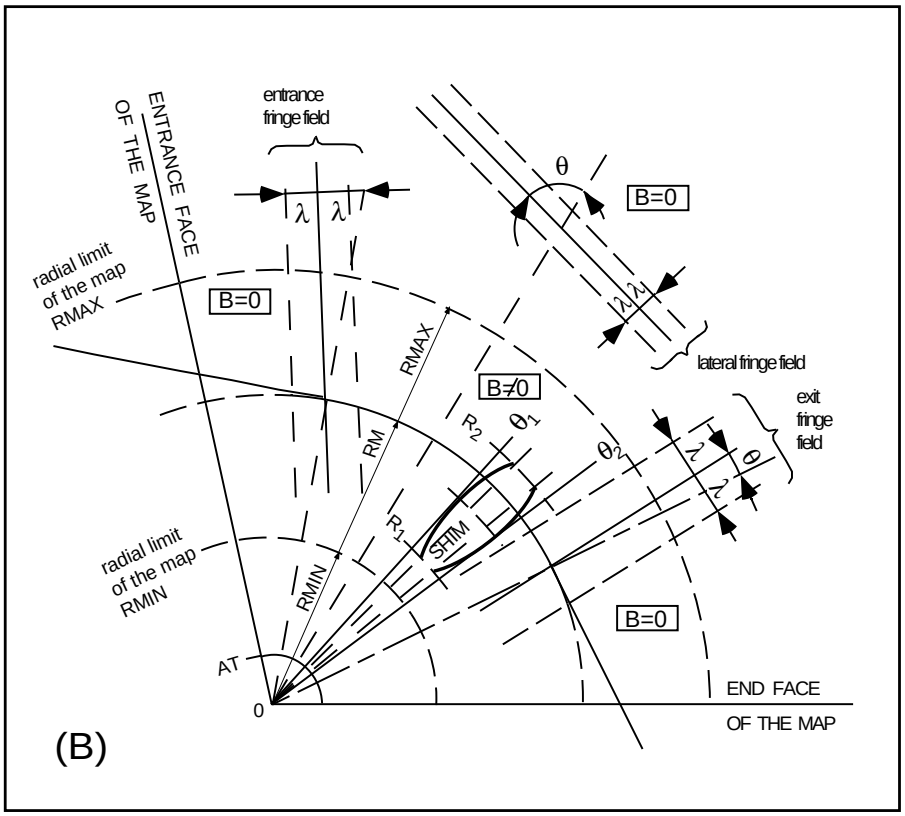

A: Parameters used to define the field map and geometric boundaries.
B: Parameters used to define the field map and fringe fields.

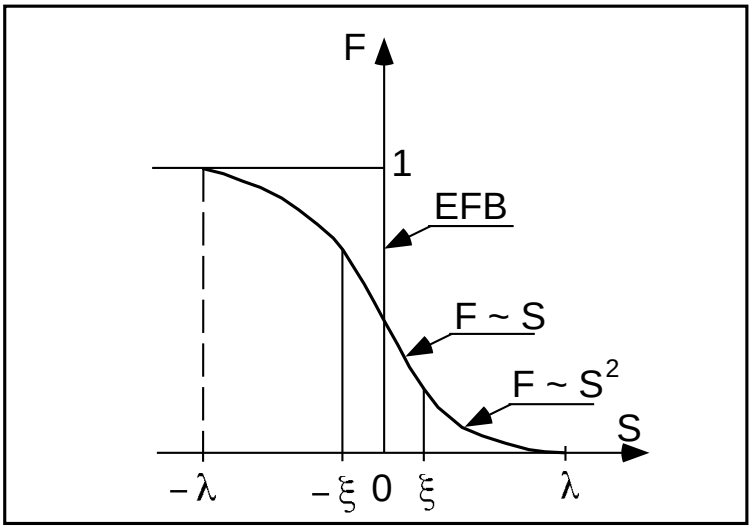

Second order type fringe field.

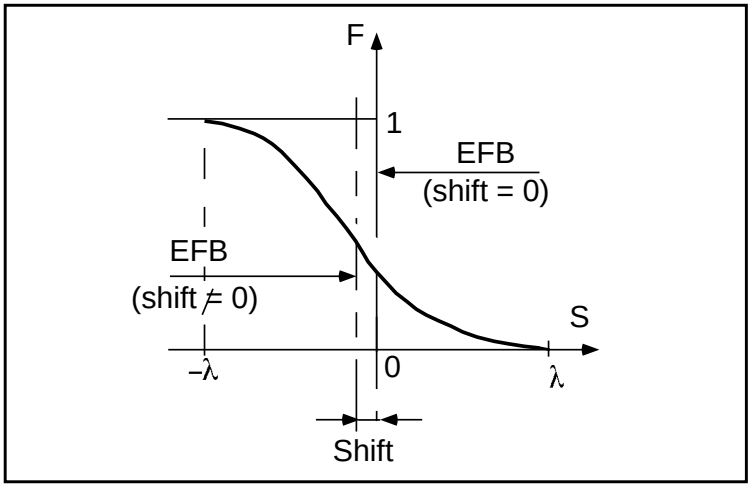

Exponential type fringe field.

AUTOREF **Automatic transformation to a new reference frame**

I	1: Equivalent to *CHANGREF* ($XCE = 0$, $YCE = Y(1)$, $ALE = T(1)$)	1-2	I
	2: Equivalent to *CHANGREF* (XW, YW, $T(1)$), with (XW, YW) being the position of the intersection (waist) of particles 1, 4 and 5 (useful with *MATRIX*, for automatic positionning of the first order focus)		
	3: Equivalent to *CHANGREF* (XW, YW, $T(I1)$), with (XW, YW) being the position of the intersection (waist) of particles $I1$, $I2$ and $I3$ (for instance: $I1$ = central trajectory, $I2$ and $I3$ = paraxial trajectories that intersect at the first order focus)		
if $I = 3$	Next record only if $I = 3$		
$I1$, $I2$, $I3$	Three particle numbers	3*(1-10^4)	3*I

BEND	**Bending magnet**		
IL	*IL* = 1, 2: print field and coordinates along trajectories (otherwise *IL* = 0)	0-2	I
XL, *Sk*, *B*1	Length; skew angle; field	cm, rad, kG	3*E
	Entrance face:		
X_E, λ_E, W_E	Integration zone extent; fringe field extent (normally $\simeq$ gap height; zero for sharp edge); wedge angle	cm, cm, rad	3*E
N, C_0–C_5	Unused; fringe field coefficients: $B(s) = B1\,F(s)$ with $F(s) = 1/(1+\exp(P(s)))$ and $P(s) = \sum_{i=0}^{5} C_i(s/\lambda)^i$	unused, 6*no dim.	I, 6*E
	Exit face:		
X_S, λ_S, W_S	See entrance face	cm, cm, rad	3*E
N, C_0–C_5		unused, 6*no dim.	I, 6*E
XPAS	Integration step	cm	E
KPOS, *XCE*, *YCE*, *ALE*	*KPOS*=1: element aligned, 2: misaligned; shifts, tilt (unused if *KPOS*=1) *KPOS* = 3: entrance and exit frames are shifted by *YCE* and tilted *wrt.* the magnet by an angle of • either ALE if ALE≠0 • or 2 Arcsin(*B*1*XL* / 2*BORO*) if ALE=0	1-2, 2*cm, rad	I, 3*E

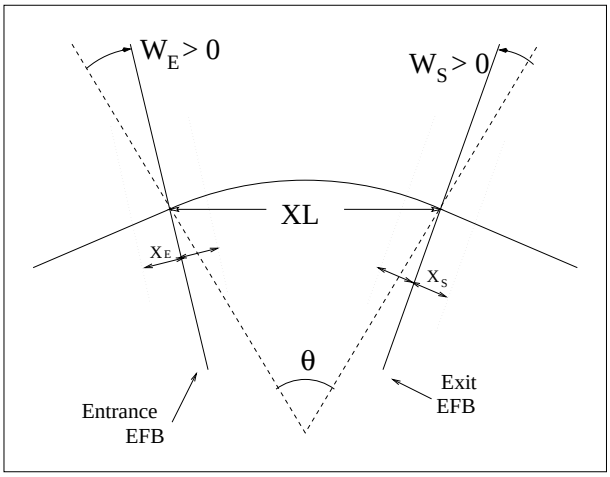

Geometry and parameters in *BEND*: *XL* = length, θ = deviation, W_E, W_S are the entrance and exit wedge angles.

BINARY	***BINARY/FORMATTED* data converter**		
NF	Number of files to convert	≤ 20	I
The next NF lines:			
FNAME	Name of the file to be translated (begin with "B_" *iff* binary)		A80

BREVOL	**1-D uniform mesh magnetic field map** X-axis cylindrical symmetry is assumed		
IC, *IL*	$IC = 1, 2$: print the map IL = 1,2: print field and coordinates along trajectories	0-2, 0-2	2*I
BNORM, XN	Field and X-coordinate normalization	2*no dim.	2*E
TIT	Title		A80
IX	Number of longitudinal nodes of the map	≤ 400	I
FNAME[1]	Filename (e.g., solenoid.map)		A80
ID, A, B, C [A', B', C' B'',etc., if $ID \geq 2$]	Integration boundary. Ineffective when $ID = 0$. ID = -1, 1 or ≥ 2 : as for *CARTEMES*	≥ -1, 2*no dim., cm [,2*no dim., cm, etc.]	I,3*E [,3*E,etc.]
IORDRE	unused	2, 4 or 25	I
XPAS	Integration step	cm	E
KPOS, *XCE*, *YCE, ALE*	*KPOS*=1: element aligned, 2: misaligned; shifts, tilt (unused if *KPOS*=1)	1-2, 2*cm, rad	I, 3*E

[1] *FNAME* contains the field data. These must be formatted according to the following *FORTRAN* sequence:

```
OPEN (UNIT = NL, FILE = FNAME, STATUS = 'OLD' [,FORM='UNFORMATTED'])
DO 1 I = 1, IX
 IF (BINARY) THEN
      READ(NL) X(I), BX(I)
 ELSE
      READ(NL,*) X(I), BX(I)
 ENDIF
  1    CONTINUE
```

where $X(I)$ and $BX(I)$ are the longitudinal coordinate and field component at node (I) of the mesh. Binary file names *FNAME* must begin with B_. 'Binary' will then automatically be set to '.TRUE.'.

CARTEMES	**2-D Cartesian uniform mesh magnetic field map** mid-plane symmetry is assumed		
IC, *IL*	$IC = 1, 2$: print the map $IL = 1, 2$: print field and coordinates along trajectories	0-2, 0-2	2*I
BNORM, XN,YN	Field and X-,Y-coordinate normalization	3*no dim.	3*E
TIT	Title[1]		A80
IX, *JY*	Number of longitudinal (IX) and transverse (JY) nodes of the map	≤ 400, ≤ 200	2*I
FNAME[2]	Filename (e.g., spes2.map)		A80
ID, A, B, C [A', B', C', A'', B'',etc., if $ID \geq 2$]	Integration boundary. Normally $ID = 0$. $ID = -1$: integration in the map begins at entrance boundary defined by $AX + BY + C = 0$. $ID = 1$: integration in the map is terminated at exit boundary defined by $AX + BY + C = 0$. $ID \geq 2$: entrance (A, B, C) and up to $ID - 1$ exit $(A', B', C', A'', B'', etc.)$ boundaries	≥ -1,2*no dim., cm [,2*no dim., cm, etc.]	I, 3*E [3*E,etc.]
IORDRE	Order of interpolation polynomial (see *DIPOLE*)	2, 4 or 25	I
XPAS	Integration step	cm	E
KPOS, *XCE*, *YCE*, *ALE*	*KPOS*=1: element aligned, 2: misaligned; shifts, tilt (unused if *KPOS*=1)	1-2, 2*cm, rad	I, 3*E

[1] Begin "Title" with "FLIP" so as to get the map flipped prior to ray-tracing.
[2] *FNAME* contains the field data. These must be formatted according to the following *FORTRAN* sequence:

```
OPEN (UNIT = NL, FILE = FNAME, STATUS = 'OLD' [,FORM='UNFORMATTED'])
IF (BINARY) THEN
  READ(NL) (Y(J), J=1, JY)
ELSE
        READ(NL,100) (Y(J), J=1, JY)
      ENDIF
100    FORMAT(10 F8.2)
      DO 1 I=1,IX
  IF (BINARY) THEN
    READ(NL) X(I), (BMES(I,J), J=1, JY)
ELSE
   READ(NL,101) X(I), (BMES(I,J), J=1, JY)
101  FORMAT(10 F8.2)
      ENDIF
 1     CONTINUE
```

where $X(I)$ and $Y(J)$ are the longitudinal and transverse coordinates and *BMES* is the Z field component at a node (I, J) of the mesh. For binary files, *FNAME* must begin with B_.'Binary' will then automatically be set to '.TRUE.'

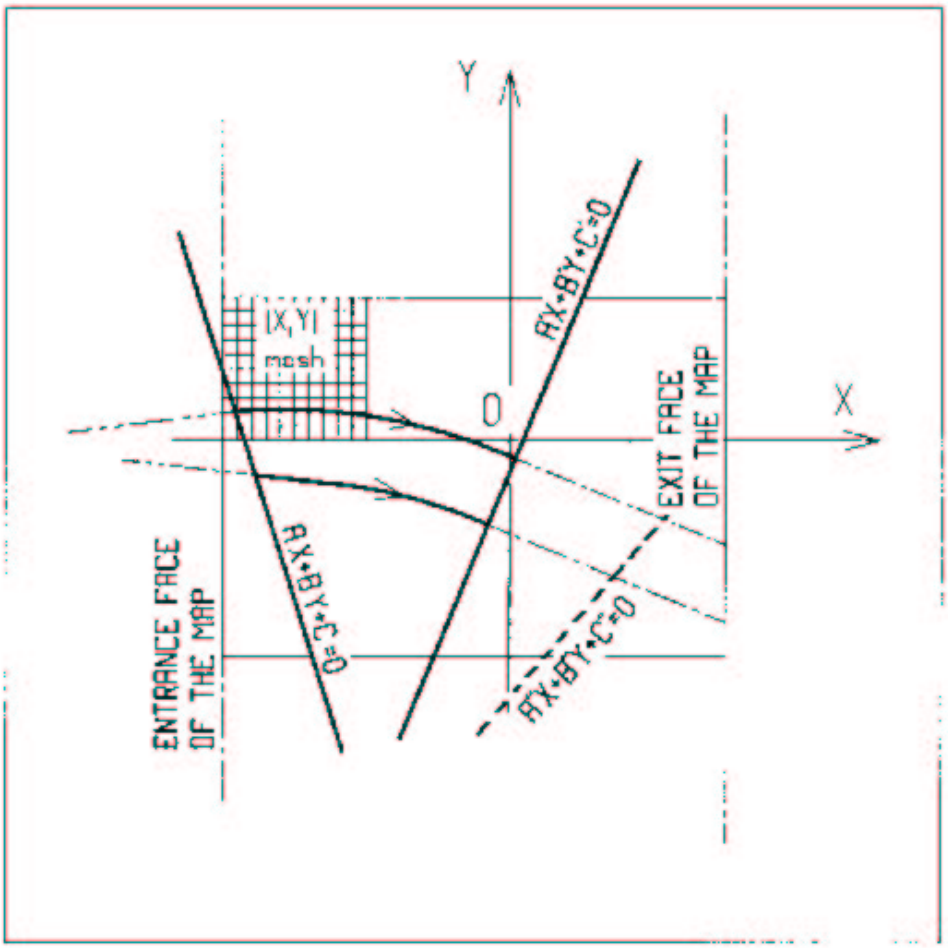

OXY is the coordinate system of the mesh. Integration zone limits may be defined, using $ID \neq 0$: particle coordinates are extrapolated linearly from the entrance face of the map, into the plane $A'X + B'Y + C' = 0$; after ray-tracing inside the map and terminating on the integration boundary $AX + BY + C = 0$, coordinates are extrapolated linearly to the exit face of the map.

CAVITE[1]	**Accelerating cavity** $\Delta W = qV sin(2\pi h f \Delta t + \varphi_s)$		
IOPT	Option	0-3	I
If IOPT=0	Element inactive		
X, X	unused		
If IOPT=1[2]	f_{RF} follows the timing law given by *SCALING*		
$\mathcal{L}$, h	Reference closed orbit length; harmonic number	m, no dim.	2*E
$\hat{V}$, X	R.F. peak voltage; unused	V, unused	2*E
If IOPT=2 $\mathcal{L}$, h	f_{RF} follows $\Delta W_s = q\hat{V} sin\phi_s$ Reference closed orbit length; harmonic number	m, no dim.	2*E
$\hat{V}$,ϕ_s	R.F. peak voltage; synchronous phase	V, rad	2*E
If IOPT=3	No synchrotron motion: $\Delta W = q\hat{V} sin\phi_s$		
X, X	unused; unused	2*unused	2*E
$\hat{V}$, ϕ_s	R.F. peak voltage; synchronous phase	V, rad	2*E

[1] Use *PARTICUL* to declare mass and charge.
[2] For ramping the R.F. frequency following $B\rho(t)$, use *SCALING*, with family *CAVITE*.

CHAMBR	**Long transverse aperture limitation**[1]		
IA	0: element inactive 1: (re)definition of the aperture 2: stop testing and reset counters, print information on stopped particles.	0-2	I
IFORM, YL[2], ZL, YC, ZC	Taken into account only if $IA = 1$. *IFORM* $= 1$: rectangular chamber; horizontal (vertical) dimension $\pm YL$ ($\pm ZL$); centered at YC, ZC. *IFORM* $= 2$: elliptical chamber; horizontal (vertical) axis $\pm YL(\pm ZL)$; centered at YC, ZC.	1-2, 4*cm	I, 4*E

[1] Any particle out of limits is stopped.

[2] When used with an optical element defined in polar coordinates (e.g. *DIPOLE*) YL is the radius and YC stands for the mean radius (normally, $YC \simeq RM$).

CHANGREF	**Transformation to a new reference frame**		
XCE, YCE, ALE	Longitudinal and transverse shifts, followed by Z-axis rotation	2*cm, deg	3*E

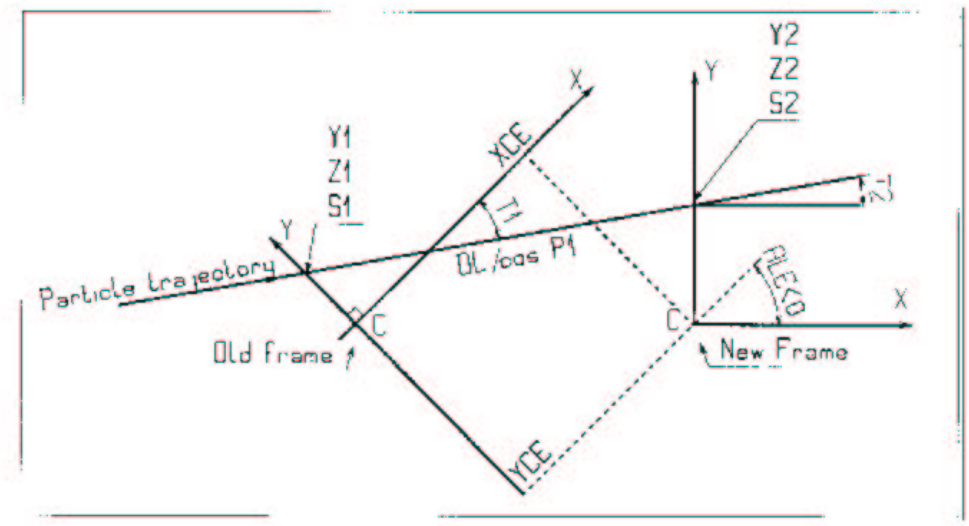

Scheme of the *CHANGREF* procedure.

CIBLE, TARGET **Generate a secondary beam from target interaction**

M_1, M_2, M_3, Q T_2, θ, β	Target, incident and scattered particle masses; Q of the reaction; incident particle kinetic energy; scattering angle; angle of the target	$5*\frac{MeV}{c^2}$, 2*deg	7*E
NT, NP	Number of samples in T and P coordinates after *CIBLE*		2*I
TS, PS, DT	Sample step sizes; tilt angle	3*mrad	3*E
BORO	New reference rigidity after *CIBLE*	kG.cm	E

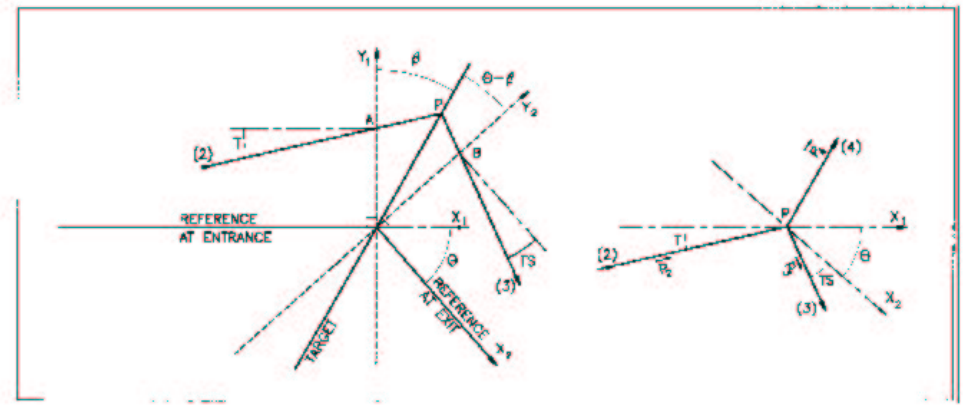

Scheme of the principles of *CIBLE (TARGET)*

A, T = position, angle of incoming particle 2 in the entrance reference frame
P = position of the interaction
B, T = position, angle of the secondary particle in the exit reference frame
θ = angle between entrance and exit frames
β = tilt angle of the target

CLORB	**Beam centroid path; closed orbit**		
N	0: inactive ≥ 1: total number of *LABEL*'s at which beam centroid is to be recorded	≥ 0	I
For I = 1, N	A list of N records follows		
LABEL's	N labels at which beam centroid is to be recorded	strings	N*A8

COLLIMA	**Collimator**[1]		
IA	0: element inactive 1: element active 2: element active and print information on stopped particles	0-2	I
Physical-space collimator			
IFORM, *YL*, *ZL*, *YC*, *ZC*	*IFORM* = 1: rectangular collimator; horizontal (vertical) dimension $\pm YL$ ($\pm ZL$); centered at *YC*, *ZC*. *IFORM* = 2: elliptical collimator; horizontal (vertical) axis $\pm YL$ ($\pm ZL$); centered at *YC*, *ZC*.	1-2, 4*cm	I, 4*E
Longitudinal phase-space collimation			
IFRM.J, H_{min}, H_{max}, V_{min}, V_{max}	*IFRM* = 6 or 7 for horizontal variable resp[ly] S (cm) or Time (μs), J=1 or 2 for vertical variable resp[ly] 1+dp/p, kinetic-E (MeV); horizontal and vertical limits		I, 4*E
Phase-space collimator			
IFORM, α, β, ϵ/π, N_σ	*IFORM* = 11, 14: horizontal collimation; horizontal ellipse parameters (unused if 14), emittance, cut-off *IFORM* = 12, 15: vertical collimation; vertical ellipse parameters (unused if 15), emittance, cut-off *IFORM* = 13, 16: longitudinal collimation; *to be implemented*	11-16, no.dim, m m.rad, no.dim	I, 4*E

[1] Any particle out of limits is stopped.

DECAPOLE	**Decapole magnet**		
IL	$IL = 1, 2$: print field and coordinates along trajectories	0-2	I
XL, R_0, B_0	Length; radius and field at pole tip	2*cm, kG	3*E
X_E, λ_E	Entrance face: Integration zone extent; fringe field extent ($\lesssim 2R_0$, $\lambda_E = 0$ for sharp edge)	2*cm	2*E
NCE, $C_0 - C_5$	*NCE* = unused $C_0 - C_5$ = Fringe field coefficients such that $G(s) = G_0/(1 + \exp P(s))$, with $G_0 = B_0/R_0^4$ and $P(s) = \sum_{i=0}^{5} C_i(s/\lambda)^i$	unused, 6*no dim.	I, 6*E
X_S, λ_S	Exit face: see entrance face	2*cm	2*E
NCS, $C_0 - C_5$		0-6, 6*no dim.	I, 6*E
XPAS	Integration step	cm	E
KPOS, *XCE*, *YCE*, *ALE*	*KPOS*=1: element aligned, 2: misaligned; shifts, tilt (unused if *KPOS*=1)	1-2, 2*cm, rad	I, 3*E

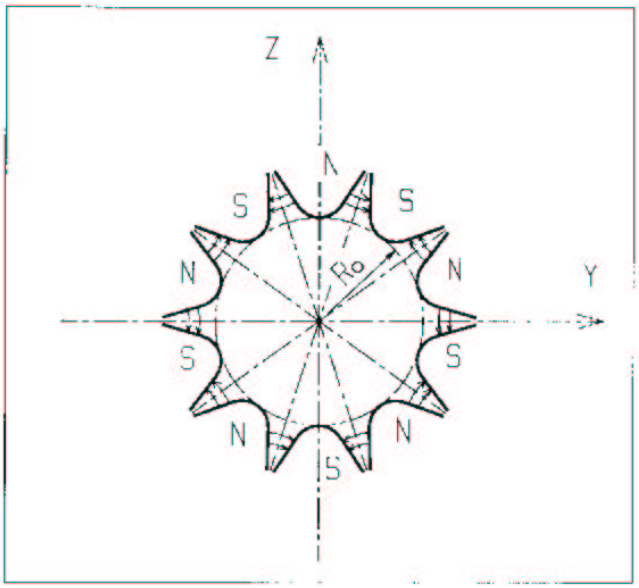

DIPOLE **Generation of a dipole magnet 2-D map**

$B_Z = \mathcal{F} B_0 \left(1 - N\left(\frac{R-RM}{RM}\right) + B\left(\frac{R-RM}{RM}\right)^2 + G\left(\frac{R-RM}{RM}\right)^3\right)$

NFACE, *IC*, *IL*	Number of field boundaries $IC = 1, 2$: print field map $IL = 1, 2$: print field and coordinates on trajectories	2-3, 0-2, 0-2	3*I
IAMAX, *IRMAX*	Azimuthal and radial number of nodes of the mesh	≤ 400, ≤ 200	2*I
B_0, N, B, G	Field and field indices	kG, 3* no dim.	4*E
AT, *ACENT*, *RM*, *RMIN* , *RMAX*	Mesh parameters: total angle of the map; azimuth for positioning of EFB's; mean radius; minimum and maximum radii	2*deg, 3*cm	5*E
	ENTRANCE FIELD BOUNDARY		
λ, ξ	Fringe field extent (normally $\simeq$ gap size); unused Exponential type fringe field is used: $F = 1\,/\,(1 + \exp(P(s)))with$ $P(s) = C_0 + C_1(\frac{s}{\lambda}) + C_2(\frac{s}{\lambda})^2 + ... + C_5(\frac{s}{\lambda})^5$	cm, unused	2*E
NC, $C_0 - C_5$, shift	unused; C_0 to C_5: see above; EFB shift	0-6, 6* no dim., cm	I,7*E
ω^+, θ, R_1, U_1, U_2, R_2	Azimuth of entrance EFB with respect to *ACENT*; wedge angle of EFB; radii and linear extents of EFB (use $\mid U_{1,2} \mid = \infty$ when $R_{1,2} = \infty$) (Note : $\lambda = 0$, $\omega^+ = ACENT$ and $\theta = 0$ for sharp edge)	2*deg, 4*cm	6*E
	EXIT FIELD BOUNDARY (See ENTRANCE FIELD BOUNDARY)		
λ, ξ NC, $C_0 - C_5$, shift	Fringe field parameters	cm, unused 0-6, 6*no dim., cm	2*E 1, 7*E
ω^-, θ, R_1, U_1, U_2, R_2	Positioning and shape of the exit EFB (Note : $\lambda = 0$, $\omega^- = -AT + ACENT$ and $\theta = 0$ for sharp edge)	2*deg, 4*cm	6*E

if NFACE = 3	LATERAL FIELD BOUNDARY (See ENTRANCE FIELD BOUNDARY) Next 3 records *only* if *NFACE* = 3		
λ, ξ	Fringe field parameters	cm, unused	2*E
NC, $C_0 - C_5$, shift		0-6, 6* no dim., cm	I,7*E
ω^-, θ, R_1, U_1, U_2, R_2, *RM3*	Positioning and shape of the lateral EFB; *RM3* is the radial position on azimut *ACENT*	2*deg, 5cm	7*E
NBS	Option index for perturbations to the field map	normally 0	I
if NBS = 0	Normal value. No other record required		
if NBS = -2	The map is modified as follows:		
$R_0, \Delta B/B_0$	B transforms to $B * \left(1 + \frac{\Delta B}{B_0} \frac{R - R_0}{RMAX - RMIN}\right)$	cm, no dim.	2*E
if NBS = -1	The map is modified as follows:		
θ_0, $\Delta B/B_0$	B transforms to $B * \left(1 + \frac{\Delta B}{B_0} \frac{\theta - \theta_0}{AT}\right)$	deg,no dim.	2*E
if NBS ≥ 1	Introduction of NBS shims		
For I = 1, NBS	The following 2 records must be repeated *NBS* times		
R_1, R_2, θ_1, θ_2, λ	Radial and angular limits of the shim; λ is unused	2*cm, 2*deg, cm	5*E
γ, α, μ, β	Geometrical parameters of the shim	2*deg, 2*no dim.	4*E
IORDRE	Order of interpolation polynomial: 2 = second order, 9-point grid 25 = second order, 25-point grid 4 = fourth order, 25-point grid	2, 4 or 25	I
XPAS	Integration step	cm	E
KPOS	Positioning of the map, normally 2. Two options:	1-2	I
if KPOS = 2 RE, TE, RS, TS	Positioning as follows: Radius and angle of reference, respectively, at entrance and exit of the map	cm, rad, cm, rad	4*E
if KPOS = 1 DP	Automatic positioning of the map, by means of reference relative momentum	no dim.	E

DODECAPO **Dodecapole magnet**

IL	*IL* = 1, 2: print field and coordinates along trajectories	0-2	I
XL, R_0, B_0	Length; radius and field at pole tip	2*cm, kG	3*E
X_E, λ_E	Entrance face: Integration zone extent; fringe field extent ($\lesssim 2R_0$, $\lambda_E = 0$ for sharp edge)	2*cm	2*E
NCE, $C_0 - C_5$	*NCE* = unused $C_0 - C_5$ = Fringe field coefficients such that $G(s) = G_0/(1 + \exp P(s))$, with $G_0 = B_0/R_0^5$ and $P(s) = \sum_{i=0}^{5} C_i(s/\lambda)^i$	unused, 6*no dim.	I, 6*E
X_S, λ_S	Exit face: see entrance face	2*cm	2*E
NCS, $C_0 - C_5$		0-6, 6*no dim.	I, 6*E
XPAS	Integration step	cm	E
KPOS, *XCE*, *YCE*, *ALE*	*KPOS*=1: element aligned, 2: misaligned; shifts, tilt (unused if *KPOS*=1)	1-2, 2*cm, rad	I, 3*E

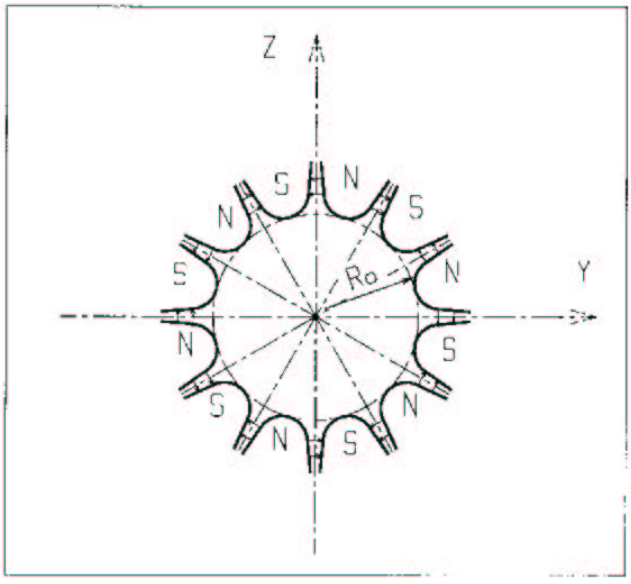

DRIFT, ESL **Field free drift space**

XL	length	cm	E

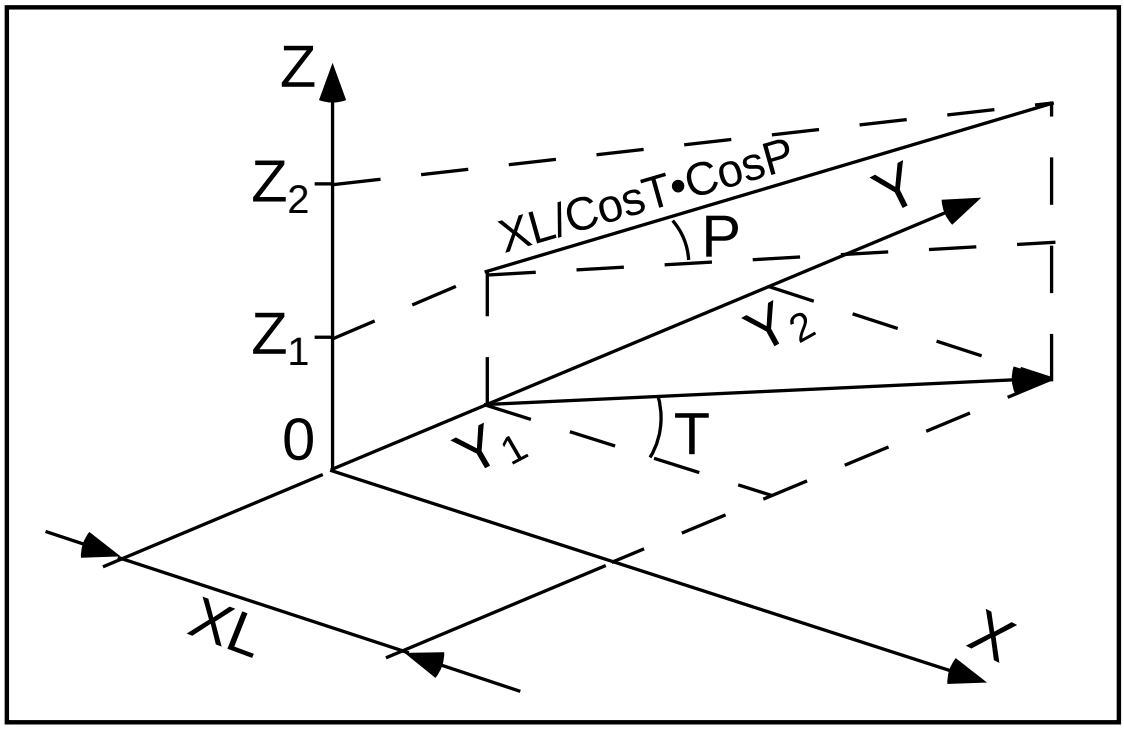

EBMULT[1]	**Electro-magnetic multipole**		
IL	*IL* = 1, 2: print field and coordinates along trajectories	0-2	I
	Electric poles		
XL, R_0, *E*1, *E*2, ..., *E*10	Length of element; radius at pole tip; field at pole tip for dipole, quadrupole, ..., 20-pole electric components	2*cm, 10*V/m	12*E
	Entrance face		
X_E, λ_E, E_2, ..., E_{10}	Integration zone; fringe field extent: dipole fringe field extent = λ_E; quadrupole fringe field extent = $\lambda_E * E_2$; ... 20-pole fringe field extent = $\lambda_E * E_{10}$ (for any component: sharp edge if field extent is zero)	2*cm, 9*no dim.	11*E
NCE,$C_0 - C_5$	same as *QUADRUPO*	0-6, 6*no dim.	I,6*E
	Exit face		
X_S, λ_S, S_2, ..., S_{10}	Integration zone; as for entrance	2*cm, 9*no dim.	11*E
NCS, $C_0 - C_5$		0-6, 6*no dim.	I, 6*E
*R*1, *R*2, *R*3, ..., *R*10	Skew angles of electric field components	10*rad	10*E
	Magnetic poles		
XL, R_0, *B*1, *B*2, ..., *B*10	Length of element; radius at pole tip; field at pole tip for dipole, quadrupole, ..., 20-pole magnetic components	2*cm, 10*kG	12*E
	Entrance face		
X_E, λ_E, E_2, ..., E_{10}	Integration zone; fringe field extent: dipole fringe field extent = λ_E; quadrupole fringe field extent = $\lambda_E * E_2$; ... 20-pole fringe field extent = $\lambda_E * E_{10}$ (for any component: sharp edge if field extent is zero)	2*cm, 9*no dim.	11*E
NCE,$C_0 - C_5$	same as *QUADRUPO*	0-6, 6*no dim.	I,6*E

[1] Use *PARTICUL* to declare mass and charge.

	Exit face		
X_S, λ_S, S_2, ..., S_{10}	Integration zone; as for entrance	2*cm, 9*no dim.	11*E
NCS, $C_0 - C_5$		0-6, 6*no dim.	I, 6*E
$R1$, $R2$, $R3$, ..., $R10$	Skew angles of magnetic field components	10*rad	10*E
XPAS	Integration step	cm	E
KPOS, *XCE*, *YCE*, *ALE*	*KPOS*=1: element aligned, 2: misaligned; shifts, tilt (unused if *KPOS*=1)	1-2, 2*cm, rad	I, 3*E

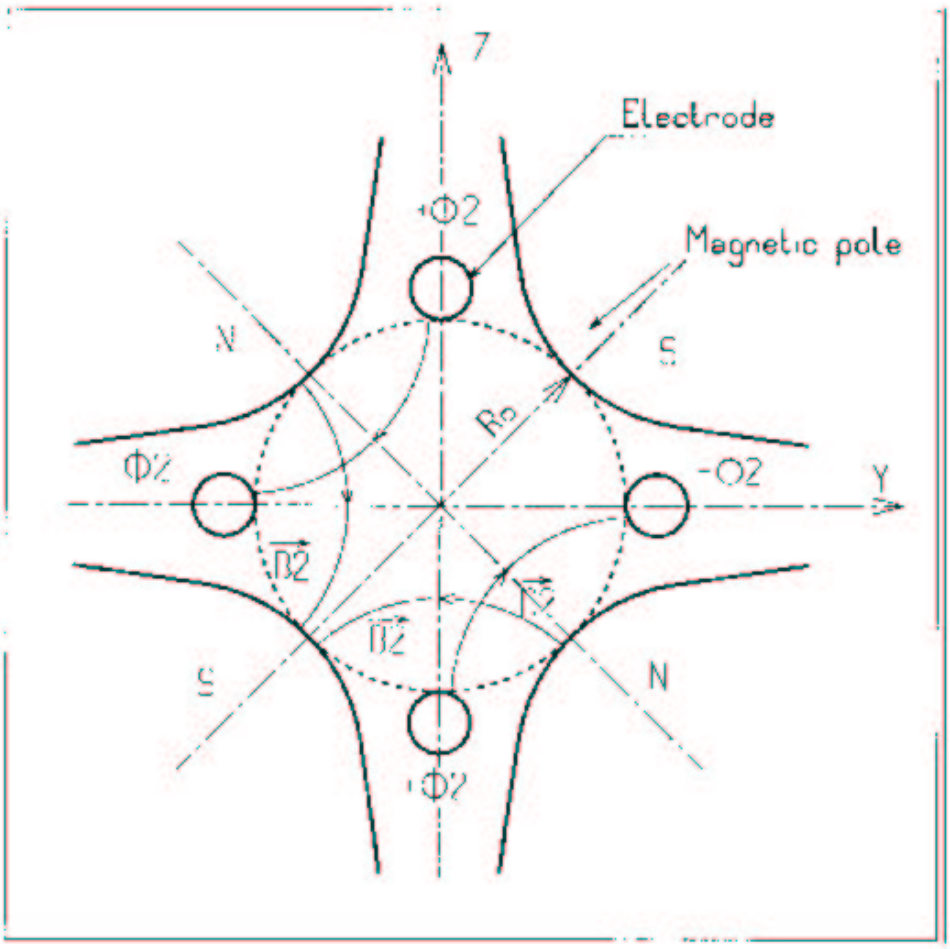

EL2TUB[1]	**Two-tube electrostatic lens**		
IL	$IL = 1, 2$: print field and coordinates along trajectories	0-2	I
X_1, D, X_2, R_0	Length of first tube; distance between tubes; length of second tube; inner radius	3*m	4*E
V_1, V_2	Potentials	2*V	2*E
XPAS	Integration step	cm	E
KPOS, *XCE*, *YCE*, *ALE*	*KPOS*=1: element aligned, 2: misaligned; shifts, tilt (unused if *KPOS*=1)	1-2, 2*cm, rad	I, 3*E

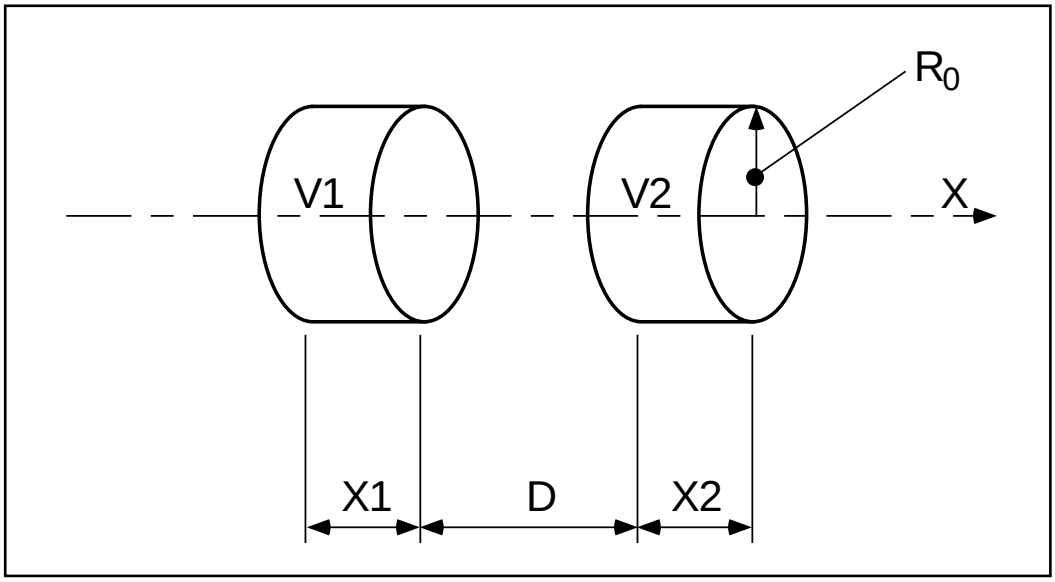

Two-electrode cylindrical electric lens.

[1] Use *PARTICUL* to declare mass and charge.

ELMIR	**Electrostatic N-electrode mirror/lens, straight slits**		
IL	$IL = 1, 2$: print field and coordinates along trajectories	0-2	I
N,*L*1, ..., *LN*, *D*, *MT*	Number of electrodes; electrode lengths; gap; mode (11/H-mir, 12/V-mir, 21/V-lens, 22/H-lens)	2 – 7, N*m, m	I, N*E, E, I
*V*1, ..., *VN*	Electrode potentials (normally $V1 = 0$)	N*V	N*E
XPAS	Integration step	cm	E
KPOS, *XCE*, *YCE*, *ALE*	*KPOS*=1: element aligned; 2: misaligned; shifts, tilt (unused if *KPOS*=1); 3: automatic positioning, YCE = pitch, ALE = half-deviation	1-2, 2*cm, rad	I, 3*E

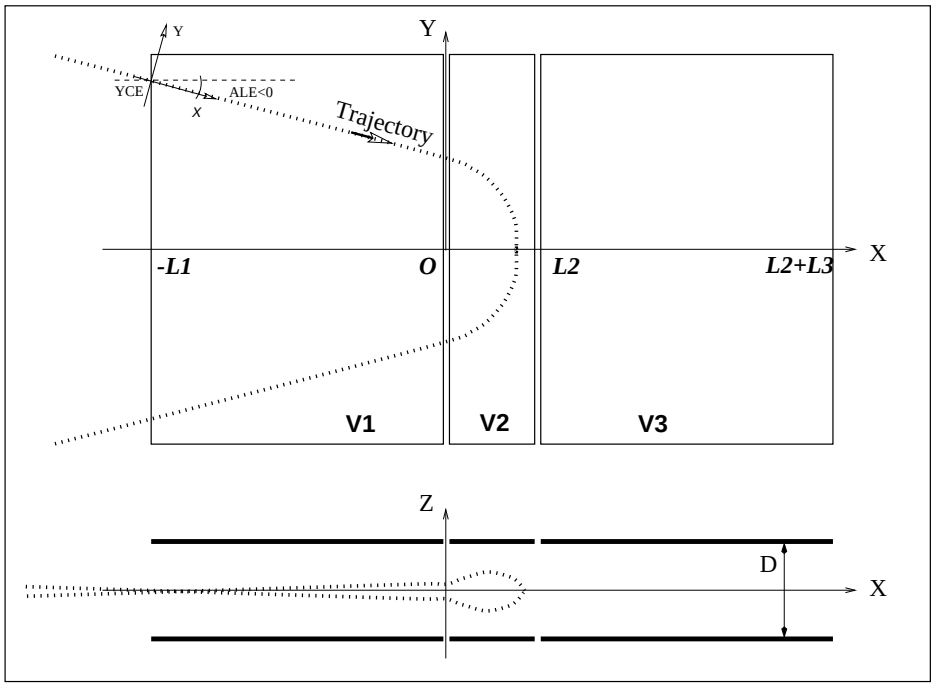

Electrostatic N-electrode mirror/lens, straight slits, in the case $N = 3$, in horizontal mirror mode ($MT = 11$). Possible non-zero entrance quantities YCE, ALE should be specified using *CHANGREF*, or using *KPOS*=3 with YCE=pitch, ALE=half-deviation.

ELMIRC	**Electrostatic N-electrode mirror/lens, circular slits**		
IL	$IL = 1, 2$: print field and coordinates along trajectories	0-2	I
$R1$, $R2$, AT, D	Radius of first and second slits; total deviation angle; gap	4*m 2*m, rad, m	4*E 4*E
$V - VA$, $VB - V$	Potential difference	2*V	2*E
XPAS	Integration step	cm	E
KPOS RE, TE, RS, TS	Normally $KPOS = 2$ for positioning; Radius and angle at respectively entrance and exit.	1-2 cm, rad, cm, rad	I 4*E

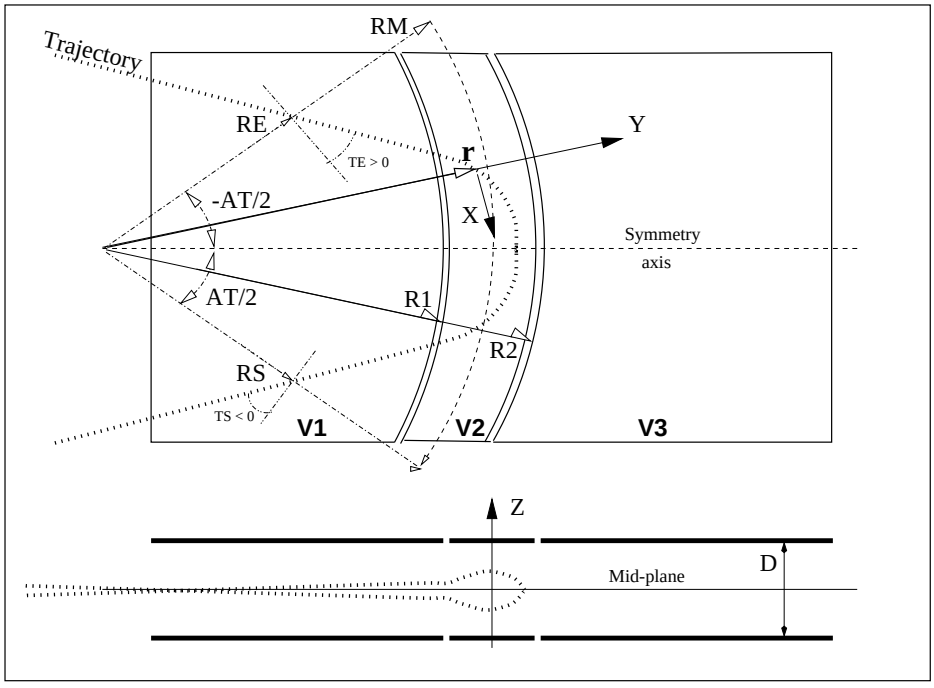

Electrostatic N-electrode mirror/lens, circular slits, in the case $N = 3$, in horizontal mirror mode.

ELMULT[1]	**Electric multipole**		
IL	*IL* = 1, 2: print field and coordinates along trajectories	0-2	I
XL, R_0, *E*1, *E*2, ..., *E*10	Length of element; radius at pole tip; field at pole tip for dipole, quadrupole, ..., dodecapole components	2*cm, 10*V/m	12*E
	Entrance face		
X_E, λ_E, E_2, ..., E_{10}	Integration zone; fringe field extent: dipole fringe field extent = λ_E; quadrupole fringe field extent = $\lambda_E * E_2$; ... 20-pole fringe field extent = $\lambda_E * E_{10}$ (sharp edge if field extent is zero)	2*cm, 9*no dim.	11*E
NCE, $C_0 - C_5$	same as *QUADRUPO*	0-6, 6*no dim.	I, 6*E
	Exit face		
X_S, λ_S, S_2, ..., S_{10}	Integration zone; as for entrance	2*cm, 9*no dim.	11*E
NCS, $C_0 - C_5$		0-6, 6*no dim.	I, 6*E
*R*1, *R*2, *R*3, ..., *R*10	Skew angles of field components	10*rad	10*E
XPAS	Integration step	cm	E
KPOS, *XCE*, *YCE*, *ALE*	*KPOS*=1: element aligned, 2: misaligned; shifts, tilt (unused if *KPOS*=1)	1-2, 2*cm, rad	I, 3*E

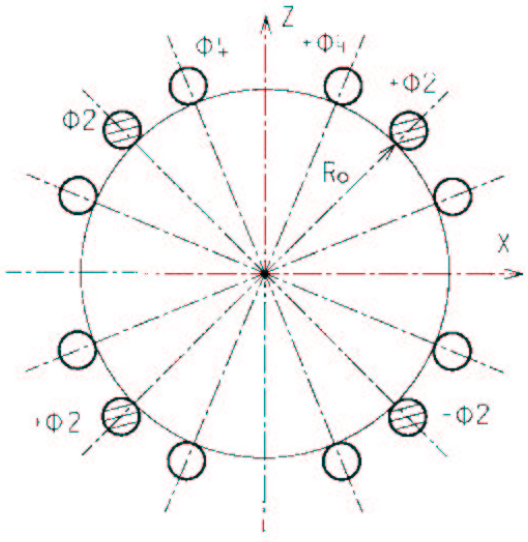

[1] Use *PARTICUL* to declare mass and charge.

ELREVOL[1]	**1-D uniform mesh electric field map** X-axis cylindrical symmetry is assumed		
IC, *IL*	$IC = 1, 2$: print the map $IL = 1, 2$: print field and coordinates along trajectories	0-2, 0-2	2*I
ENORM, X-NORM	Field and X-coordinate normalization	2*no dim.	2*E
TIT	Title		A80
IX	Number of longitudinal nodes of the map	≤ 400	I
FNAME[2]	Filename (e.g., elens.map)		A80
ID, *A*, *B*, *C* [A', B', C' B'',etc., if $ID \geq 2$]	Integration boundary. Ineffective when $ID = 0$. ID = -1, 1 or ≥ 2 : as for *CARTEMES*	≥ -1, 2*no dim., cm [,2*no dim., cm, etc.]	I,3*E [,3*E,etc.]
IORDRE	unused	2, 4 or 25	I
XPAS	Integration step	cm	E
KPOS, *XCE*, *YCE, ALE*	*KPOS*=1: element aligned, 2: misaligned; shifts, tilt (unused if *KPOS*=1)	1-2, 2*cm, rad	I, 3*E

[1] Use *PARTICUL* to declare mass and charge.

[2] *FNAME* contains the field data. These must be formatted according to the following *FORTRAN* sequence:

```
OPEN (UNIT = NL, FILE = FNAME, STATUS = 'OLD' [,FORM='UNFORMATTED'])
DO 1 I = 1, IX
  IF (BINARY) THEN
    READ(NL) X(I), EX(I)
  ELSE
    READ(NL,*) X(I), EX(I)
  ENDIF
1    CONTINUE
```

where $X(I)$ and $EX(I)$ are the longitudinal coordinate and field component at node (I) of the mesh.
Binary file names *FNAME* must begin with B_. 'Binary' will then automatically be set to '.TRUE.'

FAISCEAU **Print particle coordinates**

Print particle coordinates at the location where the keyword is introduced in the structure.

FAISCNL **Store particle coordinates in file FNAME**

FNAME[1]	Name of storage file (e.g., zgoubi.fai, or b_zgoubi.fai for binary storage).	A80

FAISTORE **Store coordinates every IP other pass [,at labeled elements]**

FNAME[1] [, *LABEL(s)*]	Name of storage file (e.g. zgoubi.fai) [; label(s) of the element(s) at the exit of which the store occurs (10 labels maximum)].	A80 [, 10*A10]
IP	Store every IP other pass (when using *REBELOTE* with $NPASS \geq IP - 1$).	I

[1] Stored data can be read again using *OBJET*, $KOBJ = 3$.

FIN, END **End of input data list**

Any information following these keywords will be ignored

FIT	**Fitting procedure**		
NV	Number of physical parameters to be varied	≤ 20	I
For I = 1, NV	repeat NV times the following sequence		
IR, *IP*, *XC*, *DV*	Number of the element in the structure; number of the physical parameter in the element; coupling switch (off = 0); allowed ± range of variation of the parameter.	≤ 200, ≤ 99, ± 200.99, relative	2*I, 2*E
NC	Number of constraints	≤ 20	I
For I = 1, NC	repeat NC times the following sequence		
IC, *I*, *J*, *IR*, V[1], *WV*	*IC*, *I* and *J* define the type of constraint (see table below); number of the element at the exit of which the constraint applies; value; weight of the constraint (the lower the stronger).	0-3, 1-200, current unit[1], no dim.	4*I, 2*E

Type of constraint	**Parameters defining the constraint**			
	IC	**I**	**J**	**Constraint**
Beam matrix[2]	0	1 - 4	1 - 4	σ_{IJ}
First order transfer coefficients[2]		1 - 6	1 - 6	R_{IJ}
	1	7	any	Y-determinant
		8	any	Z-determinant
Second order transfer coefficients[3]	2	1 - 6	11 - 66	$T_{I,j,k}$ $(j = [J/10], k = J - 10[J/10])$
Trajectory coordinate[4]	3	1 - *IMAX*	1 - 6[5]	$F(J, I)$
Periodic coefficients[2]	4	1 - 6	1 - 6	σ_{IJ}[6]
		7	any	Y-tune
		8	any	Z-tune

[1] The unit of V is that specified in the corresponding keyword.
[2] It is advised to use *OBJET* and *KOBJ* = 5, for the definition of the initial coordinates.
[3] It is advised to use *OBJET* and *KOBJ* = 6, for the definition of the initial coordinates.
[4] For use normally with object definition by *OBJET*. Thus, *I* = trajectory number = 1 to *IMAX* if *KOBJ* ≠ 2; *I* = trajectory number = 1 to 7 if *KOBJ* = 2.
[5] *J* = coordinate number = 1 to 6 for respectively D, Y, T, Z, P or X.
[6] Twiss functions: $\sigma_{11} = \beta_Y, \sigma_{12} = \sigma_{21} = -\alpha_Y, \sigma_{22} = \gamma_Y$, $\sigma_{33} = \beta_Z, \sigma_{34} = \sigma_{43} = -\alpha_Z, \sigma_{44} = \gamma_Z$; periodic dispersion: $\sigma_{16} = D_Y$, $\sigma_{26} = D'_Y$, $\sigma_{36} = D_Z, \sigma_{46} = D'_Z$

FOCALE **Particle coordinates and horizontal beam dimension at distance** XL

XL	Distance from the position of the keyword	cm	E

FOCALEZ **Particle coordinates and vertical beam dimension at distance** XL

XL	Distance from the position of the keyword	cm	E

GASCAT	**Gas scattering**		
KGA	Off/On switch	0, 1	I
AI, *DEN*	Atomic number; density		2*E

HISTO **1-D histogram**

J, $X_{\min}$, $X_{\max}$, *NBK*, *NH*	J = type of coordinate to be histogramed; the following are available: • current coordinates: $1(D)$, $2(Y)$, $3(T)$, $4(Z)$, $5(P)$, $6(S)$, • initial coordinates: $11(D_0)$, $12(Y_0)$, $13(T_0)$, $14(Z_0)$, $15(P_0)$, $16(S_0)$, • spin: $21(S_x)$, $22(S_y)$, $23(S_z)$, $24(< S >)$; $X_{\min}$, $X_{\max}$ = limits of the histogram, in units of the coordinate of concern; *NBK* = number of channels; *NH* = number of the histogram (for independency of histograms of the same coordinate)	1-24, 2* current units, < 120, 1-5	I, 2*E, 2*I
NBL, KAR, NORM, TYP	Number of lines (= vertical amplitude); alphanumeric character; normalization if *NORM* = 1, otherwise *NORM* = 0; *TYP* = 'P': primary particles are histogramed, or 'S': secondary, or Q: all particles - for use with *MCDESINT*	normally 10-40, char., 1-2, P-S-Q	I, A1, I, A1

IMAGE **Localization and size of horizontal waist**

IMAGES **Localization and size of horizontal waists**

For each momentum group, as classified by means of *OBJET*, *KOBJ* = 1, 2 or 4

IMAGESZ **Localization and size of vertical waists**

For each momentum group, as classified by means of *OBJET*, *KOBJ* = 1, 2 or 4

IMAGEZ **Localization and size of vertical waist**

MAP2D **2-D Cartesian uniform mesh field map - arbitrary magnetic field**

IC, *IL*	*IC* = 1, 2: print the field map *IL* = 1, 2: print field and coordinates along trajectories	0-2, 0-2	2*I
BNORM, XN,YN	Field and X-,Y-coordinate normalization	3*no dim.	3*E
TIT	Title[1]		A80
IX, *JY*	Number of longitudinal and horizontal-transverse nodes of the mesh (the Z elevation is arbitrary)	≤ 400, ≤ 200	2*I
FNAME[2]	File name (e.g., magnet.map)		A80
ID, *A*, *B*, *C* [A', B', C' B'',etc., if $ID \geq 2$]	Integration boundary. Ineffective when $ID = 0$. ID = -1, 1 or ≥ 2 : as for *CARTEMES*	≥ -1, 2*no dim., cm [,2*no dim., cm, etc.]	I,3*E [,3*E,etc.]
IORDRE	Order of polynomial interpolation	2, 4	I
XPAS	Integration step	cm	E
KPOS, *XCE*, *YCE, ALE*	*KPOS*=1: element aligned, 2: misaligned; shifts, tilt (unused if *KPOS*=1)	1-2, 2*cm, rad	I, 3*E

[1] Begin "Title" with "FLIP" so as to get the map flipped prior to ray-tracing.
[2] *FNAME* contains the field map data. These must be formatted according to the following *FORTRAN* read sequence (normally compatible with *TOSCA* code *OUTPUTS*):

```
    OPEN (UNIT = NL, FILE = FNAME, STATUS = 'OLD')
    DO 1 J = 1, JY
      DO 1 I = 1, IX
        IF (BINARY) THEN
              READ(NL) Y(J), Z(1), X(I), BY(I,J), BZ(I,J), BX(I,J)
        ELSE
              READ(NL,100) Y(J), Z(1), X(I), BY(I,J), BZ(I,J), BX(I,J)
100             FORMAT (1X, 6E11.4)
            ENDIF
1       CONTINUE
```

where $X(I)$, $Y(J)$ are the longitudinal, horizontal coordinates in the at nodes (I, J) of the mesh, $Z(1)$ is the vertical elevation of the map, and BX, BY, BZ are the components of the field.

For binary files, *FNAME* must begin with B_;
'Binary' will then automatically be set to '.TRUE.'

MAP2D-E **2-D Cartesian uniform mesh field map - arbitrary electric field**

IC, *IL*	*IC* = 1, 2: print the field map *IL* = 1, 2: print field and coordinates along trajectories	0-2, 0-2	2*I
ENORM, X-,Y-NORM	Field and X-,Y-coordinate normalization	2*no dim.	2*E
TIT	Title[1]		A80
IX, *JY*	Number of longitudinal and horizontal-transverse nodes of the mesh (the Z elevation is arbitrary)	≤ 400, ≤ 200	2*I
FNAME[2]	File name (e.g., mirror.map)		A80
ID, *A*, *B*, *C* [A', B', C' B'',etc., if $ID \geq 2$]	Integration boundary. Ineffective when $ID = 0$. *ID* = -1, 1 or ≥ 2 : as for *CARTEMES*	≥ -1, 2*no dim., cm [,2*no dim., cm, etc.]	I,3*E [,3*E,etc.]
IORDRE	Order of polynomial interpolation	2, 4	I
XPAS	Integration step	cm	E
KPOS, *XCE*, *YCE*, *ALE*	*KPOS*=1: element aligned, 2: misaligned; shifts, tilt (unused if *KPOS*=1)	1-2, 2*cm, rad	I, 3*E

[1] Begin "Title" with "FLIP" so as to get the map flipped prior to ray-tracing.
[2] *FNAME* contains the field map data. These must be formatted according to the following *FORTRAN* read sequence:

```
      OPEN (UNIT = NL, FILE = FNAME, STATUS = 'OLD')
      DO 1 J = 1, JY
        DO 1 I = 1, IX
          IF (BINARY) THEN
                READ(NL) Y(J), Z(1), X(I), EY(I,J), EZ(I,J), EX(I,J)
          ELSE
                READ(NL,100) Y(J), Z(1), X(I), EY(I,J), EZ(I,J), EX(I,J)
  100           FORMAT (1X, 6E11.4)
              ENDIF
  1       CONTINUE
```

where $X(I)$, $Y(J)$ are the longitudinal, horizontal coordinates in the at nodes (I, J) of the mesh, $Z(1)$ is the vertical elevation of the map, and EX, EY, EZ are the components of the field.

For binary files, *FNAME* must begin with B_;
'Binary' will then automatically be set to '.TRUE.'

MATPROD	**Matrix transfer**		
IORDRE	Transfer matrix order	1-2	I
XL	Length (ineffective, for updating)	m	E
For $IA = 1, 6$:			
$R(IA, IB)$, $IB = 1, 6$	First order matrix	m, rad	6 lines 6*E each
If IORDRE = 2	Following records *only* if $IORDRE = 2$		
$T(IA, IB, IC)$,	Second order matrix, six 6*6 blocks	m, rad	36 lines 6*E each

MATRIX **Calculation of transfer coefficients, periodic parameters**

IORD, IFOC	Options : *IORD* = 0: Same effect as *FAISCEAU* 1: First order transfer matrix; periodic beam matrix, tune numbers if *IFOC* > 0 2: First order transfer matrix R_{ij}, second order array T_{ijk} and higher order transfer coefficients; periodic parameters, chromaticities, etc. if *IFOC* > 0 *IFOC* = 0: matrix at actual position, reference ≡ particle # 1 1: matrix at the closest first order horizontal focus, reference ≡ particle # 1 10 + NPER: same as *IFOC* = 0, and also calculates the twiss parameters, tune numbers, etc. (assuming that the DATA file describes one period of a NPER-period structure).	0-2, 0-1 or > 10	2*I

MCDESINT[1] **Monte-Carlo simulation of in-flight decay**
M1 → M2 + M3

$M2$, $M3$	Masses of the two decay products	2*MeV/c^2	2*E
$I1$, $I2$, $I3$	Seeds for random number generators	3*$\simeq 10^6$	3*I

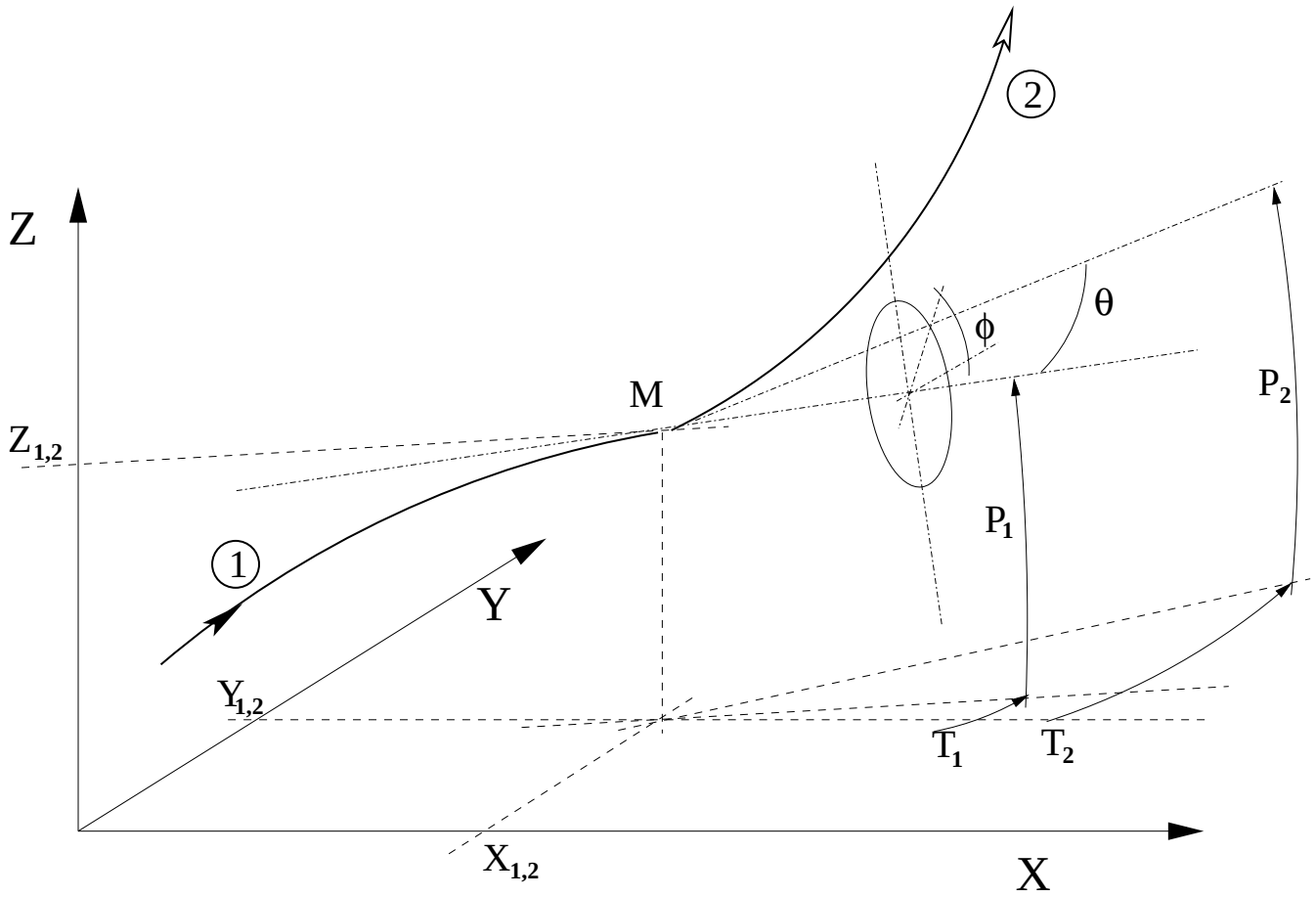

Particle 1 decays into 2 and 3; **zgoubi** then calculates trajectory of 2, while 3 is discarded. θ and ϕ are the scattering angles of particle 2 relative to the direction of the incoming particle 1. They transform to T_2 and P_2 in Zgoubi frame.

[1] *MCDESINT* must be preceded by *PARTICUL*, for the definition of the mass and lifetime of the incoming particle M1.

MCOBJET	**Monte-Carlo generation of a 6-D object**		
BORO	Reference rigidity	kG.cm	E
KOBJ	Type of support of the random distribution *KOBJ* = 1: window *KOBJ* = 2: grid *KOBJ* = 3: phase-space ellipses	1-3	I
IMAX	Number of particles to be generated	$\leq 10^4$	I
KY, KT, KZ, KP, KX, KD[1]	Type of probability density	6*(1-3)	6*I
Y_0, T_0, Z_0, P_0, X_0, D_0	Mean value of coordinates ($D_0 = B\rho/BORO$)	m, rad, m, rad, m, no dim.	6*E
if KOBJ = 1	**In a window**		
δY, δT, δZ, δP, δX, δD	Distribution widths, depending on KY, KT etc.[1]	m, rad, m, rad, m, no dim.	6*E
$N_{\delta Y}$, $N_{\delta T}$, $N_{\delta Z}$, $N_{\delta P}$, $N_{\delta X}$, $N_{\delta D}$	Sorting cut-offs (used only for Gaussian density)	units of σ_Y, σ_T, etc.	6*E
N_0, C_0, C_1, C_2, C_3	Parameters involved in calculation of P(D) (unused if $KD = 1$)	no dim.	5*E
$IR1$, $IR2$, $IR3$	Random sequence seeds	3*$\simeq 10^6$	3*I

[1] Let $x = Y, T, Z, P$ or X. KY, KT, KZ, KP and KX can take the values
1: uniform, $p(x) = 1$ if $-\delta x \leq x \leq \delta x$
2: Gaussian, $p(x) = \exp(-x^2/2\delta x^2)/\delta x\sqrt{2\pi}$
3: parabolic, $p(x) = 3(1 - x^2/\delta x^2)/4\delta x$ if $-\delta x \leq x \leq \delta x$
KD can take the values
1: uniform, $p(D) = 1$ if $-\delta D \leq x \leq \delta D$
2: exponential, $p(D) = \text{No } \exp(C_0 + C_1 l + C_2 l^2 + C_3 l^3)$ if $-\delta D \leq x \leq \delta D$
3: kinematic, $D = \delta D * T$

If KOBJ = 2	**On a grid**		
IY, IT, IZ, IP, IX, ID	Number of bars of the grid		6*I
PY, PT, PZ, PP, PX, PD	Distances between bars	m, rad, m rad, m, no dim.	6*E
δY, δT, δZ, δP, δX, δD	Width of the bars ($\pm$) if uniform, Sigma value if Gaussian distribution	*ibidem*	6*E
$N_{\delta Y}$, $N_{\delta T}$, $N_{\delta Z}$, $N_{\delta P}$, $N_{\delta X}$, $N_{\delta D}$	Sorting cut-offs (used only for Gaussian density)	units of σ_Y, σ_T,etc.	6*E
N_0, C_0, C_1, C_2, C_3	Parameters involved in calculation of $P(D)$ (unused if $KOBJ = 3$)	no dim.	5*E
$IR1$, $IR2$, $IR3$	Random sequence seeds	3*$\simeq 10^6$	3*I
if KOBJ = 3	**On a phase-space ellipse**[1]		
α_Y, β_Y, ε_Y/π, $N_{\sigma_{\epsilon_Y}}$ [, $N'_{\sigma_{\epsilon_Y}}$ if $N_{\sigma_{\epsilon_Y}} < 0$][2]	Ellipse parameters and emittance, Y-T phase-space; cut-off	no dim., m/rad, m.rad, units of $\sigma(\varepsilon_Y)$	3*E, I
α_Z, β_Z, ε_Z/π, $N_{\sigma_{\epsilon_Z}}$ [, $N'_{\sigma_{\epsilon_Z}}$ if $N_{\sigma_{\epsilon_Z}} < 0$][2]	Ellipse parameters and emittance, Z-P phase-space; cut-off	no dim., m/rad, m.rad, units of $\sigma(\varepsilon_Z)$	3*E, I
α_X, β_X, ε_X/π, $N_{\sigma_{\epsilon_X}}$ [, $N'_{\sigma_{\epsilon_X}}$ if $N_{\sigma_{\epsilon_X}} < 0$][2]	Ellipse parameters and emittance, X-D phase-space; cut-off	no dim., m/rad, m.rad, units of $\sigma(\varepsilon_X)$	3*E, I [,I]
$IR1$, $IR2$, $IR3$	Random sequence seeds	3*$\simeq 10^6$	3*I

[1] Similar possibilities, non-random, are offered with *OBJET*, KOBJ=8 (p. 180)

[2] With Gaussian density type only: sorting within the ellipse frontier

$$\frac{1+\sigma_Y^2}{\beta_Y^2}Y^2 + 2\alpha_Y YT + \beta_Y T^2 = \frac{\varepsilon_Y}{\pi}$$

if $N_{\sigma_{\epsilon_Y}} > 0$, or, if $N_{\sigma_{\epsilon_Y}} < 0$ sorting within the ring

$$[\,|N_{\sigma_{\epsilon_Y}}|, N'_{\sigma_{\epsilon_Y}}\,]$$

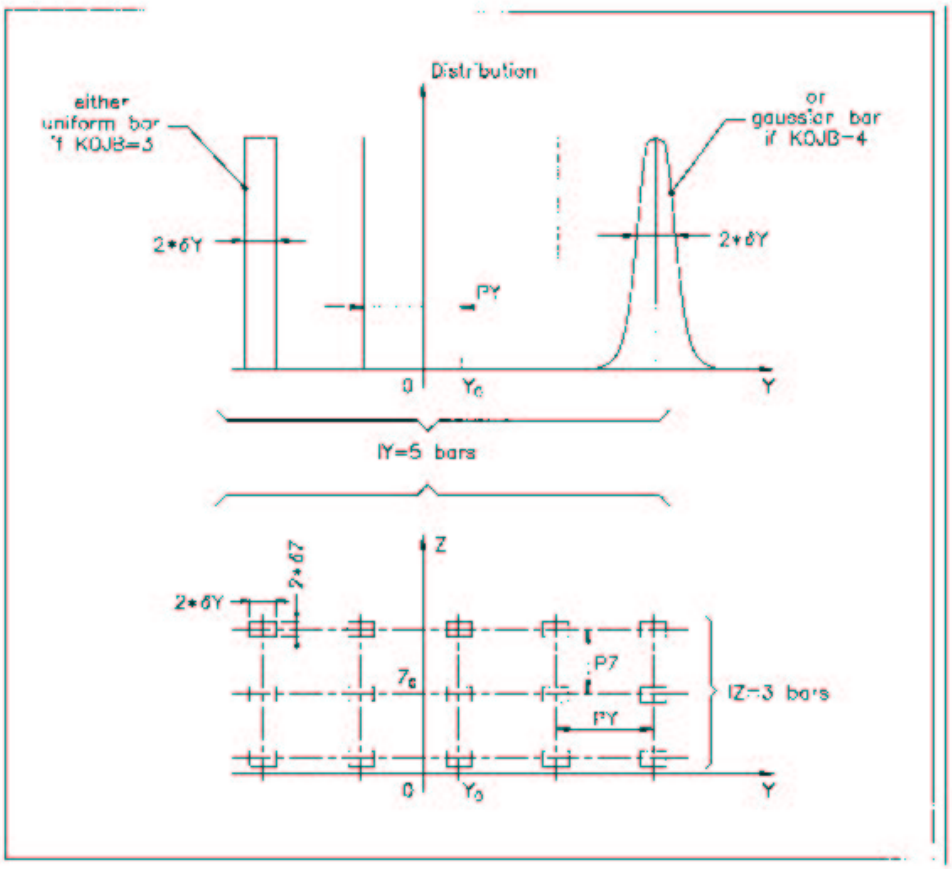

Scheme of the input parameters to *MCOBJET* when $KOBJ = 3, 4$

A: A distribution of the Y coordinate
B: 2-D grid in (Y, Z) space.

MULTIPOL	**Magnetic Multipole**		
IL	$IL = 1, 2$: print field and coordinates along trajectories	0-2	I
XL, R_0, $B1$, $B2$, ..., $B10$,	Length of element; radius at pole tip; field at pole tip for dipole, quadrupole, ..., dodecapole components	2*cm,10*kG	12*E
	Entrance face		
X_E, λ_E, E_2, ..., E_{10}	Integration zone; fringe field extent: dipole fringe field extent = λ_E; quadrupole fringe field extent = $\lambda_E * E_2$; ... 20-pole fringe field extent = $\lambda_E * E_{10}$ (sharp edge if field extent is zero)	2*cm,9*no dim.	11*E
NCE, $C_0 - C_5$	same as *QUADRUPO*	0-6, 6*no dim.	I, 6*E
	Exit face		
X_S, λ_S, S_2, ..., S_{10}	Integration zone; as for entrance	2*cm, 9*no dim.	11*E
NCS, $C_0 - C_5$		0-6, 6*no dim.	I, 6*E
$R1$, $R2$, $R3$, ..., $R10$	Skew angles of field components	10*rad	10*E
XPAS	Integration step	cm	E
KPOS, *XCE*, *YCE*, *ALE*	*KPOS*=1: element aligned, 2: misaligned; shifts, tilt (unused if *KPOS*=1) for *QUADRUPO*. *KPOS* = 3: effective only if $B1 \neq 0$: entrance and exit frames are shifted by *YCE* and tilted *wrt.* the magnet by an angle of • either ALE if ALE≠0 • or 2 Arcsin($B1\,XL\,/\,2BORO$) if ALE=0	1-2, 2*cm, rad	I, 3*E

OBJET	**Generation of an object**		
BORO	Reference rigidity	kG.cm	E
KOBJ	Option index	1-6	I
if KOBJ = 1[.1]	[Non-] Symmetric object		
IY, IT, IZ, IP, IX, ID	Ray-Tracing assumes mid-plane symmetry Total number of points in $\pm Y$, $\pm T$, $\pm Z$, $\pm P$ [$+Z$, $+P$ with KOBJ = 1.1], $\pm X$. IY*IT*IZ*IP* and $\pm D$ coordinates ($IY \leq 20$,...,$ID \leq 20$)	6*1 *IX*ID $\leq 10^4$	
PY, PT, PZ, PP, PX, PD	Step size in Y, T, Z, P, X and momentum ($PD = \delta B\rho/BORO$)	cm, mrad, cm, mrad, cm, no dim.	6*E
YR, TR, ZR, PR, XR, DR	Reference ($DR = B\rho/BORO$)	cm, mrad, cm, mrad, cm, no dim.	6*E
if KOBJ = 2	All the initial coordinates must be entered explicitly		
IMAX , *IDMAX*	total number of particles ; number of distinct momenta (if $IDMAX > 1$, group particles of same momentum)	*IMAX* $\leq 10^4$	2*I
For I = 1, IMAX	Repeat *IMAX* times the following line		
Y, T, Z, P, X, D, *LET*	Coordinates and tagging character of the *IMAX* particles ($D = B\rho/BORO$)	cm, mrad, cm, mrad, cm, no dim., char.	6*E, A1
IEX($I = 1$, *IMAX*)	*IMAX* times 1 or -2. If $IEX(I) = 1$, trajectory number I is calculated. If $IEX(I) = -2$, it is not calculated	1 or -2	*IMAX* I
If KOBJ=3[.1]	Reads coordinates from a storage file		
IT1, IT2, ITStep	Read particles numbered IT1 to IT2, step ITStep (For more than 10^4 particles stored in *FNAME*, use '*REBELOTE*')	≥ 1, $\geq IT1$, ≥ 1	3*I
IP1, IP2, IPStep	Read particles that belong in pass numbered IP1 to IP2, step IPStep	≥ 1, $\geq IP1$, ≥ 1	3*I
YR, TR, ZR, PR, XR, DR	Reference ($DR = B\rho/BORO$)	cm, mrad, cm, mrad, cm, no dim.	6*E
InitC	0 to force new starting coordinates to old initial ones 1 to force new starting coordinates to old final ones	0-1	I
FNAME	File name (e.g., zgoubi.fai) (KOBJ=3 or KOBJ=3.1 determines storage FORMAT)		A80
If KOBJ = 5[.1]	**Generation of 11 particles** (for use with *MATRIX*, $IORD = 1$)		

PY, PT, PZ, PP, PX, PD	Step sizes in Y, T, Z, P, X and D	cm, mrad, cm, mrad, cm, no dim.	6*E
YR, TR, ZR, PR, XR, DR	Reference trajectory; $DR = B\rho/BORO$	cm, mrad, cm, mrad, cm, no dim.	6*E
Iff KOBJ = 5.1	additional data line		
α_Y, β_Y, α_Z, β_Z, α_X, β_X	Initial beam ellipse parameters	2*(no dim.,m),(?,?)	6*E
If KOBJ = 6	**Generation of 61 particles** (for use with *MATRIX*, $IORD = 2$)		
PY, PT, PZ, PP, PX, PD	Step sizes in Y, T, Z, P, X and D cm, no dim.	cm, mrad, cm, mrad	6*E
YR, TR, ZR, PR, XR, DR	Reference trajectory; $DR = B\rho/BORO$	cm, mrad, cm, mrad, cm, no dim.	6*E
If KOBJ = 7	**Object with kinematics**		
IY, IT, IZ, IP, IX, ID	Number of points in $\pm Y$, $\pm T$,$\pm Z$, $\pm P$, $\pm X$; ID is not used	IY*IT*IZ*IZ*IX* $IP \leq 10^4$	6*I
PY, PT, PZ, PP, PX, PD	Step sizes in Y, T, Z, P and X; PD = kinematic coefficient, such that $D(T) = DR + PD * T$	cm, mrad, cm, mrad, cm, mrad^{-1}	6*E
YR, TR, ZR, PR, XR, DR	Reference ($DR = B\rho/BORO$)	cm, mrad, cm, mrad, cm no dim.	6*E
If KOBJ = 8	**Generation of phase-space coordinates on ellipses**[1]		
IY, IZ, IX	Number of samples in each 2-D phase-space; if zero the central value (below) is assigned	$0 \leq IX, IY, IZ \leq IMAX$, $1 \leq IX * IY * IZ \leq IMAX$	3*I
Y_0, T_0, Z_0, P_0, X_0, D_0	Central values ($D_0 = B\rho/BORO$)	m, rad, m, rad, m, no dim.	6*E
α_Y, β_Y, ε_Y/π	ellipse parameters and emittances	no dim., m/rad, m.rad	3*E
α_Z, β_Z, ε_Z/π		no dim., m/rad, m.rad	3*E
α_X, β_X, ε_X/π		no dim., m/rad, m.rad	3*E

[1] Similar possibilities, random, are offered with *MCOBJET*, KOBJ=3 (p. 176)

OBJETA	**Object from Monte-Carlo simulation of decay reaction**		
	$M1 + M2 \longrightarrow M3 + M4$ and $M4 \longrightarrow M5 + M6$		
BORO	Reference rigidity	kG.cm	E
IBODY, KOBJ	Body to be tracked: $M3(IBODY = 1)$, $M5(IBODY = 2)$ $M6(IBODY = 3)$; type of distribution for Y_0 and Z_0: uniform ($KOBJ = 1$) or Gaussian ($KOBJ = 2$)	1-3,1-2	2*I
IMAX	Number of particles to be generated (use '*REBELOTE*' for more)	$\leq 10^4$	I
$M_1 - M_5$	Rest masses of the bodies	5*GeV/c^2	5*E
T_1	Kinetic energy of incident body	GeV	E
Y_0, T_0, Z_0, P_0, D_0	Only those particles in the range $Y_0 - \delta Y \leq Y \leq Y_0 + \delta Y$ ..... $D_0 - \delta D \leq D \leq D_0 + \delta D$ will be retained	cm, mrad, cm, mrad, no dim.	5*E
δY, δT, δZ, δP, δD		cm, mrad, cm, mrad, no dim.	5*E
XL	Half length of object: $-XL \leq X_0 \leq XL$ (uniform random distribution)	cm	E
$IR1$, $IR2$	Random sequence seeds	2*$\simeq 0^6$	2*I

OCTUPOLE	**Octupole magnet**		
IL	$IL = 1, 2$: print field and coordinates along trajectories	0-2	I
XL, R_0, B_0	Length; radius and field at pole tip of the element	2*cm, kG	3*E
	Entrance face:		
X_E, λ_E	Integration zone; Fringe field extent ($\lambda_E = 0$ for sharp edge)	2*cm	2*E
NCE, $C_0 - C_5$	NCE = unused $C_0 - C_5$ = fringe field coefficients such that: $G(s) = G_0/(1 + \exp\ P(s))$, with $G_0 = B_0/R_0^3$ and $P(s) = \sum_{i=0}^{5} C_i(s/\lambda)^i$	any, 6*no dim.	I, 6*E
	Exit face:		
X_S, λ_S	Parameters for the exit fringe field; see entrance	2*cm	2*E
NCS, $C_0 - C_5$		0-6, 6*no dim.	I, 6*E
XPAS	Integration step	cm	E
KPOS, *XCE*, *YCE*, *ALE*	*KPOS*=1: element aligned, 2: misaligned; shifts, tilt (unused if *KPOS*=1)	1-2, 2*cm, rad	I, 3*E

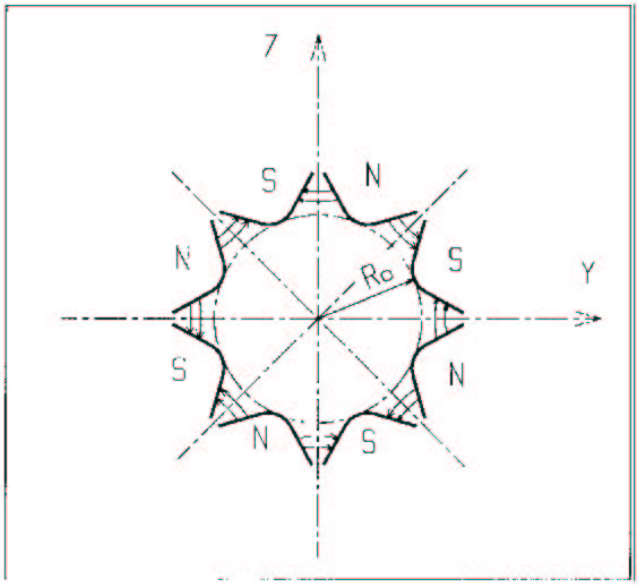

Octupole magnet

ORDRE	**Taylor expansions order**		
IO	Taylor expansions of $\vec{R}$ and $\vec{u}$ up to $\vec{u}^{(IO)}$ (default is $IO = 4$)	2-5	I

PARTICUL **Particle characteristics**

M, Q, G, τ, X	Mass; charge; gyromagnetic factor; COM life-time; unusued	MeV/c^2, C, no dim., s 5*E

NOTE : Only the parameters of concern need their value be specified (for instance M, Q for electric lenss); others can be set to zero.

PLOTDATA **Intermediate output for the PLOTDATA graphic software** [27]

To be documented.

POISSON **Read magnetic field data from *POISSON* output**

IC, *IL*	*IC* = 1, 2: print the field map *IL* = 1, 2: print field and coordinates along trajectories	0-2, 0-2	2*I
BNORM, XN,YN	Field and X-,Y-coordinate normalization	3*no dim.	3*E
TIT	Title		A80
IX, *IY*	Number of longitudinal and transverse nodes of the uniform mesh	≤ 400, ≤ 200	2*I
FNAME[1]	Filename (normally, outpoi.lis)		A80
ID, *A*, *B*, *C* [*A′*, *B′*, *C′* *B″*,etc., if $ID \geq 2$]	Integration boundary. Ineffective when $ID = 0$. *ID* = -1, 1 or ≥ 2 : as for *CARTEMES*	≥ -1, 2*no dim., cm [,2*no dim., cm, etc.]	I,3*E [,3*E,etc.]
IORDRE	Order of interpolation polynomial as for *DIPOLE*	2, 4 or 25	I
XPAS	Integration step	cm	E
KPOS, *XCE*, *YCE, ALE*	*KPOS*=1: element aligned, 2: misaligned; shifts, tilt (unused if *KPOS*=1)	1-2, 2*cm, rad	I, 3*E

[1] *FNAME* contains the field map data. These must be formatted according to the following *FORTRAN* read sequence:

```
      I = 0
   11  CONTINUE
      I = I+1
      READ(LUN,101,ERR=99,END=10) K, K, K, R, X(I), R, R, B(I)
  101   FORMAT(I1, I3, I4, E15.6, 2F11.5, 2F12.3)
      GOTO II
   10   CONTINUE
```

where $X(I)$ is the longitudinal coordinate, and $B(I)$ is the Z component of the field at a node (I) of the mesh. K's and R's are variables appearing in the *POISSON* output file outpoi.lis, not used here.

POLARMES	**2-D polar mesh magnetic field map** mid-plane symmetry is assumed		
IC, *IL*	$IC = 1, 2$: print the map $IL = 1, 2$: print field and coordinates along trajectories	0-2, 0-2	2*I
BNORM, AN,RN	Field and A-,R-coordinate normalization	3*no dim.	3*E
TIT	Title		A80
IA, *JR*	Number of angular (≤ 400) and radial (≤ 200) nodes of the map	2*I	
FNAME[1]	Filename (e.g., spes2.map)		A80
ID, *A*, *B*, *C* [A', B', C' B'',etc., if $ID \geq 2$]	Integration boundary. Ineffective when $ID = 0$. ID = -1, 1 or ≥ 2 : as for *CARTEMES*	≥ -1, 2*no dim., cm [,2*no dim., cm, etc.]	I,3*E [,3*E,etc.]
IORDRE	Order of interpolation polynomial (see *DIPOLE*)	2, 4 or 25	I
XPAS	Integration step	cm	E
KPOS	as for *DIPOLE*. Normally 2.	1-2	I
If KPOS = 2			
RE, *TE*, *RS*, *TS*		cm, rad, cm, rad	4*E
If KPOS = 1			
DP		no dim.	E

[1] *FNAME* contains the field data. These must be formatted according to the following *FORTRAN* sequence:

```
OPEN (UNIT = NL, FILE = FNAME, STATUS = 'OLD' [,FORM='UNFORMATTED'])
IF (BINARY) THEN
  READ(NL) (Y(J), J=1, JY)
ELSE
        READ(NL,100) (Y(J), J=1, JY)
      ENDIF
100    FORMAT(10 F8.2)
      DO 1 I = 1,IX
  IF (BINARY) THEN
    READ (NL) X(I), (BMES(I,J), J=1, JY)
  ELSE
    READ(NL,101) X(I), (BMES(I,J), J=1, JY)
101   FORMAT(10 F8.1)
        ENDIF
  1    CONTINUE
```

where $X(I)$ and $Y(J)$ are the longitudinal and transverse coordinates and *BMES* is the Z field component at a node (I, J) of the mesh. For binary files, *FNAME* must begin with B_ .'Binary' will then automatically be set to '.TRUE.'

PS170	**Simulation of a round shape dipole magnet**		
IL	$IL = 1, 2$: print field and coordinates along trajectories	0-2	I
XL, R_0, B_0	Length of the element, radius of the circular dipole, field	2*cm, kG	3*E
XPAS	Integration step	cm	E
KPOS, *XCE*, *YCE*, *ALE*	*KPOS*=1: element aligned, 2: misaligned; shifts, tilt (unused if *KPOS*=1)	1-2, 2*cm, rad	I, 3*E

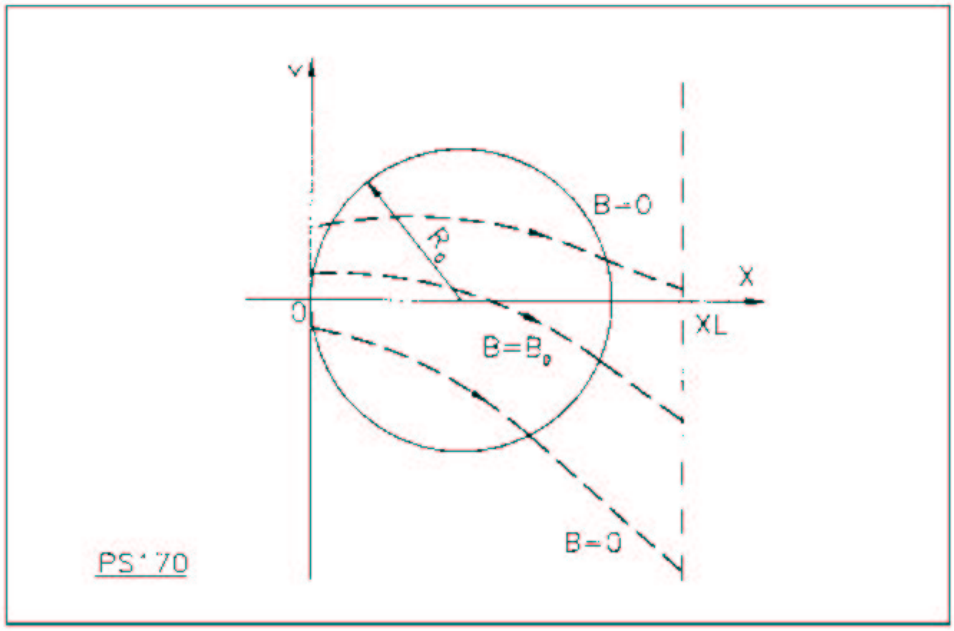

Scheme of the PS170 magnet simulation.

QUADISEX **Sharp edge magnetic multipoles**

$B_Z\,|_{Z=0} = B_0\left(1 + \frac{N}{R_0}Y + \frac{B}{R_0^2}Y^2 + \frac{G}{R_0^3}Y^3\right)$

IL	$IL = 1, 2$: print field and coordinates along trajectories	0-2	I
XL, R_0, B_0	Length of the element; normalization distance; field	2*cm, kG	3*E
N, $EB1$, $EB2$, $EG1$, $EG2$	Coefficients for the calculation of B. if $Y > 0$: $B = EB1$ and $G = EG1$; if $Y < 0$: $B = EB2$ and $G = EG2$.	5*no dim.	5*E
XPAS	Integration step	cm	E
KPOS, *XCE*, *YCE*, *ALE*	*KPOS*=1: element aligned, 2: misaligned; shifts, tilt (unused if *KPOS*=1)	1-2, 2*cm, rad	I, 3*E

QUADRUPO	**Quadrupole magnet**		
IL	$IL = 1, 2$: print field and coordinates along trajectories	0-2	I
XL, R_0, B_0	Length; radius and field at pole tip	2*cm, kG	3*E
	Entrance face:		
X_E, λ_E	Integration zone extent; fringe field extent ($\simeq 2R_0$, $\lambda_E = 0$ for sharp edge)	2*cm	2*E
NCE,$C_0 - C_5$	NCE = unused $C_0 - C_5$= Fringe field coefficients such that $G(s) = G_0/(1 + \exp P(s))$, with $G_0 = B_0/R_0$ and $P(s) = \sum_{i=0}^{5} C_i(s/\lambda)^i$	any, 6*no dim.	I, 6*E
	Exit face		
X_S, λ_S	See entrance face	2*cm	2*E
NCS, $C_0 - C_5$		0-6, 6*no dim.	I, 6*E
XPAS	Integration step	cm	E
KPOS, *XCE*, *YCE*, *ALE*	*KPOS*=1: element aligned, 2: misaligned; shifts, tilt (unused if *KPOS*=1)	1-2, 2*cm, rad	I, 3*E

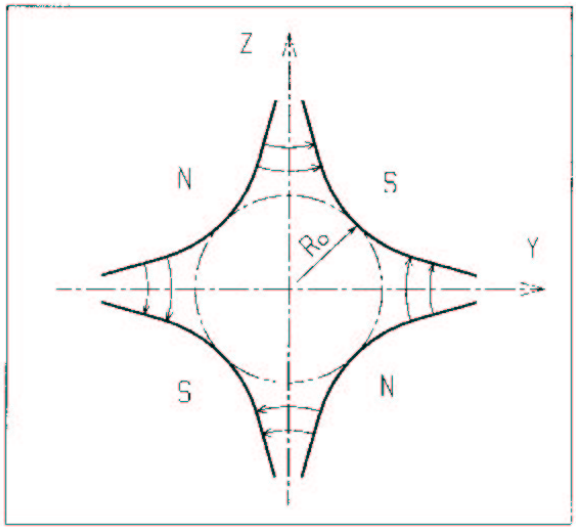

Quadrupole magnet

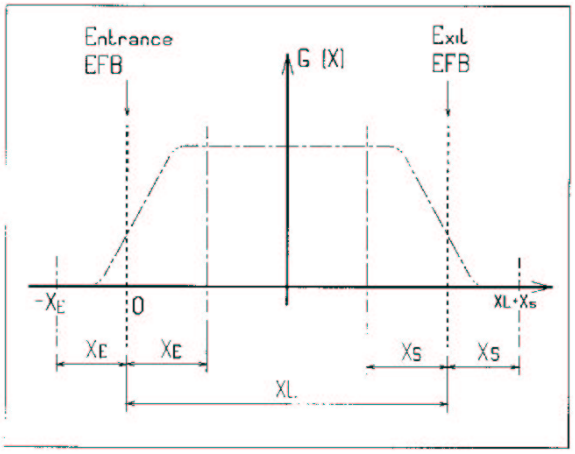

Scheme of the elements *QUADRUPO*, *SEXTUPOL*, *OCTUPOLE*, *DECAPOLE*, *DODECAPO* and *MULTIPOL*
(OX) is the longitudinal axis of the reference frame $(0, X, Y, Z)$ of **zgoubi** .
The length of the element is XL, but trajectories are calculated from $-X_E$ to $XL + X_S$, by means of automatic prior and further X_E and X_S translations.

REBELOTE **Jump to the beginning of zgoubi input data file**

NPASS, *KWRIT*, *K*	Number of runs; *KWRIT* = 0 inhibits the *FORTRAN WRITE* statements; *K* = option *K* = 0: initial conditions (coordinates and spins) are generated following the regular functioning of object definitions. If random generators are used (e.g. in *MCOBJET*) their seeds will not be reset *K* = 99: the coordinates resulting from the previous run are used as initial coordinates for the next run; idem for spin components.	arbitrary, 0-1, 0 or 99	3*I

RESET **Reset counters and flags**

Resets counters involved in *CHAMBR*, *COLLIMA* *HISTO* and *INTEG* procedures

Switches off *CHAMBR*, *MCDESINT*, *SCALING* and *SPNTRK* options

SCALING	**Time scaling of power supplies and R.F.**		
IOPT, NFAM	*IOPT* = 0 (inactive) or 1 (active); *NFAM* = number of families to be scaled	0-1; 1-9	2*I
For NF=1, NFAM:	repeat *NFAM* times the following sequence:		
NAMEF	Name of the family (i.e., keyword of concern)		A8
NT	Number of timings	1-10	I
$SCL(I),\ I = 1,\ NT$	Scaling values	relative	NT*E
$TIM(I),\ I = 1,\ NT$	Corresponding timings. Out of this range, the scaling factor is 1.	turn number	NT*I

SEPARA[1] **Wien Filter - analytical simulation**

IA, *XL*, *E*, *B*,	*IA* = 0: element inactive *IA* = 1: horizontal separation *IA* = 2: vertical separation; Length of the separator; electric field; magnetic field.	0-2, m, V/m, T	I, 3*E

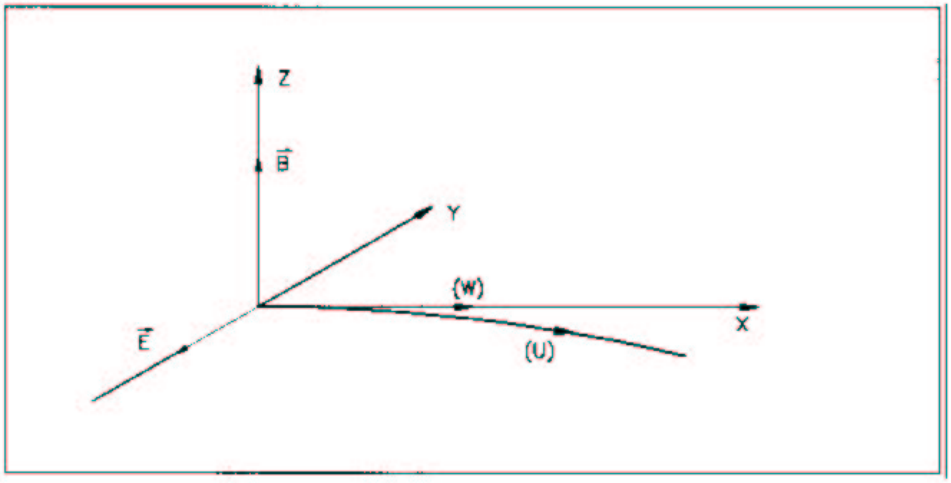

Horizontal separation between a wanted particle, (W), and an unwanted particle, (U). (W) undergoes a linear motion while (U) undergoes a cycloidal motion.

[1] *SEPARA* must be preceded by *PARTICUL* for the definition of mass and charge of the particles.

SEXQUAD **Sharp edge magnetic multipole**

$B_Z\ |_{Z=0} = B_0 \left(\frac{N}{R_0}Y + \frac{B}{R_0^2}Y^2 + \frac{G}{R_0^3}Y^3\right)$

IL	$IL = 1, 2$: print field and coordinates along trajectories	0-2	I
XL, R_0, B_0	Length of the element; normalization distance; field	2*cm, kG	3*E
N, $EB1$, $EB2$, $EG1$, $EG2$	Coefficients for the calculation of B. if $Y > 0$: $B = EB1$ and $G = EG1$; if $Y < 0$: $B = EB2$ and $G = EG2$.	5*no dim.	5*E
XPAS	Integration step	cm	E
KPOS, *XCE*, *YCE*, *ALE*	*KPOS*=1: element aligned, 2: misaligned; shifts, tilt (unused if *KPOS*=1)	1-2, 2*cm, rad	I, 3*E

SEXTUPOL	**Sextupole Magnet**		
IL	$IL = 1, 2$: print field and coordinates along trajectories	0-2	I
XL, R_0,B_0	Length; radius and field at pole tip of the element	2*cm, kG	3*E
	Entrance face:		
X_E, λ_E	Integration zone; fringe field extent ($\lambda_E = 0$ for sharp edge)	2*cm	2*E
NCE,$C_0 - C_5$	NCE = unused $C_0 - C_5$ = Fringe field coefficients such that $G(s) = G_0/(1 + \exp P(s))$, with $G_0 = B_0/R_0^2$ and $P(s) = \sum_{i=0}^{5} C_i(s/\lambda)^i$	any, 6* no dim.	I, 6*E
	Exit face:		
X_S, λ_S	Parameters for the exit fringe field; see entrance	2*cm	2*E
NCS, $C_0 - C_5$		0-6, 6*no dim.	I, 6*E
$XPAS$	Integration step	cm	E
$KPOS$, XCE, YCE, ALE	$KPOS$=1: element aligned, 2: misaligned; shifts, tilt (unused if $KPOS$=1)	1-2, 2*cm, rad	I, 3*E

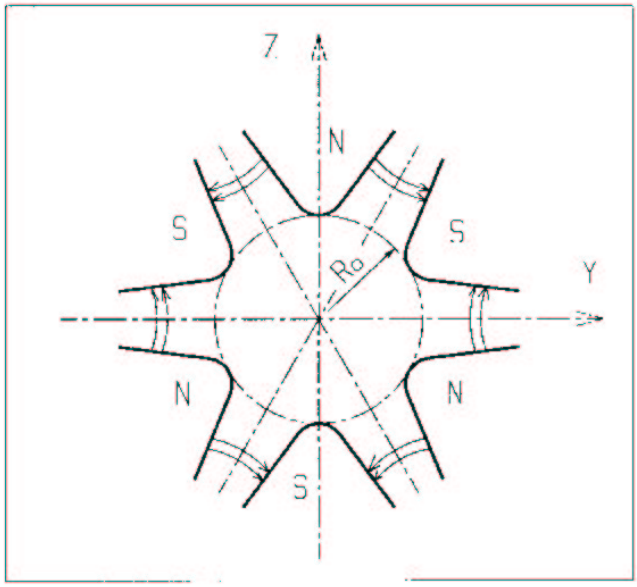

Sextupole magnet

SOLENOID **Solenoid**

IL	$IL = 1, 2$: print field and coordinates along trajectories	0-2	I
XL, R_0, B_0	Length; radius; asymptotic field ($=\mu_0 NI/XL$)	2*cm, kG	3*E
X_E, X_S	Entrance and exit integration zones	2*cm	2*E
XPAS	Integration step	cm	E
KPOS, *XCE*, *YCE*, *ALE*	*KPOS*=1: element aligned, 2: misaligned; shifts, tilt (unused if *KPOS*=1)	1-2, 2*cm, rad	I, 3*E

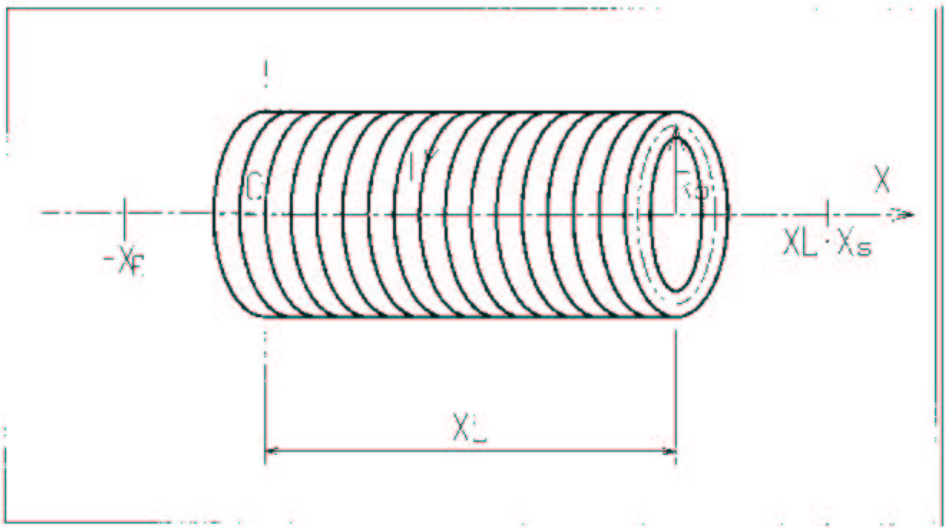

SPNPRNL **Store spin coordinates in file *FNAME***

FNAME[1]	Name of storage file (e.g. zgoubi.spn)		A80

SPNPRNLA **Store spin coordinates every IP other pass**

FNAME[1]	Name of storage file (e.g. zgoubi.spn)		A80
IP	Store every IP other pass (when using *REBELOTE* with *NPASS* $\geq IP-1$)	$\leq NPASS$	I

SPNPRT **Print spin coordinates**

Print spin coordinates at the location where this keyword is introduced in the structure.

[1] *FNAME* contains the spin coordinates and other informations, stored following the *FORTRAN* sequence below:

```
OPEN (UNIT = NL, FILE = FNAME)
DO  1  I = 1, IMAX
   WRITE(NL,100) LET(I),IEX(I),SXO(I),SYO(I),SZO(I),SO(I),SX(I),SY(I),SZ(I),S(I),γ,I,IMAX,IPASS,NOEL
 100     FORMAT(1X, A1, I2, 1P , 6E15.7, /, E15.7, 2I3, I6)
  1      CONTINUE
```

where SX, SY, SZ are the spin components (suffix O stands for origin). $S = (SX^2 + SY^2 + SZ^2)^{1/2}$, γ = Lorentz factor, I = particle number, *IMAX* = total number of particles per pass, *IPASS* = pass number (as incremented by *REBELOTE*), *NOEL* = position of the keyword *SPNPRNL[A]* in the zgoubi.dat data list. See *OBJET* and *SPNTRK* for more details.

SRPRNT **Print SR loss statistics**
into zgoubi.res

SPNTRK[1]	**Spin tracking**		
KSO	Initial conditions options	1-5	I
If KSO = 1 – 3	$KSO = 1$ (respectively 2, 3): all particles have their spin automatically set to (1,0,0) – longitudinal [respectively (0,1,0) – horizontal and (0,0,1) – vertical]		
If KSO = 4	Repeat *IMAX* times (corresponding to *IMAX* particles, cd '*OBJET*') the following sequence:		
S_x, S_y, S_z	X, Y and Z components of the spin	3*no dim.	3*E
If KSO = 5	Random distribution in a cone (see figure) Enter the following two sequences:		
TO, PO, A, δA	Angles of average polarization: A = angle of the cone; δA = standard deviation of distribution around A	4*rad	4*E
IR	Random sequence seed	$\lesssim 10^6$	I

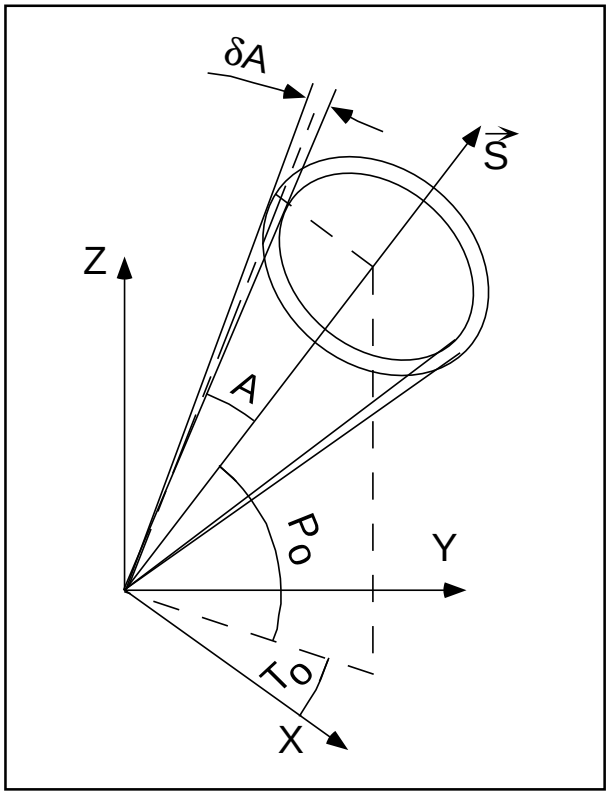

Spin distribution as obtained with option $KSO = 5$
The spins are distributed within an annular strip δA (standard deviation)
at an angle A with respect to the axis of mean polarization (S) defined by T_0 and P_0.

[1] *SPNTRK* must be preceded by *PARTICUL* for the definition of G and mass.

SRLOSS	**Synchrotron radiation loss**		
KSR, IR	Switch; seed	$0-1, >10^5$	2*I

SYNRAD	**Synchrotron radiation spectral-angular densities**		
KSR	Switch 0: inhibit SR calculations 1: start 2: stop	0-2	I
If KSR = 0			
$D1$, $D2$, $D3$	Dummies		3*E
If KSR = 1			
$X0$, $Y0$, $Z0$	Observer position in frame of magnet next to *SYNRAD*	3*m	3*E
If KSR = 2			
ν_1, ν_2, N	Frequency range and sampling	2*eV, no dim.	2*E, I

TOSCA **2-D and 3-D Cartesian uniform mesh magnetic field map**

IC, *IL*	see *CARTEMES*	0-2, 0-2	2*I
BNORM, *XN [,YN,ZN]*	Field and X- (if $IZ = 1$ below), or X-,Y-,Z- (if $IZ \neq 1$) -coordinate normalization	2[4]*no dim.	2[4]*E
TIT	Title[1]		A80
IX, *IY*, *IZ*	Number of nodes of the mesh in the X, Y and Z directions. $IZ = 1$ for 2-D maps; $IZ < 0$ for 3-D maps with no symmetry hypothesis.	≤ 400, ≤ 200, $3 \leq \|IZ\|$	3*I
FNAME[2] $(K = 1, NF)$	Names of the NF files containing the maps, ordered from $Z(1)$ to $Z(NF)$. If $IZ > 0$: $NF = 1 + [IZ/2]$, the NF maps are symmetrized with respect to the $Z(1) = 0$ plane. If $IZ < 0$: $NF = \|IZ\|$, no symmetry assumed; $Z(1) = Z_{max}$, $Z(1 + [\,\|IZ\|/2]) = 0$ and $Z(NF) = -Z_{max}$.		A80
ID, *A*, *B*, *C* [A', B', C' B'',etc., if $ID \geq 2$]	Integration boundary. Ineffective when $ID = 0$. ID = -1, 1 or ≥ 2 : as for *CARTEMES*	≥ -1, 2*no dim., cm [,2*no dim., cm, etc.]	I,3*E [,3*E,etc.]
IORDRE	If $IZ = 1$: as in *CARTEMES* If $IZ \neq 1$: unused	2, 4 or 25	I
XPAS	Integration step	cm	E
KPOS, *XCE*, *YCE*, *ALE*	*KPOS*=1: element aligned, 2: misaligned; shifts, tilt (unused if *KPOS*=1)	1-2, 2*cm, rad	I, 3*E

[1]Begin "Title" with "FLIP" so as to get the map flipped prior to ray-tracing.
[2]Each file *FNAME(K)* contains the field map at elevation $Z(K)$ and must be formatted according to the following *FORTRAN* read sequence (that normally fits *TOSCA* code *OUTPUTS*):

```
DO  2  K = 1, NF
  OPEN (UNIT = NL, FILE = FNAME(K), STATUS = 'OLD' [,FORM='UNFORMATTED'])
  DO  1  J = 1,  JY
    DO  1 I = 1, IX
          IF (BINARY) THEN
            READ(NL) Y(J), Z(K), X(I), BY(J,K,I), BZ(J,K,I), BX(J,K,I)
          ELSE
            READ(NL,100) Y(J), Z(K), X(I), BY(J,K,I), BZ(J,K,I), BX(J,K,I)
100           FORMAT(1X, 6E11.2)
          ENDIF
1     CONTINUE
      NL = NL + 1
2   CONTINUE
```

where $X(I)$, $Y(J)$, $Z(K)$ are the longitudinal, horizontal and vertical coordinates and BX, BY, BZ are the components of the field at node (I, J, K) of the mesh. For 2-D maps $B'X$ and $B'Y$ are assumed zero at all nodes of the 2D mesh, regardless of BX(J,1,I), BY(J,1,I) values.
For binary files, *FNAME* must begin with B_.'Binary' will then automatically be set to '.TRUE.'

TRAROT	**Translation-Rotation**		
TX, TY, TZ, RX, RY, RZ	Translations, rotations	3*m, 3*rad	6*E

TWISS **Calculation of optical parameters ; periodic parameters**

KTWISS	Options : 0: No effect 1: First and second order quantities are computed 2: Higher orders	0-2	2*I

UNDULATOR	**Undulator magnet**		
IL	$IL = 1, 2$: print field and coordinates along trajectories (otherwise $IL = 0$)	0-2	I
XL, Sk, $B1$	Length; skew angle; field	cm, rad, kG	3*E
	Entrance face:		
X_E, λ_E, W_E	Integration zone extent; fringe field extent (normally $\simeq$ gap height; zero for sharp edge); wedge angle	cm, cm, rad	3*E
N, C_0–C_5	Unused; fringe field coefficients: $B(s) = B1\,F(s)$ with $F(s) = 1/(1+\exp(P(s)))$ and $P(s) = \sum_{i=0}^{5} C_i (s/\lambda)^i$	unused, 6*no dim.	I, 6*E
	Exit face:		
X_S, λ_S, W_S	See entrance face	cm, cm, rad	3*E
N, C_0–C_5		unused, 6*no dim.	I, 6*E
XPAS	Integration step	cm	E
KPOS, *XCE*, *YCE*, *ALE*	*KPOS*=1: element aligned, 2: misaligned; shifts, tilt (unused if *KPOS*=1)	1-2, 2*cm, rad	I, 3*E

Undulator magnet.

UNIPOT	**Unipotential electrostatic lens**		
IL	*IL* = 1, 2: print field and coordinates along trajectories	0-2	I
X_1, D, X_2, X_3, R_0	Length of first tube; distance between tubes; length of second and third tubes; radius	5*m	5*E
V_1, V_2	Potentials	2*V	2*E
XPAS	Integration step	cm	E
KPOS, *XCE*, *YCE*, *ALE*	*KPOS*=1: element aligned, 2: misaligned; shifts, tilt (unused if *KPOS*=1)	1-2, 2*cm, rad	I, 3*E

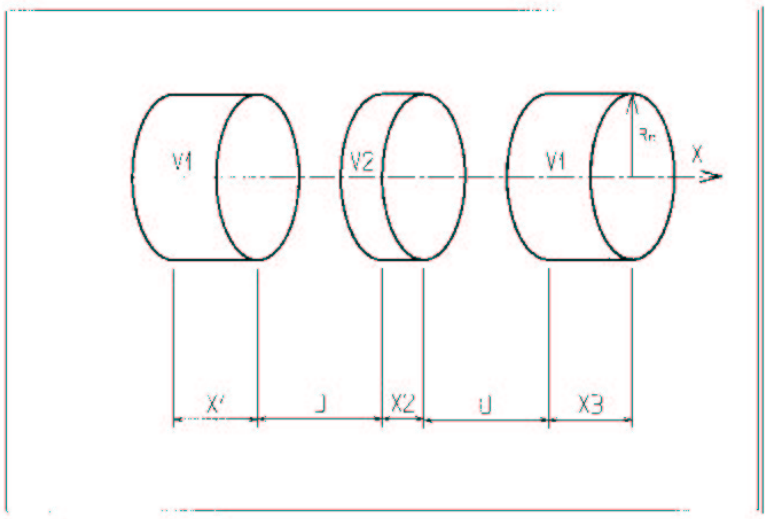

VENUS	**Simulation of a rectangular dipole magnet**		
IL	$IL = 1, 2$: print field and coordinates on trajectories	0-2	I
XL, YL, B_0	Length; width $= \pm YL$; field	2*cm, kG	3*E
XPAS	Integration step	cm	E
KPOS, *XCE*, *YCE*, *ALE*	*KPOS*=1: element aligned, 2: misaligned; shifts, tilt (unused if *KPOS*=1)	1-2, 2*cm, rad	I, 3*E

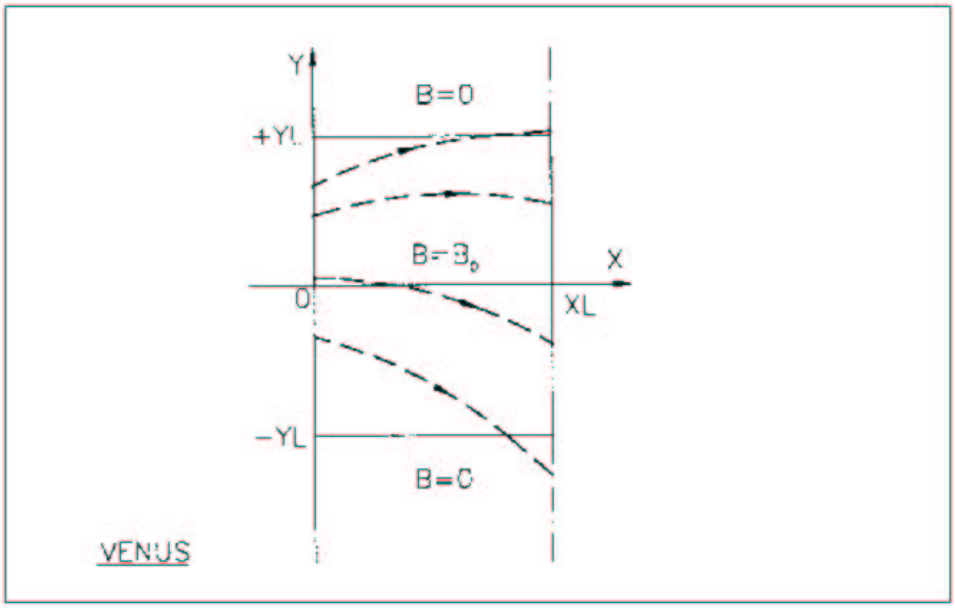

Scheme of *VENUS* rectangular dipole.

WIENFILT[1]	**Wien filter**		
IL	$IL = 1, 2$: print field and coordinates along trajectories (otherwise $IL = 0$)	0-2	I
XL, E, B, HV	Length; electric field; magnetic field; option: element inactive ($HV = 0$) horizontal ($HV = 1$) or vertical ($HV = 2$) separation	m, V/m, T, 0-2	3*E, I
	Entrance face:		
X_{E}, λ_{E_E}, λ_{B_E}	Integration zone extent; fringe field extent ($\simeq$ gap height)	3*cm	3*E
C_{E0}–C_{E5}	Fringe field coefficients for E	6*no dim.	6*E
C_{B0}–C_{B5}	Fringe field coefficients for B	6*no dim.	6*E
	Exit face:		
X_S, λ_{E_S}, λ_{B_S}	See entrance face	3*cm	3*E
C_{E0}–C_{E5}		6*no dim.	6*E
C_{B0}–C_{B5}		6*no dim.	6*E
XPAS	Integration step	cm	E
KPOS, *XCE*, *YCE*, *ALE*	*KPOS*=1: element aligned, 2: misaligned; shifts, tilt (unused if *KPOS*=1)	1-2, 2*cm, rad	I, 3*E

[1] Use *PARTICUL* to declare mass and charge.

YMY **Reverse signs of Y and Z axes**

Equivalent to a 180° rotation with respect to X-axis

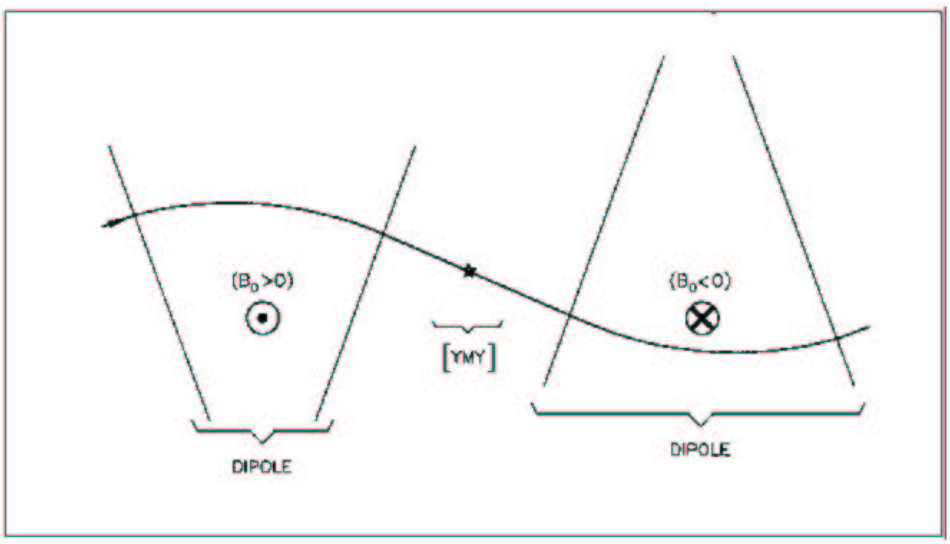

The use of YMY in a sequence of two identical dipoles of opposite signs.

PART C

Examples of input data files and output result files

INTRODUCTION

Several examples of the use of **zgoubi** are given here. They show the contents of the input and output data files, and are also intended to help understanding some subtleties of the data definition.

Example 1: checks the resolution of the QDD spectrometer SPES 2 of SATURNE Laboratory [31], by means of a *Monte Carlo initial object* and an *analysis of images* at the focal plane with histograms. The *measured field maps* of the spectrometer are used for that purpose. The design of SPES 2 is given in Fig. 40.

Example 2: calculates the *first and second order transfer matrices* of an 800 MeV/c kaon beam line [32] at each of its four foci: at the end of the first separation stage (vertical focus), at the intermediate momentum slit (horizontal focus), at the end of the second separation stage (vertical focus), and at the end of the line (double focusing). The first bending is represented by its *3-D map* previously calculated with the TOSCA magnet code. The second bending is simulated with *DIPOLE*. The design of the line is given in Fig. 41.

Example 3: illustrates *the use of MCDESINT and REBELOTE* with a simulation of the *in-flight decay*

$$K \longrightarrow \mu + \nu$$

in the SATURNE Laboratory spectrometer SPES 3 [16]. The angular acceptance of SPES 3 is ±50 mrd horizontally and ±50 mrd vertically; its momentum acceptance is ±40%. The bending magnet is simulated with *DIPOLE*. The design of SPES 3 is given in Fig. 42.

Example 4: illustrates the functioning of *the fitting procedure*: a quadrupole triplet is tuned from -0.7/0.3 T to field values leading to transfer coefficients R12=16.6 and R34=-.88 at the end of the beam line. Other example can be found in [33].

Example 5: shows the use of the *spin and multiturn tracking procedures*, applied to the case of the SATURNE 3 GeV synchrotron [5, 8, 29]. Protons with initial vertical spin ($\vec{S} \equiv \vec{S}_Z$) are accelerated through the $\gamma G = 7 - \nu_Z$ depolarizing resonance. For easier understanding, some results are summarized in Figs. 44, 45 (obtained with the graphic post-processor, see Part D).

Example 6: shows *ray-tracing through a micro-beam line* that involves *electro-magnetic quadrupoles* for the suppression of second order (chromatic) aberrations [4]. The extremely small beam spot sizes involved (less than 1 micrometer) reveal the high accuracy of the ray-tracing (Figs. 46).

1 MONTE CARLO IMAGES IN SPES 2

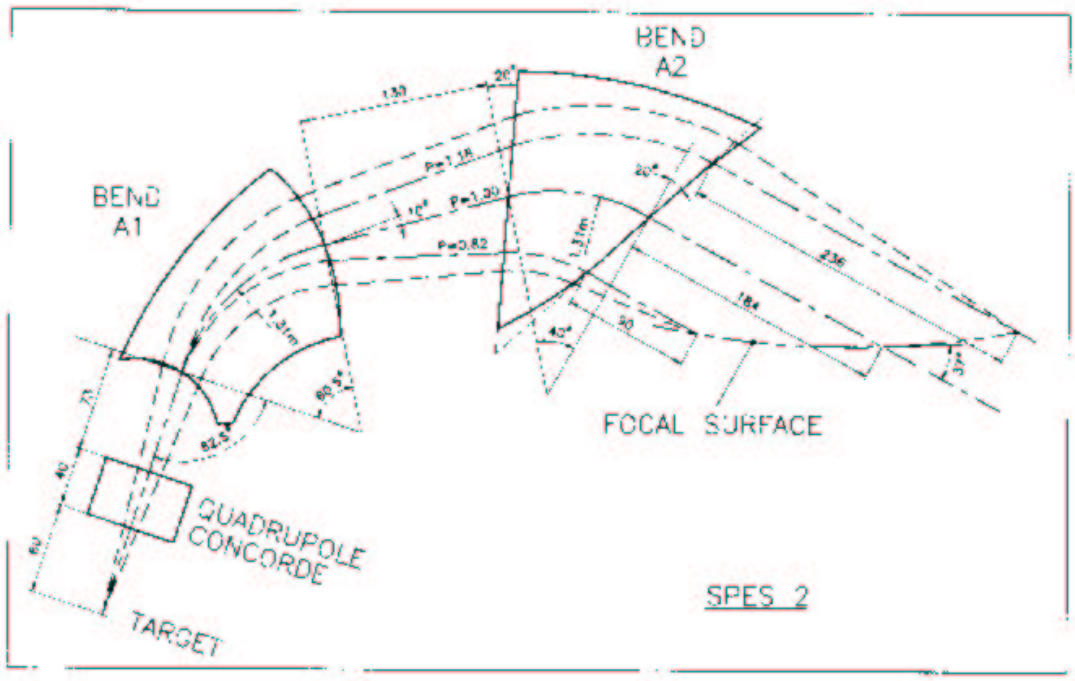

Figure 40: Design of SPES 2.

zgoubi data file.

```
 SPES2 WITH FIELD MAPS ;  MONTE-CARLO MOMENTUM GRID OBJECT.
'MCOBJET'                                                          1
2335.                              REFERENCE  RIGIDITY.
2                                  DISTRIBUTION  IN  GRID.
200                                NUMBER  OF  PARTICLES.
1   1   1   1   1   1              UNIFORM DISTRIBUTIONS
0.  0.  0.  0.  0.  1.             CENTRAL  VALUES  OF  BARS.
1   1   1   1   1   5              NUMBER  OF  BARS  IN  MOMENTUM.
0.  0.  0.  0.  0.  .001           SPACE  BETWEEN  MOMENTUM  BARS.
0.  50.e-3 0.  50.e-3 0.  0.       WIDTH  OF  BARS.
1.  1.  1.  1.  1.  1.             SORTING CUT-OFFS (UNUSED)
9   9. 9. 9. 9.                    FOR P(D) (UNUSED)
186387 548728 472874               SEEDS.
 'HISTO'                                                           2
 1   .997   1.003  80  1          HISTO  OF  D.
 20  'D'  1  'Q'
 'HISTO'                                                           3
 3   -60.  60.     80  1          HISTO  OF  THETAO.
 20  'T'  1  'Q'
 'HISTO'                                                           4
 5   -60.  60.     80  1          HISTO  OF  PHIO.
 20  'P'  1  'Q'
'DRIFT'                                                            5
41.5
'CARTEMES'                         QUADRUPOLE  MAP.                6
 0  0                              IC  IL.
 -.96136E-3                        BNORM.
++++  CONCORDE ++++
 39  23                            IX  IY.
 ../spes2/concord.map
 0  0 0 0                          NO  LIMIT  PLANE.
2                                  IORDRE.
2.5                                XPAS.
2 0 0 0                            KPOS.
'DRIFT'                                                            7
21.8
'CHANGREF'                         POSITIONING  OF  THE            8
0. 32.5 -35.6                      1-ST  BENDING.
'CARTEMES'                                                         9
 0 0
 1.04279E-3
++++  A1 ++++
 117  52
 ../spes2/a1.map
 0  0 0 0
2
2.5
2 0 0 0
'CHANGREF'                         POSITIONING  OF  THE           10
0. -28.65  -27.6137                EXIT  FRAME.
'DRIFT'                                                           11
33.15
'CHANGREF'                         POSITIONING  OF  THE           12
0. 27.5  -19.88                    2-ND  BENDING.
'CARTEMES'                                                        13
 0 0
 1.05778E-3
++++  A2 ++++
 132  80
../spes2/a2.map
 0  0 0 0
2
2.5
2 0 0 0
'CHANGREF'                         POSITIONING  OF  THE           14
41.  -81.  -21.945                 EXIT  FRAME.
'DRIFT'                                                           15
3.55
 'HISTO'                           HISTO  OF  Y :                 16
 2  -.5  2.     80  1             SHOWS  THE  RESOLUTION
 20  'Y'  1  'Q'                   OF  THE  SPECTROMETER.
 'REBELOTE'                       (9+1)  PASSES,  FOR  RAY-TRACING 17
 9  0.1  0                        (9+1)*200  TRAJECTORIES.
'END'                                                             18
```

Excerpt from zgoubi output : histograms of initial beam coordinates.

```
********************************************************************************************************
     2  HISTO

                        HISTOGRAMME  DE  LA  COORDONNEE    D
                        PARTICULES  PRIMAIRES  ET  SECONDAIRES
                        DANS  LA  FENETRE :   9.9700E-01 /   1.0030E+00
                        NORMALISE

  20
  19
  18                                    D
  17                                    D                                       D
  16                      D             D             D                         D
  15                      D             D             D             D           D
  14                      D             D             D             D           D
  13                      D             D             D             D           D
  12                      D             D             D             D           D
  11                      D             D             D             D           D
  10                      0             0             0             0           0
   9                      D             D             D             D           D
   8                      D             D             D             D           D
   7                      D             D             D             D           D
   6                      D             D             D             D           D
   5                      D             D             D             D           D
   4                      D             D             D             D           D
   3                      D             D             D             D           D
   2                      D             D             D             D           D
   1                      D             D             D             D           D

                123456789012345678901234567890123456789012345678901234567890123456789012345678901
                         2         3         4         5         6         7         8         9


            TOTAL  COMPTAGE                :    2000  SUR   2000
            NUMERO   DU  CANAL  MOYEN      :      51
            COMPTAGE  AU   "       "       :     394
            VAL. PHYS. AU  "       "       :  1.000E+00
            RESOLUTION  PAR  CANAL         :  7.500E-05

            PARAMETRES  PHYSIQUES  DE  LA  DISTRIBUTION :
                        COMPTAGE =   2000  PARTICULES
                        MIN =  9.9800E-01, MAX =  1.0020E+00, MAX-MIN =  4.0000E-03
                        MOYENNE =  9.9999E-01
                        SIGMA =  1.4158E-03
********************************************************************************************************
     3  HISTO

                        HISTOGRAMME  DE  LA  COORDONNEE  THETA
                        PARTICULES  PRIMAIRES  ET  SECONDAIRES
                        DANS  LA  FENETRE :  -6.0000E+01 /   6.0000E+01 (MRD)
                        NORMALISE

  20
  19
  18
  17                      T                                               T
  16                      T                   T             T           T     T
  15                      T                   TT            T           T     T
  14                      T               T     T TT          T           TT    T
  13                      T  T     T     T TT    TTTT          T           TT    T
  12                      T  TT T  T  T T TT    TTTT   T    T    T T         TT TT TTTT
  11                    T  T  TT T TT  T T TT T TTTTT   TT  TT  TTT T  TTTTT TTT TT TTTT
  10                    00 00 0000000 00 0000 0000000   000000  000 0  000000000 00 0000 0
   9                    TTTTT TTTTTTTTTTTTTTTT TTTTTTTTTTTTTTTTTTT TTT TTTTTTTTTTTTTTTTTTTTT T
   8                    TTTTTTTTTTTTTTTTTTTTTTTTTTTTTTTTTTTTTTTTTTTTTTTTTTTTTTTTTTTTTTTTTTTTTTT
   7                   TTTTTTTTTTTTTTTTTTTTTTTTTTTTTTTTTTTTTTTTTTTTTTTTTTTTTTTTTTTTTTTTTTTTTTTT
   6                   TTTTTTTTTTTTTTTTTTTTTTTTTTTTTTTTTTTTTTTTTTTTTTTTTTTTTTTTTTTTTTTTTTTTTTTT
   5                   TTTTTTTTTTTTTTTTTTTTTTTTTTTTTTTTTTTTTTTTTTTTTTTTTTTTTTTTTTTTTTTTTTTTTTTT
   4                   TTTTTTTTTTTTTTTTTTTTTTTTTTTTTTTTTTTTTTTTTTTTTTTTTTTTTTTTTTTTTTTTTTTTTTTT
   3                   TTTTTTTTTTTTTTTTTTTTTTTTTTTTTTTTTTTTTTTTTTTTTTTTTTTTTTTTTTTTTTTTTTTTTTTT
   2                   TTTTTTTTTTTTTTTTTTTTTTTTTTTTTTTTTTTTTTTTTTTTTTTTTTTTTTTTTTTTTTTTTTTTTTTT
   1                   TTTTTTTTTTTTTTTTTTTTTTTTTTTTTTTTTTTTTTTTTTTTTTTTTTTTTTTTTTTTTTTTTTTTTTTT

                123456789012345678901234567890123456789012345678901234567890123456789012345678901
                         2         3         4         5         6         7         8         9


            TOTAL  COMPTAGE                :    2000  SUR   2000
            NUMERO   DU  CANAL  MOYEN      :      51
            COMPTAGE  AU   "       "       :      32
            VAL. PHYS. AU  "       "       :  0.000E+00 (MRD)
            RESOLUTION  PAR  CANAL         :  1.500E+00 (MRD)

            PARAMETRES  PHYSIQUES  DE  LA  DISTRIBUTION :
                        COMPTAGE =   2000  PARTICULES
                        MIN = -4.9880E+01, MAX =  4.9955E+01, MAX-MIN =  9.9835E+01 (MRD)
                        MOYENNE =  3.1889E-01 (MRD)
                        SIGMA =  2.8881E+01 (MRD)
```

```
*********************************************************************************************
     4  HISTO

                        HISTOGRAMME  DE  LA  COORDONNEE  PHI
                        PARTICULES  PRIMAIRES  ET  SECONDAIRES
                        DANS  LA  FENETRE :  -6.0000E+01 /   6.0000E+01 (HRD)
                        NORMALISE

   20
   19
   18                                                P
   17                                                P
   16                                                P   P                           P
   15                      P                P        P P P          P         P     P
   14                      P            PP   P          PP PP P P          P         P     P
   13                    P P P          PPPP P     P    PP PPPP P  P  PPP  P P P    P P   P
   12                    P P P   P    PPPPPP P P   P P  PP PPPP P  PP PPPP P P PPP  P P  PP
   11                    PPP PP  PPP PPPPPPPPPP   P PPPPP PPPP P  PP PPPP P P PPP PP PP PP
   10                    000000  000 000000000000  0 0000000000 00000 0000 0 00000 00000 000
    9                    PPPPPPP PPP PPPPPPPPPPPPPPPPPPPPPPPPPPPPPPPPPPPPPP PPPPPPPPPPPPPPPP
    8                    PPPPPPPPPPPPPPPPPPPPPPPPPPPPPPPPPPPPPPPPPPPPPPPPPP PPPPPPPPPPPPPPPP
    7                    PPPPPPPPPPPPPPPPPPPPPPPPPPPPPPPPPPPPPPPPPPPPPPPPPP PPPPPPPPPPPPPPPP
    6                    PPPPPPPPPPPPPPPPPPPPPPPPPPPPPPPPPPPPPPPPPPPPPPPPPPPPPPPPPPPPPPPPPPP
    5                    PPPPPPPPPPPPPPPPPPPPPPPPPPPPPPPPPPPPPPPPPPPPPPPPPPPPPPPPPPPPPPPPPPP
    4                    PPPPPPPPPPPPPPPPPPPPPPPPPPPPPPPPPPPPPPPPPPPPPPPPPPPPPPPPPPPPPPPPPPP
    3                    PPPPPPPPPPPPPPPPPPPPPPPPPPPPPPPPPPPPPPPPPPPPPPPPPPPPPPPPPPPPPPPPPPP
    2                    PPPPPPPPPPPPPPPPPPPPPPPPPPPPPPPPPPPPPPPPPPPPPPPPPPPPPPPPPPPPPPPPPPP
    1                    PPPPPPPPPPPPPPPPPPPPPPPPPPPPPPPPPPPPPPPPPPPPPPPPPPPPPPPPPPPPPPPPPPP

              1234567890123456789012345678901234567890123456789012345678901234567890123456789012345678901
                        2         3         4         5         6         7         8         9


              TOTAL  COMPTAGE                 :    2000  SUR   2000
              NOMBRE   DU  CANAL  MOYEN       :      51
              COMPTAGE  AU   "      "         :      25
              VAL. PHYS. AU  "      "         :  0.000E+00 (HRD)
              RESOLUTION  PAR  CANAL          :  1.500E+00 (HRD)

              PARAMETRES  PHYSIQUES  DE  LA  DISTRIBUTION :
                          COMPTAGE =   2000  PARTICULES
                          MIN = -4.9968E+01, MAX =  4.9980E+01, MAX-MIN =  9.9949E+01 (HRD)
                          MOYENNE =  1.8122E-01 (HRD)
                          SIGMA =  2.8843E+01 (HRD)
*********************************************************************************************
```

Excerpt of zgoubi output : the final momentum resolution histogram at the spectrometer focal surface.

```
                        HISTOGRAMME  DE  LA  COORDONNEE  Y
                        PARTICULES  PRIMAIRES  ET  SECONDAIRES
                        DANS  LA  FENETRE :  -5.0000E-01 /   2.0000E+00 (CM)
                        NORMALISE


   20
   19
   18                                                Y
   17                                                Y         Y
   16                                                Y         Y
   15                                                Y         Y
   14                                                Y         Y
   13                                                Y         Y
   12                                                Y         Y
   11                                     Y          Y         Y
   10                                     0          0         0         0
    9                                     YY         Y         Y         Y
    8                                     YY         Y         Y         YY
    7                                    YYY         Y         YY        YYY
    6                                 YY  YYY        YY        YY       YYYY
    5                                 YY Y  YYY       YYY       YY       YYYY
    4                                 YY Y   YYYY      YYY       YY       YYYY
    3                                YYY YY    YYYYY     YYYY      YYYY     YYYYY
    2                                YYY YYY   YYYYY     YYYYY     YYYYY    YYYYYY
    1                               YYYYYYYYYY YYYYYYYYYYYYYYYYYYY YYYYYYYYYY  YYYYYYY  Y

              1234567890123456789012345678901234567890123456789012345678901234567890123456789012345678901
                        2         3         4         5         6         7         8         9


              TOTAL  COMPTAGE                 :    2000  SUR   2000
              NOMBRE   DU  CANAL  MOYEN       :      51
              COMPTAGE  AU   "      "         :      48
              VAL. PHYS. AU  "      "         :  7.500E-01 (CM)
              RESOLUTION  PAR  CANAL          :  3.125E-02 (CM)

              PARAMETRES  PHYSIQUES  DE  LA  DISTRIBUTION :
                          COMPTAGE =   2000  PARTICULES
                          MIN = -1.3931E-01, MAX =  1.6491E+00, MAX-MIN =  1.7884E+00 (CM)
                          MOYENNE =  7.5224E-01 (CM)
                          SIGMA =  4.6760E-01 (CM)

TRAJ #1  D,Y,T,Z,P,S,IEX : 9.9900E-01  3.5955E-01 -8.0215E+01  9.8989E-02  2.0665E+00  7.46951E+02  1

*********************************************************************************************
```

2 TRANSFER MATRICES ALONG A TWO-STAGE SEPARATION KAON BEAM LINE

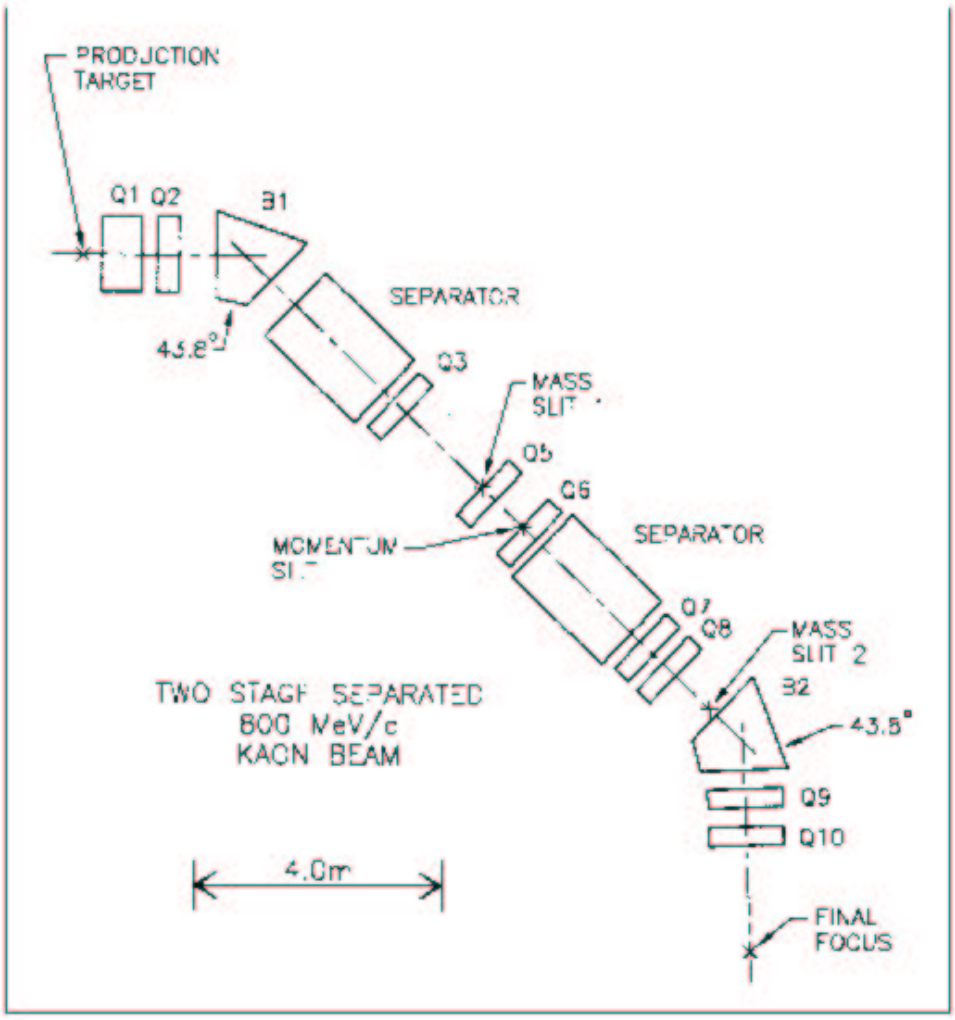

Figure 41: Design of 800 MeV/c kaon beam line.

zgoubi data file.

```
  800 MeV/c KAON BEAM LINE. CALCULATION OF TRANSFER COEFFICIENTS.
 'OBJET'                                                          1
 2668.5100                          AUTOMATIC  GENERATION  OF
 6                                  AN  OBJECT  FOR  CALCULATION
 .1  .1  .1  .1 0.  .001      OF  THE  FIRST  ORDER  TRANSFER
 0. 0. 0. 0. 0. 1.                  COEFFICIENTS  WITH  'MATRIX'
 'PARTICUL'                                                       2
  493.646 1.60217733E-19 0. 0. 0.   KAON M & Q, FOR USE IN WIEN FILTER
 'DRIFT'                                                          3
  35.00000
 'QUADRUPO'                         Q1                            4
 0
   76.2  15.24  13.6
  30.  30.
  4    0.2490   5.3630  -2.4100   0.9870   0.   0.
  30. 30.
  4    0.2490   5.3630  -2.4100   0.9870   0.   0.
   1.1
  1  0. 0. 0.
 'DRIFT'                                                          5
   25.00000
 'QUADRUPOLE'                       Q2                            6
 0
 45.72  15.24   -11.357
  30. 30.
  4    0.2490   5.3630  -2.4100   0.9870   0.   0.
  30. 30.
  4    0.2490   5.3630  -2.4100   0.9870   0.   0.
   1.1
  1  0. 0. 0.
 'DRIFT'                                                          7
  -1.898
 'TOSCA'                          3-D  MAP  THE  OF  FIRST        8
  0  0                                          BENDING  MAGNET
 1.0313E-3  1. 1. 1.              B, X, Y, Z normalization coefficients
 1D map at z=0, from TOSCA
 59  39  1
 bz6_0.map
 0  0. 0. 0.
 2
   1.1
 1 0 0 0
 'CHANGREF'                                                       9
 0.  -70.78  -43.8
'FAISCEAU'                                                       10
  'DRIFT'                                                         11
    -49.38
 'OCTUPOLE'                                                      12
 0
  10. 15.24  .6
  0. 0.
  4    0.2490   5.3630  -2.4100   0.9870   0.   0.
  0. 0.
  4    0.2490   5.3630  -2.4100   0.9870   0.   0.
  .4
  1  0. 0. 0.
 'SEXTUPOL'                         SX1, COMPENSATION             13
 0                                  OF  THE  Theta.Phi  ABERRATION
 10.  15.24  2.4                   AT  VF1
  0.  0. 0. 0.
  4    0.2490   5.3630  -2.4100   0.9870   0.   0.
  0. 0.  0. 0.
  4    0.2490   5.3630  -2.4100   0.9870   0.   0.
   .4
  1  0. 0. 0.
 'DRIFT'                                                         14
   50.0
  'WIENFILT'                        FIRST  VERTICAL  WIEN  FILTER   15
  0
 2.16  55.E5  -.0215576  2
 20. 10. 10.
 0.2401  1.8639  -0.5572  0.3904 0. 0.
 0.2401  1.8639  -0.5572  0.3904 0. 0.
 20. 10. 10.
 0.2401  1.8639  -0.5572  0.3904 0. 0.
 0.2401  1.8639  -0.5572  0.3904 0. 0.
 1.
1. 0. 0. 0.
 'DRIFT'                                                         16
   30.
 'QUADRUPO'                         Q3                           17
 0
   45.72  15.24  -6.34
  30. 30.
  4    0.2490   5.3630  -2.4100   0.9870   0.   0.
  30. 30.
  4    0.2490   5.3630  -2.4100   0.9870   0.   0.
   1.1
  1  0. 0. 0.
 'DRIFT'                                                         18
  10.0
 'MULTIPOL'                         SX2 + OCTU, COMPENSATION      19
 0                                  OF  THE  D.Phi  AND  D2.Phi
 10.  15.24   0. 0. -8.  1.2  0. 0. 0. 0. 0.    ABERRATIONS  AT  VF1
  0. 0. 0. 0. 0. 0. 0. 0. 0. 0. 0.
  4    0.2490   5.3630  -2.4100   0.9870   0.   0.
  0. 0. 0. 0. 0. 0. 0. 0. 0. 0. 0.
  4    0.2490   5.3630  -2.4100   0.9870   0.   0.
 0. 0. 0. 0. 0. 0. 0. 0. 0. 0.
   .4
  1  0. 0. 0.
 'DRIFT'                                                         20
   90.0
 'MATRIX'                           TRANSFER  COEFFICIENTS        21
 2 0
 'COLLIMA'                          FIRST  VERTICAL  FOCUS,       22
  2                                 MASS  SLIT
 2  14.6  .15E10  0. 0.
 'DRIFT'                                                         23
   20.0
 'QUADRUPO'                         Q5                           24
 0
  45.72  15.24   10.93
  30. 30.
  4    0.2490   5.3630  -2.4100   0.9870   0.   0.
  30. 30.
  4    0.2490   5.3630  -2.4100   0.9870   0.   0.
 1.1
  1  0. 0. 0.
 'DRIFT'                                                         25
   10.0
 'MULTIPOL'                         COMPENSATION  OF              26
 0                                  ABERRATIONS  AT  VF2
  10.  15.24  0. 0.  0.  1.  0. 0. 0. 0. 0. 0.
  0. 0.  0. 0. 0. 0. 0. 0. 0. 0. 0.
  4    0.2490   5.3630  -2.4100   0.9870   0.   0.
  0. 0.  0. 0. 0. 0. 0. 0. 0. 0. 0.
  4    0.2490   5.3630  -2.4100   0.9870   0.   0.
 0. 0. 0. 0. 0. 0. 0. 0. 0. 0.
  .4
  1  0. 0. 0.
 'DRIFT'                                                         27
   10.0
 'QUADRUPO'                         Q6                           28
 0
  45.72  15.24  -11.18
  30. 30.
  4    0.2490   5.3630  -2.4100   0.9870   0.   0.
  30. 30.
  4    0.2490   5.3630  -2.4100   0.9870   0.   0.
   1.1
  1  0. 0. 0.
 'DRIFT'                                                         29
   50.0
  'WIENFILT'                        SECOND  VERTICAL  WIEN  FILTER  30
  0
 2.16  -55.E5  .0215576  2
 20. 10. 10.
 0.2401  1.8639  -0.5572  0.3904 0. 0.
 0.2401  1.8639  -0.5572  0.3904 0. 0.
 20. 10. 10.
 0.2401  1.8639  -0.5572  0.3904 0. 0.
 0.2401  1.8639  -0.5572  0.3904 0. 0.
 1.
1. 0. 0. 0.
 'DRIFT'                                                         31
   30.0
 'QUADRUPO'                         Q7                           32
 0
  45.72  15.24  -6.44
  30. 30.
  4    0.2490   5.3630  -2.4100   0.9870   0.   0.
  30. 30.
  4    0.2490   5.3630  -2.4100   0.9870   0.   0.
  1.1
  1  0. 0. 0.
 'DRIFT'                                                         33
   25.00000
 'QUADRUPO'                         Q8                           34
 0
  45.72  15.24  8.085
  30. 30.
  4    0.2490   5.3630  -2.4100   0.9870   0.   0.
  30. 30.
  4    0.2490   5.3630  -2.4100   0.9870   0.   0.
   1.1
  1  0. 0. 0.
 'DRIFT'                                                         35
   40.0
 'COLLIMA'                          SECOND  VERTICAL  FOCUS,       36
  2                                 MASS  SLIT
 1  17.   .2E10   0. 0.
 'MATRIX'                           TRANSFER  COEFFICIENTS        37
 2 0
 'DRIFT'                                                         38
 -25.0
 'DIPOLE'                           SIMULATION  OF  THE  MAP       39
  2 0 0                             OF  THE  SECOND  BENDING  MAGNET
  150  60              (upgraded version of keyword 'AIMANT')
   18.999   0. 0. 0.
   79.3329   17.7656  140.4480   110.  170.
  15. -1.
  4  .1455   2.2670  -.6395  1.1558  0. 0.  0.
  0.00    21.90  1.E6 -1.E6  1.E6  1.E6
  15. -1.
  4  .1455   2.2670  -.6395  1.1558  0. 0.  0.
 -43.80  -21.90 -1.E6 -1.E6  1.E6 -1.E6
  0
  2
   2.5
  2
  147.48099   -0.31007  147.48099    0.31007
 'DRIFT'                                                         40
 -15.00000
 'QUADRUPO'                         Q9                           41
 0
  35.56  12.7  -13.69  -13.91
  30.  25.4
  4    0.2490   5.3630  -2.4100   0.9870   0.   0.
  30.  25.4
  4    0.2490   5.3630  -2.4100   0.9870   0.   0.
   .5
  1  0. 0. 0.
```

```
'DRIFT'                                                          42
  25.00000
'QUADRUPO'                          Q10                          43
0
  35.56  12.7  11.97
 30.  25.4
 4    0.2490   5.3630  -2.4100   0.9870   0.   0.
 30.  25.4
 4    0.2490   5.3630  -2.4100   0.9870   0.   0.
  1.1
 1  0. 0. 0.
'DRIFT'                                                          44
 200.0
'MATRIX'                            TRANSFER  COEFFICIENTS       45
2 0                                 AT  THE  FINAL  FOCUS
'END'                                                            46
```

Excerpt of zgoubi output : first and second order transfer matrices and higher order coefficients at the end of the line.

```
            FIRST  ORDER  COEFFICIENTS  ( MKSA ):

         3.60453       -4.453265E-02   -3.049728E-04   -1.165832E-04     0.00000       -5.229783E-02
        -2.05368        0.270335        4.700517E-05    1.763910E-05     0.00000       -9.561918E-02
        2.240965E-05   -8.687757E-07    -3.60817       -1.731805E-02     0.00000       -7.815367E-02
        1.185290E-05   -4.356398E-07    -2.05043       -0.286991         0.00000       -3.983392E-02
       -0.387557        2.313953E-02    -2.264218E-05   -8.015244E-06    1.00000        0.374917
        0.00000         0.00000          0.00000         0.00000         0.00000         1.00000

        DetY-1 =      -0.1170246601,    DetZ-1 =       0.0000034613

        R12=0 at   0.1647     m,        R34=0 at  -0.6034E-01 m

    First order sympletic conditions (expected values = 0) :
      -0.1170        3.4614E-06   -1.8207E-04    3.0973E-05    4.6007E-04   -8.0561E-05

            SECOND  ORDER  COEFFICIENTS  ( MKSA ):

1 11   7.34       1 21  -1.78       1 31  1.399E-02   1 41  1.456E-02   1 51   0.00       1 61   36.3
1 12  -1.78       1 22  -530.       1 32 -1.308E-03   1 42 -1.743E-03   1 52   0.00       1 62   12.3
1 13  1.399E-02   1 23 -1.308E-03   1 33 -0.611       1 43 -0.522       1 53   0.00       1 63 -2.771E-02
1 14  1.456E-02   1 24 -1.743E-03   1 34 -0.522       1 44  0.163       1 54   0.00       1 64 -2.211E-02
1 15   0.00       1 25   0.00       1 35   0.00       1 45   0.00       1 55   0.00       1 65   0.00
1 16   36.3       1 26   12.3       1 36 -2.771E-02   1 46 -2.211E-02   1 56   0.00       1 66   2.88


2 11  -303.       2 21   3.81       2 31  3.684E-02   2 41  3.581E-02   2 51   0.00       2 61   144.
2 12   3.81       2 22  -62.9       2 32 -5.821E-04   2 42 -1.638E-04   2 52   0.00       2 62 -0.759
2 13  3.684E-02   2 23 -5.821E-04   2 33   1.05       2 43   1.94       2 53   0.00       2 63 -1.031E-02
2 14  3.581E-02   2 24 -1.638E-04   2 34   1.94       2 44   6.70       2 54   0.00       2 64 -4.285E-02
2 15   0.00       2 25   0.00       2 35   0.00       2 45   0.00       2 55   0.00       2 65   0.00
2 16   144.       2 26 -0.759       2 36 -1.031E-02   2 46 -4.285E-02   2 56   0.00       2 66  -65.3


3 11 -0.145       3 21  2.158E-02   3 31   20.6       3 41   86.0       3 51   0.00       3 61 -0.201
3 12  2.158E-02   3 22   64.6       3 32   1.61       3 42  0.496       3 52   0.00       3 62  8.793E-02
3 13   20.6       3 23   1.61       3 33  0.710       3 43  0.128       3 53   0.00       3 63   39.1
3 14   86.0       3 24  0.496       3 34  0.128       3 44   64.8       3 54   0.00       3 64   7.17
3 15   0.00       3 25   0.00       3 35   0.00       3 45   0.00       3 55   0.00       3 65   0.00
3 16 -0.201       3 26  8.793E-02   3 36   39.1       3 46   7.17       3 56   0.00       3 66   1.46


4 11 -8.254E-02   4 21  1.146E-02   4 31   10.7       4 41   47.3       4 51   0.00       4 61 -0.127
4 12  1.146E-02   4 22   33.0       4 32  0.787       4 42  0.157       4 52   0.00       4 62  3.566E-02
4 13   10.7       4 23  0.787       4 33  0.365       4 43  6.774E-02   4 53   0.00       4 63   17.5
4 14   47.3       4 24  0.157       4 34  6.774E-02   4 44   33.1       4 54   0.00       4 64   1.05
4 15   0.00       4 25   0.00       4 35   0.00       4 45   0.00       4 55   0.00       4 65   0.00
4 16 -0.127       4 26  3.566E-02   4 36   17.5       4 46   1.05       4 56   0.00       4 66  0.715


5 11   568.       5 21  -7.67       5 31 -5.970E-02   5 41 -5.682E-02   5 51   0.00       5 61  -251.
5 12  -7.67       5 22   225.       5 32  1.283E-03   5 42  6.947E-04   5 52   0.00       5 62   2.77
5 13 -5.970E-02   5 23  1.283E-03   5 33   19.2       5 43   10.2       5 53   0.00       5 63  0.215
5 14 -5.682E-02   5 24  6.947E-04   5 34   10.2       5 44   1.59       5 54   0.00       5 64  0.129
5 15   0.00       5 25   0.00       5 35   0.00       5 45   0.00       5 55   0.00       5 65   0.00
5 16  -251.       5 26   2.77       5 36  0.215       5 46  0.129       5 56   0.00       5 66   112.

            HIGHER  ORDER  COEFFICIENTS  ( MKSA ):

         Y/Y3            5784.8
         Y/T3           9.40037E+05
         Y/Z3           0.70673
         Y/P3           0.42104

         T/Y3           -18607.
         T/T3           1.04607E+05
         T/Z3          -0.10234
         T/P3           5.25793E-02

         Z/Y3            32.161
         Z/T3            18.425
         Z/Z3           -872.50
         Z/P3           -785.20

         P/Y3            15.460
         P/T3            7.5264
         P/Z3           -409.98
         P/P3           -389.15
```

3 IN-FLIGHT DECAY IN SPES 3

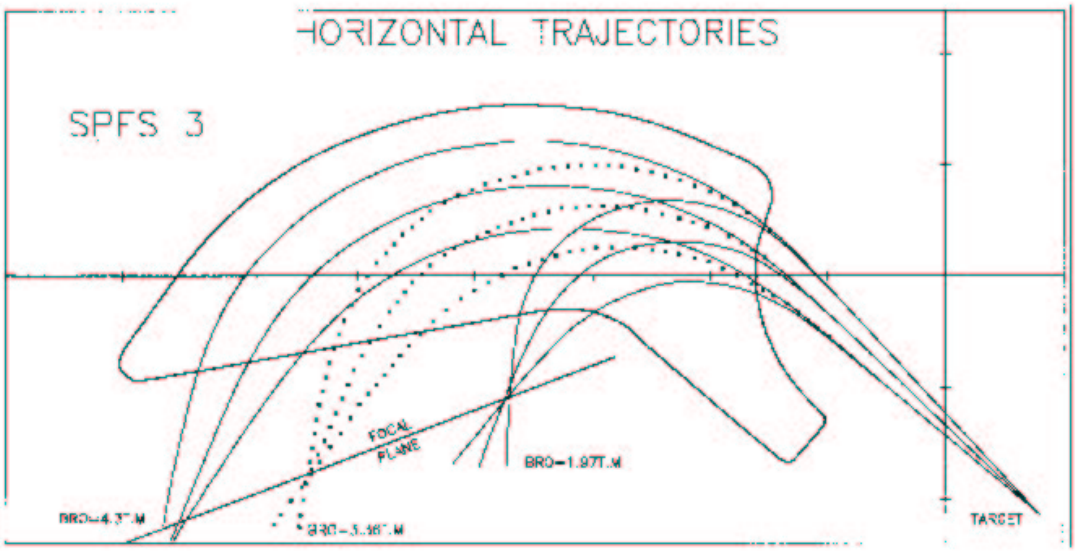

Figure 42: Design of SPES 3.

zgoubi data file

```
SIMULATION  OF  PION  IN-FLIGHT  DECAY  IN  SPES3
'MCOBJET'                                                          1
3360.                              REFERENCE  RIGIDITY (PION).
1                                  DISTRIBUTION  IN  WINDOW.
200                                BUNCHES  OF  200  PARTICLES.
1     1       1     1      1    1   UNIFORM DISTRIBUTION
0.    0.      0.    0.     0.   1.  CENTRAL  VALUES  OF  BARS.
.5e-2 50.e-3 .5e-2  50.e-3 0.  0.4  WIDTH  OF  BARS.
1     1       1     1      1    1   CUT-OFFS (UNUSED)
9   9. 9. 9. 9.                    UNUSED.
186387 548728 472874               SEEDS.
'PARTICUL'                                                         2
139.6000 0. 0. 26.03E-9 0.         PION MASS AND LIFE TIME
'MCDESINT'                                                         3
105.66   0.                        PION -> MUON + NEUTRINODECAY
136928 768370 548375
'ESL'                                                              4
77.3627
'CHAMBR'                           STOPS  ABERRANT  MUONS.         5
1
1   100. 10. 245.  0.
'DIPOLE'                                                           6
2 0 0
180  130
30     0. 0. 0.
80.   33.     208.5  140.  350.
46. -1.
4. .14552 5.21405 -3.38307 14.0629 0. 0. 0.
 15.   0.      -65.  0.    0.  -65.
46. -1.
4. .14552 5.21405 -3.38307 14.0629 0. 0. 0.
-15.  69.       85.  0.    1.E6  1.E6
0
2
4.
2
164.755 .479966 233.554 -.057963
'CHAMBR'                                                           7
2
1   100. 10. 245.  0.
'CHANGREF'                         TILT  ANGLE  OF                 8
0.   0.   -49.                     FOCAL  PLANE.
'HISTO'                            TOTAL  SPECTRUM (PION + MUON).  9
2  -170.  130.  60  1
20  'Y'  1  'Q'
'HISTO'                            PION  SPATIAL  SPECTRUM        10
2  -170.  130.  60  2              AT  FOCAL  PLANE.
20  'P'  1  'P'
'HISTO'                            MUON  SPATIAL  SPECTRUM        11
2  -170.  130.  60  3              AT  FOCAL  PLANE.
20  'y'  1  'S'
'HISTO'                            MUON  MOMENTUM  SPECTRUM       12
1    .2   1.7   60  3             AT  FOCAL  PLANE.
20  'd'  1  'S'
'REBELOTE'                         (49+1)  RUNS =  CALCULATION  OF 13
49  0.1  0                        (49+1)*200  TRAJECTORIES.
'END'                                                              14
```

Excerpt of zgoubi output : histograms of primary and secondary particles at focal surface of SPES3.

```
 9  HISTO     TOTAL     SPECTRUM

                       HISTOGRAMME  DE  LA  COORDONNEE  Y
                       PARTICULES  PRIMAIRES  ET  SECONDAIRES
                       DANS  LA  FENETRE :  -1.7000E+02 /   1.3000E+02 (CH)
                       NORMALISE

  20                                                                                
  19                                                                                
  18                                                                                
  17                                      Y     YY        Y  Y      Y              
  16                                     Y YYYYY YY YYY  Y YY Y Y  YYYY            
  15                                     Y YYYYY YYYYYYYYYYYYY YYYYYYYY YY         
  14                                    YYYYYYYYY YYYYYYYYYYYYYYYYYYYYYYYYY        
  13                                    YYYYYYYYY YYYYYYYYYYYYYYYYYYYYYYYYY        
  12                                    YYYYYYYYYYYYYYYYYYYYYYYYYYYYYYYYYYY        
  11                                    YYYYYYYYYYYYYYYYYYYYYYYYYYYYYYYYYYY        
  10                                    000000000000000000000000000000000000      
   9                                    YYYYYYYYYYYYYYYYYYYYYYYYYYYYYYYYYYY        
   8                                    YYYYYYYYYYYYYYYYYYYYYYYYYYYYYYYYYYY        
   7                                    YYYYYYYYYYYYYYYYYYYYYYYYYYYYYYYYYYY        
   6                                    YYYYYYYYYYYYYYYYYYYYYYYYYYYYYYYYYYY        
   5                                    YYYYYYYYYYYYYYYYYYYYYYYYYYYYYYYYYYY        
   4                                    YYYYYYYYYYYYYYYYYYYYYYYYYYYYYYYYYYY        
   3                                    YYYYYYYYYYYYYYYYYYYYYYYYYYYYYYYYYYY        
   2                                   YYYYYYYYYYYYYYYYYYYYYYYYYYYYYYYYYYYY       
   1                                   YYYYYYYYYYYYYYYYYYYYYYYYYYYYYYYYYYYY       

                       123456789012345678901234567890123456789012345678901234567890
                                3         4         5         6         7         8


            TOTAL  COMPTAGE                :    9887  SUR  10000
            NUMERO   DU  CANAL  MOYEN      :      55
            COMPTAGE  AU   "      "        :     281
            VAL. PHYS. AU  "      "        :  0.000E+00 (CH)
            RESOLUTION  PAR  CANAL         :  5.000E+00 (CH)

            PARAMETRES  PHYSIQUES  DE  LA  DISTRIBUTION :
                        COMPTAGE =   9887  PARTICULES
                        MIN = -1.6687E+02, MAX = 9.4131E+01, MAX-MIN = 2.6100E+02(CH)
                        MOYENNE = -9.2496E-01 (CH)
                        SIGMA =  5.3583E+01 (CH)
```

```
 11  HISTO     MUON      SPATIAL

                       HISTOGRAMME  DE  LA  COORDONNEE  Y
                       PARTICULES  SECONDAIRES
                       DANS  LA  FENETRE :  -1.7000E+02 /   1.3000E+02 (CH)
                       NORMALISE

  20                                                                                
  19                                                                                
  18                                                 y                              
  17                                                 y        yy                    
  16                                                 y        yy                    
  15                                             y   y y     yyy   y                
  14                                             y   y y  y  yyyy  y                
  13                                             y   yyy  yy yyyy  y                
  12                                            yy y yyy yyy yyyyy y    y          
  11                                           yyy y yyy yyy yyyyy y    y   y      
  10                                           000 0 000 000000000000   0   00     
   9                                           yyyyy yyy yyyyyyyyyyyy y y   yy     
   8                                           yyyyyyyyyy yyyyyyyyyyyyyy y   yy    
   7                                         yyyyyyyyyyyyyyyyyyyyyyyyyy y  yyy     
   6                                         yyyyyyyyyyyyyyyyyyyyyyyyyy y yyyy     
   5                                      y  yyyyyyyyyyyyyyyyyyyyyyyyyyyyyyyyyyy yyy
   4                                      y  yyyyyyyyyyyyyyyyyyyyyyyyyyyyyyyyyyyyyy
   3                                      y  yyyyyyyyyyyyyyyyyyyyyyyyyyyyyyyyyyyyyy
   2                                   yy   yy  yyyyyyyyyyyyyyyyyyyyyyyyyyyyyyyyyyyyy
   1                                   yy  yyyyyyyyyyyyyyyyyyyyyyyyyyyyyyyyyyyyyyyyyy

                       123456789012345678901234567890123456789012345678901234567890
                                3         4         5         6         7         8


            TOTAL  COMPTAGE                :     605  SUR  10000
            NUMERO   DU  CANAL  MOYEN      :      50
            COMPTAGE  AU   "      "        :      14
            VAL. PHYS. AU  "      "        : -2.500E+01 (CH)
            RESOLUTION  PAR  CANAL         :  5.000E+00 (CH)

            PARAMETRES  PHYSIQUES  DE  LA  DISTRIBUTION :
                        COMPTAGE =    605  PARTICULES
                        MIN= -1.6687E+02, MAX = 9.4131E+01, MAX-MIN = 2.6100E+02 (CH)
                        MOYENNE = -2.2782E+01 (CH)
                        SIGMA =  5.4452E+01 (CH)
```

```
 10  HISTO     PION      SPATIAL

                       HISTOGRAMME  DE  LA  COORDONNEE  Y
                       PARTICULES  PRIMAIRES
                       DANS  LA  FENETRE :  -1.7000E+02 /   1.3000E+02 (CH)
                       NORMALISE

  20                                                                                
  19                                                                                
  18                                                P                               
  17                                           P     PP        P  P      P          
  16                                           PP    PP PPP  P PP P P  PPPPP       
  15                                          P PPPPP PPPPPPPPPPPPPPPPPPPPP PP      
  14                                       PPPPPPPPP PPPPPPPPPPPPPPPPPPPPPPPPPP     
  13                                       PPPPPPPPPPPPPPPPPPPPPPPPPPPPPPPPPPP     
  12                                       PPPPPPPPPPPPPPPPPPPPPPPPPPPPPPPPPPP     
  11                                       PPPPPPPPPPPPPPPPPPPPPPPPPPPPPPPPPPP     
  10                                       000000000000000000000000000000000000    
   9                                       PPPPPPPPPPPPPPPPPPPPPPPPPPPPPPPPPPP     
   8                                       PPPPPPPPPPPPPPPPPPPPPPPPPPPPPPPPPPP     
   7                                       PPPPPPPPPPPPPPPPPPPPPPPPPPPPPPPPPPP     
   6                                       PPPPPPPPPPPPPPPPPPPPPPPPPPPPPPPPPPP     
   5                                       PPPPPPPPPPPPPPPPPPPPPPPPPPPPPPPPPPP     
   4                                       PPPPPPPPPPPPPPPPPPPPPPPPPPPPPPPPPPP     
   3                                       PPPPPPPPPPPPPPPPPPPPPPPPPPPPPPPPPPP     
   2                                      PPPPPPPPPPPPPPPPPPPPPPPPPPPPPPPPPPPP    
   1                                      PPPPPPPPPPPPPPPPPPPPPPPPPPPPPPPPPPPPP   

                       123456789012345678901234567890123456789012345678901234567890
                                3         4         5         6         7         8


            TOTAL  COMPTAGE                :    9282  SUR  10000
            NUMERO   DU  CANAL  MOYEN      :      55
            COMPTAGE  AU   "      "        :     264
            VAL. PHYS. AU  "      "        :  0.000E+00 (CH)
            RESOLUTION  PAR  CANAL         :  5.000E+00 (CH)

            PARAMETRES  PHYSIQUES  DE  LA  DISTRIBUTION :
                        COMPTAGE =   9282  PARTICULES
                        MIN= -9.5838E+01, MAX = 9.3504E+01, MAX-MIN = 1.8934E+02 (CH)
                        MOYENNE =  4.9971E-01 (CH)
                        SIGMA =  5.3215E+01 (CH)
```

```
 12  HISTO     MUON      HORENTUM

                       HISTOGRAMME  DE  LA  COORDONNEE    D
                       PARTICULES  SECONDAIRES
                       DANS  LA  FENETRE :   2.0000E-01 /   1.7000E+00
                       NORMALISE

  20                                                                                
  19                                                                                
  18                                                   d   d                        
  17                                                   d   d                        
  16                                                   d   dd                       
  15                                                  dd   dd                       
  14                                                 ddd d dd                       
  13                                                 ddd d dd     dd                
  12                                                 ddd d dd     dd                
  11                                                 ddd d ddd d  dd                
  10                                                 0000 0 000 0  00               
   9                                                ddddd ddddd dd dd               
   8                                               ddddddddddddddd ddddd            
   7                                               ddddddddddddddddddddddd          
   6                                              ddddddddddddddddddddddddd ddd     
   5                                             ddddddddddddddddddddddddddddddddd  
   4                                           ddddddddddddddddddddddddddddddddddd  
   3                                           ddddddddddddddddddddddddddddddddddd  d
   2                                         ddddddddddddddddddddddddddddddddddddddd 
   1                                         ddddddddddddddddddddddddddddddddddddddd 

                       123456789012345678901234567890123456789012345678901234567890
                                3         4         5         6         7         8


            TOTAL  COMPTAGE                :     605  SUR  10000
            NUMERO   DU  CANAL  MOYEN      :      46
            COMPTAGE  AU   "      "        :      16
            VAL. PHYS. AU  "      "        :  8.250E-01
            RESOLUTION  PAR  CANAL         :  2.500E-02

            PARAMETRES  PHYSIQUES  DE  LA  DISTRIBUTION :
                        COMPTAGE =    605  PARTICULES
                        MIN =  3.7184E-01, MAX =  1.3837E+00, MAX-MIN =  1.0119E+00
                        MOYENNE =  8.1693E-01
                        SIGMA =  2.2849E-01
```

4 USE OF THE FITTING PROCEDURE

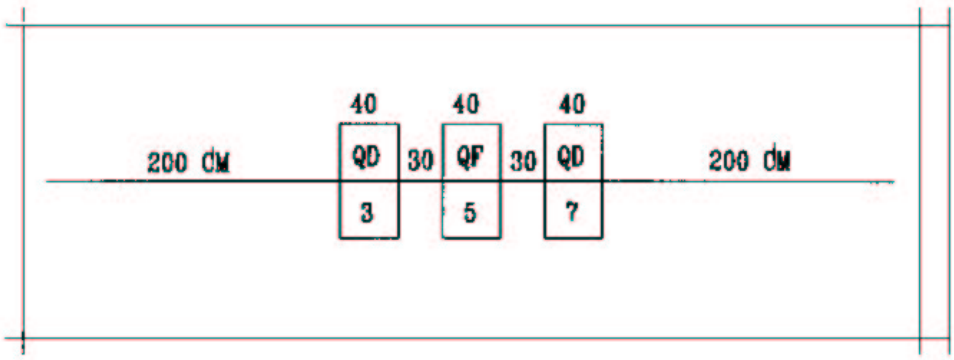

Figure 43: Vary B in all quadrupoles, for fitting of the transfer coefficients R_{12} and R_{34} at the end of the line. The first and last quadrupoles are coupled so as to present the same value of B.

zgoubi data file.

```
HATCHING A SYMMETRIC QUADRUPOLE TRIPLET
'OBJET'                                                              1
2501.73                        750MeV/c PROTONS
5                              11 PARTICLES FOR USE OF MATRIX
2.  2.  2.   2.  0. .001
0.  0.  0.   0.  0.  1.
'ESL   '                                                            2
200.
'QUADRUPO'    3                                                     3
 0
40.  15.  -7.
0.  0.
6  .1122 6.2671 -1.4982 3.5882 -2.1209 1.723
0.   0.
6  .1122 6.2671 -1.4982 3.5882 -2.1209 1.723
5.
1 0. 0. 0.
'ESL'                                                               4
30.
'QUADRUPO'     5                                                    5
 0
40.  15.  3.
0.  0.
6  .1122 6.2671 -1.4982 3.5882 -2.1209 1.723
0.   0.
6  .1122 6.2671 -1.4982 3.5882 -2.1209 1.723
5.
1 0. 0. 0.
'ESL'                                                               6
30.
'QUADRUPO'      7                                                   7
 0
40.  15.  -7.
0.  0.
6  .1122 6.2671 -1.4982 3.5882 -2.1209 1.723
0.   0.
6  .1122 6.2671 -1.4982 3.5882 -2.1209 1.723
5.
1 0. 0. 0.
'ESL'                                                               8
200.
'MATRIX'                                                            9
1  0
'FIT'              VARY B IN QUADS FOR FIT OF R12 AND R34           10
2                  FIRST ORDER TRANSFER COEFFICIENTS
3  12 7.12  2.     SYMMETRIC TRIPLET => QUADS #1 AND #3 ARE COUPLED
5  12  0.   2.     PARAMETER #12 OF ELEMENTS #3, 5 AND 7 IS FIELD VALUE
2
1  1 2 8 16.6 1.   FIRST CONSTRAINT: R12=16.6, AFTER ELEMENT #8 (LAST DRIF
1  3 4 8 -.88 1.   SECOND CONSTRAINT: R34=-.88
'END'                                                               11
```

Excerpt of zgoubi output : first order transfer matrices prior to and after fitting.

```
*******************************************************************************************
 TRANSFER MATRIX WITH STARTING  CONDITIONS :


                  MATRICE  DE  TRANSFERT  ORDRE  1  ( MKSA )

         5.43642  17.02625   0.00000   0.00000   0.00000   0.00000
         1.67617   5.43442   0.00000   0.00000   0.00000   0.00000
         0.00000   0.00000  -1.27013  -0.97430   0.00000   0.00000
         0.00000   0.00000  -0.62915  -1.27004   0.00000   0.00000
         0.00000   0.00000   0.00000   0.00000   1.00000   0.00000
         0.00000   0.00000   0.00000   0.00000   0.00000   1.00000


*******************************************************************************************

STATE OF VARIABLES  AFTER  MATCHING :


          VARIABLE  ELEMENT    3,  PRMTR #12 :
              COUPLED  WITH  ELEMENT    7,  PRMTR #12

 STATUS OF VARIABLES
 LMNT  VAR  PARAM  MINIMUM      INITIAL        FINAL         MAXIMUM      STEP
   3    1    12  -8.384E+00  -6.986E+00  -6.98648097E+00 -5.590E+00  2.424E-16
   5    2    12   2.585E+00   3.230E+00   3.22956371E+00  3.877E+00  1.208E-16
 STATUS OF CONSTRAINTS
 TYPE  I   J  LMNT#       DESIRED          WEIGHT         REACHED         KI2
   1   1   2     8      1.6600E+01     1.0000E+00    1.6600000E+01   8.2185E-02
   1   3   4     8     -8.8000E-01     1.0000E+00   -8.8000000E-01   9.1781E-01

*******************************************************************************************

FINAL RUN, WITH NEW VARIABLES :

      9  MATRIX    9

           Frame for MATRIX calculation moved by :
            XC =    0.000 CM , YC =    0.000  CM ,   A =  0.00000 DEG  ( = 0.000000 RD )
            Path length of particle #1 :    580.0000 m



                  MATRICE  DE  TRANSFERT  ORDRE  1  ( MKSA )

         5.272531  16.600000   0.000000   0.000000   0.000000   0.000000
         1.614433   5.272531   0.000000   0.000000   0.000000   0.000000
         0.000000   0.000000  -1.244124  -0.880000   0.000000   0.000000
         0.000000   0.000000  -0.622552  -1.244124   0.000000   0.000000
         0.000000   0.000000   0.000000   0.000000   1.000000   0.000000
         0.000000   0.000000   0.000000   0.000000   0.000000   1.000000

      Determinants  :        DetY-1 = -.0000011112
                             DetZ-1 = -.0000000156

       R12=0  at       -3.1484  meters
       R34=0  at       -0.7073  meters

      First order sympletic conditions (expected values = 0) :
        -1.1112E-06   -1.5616E-08    0.0000E+00    0.0000E+00    0.0000E+00    0.0000E+00
*******************************************************************************************
```

5 MULTITURN SPIN TRACKING IN SATURNE 3 GeV SYNCHROTRON

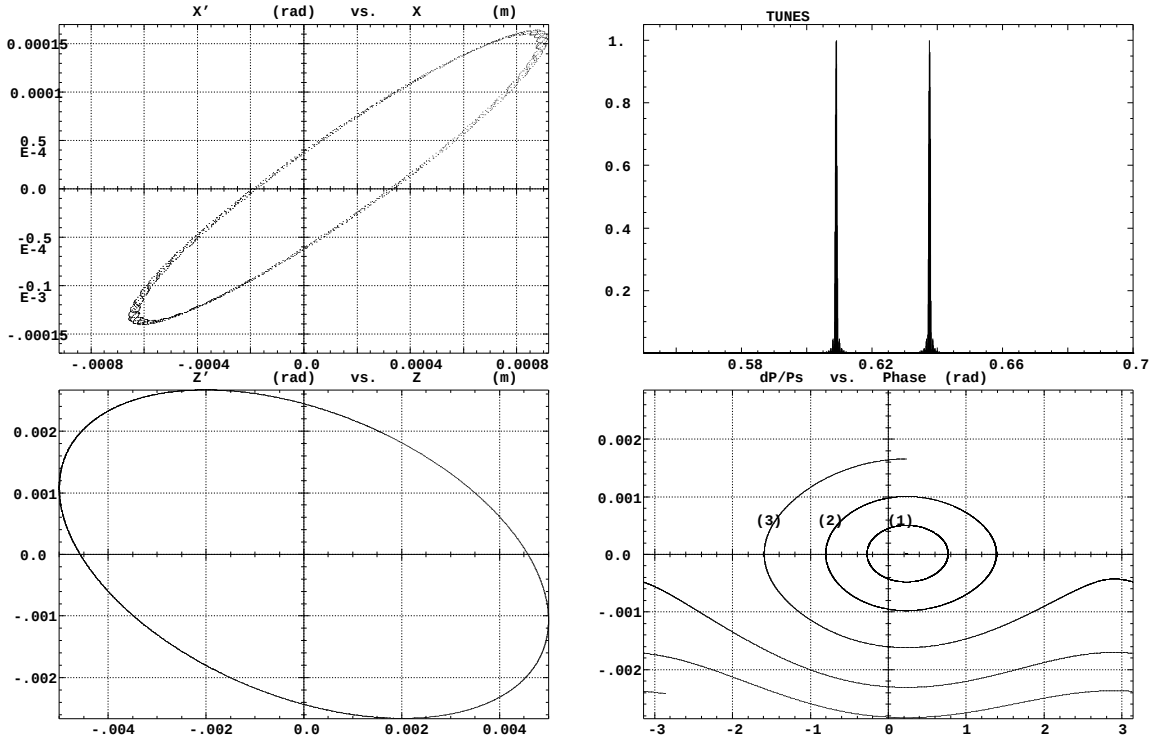

Figure 44: Tracking over 3000 turns. These simulations exhibit the first order parameters and motions as produced by the multiturn ray-tracing.
(A) Horizontal phase-space: the particle has been launched near to the closed orbit (the fine structure is due to $Y - Z$ coupling induced by bends fringe fields, also responsible of the off-centering of the local closed orbit - at ellipse center).
(B) Vertical phase-space: the particle has been launched with $Z_0 = 4.58\ 10^{-3}$ m, $Z_0' = 0$. A least-square fit by $\gamma_Z Z^2 + 2\alpha_Z Z Z' + \beta_Z Z'^2 = \varepsilon_Z/\pi$ yields $\beta_Z = 2.055$ m, $\alpha_Z = 0.444$, $\gamma_Z = 0.582$ m^{-1}, $\varepsilon_Z/\pi = 12\ 10^{-6}$ m.rad in agreement with matrix calculations.
(C) Fractional tune numbers obtained by Fourier analysis for $\varepsilon_Y/\pi = \varepsilon_Z/\pi \simeq 12\ 10^{-6}$ m.rad: $\nu_Y = 0.63795$, $\nu_Z = 0.60912$ (the integer part is 3 for both).
(D) Longitudinal phase-space (DP, phase): articles with initial momentum dispersion of $5\ 10^{-4}$ (1), 10^{-3} (2), $1.65\ 10^{-3}$ (3) (out of acceptance), are accelerated at 1405 eV/turn ($\dot{B} = 2.1$ T/s); analytical calculations give accordingly momentum acceptance of $1.65\ 10^{-3}$.

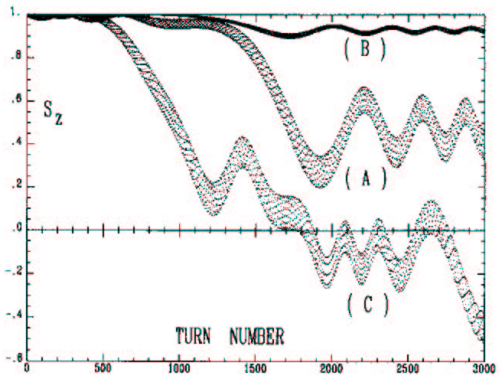

Figure 45: Crossing of $\gamma G = 7 - \nu_Z$, at $\dot{B} = 2.1$ T/s.
(A) $\varepsilon_Z/\pi = 12.2\ 10^{-6}$ m.rad. The strength of the resonance is $\mid \varepsilon \mid = 3.3\ 10^{-4}$. As expected from the Froissart-Stora formula the asymptotic polarization is about 0.44.
(B) The emittance is now $\varepsilon_Z/\pi = 1.2\ 10^{-6}$ m.rad; comparison with (A) shows that $\mid \varepsilon \mid$ is proportional to $\sqrt{\varepsilon_Z}$.
(C) Crossing of this resonance for a particle having a momentum dispersion of 10^{-3}.

zgoubi data file (begining and end).

```
 SATURNE. CROSSING GammaG=7-Nuz, Nuz=3.60877(perturbed)
 'OBJET'
 5015.388                                          834.04 MeV, proton
 2
  4  1
6.2E-02     6.5E-02    .458  0.  0.  1.00    'o'   EpsilonY/pi = 0. (Closed orbit)
0.356       0.379      .458  0.  0.  1.0005  '1'
0.647       0.689      .458  0.  0.  1.001   '2'
1.024       1.09       .458  0.  0.  1.0016  '3'
1 1 1 1
'SCALING'
1  4
  MULTIPOL
  2                                  CROSSING GammaG=7-Nuz+/-14E, E=3.3E-4
  5015.388E-3  5034.391E-3           AT 2.1 T/s, IN 3442 MACHINE TURNS,
  1            3442                  FROM 834.041 TO  838.877 MeV
  QUADRUPO
  2
  5015.388E-3  5034.391E-3
  1            3442
  BEND
  2
  5015.388E-3  5034.391E-3
  1            3442
  CAVITE
  2
  1.           1.00378894            RELATIVE CHANGE OF SYNCHRONOUS RIGIDITY
  1            3442
'PARTICUL'
 938.2723  1.6021892E-19  1.7928474 0. 0.
'SPNTRK'
3
'QUADRUPO'                 QP  1                                          5
  0
 46.723  10.  .763695                             .763695  = FIELD FOR BORO=1 T.m
 0.  0.
 6  .1122 6.2671 -1.4982 3.5882 -2.1209 1.723
 0.  0.
 6  .1122 6.2671 -1.4982 3.5882 -2.1209 1.723
 #30|50|30 Quad
 1 0. 0. 0.
 'ESL'                     SD  2                                           6
 71.6256
  'BEND'                   DIP 3 4 3                                       7
   0
  247.30039  0.  1.57776
    20. 8. .04276056667
  4 .2401  1.8639  -.5572  .3904 0. 0. 0.
    20. 8. .04276056667         20.  8.
  4 .2401  1.8639  -.5572  .3904 0. 0. 0.
  #30|120|30   bend    3 0. 0. 0. -.1963495408
 'ESL'                     SD  2                                           8
 71.6256
 'MULTIPOL'                QP  5                                           9
  0
 48.6273  10. 0. -.77319 0. 0. .0 .0   0. 0. 0. 0.      -.77319=-.765533+QUAD DEFECT
 0.  0. 0. 0. 0. .0 .0  0. 0. 0. 0.                     FOR EXCITING THE DEPOLARIZING
 6  .1122 6.2671 -1.4982 3.5882 -2.1209 1.723          RESONNANCE.
 0.  0. 0. 0. 0.  0. 0.   0. 0. 0. 0.
 6  .1122 6.2671 -1.4982 3.5882 -2.1209 1.723
 0. 0. 0. 0. 0. 0.   0. 0. 0. 0.
 #30|50|30 Quad
 1 0. 0. 0.
'ESL'                     SD  2                                          10
 71.6256
  'BEND'                   DIP 3 4 3                                      11
   0
  247.30039  0.  1.57776
    20. 8. .04276056667
  4 .2401  1.8639  -.5572  .3904 0. 0. 0.
    20. 8. .04276056667         20.  8.
  4 .2401  1.8639  -.5572  .3904 0. 0. 0.
  #30|120|30   bend    3 0. 0. 0. -.1963495408
 'ESL'                     SD  2                                          12
 71.6256
 'QUADRUPO'                QP  1                                          13
  0
 46.723  10.  .763695
 0.  0.
 6  .1122 6.2671 -1.4982 3.5882 -2.1209 1.723
 0.  0.
 6  .1122 6.2671 -1.4982 3.5882 -2.1209 1.723
 #30|50|30 Quad
 1 0. 0. 0.
 'ESL'                     SD  2                                          14
 71.6256
  'BEND'                   DIP 3 4 3                                      15
   0
  247.30039  0.  1.57776
    20. 8. .04276056667
  4 .2401  1.8639  -.5572  .3904 0. 0. 0.
    20. 8. .04276056667         20.  8.
  4 .2401  1.8639  -.5572  .3904 0. 0. 0.
  #30|120|30   bend    3 0. 0. 0. -.1963495408
 'ESL'                     SD  2                                          16
 71.6256
 'MULTIPOL'                QP  5                                          17
  0
 48.6273  10.  0.  -.765533 0. 0. 0. 0.   0. 0. 0. 0.
 0.  0. 0. 0. 0.  0. 0.    0. 0. 0. 0.
 6  .1122 6.2671 -1.4982 3.5882 -2.1209 1.723
 0.  0. 0. 0. 0.  0. 0.    0. 0. 0. 0.
 6  .1122 6.2671 -1.4982 3.5882 -2.1209 1.723
 0. 0. 0. 0. 0. 0.   0. 0. 0. 0.
 #30|50|30 Quad
 1 0. 0. 0.
 'ESL'                     SD  2                                          18
 71.6256
  'BEND'                   DIP 3 4 3                                      19
   0
  247.30039  0.  1.57776
    20. 8. .04276056667
  4 .2401  1.8639  -.5572  .3904 0. 0. 0.
    20. 8. .04276056667         20.  8.
  4 .2401  1.8639  -.5572  .3904 0. 0. 0.
  #30|120|30   bend    3 0. 0. 0. -.1963495408
 'ESL'                     SD  2                                          20
 71.6256
 'QUADRUPO'                QP  1                                          21
  0
 46.723  10.  .763695
 0.  0.
 6  .1122 6.2671 -1.4982 3.5882 -2.1209 1.723
 0.  0.
 6  .1122 6.2671 -1.4982 3.5882 -2.1209 1.723
 #30|50|30 Quad
 1 0. 0. 0.
'ESL'                                                                      22
392.148
 'MULTIPOL'                QP  5                                          23
  0
 48.6273  10.  0.  -.765533 0. 0. 0. 0.   0. 0. 0. 0.
 0.  0. 0. 0. 0.  0. 0.    0. 0. 0. 0.
 6  .1122 6.2671 -1.4982 3.5882 -2.1209 1.723
 0.  0. 0. 0. 0.  0. 0.    0. 0. 0. 0.
 6  .1122 6.2671 -1.4982 3.5882 -2.1209 1.723
 0. 0. 0. 0. 0. 0.    0. 0. 0. 0.
 #30|50|30 Quad
 1 0. 0. 0.
'ESL'                                                                      24
392.148
 'QUADRUPO'                QP  1                                          25
  0
 46.723  10.  .763695
 0.  0.
 6  .1122 6.2671 -1.4982 3.5882 -2.1209 1.723
 0.  0.
 6  .1122 6.2671 -1.4982 3.5882 -2.1209 1.723
 #30|50|30 Quad
 1 0. 0. 0.
 'ESL'                     SD  2                                          26
 71.6256
  'BEND'                   DIP 3 4 3                                      27
   0
  247.30039  0.  1.57776
    20. 8. .04276056667
  4 .2401  1.8639  -.5572  .3904 0. 0. 0.
    20. 8. .04276056667         20.  8.
  4 .2401  1.8639  -.5572  .3904 0. 0. 0.
  #30|120|30   bend    3 0. 0. 0. -.1963495408
 'ESL'                     SD  2                                          28
 71.6256
 'MULTIPOL'                QP  5                                          29
  0
 48.6273  10.  0. -.765533  0. 0. 0. 0.   0. 0. 0. 0.
 0.  0. 0. 0. 0.  0. 0.    0. 0. 0. 0.
 6  .1122 6.2671 -1.4982 3.5882 -2.1209 1.723
 0.  0. 0. 0. 0.  0. 0.    0. 0. 0. 0.
 6  .1122 6.2671 -1.4982 3.5882 -2.1209 1.723
 0. 0. 0. 0. 0. 0.    0. 0. 0. 0.
 #30|50|30 Quad
 1 0. 0. 0.
'ESL'                     SD  2                                          30
 71.6256
  'BEND'                   DIP 3 4 3                                      31
   0
  247.30039  0.  1.57776
    20. 8. .04276056667
  4 .2401  1.8639  -.5572  .3904 0. 0. 0.
    20. 8. .04276056667         20.  8.
  4 .2401  1.8639  -.5572  .3904 0. 0. 0.
  #30|120|30   bend    3 0. 0. 0. -.1963495408

;;;;;;;;;;;;;;;;;;;;;;;;;;;;;;;;;;;;;;;;;;;;;;;;;;;;;;;;;;;;;;;;;;;;;;;;;;;;;;;;

 'ESL'                                                                      84
 392.148
 'CAVITE'                                                                   85
  1
 105.5556848673   3.
 6000.      0.                  SIN(phis) = .234162, dE=1.40497 keV/Turn.
'FAISCNL'                                                                   86
b_zgoubi.fai
 'SPNPRNL'                                                                  87
 zgoubi.spn
 'SPNPRT'                                                                   88
 'REBELOTE'                                                                 90
 2999  0.1 99                    TOTAL NUMBER OF TURNS = 3000
'END'                                                                       91
```

6 MICRO-BEAM FOCUSING WITH ELECTROMAGNETIC QUADRUPOLES

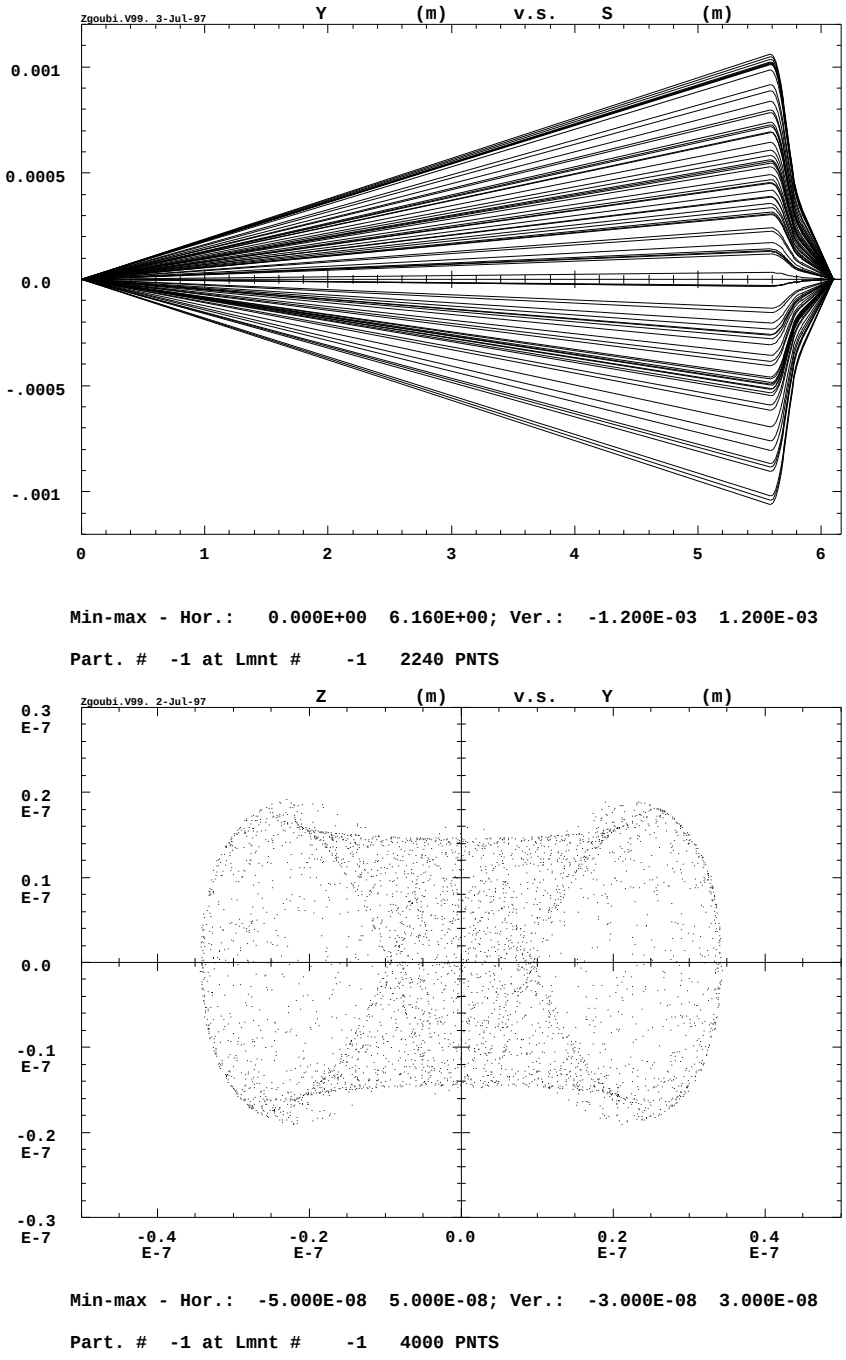

Figure 46: *Upper plot*: 50-particle beam tube ray-traced through a double focusing quadrupole doublet typical of the front end design of micro-beam lines. Initial conditions are : $Y_0 = Z_0 = 0$, angles T_0 and P_0 random uniform within ± 0.2 mrad, and momentum dispersion $\delta p/p$ uniform in $\pm 3\,10^{-4}$.
Lower plot: **(D)** sub-micronic cross-section at the image plane of a 4000-particle beam with initial conditions as above, obtained thanks to the second-order achromatic electro-magnetic quadrupole doublet (the inage size would be $\Delta Y \approx \Delta Z \approx \pm 50 \mu m$ with regular magnetic quadrupoles, due to the momentum dispersion). Note the high resolution of the ray-tracing which still reveals image structure of nanometric size.

zgoubi data file.

```
MICROBEAM LINE, WITH AN ELECTROMAGNETIC QUADRUPOLE DOUBLET.
'MCOBJET'                                RANDOM  OBJECT  DEFINITION   1
20.435                                     RIGIDITY (20keV  PROTONS).
1                                          DISTRIBUTION IN WINDOW.
200                                        NUMBER  OF  PARTICLES.
1    1     1    1     1    1              UNIFORM DISTRIBUTION.
0.   0.    0.   0.    0.   1.             CENTRAL  VALUE,  AND
0.  .2e-3  0.  .2e-3  0.   0.0003         HALF WIDTH OF DISTRIBUTION.
10.  10.   10.  10.   10.  10.            CUT-OFFS (UNUSED).
9   9. 9. 9. 9.                            FOR P(D) - UNUSED.
186387 548728 472874                       SEEDS.
 'PARTICUL'                              PARTICLE MASS AND CHARGE   2
  938.2723 1.60217733E-19 0. 0. 0.         FOR INTEGRATION IN E-FIELD.
'DRIFT'                                  DRIFT.                     3
500.
'DRIFT'                                  DRIFT.                     4
59.
'EBMULT'                                 FIRST ELECTROMAGNETIC     5
 0                                                          QUADRUPOLE.
10.2  10. 0. -9272.986  0. 0. 0. 0. 0. 0. 0.     ELECTRIC Q-POLE COMPONENT.
 0.  0.  0.  0.  0.  0.  0.  0. 0. 0. 0.          ENTRANCE EFB, SHARP EDGE.
6  .1122 6.2671 -1.4982 3.5882 -2.1209 1.723
 0.  0.  0.  0.  0.  0.  0.  0. 0. 0. 0.          EXIT EFB, SHARP EDGE.
6  .1122 6.2671 -1.4982 3.5882 -2.1209 1.723
 0. 0. 0. 0. 0. 0. 0. 0. 0. 0.
10.2  10. 0.  1.89493  0. 0. 0. 0.  0. 0. 0. 0.     MAGNETIC Q-POLE COMPONENT.
 0.  0.  0.  0.  0.  0.  0.  0. 0. 0. 0.          ENTRANCE EFB, SHARP EDGE.
6  .1122 6.2671 -1.4982 3.5882 -2.1209 1.723
 0.  0.  0.  0.  0.  0.  0.  0. 0. 0. 0.          EXIT EFB, SHARP EDGE.
6  .1122 6.2671 -1.4982 3.5882 -2.1209 1.723
0.  0. 0. 0. 0. 0. 0. 0. 0. 0.
.8
1 0. 0. 0.
'DRIFT'                                  DRIFT.                     6
4.9
'EBMULT'                                 SECOND ELECTROMAGNETIC    7
 0                                                          QUADRUPOLE.
10.2  10. 0.  13779.90  0. 0. 0. 0. 0. 0. 0.
 0.  0.  0.  0.  0.  0.  0. 0. 0. 0. 0.
6  .1122 6.2671 -1.4982 3.5882 -2.1209 1.723
 0.  0.  0.  0.  0.  0.  0. 0. 0. 0. 0.
6  .1122 6.2671 -1.4982 3.5882 -2.1209 1.723
0. 0. 0. 0. 0. 0. 0. 0. 0. 0. 0. 0.
10.2  10. 0.   -2.81592  0. 0. 0. 0. 0. 0. 0.
 0.  0.  0.  0.  0.  0.  0. 0. 0. 0. 0.
6  .1122 6.2671 -1.4982 3.5882 -2.1209 1.723
 0.  0.  0.  0.  0.  0.  0. 0. 0. 0. 0.
6  .1122 6.2671 -1.4982 3.5882 -2.1209 1.723
0. 0. 0. 0. 0. 0. 0. 0. 0. 0.
.8
1 0. 0. 0.
'DRIFT'                                  DRIFT.                     8
25.
'HISTO'                                  HISTOGRAM                  9
2  -5E-6  5E-6     60  2                   OF THE Y COORDINATE.
20  'Y'  1  'Q'
'HISTO'                                  HISTOGRAM                 10
4  -5E-6  5E-6     60  2                   OF THE Z COORDINATE.
20  'Z'  1  'Q'
'FAISCHL'                                RAYS ARE STORED IN RAYS  11
rays.out                                         FOR FURTHER PLOTTING.
'REBELOTE'                               RUN AGAIN, FOR RAY-TRACING  12
19  0.1 0                                  TOTAL OF 200*(19+1) PARTICLES.
'END'
```

zgoubi output file.

```
****************************************************************************************************************************************

     LE  PASSAGE  SUIVANT  EST  LE    20-EME  (ET  DERNIER)  PASSAGE  DANS  LA  STRUCTURE

****************************************************************************************************************************************
      1  MCOBJET   RANDOM    OBJECT
               Reference  magnetic rigidity =         20.435 KG*CM

               Object  built  up  of 200  particles
               Distribution in a Window

               Central values (MKSA units):
           Yo, To, Zo, Po, Xo, BR/BORO  :         0.000E+00  0.000E+00  0.000E+00  0.000E+00  0.000E+00  1.0000E+00

               Width  (  +/- , MKSA units ) :
           DY, DT, DZ, DP, DX, DBR/BORO :         0.000E+00  2.000E-04  0.000E+00  2.000E-04  0.000E+00  3.0000E-04

               Cut-offs  ( * +/-Width ) :
           NY, NT, NZ, NP, NX, NBR/BORO :              0.0       0.0       0.0       0.0       0.0       0.0


****************************************************************************************************************************************
      2  PARTICUL  PARTICLE  MASS
     PARTICLE PROPERTIES :
          Masse =     938.27230000000 MeV/c2
         Charge =     1.6021773300000D-19 C

****************************************************************************************************************************************
```

```
      3  DRIFT     DRIFT.

                              ESPACE  LIBRE =   500.00000  CM

  TRAJ #1  D,Y,T,Z,P,S,IEX :  1.0002E+00  1.7062E-02  3.4124E-02 -2.6802E-02 -5.3603E-02      5.00000E+02  1

*****************************************************************************************************************************
      4  DRIFT     DRIFT.

                              ESPACE  LIBRE =    59.00000  CM

  TRAJ #1  D,Y,T,Z,P,S,IEX :  1.0002E+00  1.9075E-02  3.4124E-02 -2.9964E-02 -5.3603E-02      5.59000E+02  1

*****************************************************************************************************************************
      5  EBHULT    FIRST

      -----  HULTIPOLE    :
                LONGUEUR  DE  L'ELEMENT  :   10.200  CM
                RAYON DE GORGE  RO =   10.00  CM
               V-DIPOLE       =  0.000000E+00 V
               V-QUADRUPOLE   = -9.272986E+03 V
               V-SEXTUPOLE    =  0.000000E+00 V
               V-OCTUPOLE     =  0.000000E+00 V
               V-DECAPOLE     =  0.000000E+00 V
               V-DODECAPOLE   =  0.000000E+00 V
               V-14-POLE      =  0.000000E+00 V
               V-16-POLE      =  0.000000E+00 V
               V-18-POLE      =  0.000000E+00 V
               V-20-POLE      =  0.000000E+00 V
                LENTILLE  A  GRADIENT  CREUEAU

      -----  HULTIPOLE    :
                LONGUEUR  DE  L'ELEMENT  :   10.200  CM
                RAYON DE GORGE  RO =   10.00  CM
               B-DIPOLE       =  0.000000E+00 kG
               B-QUADRUPOLE   =  1.894930E+00 kG
               B-SEXTUPOLE    =  0.000000E+00 kG
               B-OCTUPOLE     =  0.000000E+00 kG
               B-DECAPOLE     =  0.000000E+00 kG
               B-DODECAPOLE   =  0.000000E+00 kG
               B-14-POLE      =  0.000000E+00 kG
               B-16-POLE      =  0.000000E+00 kG
               B-18-POLE      =  0.000000E+00 kG
               B-20-POLE      =  0.000000E+00 kG
                LENTILLE  A  GRADIENT  CREUEAU

                    Integration step :      0.80 cm

*****************************************************************************************************************************
      6  DRIFT     DRIFT.

                              ESPACE  LIBRE =     4.90000  CM

  TRAJ #1  D,Y,T,Z,P,S,IEX :  1.0002E+00  1.1032E-02 -8.0508E-01 -4.5922E-02 -1.6008E+00      5.74100E+02  1

*****************************************************************************************************************************
      7  EBHULT    SECOND

      -----  HULTIPOLE    :
                LONGUEUR  DE  L'ELEMENT  :   10.200  CM
                RAYON DE GORGE  RO =   10.00  CM
               V-DIPOLE       =  0.000000E+00 V
               V-QUADRUPOLE   =  1.377990E+04 V
               V-SEXTUPOLE    =  0.000000E+00 V
               V-OCTUPOLE     =  0.000000E+00 V
               V-DECAPOLE     =  0.000000E+00 V
               V-DODECAPOLE   =  0.000000E+00 V
               V-14-POLE      =  0.000000E+00 V
               V-16-POLE      =  0.000000E+00 V
               V-18-POLE      =  0.000000E+00 V
               V-20-POLE      =  0.000000E+00 V
                LENTILLE  A  GRADIENT  CREUEAU

      -----  HULTIPOLE    :
                LONGUEUR  DE  L'ELEMENT  :   10.200  CM
                RAYON DE GORGE  RO =   10.00  CM
               B-DIPOLE       =  0.000000E+00 kG
               B-QUADRUPOLE   = -2.815920E+00 kG
               B-SEXTUPOLE    =  0.000000E+00 kG
               B-OCTUPOLE     =  0.000000E+00 kG
               B-DECAPOLE     =  0.000000E+00 kG
               B-DODECAPOLE   =  0.000000E+00 kG
               B-14-POLE      =  0.000000E+00 kG
               B-16-POLE      =  0.000000E+00 kG
               B-18-POLE      =  0.000000E+00 kG
               B-20-POLE      =  0.000000E+00 kG
                LENTILLE  A  GRADIENT  CREUEAU

                    Integration step :      0.80 cm

*****************************************************************************************************************************
      8  DRIFT     DRIFT.

                              ESPACE  LIBRE =    25.00000  CM

  TRAJ #1  D,Y,T,Z,P,S,IEX :  1.0002E+00  9.0257E-07 -2.3996E-01 -1.0770E-06  1.7947E+00      6.09300E+02  1


*****************************************************************************************************************************
```

```
     9  HISTO     HISTOGRA

                           HISTOGRAMME  DE  LA  COORDONNEE  Y
                           PARTICULES  PRIMAIRES  ET  SECONDAIRES
                           DANS  LA  FENETRE :  -5.0000E-06 /   5.0000E-06 (CM)
                           NORMALISE

   20
   19
   18                                              Y
   17                                              Y
   16                                              Y
   15                                              Y
   14                                            YYY     Y
   13                                          Y  YYY    YY YY
   12                                          YYYYYY YYYYYYYY             Y
   11                                  Y  Y      Y YYYYYYYYYYYYYYYYY  YY    Y  Y
   10                                  0  0   000000000000000000000000 00    0  0
    9                                  Y YYYY YYYYYYYYYYYYYYYYYYYYYYYY    Y YY
    8                                  Y YYYY YYYYYYYYYYYYYYYYYYYYYYYYY  Y YY
    7                                  YYYYYYYYYYYYYYYYYYYYYYYYYYYYYYYYYYYYYYY
    6                                  YYYYYYYYYYYYYYYYYYYYYYYYYYYYYYYYYYYYYYY
    5                                  YYYYYYYYYYYYYYYYYYYYYYYYYYYYYYYYYYYYYYY
    4                                  YYYYYYYYYYYYYYYYYYYYYYYYYYYYYYYYYYYYYYY
    3                                  YYYYYYYYYYYYYYYYYYYYYYYYYYYYYYYYYYYYYYY
    2                                  YYYYYYYYYYYYYYYYYYYYYYYYYYYYYYYYYYYYYYY
    1                                 YYYYYYYYYYYYYYYYYYYYYYYYYYYYYYYYYYYYYYYY

                           12345678901234567890123456789012345678901234567890123456789012345678901
                                    3         4         5         6         7         8

               TOTAL  COMPTAGE                :    4000  SUR   4000
               NOMBRE   DU  CANAL  MOYEN      :      51
               COMPTAGE  AU   "      "        :     109
               VAL. PHYS. AU  "      "        :  0.000E+00 (CM)
               RESOLUTION  PAR  CANAL         :  1.667E-07 (CM)

               PARAMETRES  PHYSIQUES  DE  LA  DISTRIBUTION :
                           COMPTAGE =   4000  PARTICULES
                           MIN = -3.4326E-06, MAX =  3.4347E-06, MAX-MIN =  6.8674E-06 (CM)
                           MOYENNE = -2.8531E-08 (CM)
                           SIGMA =  1.8619E-06 (CM)

  TRAJ #1  D,Y,T,Z,P,S,IEX :  1.0002E+00  9.0257E-07 -2.3996E-01 -1.0770E-06  1.7947E+00      6.09300E+02  1
*************************************************************************************************************************************
     10  HISTO     HISTOGRA

                           HISTOGRAMME  DE  LA  COORDONNEE  Z
                           PARTICULES  PRIMAIRES  ET  SECONDAIRES
                           DANS  LA  FENETRE :  -5.0000E-06 /   5.0000E-06 (CM)
                           NORMALISE

   20
   19
   18
   17                                                    Z
   16                                        Z           Z
   15                                        ZZ          Z
   14                                        ZZ          Z
   13                                        ZZ         ZZ
   12                                        ZZ         ZZ
   11                                        ZZ        ZZZ
   10                                        00        000
    9                                        ZZZZ      ZZZ
    8                                       ZZZZZZZ Z Z   ZZZZZZ
    7                                       ZZZZZZZ Z Z ZZZZZZZZZ
    6                                       ZZZZZZZZZZZZZZZZZZZZ
    5                                       ZZZZZZZZZZZZZZZZZZZZ
    4                                       ZZZZZZZZZZZZZZZZZZZZ
    3                                      ZZZZZZZZZZZZZZZZZZZZZZ
    2                                      ZZZZZZZZZZZZZZZZZZZZZZ
    1                                      ZZZZZZZZZZZZZZZZZZZZZZ

                           12345678901234567890123456789012345678901234567890123456789012345678901
                                    3         4         5         6         7         8

               TOTAL  COMPTAGE                :    4000  SUR   4000
               NOMBRE   DU  CANAL  MOYEN      :      51
               COMPTAGE  AU   "      "        :     169
               VAL. PHYS. AU  "      "        :  0.000E+00 (CM)
               RESOLUTION  PAR  CANAL         :  1.667E-07 (CM)

               PARAMETRES  PHYSIQUES  DE  LA  DISTRIBUTION :
                           COMPTAGE =   4000  PARTICULES
                           MIN = -1.9150E-06, MAX =  1.9110E-06, MAX-MIN =  3.8260E-06 (CM)
                           MOYENNE = -3.8539E-09 (CM)
                           SIGMA =  1.1232E-06 (CM)

  TRAJ #1  D,Y,T,Z,P,S,IEX :  1.0002E+00  9.0257E-07 -2.3996E-01 -1.0770E-06  1.7947E+00      6.09300E+02  1
*************************************************************************************************************************************
     11  FAISCNL   RAYS      ARE
  Print[s] occur at

*************************************************************************************************************************************
     12  REBELOTE  RUN       AGAIN,

                      ****  FIN  D'EFFET  DE  'REBELOTE'  ****
      IL  Y  A  EU        20  PASSAGES  DANS  LA  STRUCTURE
                  # PARTICULES  ENVOYEES      :      4000

*************************************************************************************************************************************
          PGM PRINCIPAL : ARRET SUR CLE   REBELOTE
*************************************************************************************************************************************
```

PART D

Running zgoubi and its post-processor/graphic interface zpop

INTRODUCTION

The basic **zgoubi** *FORTRAN* package is transportable; it has been compiled, linked and executed on several types of computers (e.g. CDC, CRAY, IBM, DEC, HP, SUN, VAX).

An additional *FORTRAN* code, **zpop**, allows the post-processing and graphic treatment of **zgoubi** output files. **zpop** is routinely used on DEC, HP and SUN stations.

1 GETTING TO RUN zgoubi AND zpop

1.1 Making the executable files zgoubi and zpop

1.1.1 The transportable package zgoubi

Compile and link the *FORTRAN* source file zgoubi.f , to create the executable **zgoubi**.

zgoubi.f is written in standard *FORTRAN* , therefore it is not necessary to link with any Library, except maybe a local math. lib.

1.1.2 The post-processor and graphic interface package zpop

Compile the *FORTRAN* source files zpop*.f.

Link **zpop** with the graphic library, libminigraf.a [28]. This will create the executable **zpop**, that can run on xterm type window.

1.2 Running zgoubi

The principles are the following:

- fill zgoubi.dat with the input data that describe the problem (see examples, Part C).
- Run **zgoubi**.
- Results of the execution will be printed into zgoubi.res and, upon options appearing in zgoubi.dat, into several other outputs files (see section 2 below).

1.3 Running zpop

- Run **zpop** on an xterm window. This will open a graphic window.
- Select options displayed on the menu.
- To access the graphic sub-menu, select option 7.
- An on-line Help provides all necessary informations on the post-processors (Fourier transform, elliptical fit, synchrotron radiation, field map contours, etc.).

2 STORAGE FILES

When explicitly requested by means of the adequate keywords, or options, extra storage files are opened by **zgoubi** (*FORTRAN "OPEN"* statement) and filled. Their content is afterwards read and post-processed when executing **zpop** and its dedicated graphic menu options.

The **zgoubi** procedures that create and fill these extra output files are the following (refer to Part A and Part B of the guide):

- Keywords *FAISCNL*, *FAISTORE*: fill a '.fai' type file (normally named zgoubi.fai) with particle coordinates and other informations.
- Option $IC = 2$, with field map keywords (e.g. *CARTEMES*, *TOSCA*) : fill zgoubi.map with 2-D field map.
- Option $IL = 2$, with magnetic and electric element keywords: fill zgoubi.plt with the particle coordinates, and experienced field, step after step, all along the optical element.
- Keyword *SPNPRNL[A]*: fill a '.spn' type file (normally named zgoubi.spn) with spin coordinates and other informations.

Typical examples of graphics that one can expect from the post-processing of these files by **zpop** are the following (see examples, Part C):

- '.fai' type files

  Phase-space plots (transverse and longitudinal), aberration curves, at the position where *FAISCNL* appears in the optical structure. Histograms of coordinates. Fourier analysis (e.g. tune numbers in multiturn tracking), calculation of Twiss parameters from phase-space ellipse matching.

- zgoubi.map

  Isomagnetic field lines of 2-D map. Superimposing trajectories read from zgoubi.plt is possible.

- zgoubi.plt

  Trajectories inside magnets and other lenses (these can be superimposed over field lines obtained from zgoubi.map). Fields experienced by the particles at the traversal of optical elements. Synchrotron radiation.

- zgoubi.spn

  Spin coordinates and histograms, at the position where *SPNPRNL* appears in the structure. Resonance crossing when performing multiturn tracking.

References

[1] F. Méot et S. Valéro, *Manuel d'utilisation de Zgoubi*, report IRF/LNS/88-13, CEA Saclay, 1988.

[2] F. Méot and S. Valéro, *Zgoubi users' guide*, report DSM/LNS/GT/90-05, CEA Saclay (1990) and TRIUMF report TRI/CD/90-02 (1990).

[3] F. Méot and S. Valéro, *Zgoubi users' guide*, report DSM/LNS/GT/93-12, CEA Saclay (1993).

[4] F. Méot, *The electrification of Zgoubi*, Saturne report DSM/LNS/GT/93-09, CEA Saclay (1993) ; F. Méot, *Generalization of the Zgoubi method for ray-tracing to include electric fields*, NIM A 340 (1994) 594-604.

[5] D. Carvounas, *Suivi numérique de particules chargées dans un solénoïde*, report de stage, CEA/LNS/GT-1991.

[6] F. Méot, *Raytracing in 3-D field maps with Zgoubi*, report DSM/LNS/GT/90-01, CEA Saclay, 1990.

[7] G. Leleux, *Compléments sur la physique des accélérateurs*, cours de DEA Univ. Paris-VI, report IRF/LNS/86-101, CEA Saclay, March 1986.

[8] F. Méot, *A numerical method for combined spin tracking and raytracing of charged particles*, NIM **A313** (1992) 492, and proc. EPAC (1992) p.747.

[9] V. Bargmann, L. Michel, V.L. Telegdi, Precession of the polarization of particles moving in a homogeneous electromagnetic field, Phys. Rev. Lett. 2 (1959) 435.

[10] F. Méot and J. Payet, *Numerical tools for the simulation of synchrotron radiation loss and induced dynamical effects in high energy transport lines*, Report DSM/DAPNIA/SEA-00-01, CEA Saclay (2000).

[11] F. Méot, *Synchrotron radiation interferences at the LEP miniwiggler*, Report CERN SL/94-22 (AP), 1994.

[12] J.D. Jackson, *Classical electrodynamics*, 2nd Ed., J. Wiley and Sons, New York, 1975.

[13] F. Méot, A theory of low frequency far-field synchrotron radiation, Particle Accelerators Vol 62, pp. 215-239 (1999).

[14] B. Mayer, personal communication, CEA Saclay, 1990.

[15] L. Farvacque *et al.*, *Beta user's guide*, Note ESRF-COMP-87-01, 1987; J. Payet, IRF/LNS, CEA Saclay, private communication; see also J.M. Lagniel, *Recherche d'un optimum*, Note IRF/LNS/SM 87/48, CEA Saclay 1987.

[16] F. Méot and N. Willis, *Raytrace computation with Monte Carlo simulation of particle decay*, internal report CEA/LNS/88-18 CEA Saclay, 1988.

[17] H.A. Enge, *Deflecting magnets*, in **Focusing of Charged Particles**, ed. A. Septier, **Vol. II**, pp 203-264, Academic Press Inc., 1967.

[18] P. Birien et S. Valéro, *Projet de spectromètre magnétique à haute résolution pour ions lourds*, **Section IV** p.62, Note CEA-N-2215, CEA Saclay, mai 1981.

[19] V. M. Kel'man and S. Ya. Yavor, Achromatic quadrupole electron lenses, Soviet Physics - Technical Physics, vol. 6, No 12, June 1962;
S. Ya. Yavor *et als.*, *Achromatic quadrupole lenses*, NIM **26** (1964) 13-17.

[20] A. Septier et J. van Acker, *Les lentilles quadrupolaires électriques*, NIM **13** (1961) 335-355; Y. Fujita and H. Matsuda, *Third order transfer matrices for an electrostatic quadrupole lens,* NIM **123** (1975) 495-504.

[21] A. Septier, Cours du DEA de physique des particules, optique corpusculaire, Université d'Orsay, 1966-67, pp. 38-39.

[22] S. P. Karetskaya et als., Mirror-bank energy analyzers, in Advances in electronics and electron physics, Vol. 89, Acad. Press (1994) 391-491.

[23] P. Akishin, JINR, Dubna, 1992.

[24] M.W. Garrett, *Calculation of fields [...] by elliptic integrals*, J. Appl. Phys., **34**, 9, sept. 1963.

[25] P.F. Byrd and M.D. Friedman, *Handbook of elliptic integrals for engineers and scientists,* pp. 282-283, Springer-Verlag, Berlin, 1954.

[26] A. Tkatchenko, *Computer program UNIPOT*, SATURNE, CEA Saclay, 1982.

[27] J.L. Chuma, *PLOTDATA*, TRIUMF Design Note TRI-CO-87-03a.

[28] J.L. Hamel, *mini graphic library LIBMINIGRAF*, CEA-DSM, Saclay, 1996.

[29] E. Grorud, J.L. Laclare, G. Leleux, Résonances de dépolarisation dans SATURNE 2, Int. report GOC-GERMA 75-48/TP-28, CEA Saclay (1975), and Home Computer Codes POLAR and POPOL, IRF/LNS/GT, CEA Saclay (1975).

[30] M. Froissart et R. Stora, Dépolarisation d'un faisceau de protons polarisés dans un synchrotron, NIM 7 (1960) 297-305.

[31] J. Thirion et P. Birien, Le spectromètre II, Internal Report DPh-N/ME, CEA Saclay, 23 Déc. 1975;
H. Catz, Le spectromètre II, Internal Report DPh-N/ME, CEA Saclay, 1980.

[32] P. Pile, I-H. Chiang, K. K. Li, C. J. Kost, J. Doornbos, F. Méot et als., A two-stage separated 800-MeV/c Kaon beamline, TRIUMF and BNL Preprint (1997).

[33] F. Méot, The raytracing code Zgoubi, CERN SL/94-82 (AP) (1994), 3rd Intern. Workshop on Optimization and Inverse Problems in Electromagnetism, CERN, Geneva, Switzerland, 19-21 Sept. 1994.

[34] W. H. Press et *als.*, Numerical recipes, Cambridge Univ. Press (1987).

[35] V. O. Kostroun, Simple numerical evaluation of modified Bessel functions and integrals [...], NIM 172 (1980) 371-374.

Index